frontiers | Research Topics

Exploring the potential for advancements in spinal neurosurgery: revolutionizing treatment pathways and improving quality of life

Edited by
Ning Li, Jiaao Gu, Lili Cui, Madiha Zahra Syeda and John Gruen

Published in
Frontiers in Neurology
Frontiers in Oncology

ISSN 1664-8714
ISBN 978-2-8325-5721-1
DOI 10.3389/978-2-8325-5721-1

Generative AI statement
Any alternative text (Alt text) provided alongside figures in the articles in this ebook has been generated by Frontiers with the support of artificial intelligence and reasonable efforts have been made to ensure accuracy, including review by the authors wherever possible. If you identify any issues, please contact us.

About Frontiers

Frontiers is more than just an open access publisher of scholarly articles: it is a pioneering approach to the world of academia, radically improving the way scholarly research is managed. The grand vision of Frontiers is a world where all people have an equal opportunity to seek, share and generate knowledge. Frontiers provides immediate and permanent online open access to all its publications, but this alone is not enough to realize our grand goals.

Frontiers journal series

The Frontiers journal series is a multi-tier and interdisciplinary set of open-access, online journals, promising a paradigm shift from the current review, selection and dissemination processes in academic publishing. All Frontiers journals are driven by researchers for researchers; therefore, they constitute a service to the scholarly community. At the same time, the *Frontiers journal series* operates on a revolutionary invention, the tiered publishing system, initially addressing specific communities of scholars, and gradually climbing up to broader public understanding, thus serving the interests of the lay society, too.

Dedication to quality

Each Frontiers article is a landmark of the highest quality, thanks to genuinely collaborative interactions between authors and review editors, who include some of the world's best academicians. Research must be certified by peers before entering a stream of knowledge that may eventually reach the public - and shape society; therefore, Frontiers only applies the most rigorous and unbiased reviews. Frontiers revolutionizes research publishing by freely delivering the most outstanding research, evaluated with no bias from both the academic and social point of view. By applying the most advanced information technologies, Frontiers is catapulting scholarly publishing into a new generation.

What are Frontiers Research Topics?

Frontiers Research Topics are very popular trademarks of the *Frontiers journals series*: they are collections of at least ten articles, all centered on a particular subject. With their unique mix of varied contributions from Original Research to Review Articles, Frontiers Research Topics unify the most influential researchers, the latest key findings and historical advances in a hot research area.

Find out more on how to host your own Frontiers Research Topic or contribute to one as an author by contacting the Frontiers editorial office: frontiersin.org/about/contact

Exploring the potential for advancements in spinal neurosurgery: revolutionizing treatment pathways and improving quality of life

Topic editors

Ning Li — Southeast University, China
Jiaao Gu — First Affiliated Hospital of Harbin Medical University, China
Lili Cui — Guangdong Medical University, China
Madiha Zahra Syeda — Zhejiang University, China
John Gruen — University of Southern California, United States

Citation

Li, N., Gu, J., Cui, L., Syeda, M. Z., Gruen, J., eds. (2025). *Exploring the potential for advancements in spinal neurosurgery: revolutionizing treatment pathways and improving quality of life*. Lausanne: Frontiers Media SA.
doi: 10.3389/978-2-8325-5721-1

Table of contents

frontiers | Frontiers in Neurology

TYPE Original Research
PUBLISHED 17 April 2024
DOI 10.3389/fneur.2024.1387801

OPEN ACCESS

EDITED BY
Alberto Albanese,
Catholic University of the Sacred Heart, Italy

REVIEWED BY
S. Ottavio Tomasi,
Paracelsus Medical University, Austria
Daniele Bongetta,
ASST Fatebenefratelli Sacco, Italy

*CORRESPONDENCE
Yuhai Wang
✉ wangyuhai1516@163.com

†These authors have contributed equally to this work

RECEIVED 18 February 2024
ACCEPTED 03 April 2024
PUBLISHED 17 April 2024

CITATION
Shu L, Mu Q, Dai F, Zhao W, Syeda MZ and Wang Y (2024) Contralateral approach using microscope and tubular retractor system for ipsilateral decompression of lumbar degenerative lateral recess stenosis associated with narrow spinal canal. *Front. Neurol.* 15:1387801. doi: 10.3389/fneur.2024.1387801

Contralateral approach using microscope and tubular retractor system for ipsilateral decompression of lumbar degenerative lateral recess stenosis associated with narrow spinal canal

Longfei Shu[1†], Qingchun Mu[2†], Feihu Dai[1], Wei Zhao[1], Madiha Zahra Syeda[3,4] and Yuhai Wang[1*]

[1]Department of Neurosurgery, Wuxi Clinical College of Anhui Medical University, 904th Hospital of Joint Logistic Support Force of PLA, Wuxi, China, [2]Department of Neurosurgery, Second Affiliated Hospital of Soochow University, Suzhou, China, [3]Keenan Research Centre for Biomedical Science, St. Michael's Hospital, Toronto, ON, Canada, [4]Faculty of Medicine, Institute of Medical Sciences, University of Toronto, Toronto, ON, Canada

Objective: To summarize the clinical effect of a single-center retrospective analysis of the contralateral approach with a microscope and tubular retractor system for ipsilateral decompression in patients with lumbar lateral recess stenosis and a narrow spinal canal.

Methods: A total of 25 patients who underwent ipsilateral decompression surgery via a contralateral approach with microscope and tubular retractor system, performed by one surgeon at a single center were retrospectively examined. The width of the lamina fenestration was compared with the preoperative distance from the root of the spinous process to the dorsal articular facet, the bilateral articular facet change in the suprapedicle notch section on CT scan, and with the changes in transverse and sagittal diameters of the canal area on MRI. Clinical efficacy was assessed using the Japanese Orthopedic Association (JOA), Visual Analog Scale (VAS), and Oswestry Disability Index (ODI) scores.

Results: In total, 25 patients were treated and the mean intraoperative time was 82.04 ± 12.48 min. There was no nerve injury, cerebrospinal fluid leakage, and infection complications. The postoperative CT revealed that the width of the contralateral laminar fenestration was less than the distance from the root of the spinous process to the dorsal articular facet. The residual widths of the ipsilateral articular facet and contralateral articular facet were greater than 2/3 of the preoperative articular facet width. The transverse and sagittal diameter of canal were significantly increased. The mean follow-up period was 12–16 months, and no recurrence or reoperation incidence were found at the last follow-up. When compared to pre-surgery, the ODI, VAS, and JOA scores were significantly improved after surgery ($p < 0.05$).

Conclusion: Based on our single-center retrospective observation of 25 cases and combined with previous literature, the contralateral approach with a microscope and tubular retractor system for ipsilateral decompression in patients with lumbar lateral recess stenosis and a narrow spinal canal can

reduce damage to the articular processes, and probably more conducive to the postoperative stability of the lumbar spine. This was a single center retrospective analysis with a small sample size and lacked randomized controlled trials (RCTs). However, larger-scale, multicenter RTCs are required for additional validation.

KEYWORDS

contralateral approach, laminectomy alone, lateral recesses stenosis, minimally invasive, microscope

Introduction

Currently, lumbar spinal stenosis is the most prevalent spinal disease affecting adults over 65 years old (1–3). Based on the location of the stenotic pathology, lumbar spinal stenosis can be anatomically classified into three types: central stenosis, lateral recess stenosis, and foraminal stenosis (4). Degenerative lateral recess stenosis is usually caused by hyperplasia of the articular facets, osteophyte formation, hypertrophied ligamentum flavum, or disc herniation (5). A hypertrophied ligamentum flavum and hyperplasia of the articular facet on the dorsal side are the main causes of spinal canal and nerve root compression (6).

The aging process contributes to an increase in the number of geriatric patients with degenerative lumbar lateral recess stenos is worldwide. These patients usually have severe symptoms, protracted illness, and poor overall health. It is important to take into account the ease, safety, and efficacy of the treatments that can be performed to alleviate pain and discomfort and improve the quality of life (7, 8). Additionally, conservative treatment yields no discernible results. The traditional posterior surgical approach typically entails decompression with foraminotomy and facetectomy (9, 10, 11). which enlarges the nerve root canal but also increases intraoperative tissue destruction, blood loss, and postoperative lumbar instability, and can be performed with lumbar fusion (12, 13).

The development of tubular retractors in 1997 and the subsequent development of endoscopic techniques have led to a pattern shift from open to minimally invasive surgeries (14, 15, 16). In 2002, Palmer et al. reported the feasibility and surgical efficacy of unilateral approach bilateral decompression (ULBD) and the use of a tubular retractor system in patients with LSS and degree I spondylolisthesis (17, 18). Further, patients who present with unilateral lateral recess or foraminal stenosis are frequently treated with an ipsilateral microscope or endoscopic approach (19, 20).

The diameter of the working tube in our center was 1.6 cm (Figure 1A), which is smaller than the width of most lamina. The ipsilateral microscopic approach was used more frequently to perform the lateral recess decompression without excessively grinding the articular joints (Figure 1B); however, in some cases, the lamina's width combined with wide spinous processes or a spinal canal that is developmentally narrower than the tubular diameter may cause problems. Surgeons using the ipsilateral microscope approach are likely to over-resect the inferior articular process, which can easily lead to excessive breakthrough of the articular joint, raising the risk of postoperative instability (Figure 1C). In contrast, the contralateral approach does not require excessive grinding of the articular joint to expose the lateral recess, and utilizes the inclination angle of the tube to complete symptomatic nerve root decompression (Figure 1D). The KOIKUTA study also showed that articular processes on the ipsilateral side suffered more damage than contralateral side during unilateral bilateral decompression (21). Alimi et al. showed that contralateral foraminotomy is a preferable option for decompression on the opposite side (22). Concordontaly, the percutaneous endoscopic contralateral technique, which has also been shown to lessen injury to the lumbar articular processes on the approach side, was employed by Hyeung Sung Kim to treat lumbar spine lateral recess stenosis (23).

Here, we reported the lamina fenestration, bilateral articular facet changes, and radiological outcomes of the standalone contralateral approach for ipsilateral lateral recess decompression, using a microscope and tubular retractor system in patients with a bilateral distance of less than 1.6 cm from the root of the spinous process to the dorsal articular facet in the suprapedicle notch section CT scan. We have discussed and compared our findings with the current literature on the contralateral approach.

Materials and methods

Characteristics of patients and study design

A retrospective study of 317 consecutive patients with lumbar spinal stenosis was conducted from September-2019 to December-2022 at the 904th Hospital of Joint Logistic Support Force of the PLA. Of these, 25 patients presented with degenerative ipsilateral recess stenosis associated with a narrow spinal canal and underwent decompression via a contralateral approach with a microscope and tubular retractor system operated by one senior surgeon at a single center.

Inclusion/exclusion criteria

All patients underwent anterior and lateral lumbar radiography, computed tomography (CT), and magnetic resonance imaging (MRI) before surgery. Every patient satisfied the following inclusion and exclusion criteria and had a diagnosis of lateral recess stenosis. Inclusion criteria: (1) aged 45 years or older; (2) width of the bilateral vertebral plate from the root of the spinous process to the dorsal articular facet in the suprapedicle notch section CT scan less than 1.6 cm; (3) lumbar spondylolisthesis less than or equal to grade I; and (4) no significant effect of conservative treatment for 6 months. Exclusion criteria: (1) acute lumbar disc herniation resulting in lateral

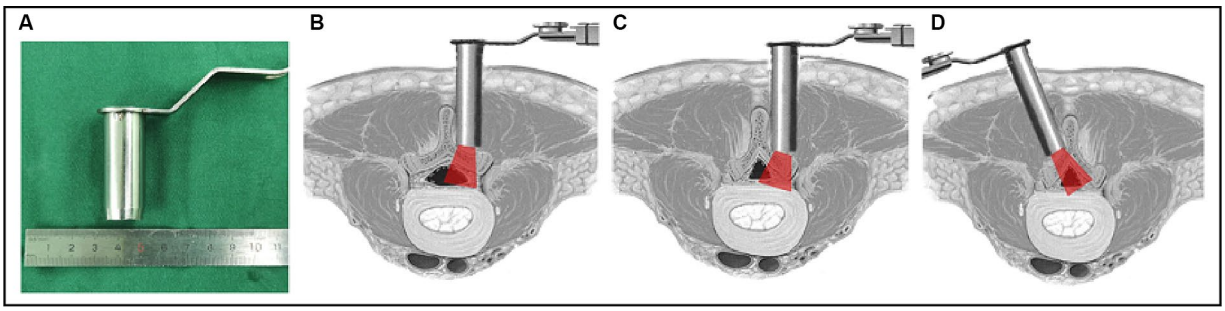

FIGURE 1
Illustration of the tube in a vertical and medially angled position to access the contralateral side. **(A)** Diameter of the tube; **(B)** a normal vertebral lamina with ipsilateral decompression through the symptomatic ipsilateral approach; **(C)** a narrow vertebral lamina with ipsilateral decompression through the symptomatic ipsilateral approach; **(D)** a narrow vertebral lamina with ipsilateral decompression through the symptomatic contralateral approach.

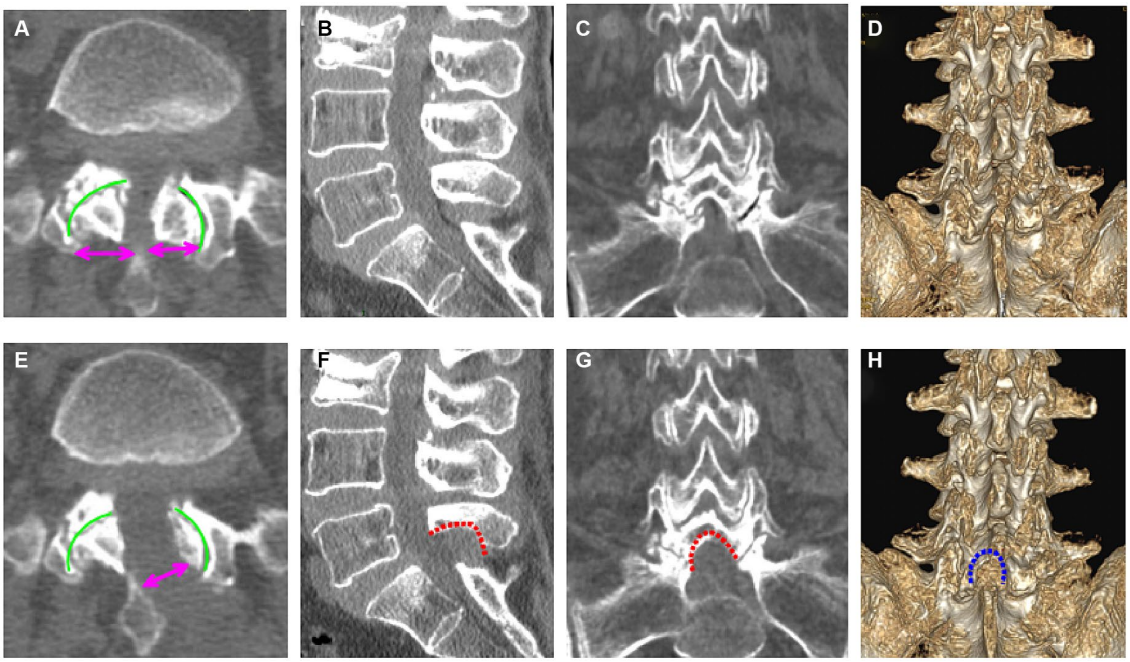

FIGURE 2
Pre- **(A–D)** and postoperative **(E–H)** computed tomography (CT) images of the lumbar spine (a 69-year-old woman). **(A)** Preoperative axial CT image of L5/S1; **(B)** preoperative sagittal CT image of L5/S1; **(C)** preoperative coronal CT image of L5/S1; **(D)** preoperative three-dimensional CT image of L5/S1; **(E)** postoperative axial CT image of L5/S1; **(F)** postoperative sagittal CT image of L5/S1; **(G)** postoperative coronal CT image of L5/S1; **(H)** three-dimensional CT image of L5/S1.

recess stenosis; (2) a distance of more than 1.6 cm from the root of the spinous facet to the articular surface on CT scan of the suprapedicle notch section; (3) bilateral lateral recess stenosis; (4) a lumbar spondylolisthesis exceeding grade I; (5) a history of lumbar spine decompression surgery, spinal tumors, or spinal tuberculosis; and (6) an unwillingness to adhere to follow-up agreements.

Radiological methods

Using the CareStream Pacs imaging system (OneX, Canada), two senior doctors measured the distance of the bilateral lamina from the spinous process root to the bilateral dorsal articular facet based on the CT image of the suprapedicular notch section as well as the width of the bilateral articular facet (Figures 2A,E). The transverse and sagittal diameters of the dural sac in the axial plane were measured via MRI (Figures 3A,C). All the indicators were measured twice, and the average value was calculated.

Surgical methods

(1) Surgical position, anesthesia and body surface positioning: Under general anesthesia and in the prone position with neuroelectrophysiological monitoring. The target level was verified using C-arm guidance, and a 1.8–2.0 cm paramedian skin incision was

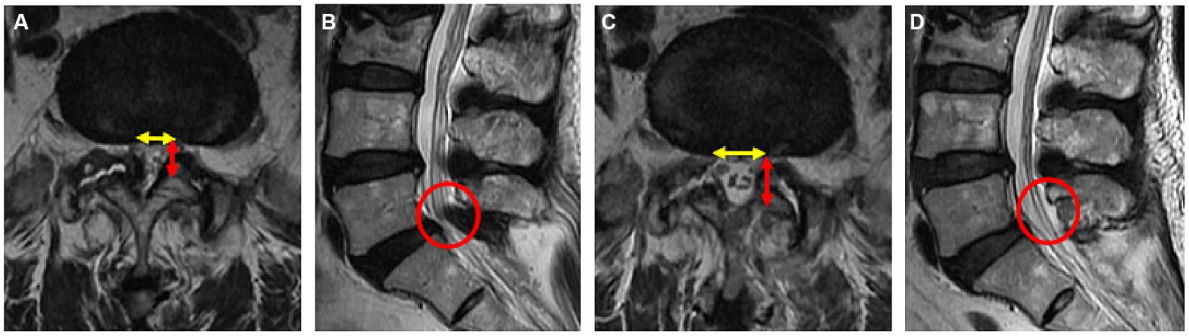

FIGURE 3
Pre- **(A,B)** and postoperative **(C,D)** magnetic resonance imaging (MRI) of the lumbar spine in a 69-year-old female patient. **(A)** Preoperative axial MR image of L5/S1; **(B)** preoperative sagittal MR image of L5/S1; **(C)** postoperative axial MR image of L5/S1; **(D)** postoperative sagittal MR image of L5/S1.

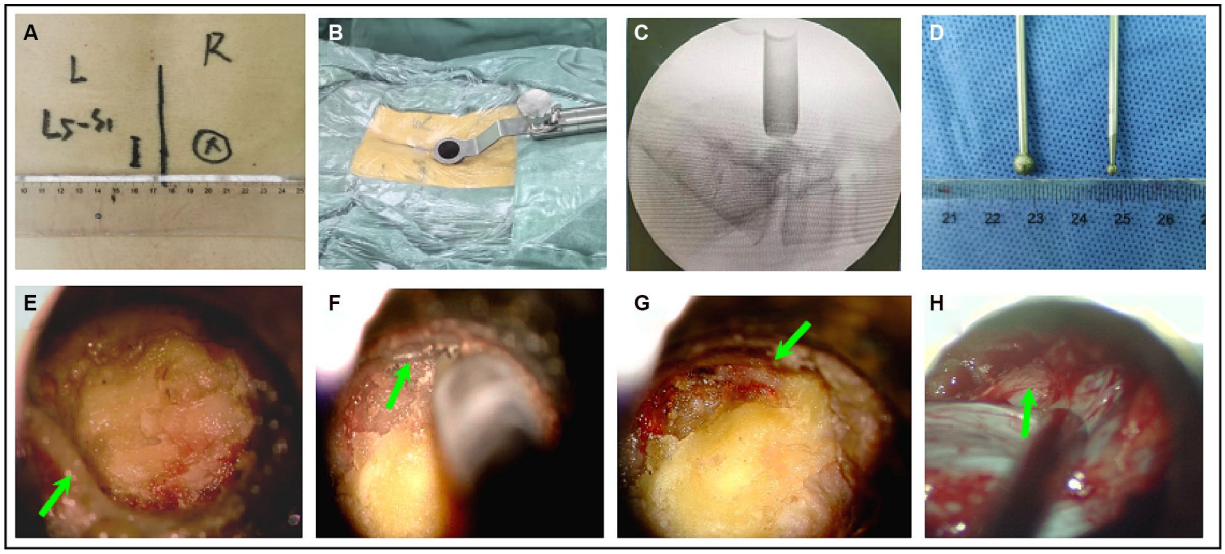

FIGURE 4
The surgical procedure for microscopic tubular reconstruction: A working tube for microchannel decompression was established **(A–C)**. **(D)** The style of the high-speed drill. The left part of the inferior articular process was removed to expose the ligamentum flavum and contralateral interlaminar region **(E,F)**. Ipsilateral osteophytes **(G)**. The ligamentum flavum and the ipsilateral nerve root were removed **(H)**.

made overlying the target level approximately 1.5–2 cm lateral to the midline on the patient's symptomatic contralateral side (Figure 4A). (2) Establishment of the spinal tubular working channel: The skin, fascia, and muscle were sequentially dilated, after which we inserted a 16-mm modified mini-retractor microscopic tube of the shortest length, usually 50 or 70 mm, that would allow adequate depth of access (Figure 4B). The surgical level was verified by C-arm guidance (Figure 4C). (3) Contralateral lamina fenestration: An operating microscope (Leica OH4, Germany) was used to view the fenestration into the field, and the paraspinal muscles were removed by an electrocautery from their bony attachments on the spinous process and lamina to expose the bony details. The inferior edge of the lamina was defined, and a hemilaminotomy was performed with a width diameter of 5 mm high-speed drill (Figure 4D) extending cranially above the attachment point of the ligamentum flavum on the inferior lamina surface, caudally on the superior lamina surface, and on the medial margin of the articular process. (4) The inner edge of the lamina was grounded on the ipsilateral side: The working tube was then angled medially to expose the anterior aspect of the spinous process, which was then removed utilizing a width diameter of 2 mm high-speed drill by microscopic angulation (Figure 4D), adhering to the inner edge of the vertebral plate on the symptomatic side with trumpeted decompression (Figures 4E,F). The inferior articular process of the upper hemilaminectomy was removed, and the inner edge of the articular facet of the articular process was revealed, than the superior articular process led to ipsilateral recess stenosis was exposed. During the use of high-speed drill, ligandum flavum removal should not be performed until sufficient medial facetectomy is performed. (5) Removed the ligamentum flavum and decompressed the nerve root: The ligamentum flavum and ipsilateral facet could be resected using Kerrison punches (Figure 4G). The dural sac was separated to the lamina fenestration side, and the exiting nerve root was completely decompressed to the internal edge of the pedicle side under direct visualization. The ipsilateral nerve root were then

completely decompressed (Figure 4H). (6) Final step: The surgical cavity was rinsed with hydrogen peroxide, diluted iodine solution, and physiological saline sequentially; the tubes were removed; the paraspinal muscles were repositioned; the muscle membrane, subcutaneous tissue, and skin were sutured sequentially; and suction drains were routinely placed.

Outcome assessment

Prior to surgery, the Japanese Orthopedic Association (JOA) score, the Disability Scale (Oswestry Disability Index [ODI]), and the Scale for Leg Pain (visual analog scale [VAS]) were used to assess the functional limits and symptoms of the patients. All the assessments were repeated at 7 days, 1 month, 3 months, 6 months and 12 months post-surgery. Postoperative CT scan was used to evaluate the width of the contralateral vertebral lamina fenestration and the remaining width of the bilateral articular facet in all patients. Similarly, postoperative MRI was used to determine the changes in the transverse and sagittal diameters of the dural sac.

Statistical analysis

Statistical analysis was performed using SPSS (version 19.0; SPSS, Inc., Chicago, IL, United States). Continuous variable data are presented as the mean ± standard deviation (SD), with discontinuous variables as percentages. For quantitative data, a *t*-test was used when the data conformed to a normal distribution. For the quantitative data, *t*-test was selected when it conforms to normal distribution. The paired *t*-test was used for the quantitative data with equal variance assumed between the two groups, and the separate variance estimation *t*-test was used for the quantitative data with equal variance not assumed. The Chi-square test was used to assess the qualitative data between the two groups. Significance was set at $p < 0.05$.

Results

Baseline clinical and demographic characteristics

A total of 25 patients with a mean age of 65.16 ± 7.43 years (range 54–82 years) were included in the study, 13 of whom were male (52%) and 12 of whom were female (48%). The symptoms persisted for 6 to 48 months. The lateral recess stenosis levels were as follows: L3-4 (in 8 patients, 32%), L4-5 (in 10 patients, 40%), and L5-S1 (in 7 patients, 28%). Twenty (80%) patients showed decreased sensation in clinical symptoms, 23 (92%) had a positive lower limb nerve tension test, and 18 (76%) had neurogenic claudication. The surgical duration was 82.04 ± 12.48 min (60–100 min), and intravenous cefazolin was administered both pre- and post-surgery. An 80 mg dose of depomedrol was given for 2 days to prevent nerve root edema. An exercise program was started after 1 day to strengthen the paravertebral muscles, and patients were allowed to leave bed with a lumbosacral corset after 2 days and discharged within 1 week. The baseline data are presented in Table 1.

Complications

There were no accidental nerve injuries, CSF leakage, or infections. Three patients experienced aggravated symptoms of lower limb numbness due to nerve root edema after surgery and recovered 1 week later of receiving hyperbaric oxygen and 80 mg of depomedrol treatment.

Radiological results

The radiological results are shown in Tables 1–3. Postoperative CT (Figures 2B–H) and MRI (Figures 3B–D) scanning demonstrated adequate decompression and no instability in all patients, and the contralateral lamina fenestration width was 9.23 ± 1.32 mm, which was less than the distance between the spinous process to the dorsal articular facet (13.46 ± 1.75 mm) ($p < 0.001$). The residual widths of the ipsilateral articular facet (15.92 ± 3.8 mm) and contralateral articular facet (15.18 ± 2.64 mm) were greater than 2/3 of their preoperative widths (12.13 ± 2.21 mm and 12.25 ± 2.8 mm, respectively) (both $p < 0.001$). The canal area significantly increased from 8.29 ± 1.39 to 13.93 ± 1.82 mm ($p < 0.001$) in transverse diameter and from 9.27 ± 1.55 mm to 13.50 ± 2.40 mm in sagittal diameter ($p < 0.001$).

Clinical outcomes

Clinical outcomes throughout the follow-up period are shown in Table 4. The mean follow-up time was 14.1 months (12–16 months). Routine radiological investigations were performed at the indicated time intervals, and follow-up data were obtained from the VAS score, ODI, and JOA score for all 25 patients. Among the 20 patients with preoperative numbness, 12 improved within 1 month, and 5 showed improvement within 6 months after surgery; however, there was no significant symptom relief in the remaining 3 patients. Prior to surgery, 23 patients had radiating lower limb pain, 16 of them experienced pain relief 1 day after surgery, and the remaining 7 patients experienced pain relief 7 days after the surgery. One month following surgery, all 18 patients with neurogenic claudication fully recovered, and no patient required reoperation for residual or recurrent spinal stenosis at the same segment(s) at the 12th–16th months period. All the patients did not develop postoperative instability, and required instrumentation-assisted secondary fusion (Table 4).

Discussion

Lumbar spinal stenosis can be subdivided into three categories according to pathological location: central stenosis, lateral recess stenosis, and foraminal stenosis (4). Lateral recess stenosis is commonly associated with neurogenic claudication, radiculopathy pain, and motor and sensory deficits, which can lead to various pathologies of spinal compression, including spondylisthesis, osteophytes, disc herniation, and ligamentum flavum hypertrophy (5). The main reasons for degenerative lateral recess stenosis are often dorsal ligamentum flavum hypertrophy and osteophyte compression (6). When conservative therapy fails, surgical treatment is usually

TABLE 1 Baseline characteristics, surgery time and lamina width change values.

Level	n	Age (Mean + SD)	Male n (%)	DS n (%)	PNTT n (%)	NC n (%)	ST min (Mean ± SD)	Lamina width (Mean ± SD)	LF mm (Mean ± SD)
								Ipsilateral contral	
L3-L4	8	63.98 ± 8.90	5(62.5)	7(87.5)	8(100)	6(75)	85.75 ± 10.99	12.38 ± 1.51 12.38 ± 1.41	8.31 ± 0.65*
L4-L5	10	66.60 ± 6.57	5(50)	8(80)	9(90)	7(70)	77.50 ± 14.03	13.20 ± 1.63 13.22 ± 1.92	9.33 ± 1.42*
L5-S1	7	64.57 ± 7.59	3(42.8)	5(71.4)	6(85.7)	5(71.4)	84.29 ± 11.34	14.20 ± 1.83 14.14 ± 1.89	9.28 ± 0.75*
Total	25	65.16 ± 7.43	13(52)	20(80)	23(92)	18(76)	82.04 ± 12.48	13.46 ± 1.75 13.54 ± 1.69	9.23 ± 1.32*

DS, decreased sensation; PNTT, positive nerve tension test; IC, neurogenic claudication; ST, surgery time; LF, lamina fenestration. $P < 0.001$ versus preoperative values.

TABLE 2 Results of articular process measurements with pre- and postsurgical values.

Level	n	Ipsilateral Mean ± SD				Contralateral Mean ± SD			
		Preop×2/3	Postop	*t*-value	*p*-value	Preop×2/3	Postop	*t*-value	*P*-value
L3-L4	8	12.67 ± 1.51	16.43 ± 1.72	8.74	<0.001	13.01 ± 1.85	16.53 ± 1.63	10.09	<0.001
L4-L5	10	12.17 ± 1.69	16.71 ± 2.13	5.32	<0.001	12.21 ± 1.21	14.89 ± 1.75	4.091	0.001
L5-S1	7	11.47 ± 1.92	14.30 ± 1.27	4.77	<0.001	11.49 ± 1.76	13.87 ± 2.23	5.65	<0.001
Total	25	12.13 ± 2.21	15.92 ± 3.88	8.46	<0.001	12.25 ± 2.8	15.18 ± 2.64	7.40	<0.001

Preop, preoperative; Postop, postoperative.

TABLE 3 Dural sac results of nuclear magnetic resonance measurements before and after surgery.

Level	n	Transverse diameter Mean ± SD				Sagittal diameter Mean ± SD			
		Preop	Postop	*t*-value	*p*-value	Preop	Postop	*t*-value	*p*-value
L3-L4	8	8.37 ± 0.96	14.26 ± 2.02	7.45	<0.001	8.87 ± 1.64	13.51 ± 2.82	4.01	0.001
L4-L5	10	7.54 ± 1.61	14.27 ± 1.87	9.64	<0.001	9.57 ± 1.69	14.76 ± 2.12	6.05	<0.001
L5-S1	7	9.27 ± 0.86	13.07 ± 1.43	6.02	<0.001	9.30 ± 1.35	11.70 ± 1.81	4.04	<0.001
Total	25	8.29 ± 1.39	13.93 ± 1.82	12.31	<0.001	9.27 ± 1.55	13.50 ± 2.40	7.40	0.002

Preop, preoperative; Postop, postoperative.

TABLE 4 Comparisons of VAS, JOA, and ODI scores before and after surgery.

Time	VAS leg pain scores	JOA	ODI (%)
Preop	6.87 ± 0.96	13.49 ± 3.50	69.22 ± 13.69
1w postop	3.91 ± 0.90*	20.09 ± 2.82*	29.00 ± 7.35*
1mo postop	2.22 ± 0.60*	23.17 ± 2.15*	22.04 ± 6.08*
3mo postop	1.44 ± 0.51*	25.09 ± 2.26*	17.57 ± 4.41*
6mo postop	0.87 ± 0.63*	26.26 ± 1.69*	14.78 ± 3.73*
12mo postop	0.48 ± 0.25*	27.22 ± 1.35*	12.78 ± 2.18*

VAS, visual analog scale; JOA, Japanese Orthopedic Association; ODI, Oswestry Disability Index; Preop, preoperative; Postop, postoperative; d, day; w, week; mo, month/month.
*$P < 0.05$ versus preoperative values.

necessary for symptomatic lateral recess stenosis. The preferred intervention for treatment is to relieve nerve root canal compression. In most centers, the conventional ipsilateral midline approach—which incorporates several decompression techniques such laminectomy, foraminotomy, and laminotomy remains an efficacious intervention strategy. However, wide excision of facet joints to access the foramen can cause instability (24). Moreover, lumbar fusion and fixation is usually needed for the repair of spinal stability. The main goal of this study was to describe the use of the contralateral minimally invasive approach as an effective method for treating ipsilateral recess stenosis, while protecting the bilateral articular joint.

Patients who present with a unilateral lateral recess are frequently treated using an ipsilateral approach (19, 20). When decompressing the ipsilateral nerve root, it is necessary to grind out too many articular processes on the ipsilateral recess side, which can easily lead to excessive removal of the articular joint and impair the stability of the posterior spine column. Preservation of facet joints is the very important in successful outcome following micro-decompression surgery, especially in patients with very narrow lamina (21, 25, 26). The concept of a contralateral approach was briefly described by Wiltse and Spencer in 1988 as a part of an open lumbar spine approach (9). In 2002, Palmer et al. reported the feasibility and surgery-related

efficacy of unilateral bilateral decompression and the utilization of a tubular retractor system in patients with LSS (17, 18) Post-surgery imaging scans reveal that the contralateral approach is more likely to result in entry into the lateral recess and intervertebral foramen space. Myung-Hoon also demonstrated good articular protection when treating lumbar spinal central stenosis with a bilateral contralateral approach (27). Ikuta et al. reported that the reduction in facet size of 22.6% and fracture of the inferior facet is up to 6% of patients with microendoscopic posterior decompress techniques (21). Matsumura et al. reported that patients whose with degenerative stenosis is more common in the lateral recess region (28). During ipsilateral decompression in this patients, the damage to facet joint would increase deformation and may lead to instability, while a contralateral approach, the facets are better preserved and thus the fusion and fixation can be avoided in such patients. Concordontaly, Alimi et al. reported less articular joint destruction and greater protection on the approach side when using a contralateral approach to treat lumbar lateral recess and intervertebral foramen stenosis via a microscope and tubular system (22).

Hamasaki et al. (29) observed biomechanical changes in the spine in fresh degenerative spinal specimens using stepwise resection of the medial aspect of the articular processes. When more than one-third of the lower edge of the bilateral upper vertebral lamina combined with the medial aspect of the articular processes was removed, both spinal flexion and rotation were affected. Ahuja et al. (30) used the finite element model to study lumbar spinal stability in young people and showed that when the facet joint was removed by more than 30%, the biomechanics of the spine changed. In our treatment of patients with partial lumbar spinal stenosis at a single-center, we discovered that vertebral lamina's width was smaller than the inner diameter of the 1.6 cm channel. To achieve ipsilateral nerve root decompression, it is necessary to remove more than one-third of the lateral articular joints. Since the narrow spinal canal allows for the easiest access to the lateral recess space, we contend that degenerative lateral recess stenosis is related to it in this study. With a contralateral approach, the ipsilateral lateral recesses and central canal can all be accessed and decompressed with a single incision, preserving mechanical stability. Our results showed that there was less damage to the bilateral articular joints, and the remaining articular facet was greater than 2/3 of its preoperative value. Since the extent of articular facet removal in the contralateral and ipsilateral approaches is equal to or less than that described in biomechanical studies, the lumbar spine stability is presumably maintained. The clinical results of our study suggest that at the mid-term follow-up, the procedure does not appear to increase the risk of fusion due to instability.

In this study, a high-speed drill with a diameter of 5 mm was used for lamina fenestration to improve the speed of removal of the vertebral plate on the fenestration side. To avoid excessive removal of the lamina and reduce ligamentum flavum compression on the dural sac, a 2 mm diameter high-speed drill was used to adhere to the inner edge of the vertebral plate on the symptomatic side. In comparison with the over-the-top decompression technique (31), also referred to as lumbar endoscopic unilateral laminotomy for bilateral decompression, we can be more efficient grinding drills and operated with bimanualness. In addition, the over-the-top technique needs to be highlighted that performing a full-endoscopic decompression is a complex technique which requires advanced endoscopic skills and should only be considered for surgeons that are already familiar with this technique. The splitting technique allows for a satisfying central decompression, with minimal sparing the facet joints and the posterior neural arch, but it is far laterally to reach the foramina and which can be insufficient decompression of lateral recess (32, 33).

Most patients had successful surgical results without any nerve damage or post-operative cerebrospinal fluid leakage (34). We exposed the whole ligamentum flavum and separated the boundary between the dural sacs with a nerve stripping ion, which is same as the En bloc resection of the ligamentum flavum technique reported by Luis M reported (35). The ligamentum flavum was not removed until sufficient medial facetectomy was performed, as this approach shields the dura mater and nerve roots from duratomy or thermal injury.

It should be noted that the term "narrow spinal canal" was defined based on the distance from the spinous process root to the bilateral dorsal articular processes in the suprapedicle notch section CT image of the lumbar spinal stenosis segment, which is less than the working tubular diameter (1.6 cm) in our center. To avoid ambiguity, the lumbar degenerative lateral recess stenosis associated with a narrow spinal canal referred to in this article does not have broad clinical representation, and its indications are limited to spinous process hyperplasia, articular process aggregation, ligamentum flavum hypertrophy, and no acute disc herniation.

Conclusion

According to our retrospective observation of 25 patients, combined with the findings of previous literature, the contralateral approach with a microscope and tubular retractor system for ipsilateral decompression in patients with lumbar lateral recess stenosis and a narrow spinal canal can reduce damage to the articular processes, which may be beneficial for postoperative stability of the lumbar spine. However, there are several limitations to this study. First, this study is a retrospective study of case series involving a small number of cases and having a short follow-up period, which prevented the detection of complications such as the development of chronic vertebral column instability and recurred lateral stenosis. Second, although we demonstrated better lateral recess decompression in our cases, but absence of a comparable control group within the same study, this is another limitation of our study. Third, measurement of the reduction change may be inaccurate in reflecting the width of the bilateral articular facet and bilateral articular facet change in the suprapedicle notch section on CT scan with bias. A further follow-up evaluation with multicenter, large-scale randomized clinical trials would be necessary to prove the efficacy of contralateral approach in the long term.

Data availability statement

The raw data supporting the conclusions of this article will be made available by the authors, without undue reservation.

Ethics statement

The studies involving human participants were reviewed and approved by Ethics Committee of Wuxi Clinical College of Anhui Medical University. Written informed consent to participate in this

study was provided by the participants' legal guardian/next of kin. The studies were conducted in accordance with the local legislation and institutional requirements. The participants provided their written informed consent to participate in this study.

Author contributions

LS: Writing – original draft, Investigation. QM: Project administration, Writing – review & editing, Visualization. FD: Writing – original draft, Project administration, Data curation. WZ: Writing – review & editing, Resources, Project administration, Methodology. MS: Writing – review & editing. YW: Writing – review & editing, Visualization, Supervision, Conceptualization.

Funding

The author(s) declare that financial support was received for the research, authorship, and/or publication of this article. This project was funded by the Hospital Fund of the 904th Hospital of PLA Joint Logistic Support Force (Grant No. MS202116) and Wuxi Health Commission Fund (Grant No. Q202363). Medical Independent Research Project of Joint Logistics Support Force fund (grant no: XK2024103).

Conflict of interest

The authors declare that the research was conducted in the absence of any commercial or financial relationships that could be construed as a potential conflict of interest.

Publisher's note

All claims expressed in this article are solely those of the authors and do not necessarily represent those of their affiliated organizations, or those of the publisher, the editors and the reviewers. Any product that may be evaluated in this article, or claim that may be made by its manufacturer, is not guaranteed or endorsed by the publisher.

References

1. Den Boogert HF, Keers JC, Marinus Oterdoom DL, Kuijlen JMA. Bilateral versus unilateral interlaminar approach for bilateral decompression in patients with single-level degenerative lumbar spinal stenosis: a multicenter retrospective study of 175 patients on postoperative pain, functional disability, and patient satisfaction. *J Neurosurg Spine*. (2015) 23:326–35. doi: 10.3171/2014.12.SPINE13994

2. Genevay S, Atlas SJ. Lumbar spinal stenosis. *Best Pract Res Clin Rheumatol*. (2010) 24:253–65. doi: 10.1016/j.berh.2009.11.001

3. Siebert E, Prüss H, Klingebiel R, Failli V, Einhäupl KM, Schwab JM. Lumbar spinal stenosis: syndrome, diagnostics and treatment. *Nat Rev Neurol*. (2009) 5:392–403. doi: 10.1038/nrneurol.2009.90

4. Katz JN, Harris MB. Clinical practice: lumbar spinal stenosis. *N Engl J Med*. (2008) 358:818–25. doi: 10.1056/NEJMcp0708097

5. Amundsen T, Weber H, Lilleas F, Nordal HJ, Abdelnoor M, Magnaes B. Lumbar spinal stenosis: clinical and radiologic features. *Spine*. (1995) 20:1178–86. doi: 10.1097/00007632-199505150-00013

6. Olszewski AD, Yaszemski MJ, White AA. The anatomy of the human lumbar ligamentum flavum: new observations and their surgical importance. *Spine*. (1996) 21:2307–12. doi: 10.1097/00007632-199610150-00001

7. Ravindra VM, Senglaub SS, Rattani A, Dewan MC, Härtl R, Bisson E, et al. Degenerative lumbar spine disease: estimating global incidence and worldwide volume. *Global Spine J*. (2018) 8:784–94. doi: 10.1177/2192568218770769

8. Lee CH, Chung CK, Kim CH, Kwon JW. Health care burden of spinal diseases in the Republic of Korea: analysis of a Nationwide database from 2012 through 2016. *Neurospine*. (2018) 15:66–76. doi: 10.14245/ns.1836038.019

9. Young S, Veerapen R, O'Laoire SA. Relief of lumbar canal stenosis using multilevel subarticular fenestrations as an alternative to wide laminectomy: preliminary report. *Neurosurgery*. (1988) 23:628–33. doi: 10.1227/00006123-198811000-00014

10. Caputy AJ, Luessenhop AJ. Long-term evaluation of decompressive surgery for degenerative lumbar stenosis. *J Neurosurg*. (1992) 77:669–76. doi: 10.3171/jns.1992.77.5.0669

11. Rahman M, Summers LE, Richter B, Mimran RI, Jacob RP. Comparison of techniques for decompressive lumbar laminectomy: the minimallyinvasive versus the "classic" open approach. *Minim Invasive Neurosurg*. (2008) 51:100–5. doi: 10.1055/s-2007-1022542

12. Sairyo K, Sakai T, Higashino K, Inoue M, Yasui N, Dezawa A. Complications of endoscopic lumbar decompression surgery. *J. Neurol. Surg. A*. (2010) 53:175–8. doi: 10.1055/s-0030-1262814

13. Austevoll IM, Gjestad R, Brox JI, Solberg TK, Storheim K, Rekeland F, et al. The effectiveness of decompression alone compared with additional fusion for lumbar spinal stenosis with degenerative spondylolisthesis: a pragmatic comparative non-inferiority observational study from the Norwegian registry for spine surgery. *Eur Spine J*. (2017) 26:404–13. doi: 10.1007/s00586-016-4683-1

14. Foley KT. Microendoscopic discectomy. *Techniq. Neurosurg*. (1997) 3:301–7.

15. Weiner BK, Walker M, Brower RS, McCulloch JA. Microdecompression for lumbar spinal canal stenosis. *Spine*. (1999) 24:2268–72. doi: 10.1097/00007632-199911010-00016

16. McCollough JA. *Essentials of spinal microsurgery*. Philadelphia: Lippincott-Raven Publishers (1998).

17. Palmer S, Turner R, Palmer R. Bilateral decompression of lumbar spinal stenosis involving a unilateral approach with microscope and tubular retractor system. *J Neurosurg*. (2002) 97:213–7. doi: 10.3171/spi.2002.97.2.0213

18. Palmer S, Turner R, Palmer R. Bilateral decompressive surgery in lumbar spinal stenosis associated with spondylolisthesis: unilateral approach and use of a microscope and tubular retractor system. *Neurosurg Focus*. (2002) 13:E4. doi: 10.3171/foc.2002.13.1.5

19. Kulkarni AG, Patel R, Dutta S, Patil V. Stand-alone lateral recess decompression without discectomy in patients presenting with Claudicant radicular pain and MRI evidence of lumbar disc herniation: a prospective study. *Spine*. (2017) 42:984–91. doi: 10.1097/BRS.0000000000001944

20. Gulsever CI, Sahin D, Ozturk S, Ahmadov T, Sabanci PA. Full-endoscopic interlaminar approach for decompression of lateral recess stenosis. *J Vis Exp*. (2023) 192:e64600. doi: 10.3791/64600

21. Ikuta K, Arima J, Tanaka T, Oga M, Nakano S, Sasaki K, et al. Short-term results of microendoscopic posterior decompression for lumbar spinal stenosis. *J Neurosurg Spine*. (2005) 2:624–33. doi: 10.3171/spi.2005.2.5.0624

22. Alimi M, Hofstetter CP, Torres-Campa JM, Navarro-Ramirez R, Cong G-T, Njoku I Jr, et al. Unilateral tubular approach for bilateral laminotomy: effect on ipsilateral and contralateral buttock and leg pain. *Eur Spine J*. (2017) 26:389–96. doi: 10.1007/s00586-016-4594-1

23. Kim HS, Paudel B, Jang JS, Oh SH, Lee S, Park JE, et al. Percutaneous full endoscopic bilateral lumbar decompression of spinal stenosis through uniportal-contralateral approach: techniques and preliminary results. *World Neurosurg*. (2017) 103:201–9. doi: 10.1016/j.wneu.2017.03.130

24. Bresnahan L, Ogden AT, Natarajan RN, Fessler RG. A biomechanical evaluation of graded posterior element removal for treatment of lumbar stenosis: comparison of a minimally invasive approach with two standard laminectomy techniques. *Spine Affil Soc Meet Abstr*. (2009) 34:17–23. doi: 10.1097/BRS.0b013e318191438b

25. Thomé C, Zevgaridis D, Leheta O, Bäzner H, Pöckler-Schöniger C, Wöhrle J, et al. Outcomeafter less-invasive decompression of lumbar spinal stenosis: a randomized comparison of nilateral laminotomy, bilateral laminotomy, and laminectomy. *J Neurosurg Spine*. (2005) 3:129–41. doi: 10.3171/spi.2005.3.2.0129

26. Hasegawa K, Kitahara K, Shimoda H, Hara T. Biomechanical evaluation of destabilization following minimally invasive decompression for lumbar spinal canal stenosis. *J Neurosurg Spine*. (2013) 18:504–10. doi: 10.3171/2013.1.SPINE12599

27. Shin MH, Kim JS, Ryu KS, Hur JW. Bilateral decompression via microscopic tubular crossing laminotomy (MTCL) for lumbar spinal stenosis: technique and early surgical result. *Neurol Med Chir*. (2015) 55:570–7. doi: 10.2176/nmc.oa.2014-0251

28. Matsumura A, Namikawa T, Terai H, Tsujio T, Suzuki A, Dozono S, et al. The influence of approach side on facet preservation in microscopic bilateral decompression

via a unilateral approach for degenerative lumbar scoliosis. *J Neurosurg*. (2010) 13:758–65. doi: 10.3171/2010.5.SPINE091001

29. Hamasaki T, Tanaka N, Kim J, Okada M, Ochi M, Hutton WC. Biomechanical assessment of minimally invasive decompression for lumbar spinal canal stenosis: a cadaver study. *J Spinal Disord Tech*. (2009) 22:486–91. doi: 10.1097/BSD.0b013e31818d7dc9

30. Ahuja S, Moideen AN, Dudhniwala AG, Karatsis E, Papadakis L, Varitis E. Lumbar stability following graded unilateral and bilateral facetectomy: a finite element model study. *Clin Biomech*. (2020) 75:105011. doi: 10.1016/j.clinbiomech.2020.105011

31. Siepe CJ, Bridts A-L, Ayman M, Sauer D, Mehren C. Full-endoscopic bilateral over-the-top decompression in lumbar central stenosis: surgical technique and outcomes. *Eur Spine J*. (2023) 32:2918–23. doi: 10.1007/s00586-023-07750-0

32. Kanbara S, Yukawa Y, Ito K, Machino M, Kato F. Surgical outcomes of modified lumbar spinous process-splitting laminectomy for lumbar spinal stenosis. *J Neurosurg Spine*. (2015) 22:353–7. doi: 10.3171/2014.9.SPINE1457

33. Tomasi SO, Umana GE, Scalia G, Raudino G, Stevanovic V, Krainz H, et al. Lumbar spinous process-splitting technique for ligamentum flavum cyst removal. *J Neurol Surg A Cent Eur Neurosurg*. (2024) 85:195–201. doi: 10.1055/a-1715-3958

34. Orpen NM, Corner JA, Shetty RR, Marshall R. Micro-decompression for lumbar spinal stenosis: the early outcome using a modified surgical technique. *J Bone Joint Surg Br*. (2010) 92:550–4. doi: 10.1302/0301-620X.92B4.22050

35. Tumialán LM. En bloc resection of ligamentum flavum with laminotomy of the caudal lamina in the minimally invasive laminectomy: surgical anatomy and technique. *Neurosurg Focus*. (2023) 54:E8. doi: 10.3171/2022.10.FOCUS22601

frontiers | Frontiers in Neurology

TYPE Review
PUBLISHED 22 April 2024
DOI 10.3389/fneur.2024.1358414

OPEN ACCESS

EDITED BY
Qingchun Mu,
Second Affiliated Hospital of Soochow University, China

REVIEWED BY
Xiaofeng Chen,
Harbin Medical University, China
Rujun Li,
Suzhou University, China
Madiha Zahra Syeda,
Zhejiang University, China

*CORRESPONDENCE
Qiang Xiao
✉ kyxq168@126.com

†These authors have contributed equally to this work and share first authorship

RECEIVED 25 December 2023
ACCEPTED 02 April 2024
PUBLISHED 22 April 2024

CITATION
Ai G, Xiong M, Deng L, Zeng J and Xiao Q (2024) Research progress on the inhibition of oxidative stress by teriparatide in spinal cord injury.
Front. Neurol. 15:1358414.
doi: 10.3389/fneur.2024.1358414

Research progress on the inhibition of oxidative stress by teriparatide in spinal cord injury

Gangtong Ai[1,2†], Moliang Xiong[2†], Liang Deng[2], Jihuan Zeng[2] and Qiang Xiao[2*]

[1]Department of Jiangxi Medical College, Nanchang University, Nanchang, Jiangxi, China, [2]Department of Orthopaedics, Jiangxi Provincial People's Hospital, The First Affiliated Hospital of Nanchang Medical College, Nanchang, Jiangxi, China

Spinal cord injury (SCI) is currently a highly disabling disease, which poses serious harm to patients and their families. Due to the fact that primary SCI is caused by direct external force, current research on SCI mainly focuses on the treatment and prevention of secondary SCI. Oxidative stress is one of the important pathogenic mechanisms of SCI, and intervention of oxidative stress may be a potential treatment option for SCI. Teriparatide is a drug that regulates bone metabolism, and recent studies have found that it has the ability to counteract oxidative stress and is closely related to SCI. This article summarizes the main pathological mechanisms of oxidative stress in SCI, as well as the relationship between them with teriparatide, and explores the therapeutic potential of teriparatide in SCI.

KEYWORDS

spinal cord injury, oxidative stress, Nrf2, teriparatide, PTH

Introduction

Spinal cord injury (SCI) refers to the varying degrees of damage to the spinal cord caused by various etiologies. It can be classified into primary injury and secondary injury. Primary injury refers to the initial acute trauma that causes damage to the neural fibers. Secondary injury, on the other hand, occurs as a result of a series of cascading reactions, such as oxidative stress, inflammatory response, neurotoxicity caused by Ca^{2+} and glutamate, which further deepen the extent of damage and expand the affected area (1). Among these reactions, oxidative stress is one of the important factors in the pathogenesis of secondary SCI (2). Currently, SCI is a challenging health problem worldwide. It has been reported that there are approximately 17,500 new cases of SCI in the United States annually, with the majority of patients experiencing severe clinical symptoms and complications, imposing significant physical, mental, and economic burdens on both the patients and their families (3). Due to the incomplete understanding of its pathogenesis, the treatment options for SCI are limited. Currently, early methylprednisolone combined with surgical intervention is the main approach (4). As the primary injury caused by direct trauma is unavoidable, there is an urgent clinical need for an effective treatment specifically targeting secondary injury.

Teriparatide is a synthetically produced analog of the parathyroid hormone (PTH), also known as recombinant human PTH 1-34. It consists of the first 34 amino acid residues of the PTH molecule. Teriparatide is the first bone metabolism drug authorized by the U.S. Food and Drug Administration for the treatment of osteoporosis (5, 6). It not only has the function of regulating bone metabolism, but also can play a role in regulating oxidative stress (7). Study have

shown that therapeutic doses of teriparatide can significantly reduce the production of reactive oxygen species (ROS) within the osteocytes of patients with osteoporosis, effectively inhibiting oxidative stress responses (7). Currently, this effect is also being investigated in the field of neuroscience (8), and it has promising experimental results. However, the evidence linking PTH and SCI mainly comes from scattered case reports (9–11), and the exact role of PTH in the SCI process remains unclear. This article aims to review the oxidative stress-related mechanisms following SCI and the connection with PTH, as well as to explore the potential therapeutic role of teriparatide in SCI (Figure 1).

The relationship between SCI with oxidative stress

Oxidative stress refers to the imbalance between oxidation and antioxidant systems in the body, leading to the overproduction of ROS, reactive nitrogen species, and other excessive free radicals that exert toxic effects (12). Free radicals derived from O_2 include O^{2-}, OH^-, and others, collectively referred to as ROS (13). Free radicals are normal byproducts of mitochondrial oxidative metabolism in the human body. During mitochondrial oxidative respiration, molecules with unpaired electrons, namely free radicals, are formed. The unpaired electrons make free radicals unstable and prone to react with other molecules, such as proteins, lipids, and DNA (14, 15).

Oxidative stress is one of the important aspects of the secondary pathological process of SCI (16). Excessive free radicals are produced due to ischemia and hypoxia during SCI, and the body's own antioxidants are depleted within days or even hours after SCI (17). The generated antioxidants are insufficient to counteract the oxidative stress caused by SCI, and the excess oxidants cause irreversible damage to nerve cells (12, 15). This leads to nerve cell death and tissue damage (18). Increasing evidence suggests that reducing the production of ROS after SCI can effectively protect nerve cells from the effects of oxidative stress, mitigate the pathological process of spinal cord damage, promote neuronal repair and axonal regeneration (19, 20).

The intracellular homeostasis is disrupted after SCI, characterized by increased excitotoxicity of glutamate, elevated levels of free iron, and increased membrane permeability of Ca^{2+} (21). The elevated intracellular Ca^{2+} levels activate the nicotinamide adenine dinucleotide, which promotes ATP production while also increasing the production of ROS (22, 23). Excessive ROS can increase the permeability of Ca^{2+} membranes, leading to an increased influx of Ca^{2+}, which causes a decrease in membrane potential. This activates the mitochondrial autophagy signaling pathway, inducing mitochondrial autophagy and further releasing excessive ROS, forming a vicious cycle (24). Recent study by Han et al. (25) have demonstrated that enhancing mitochondrial transport after SCI helps remove damaged mitochondria and replenish injured axons with normal mitochondria, thereby restoring local mitochondrial integrity and enhancing local ATP supply to meet the energy metabolic demands of axonal regeneration. This activates the intrinsic "growth program" in the central nervous system, promoting axonal regeneration and functional recovery after injury. Additionally, Ca^{2+} overload can enhance the activity of protein kinases and phospholipases, inducing protein degradation and lipid oxidation damage (26).

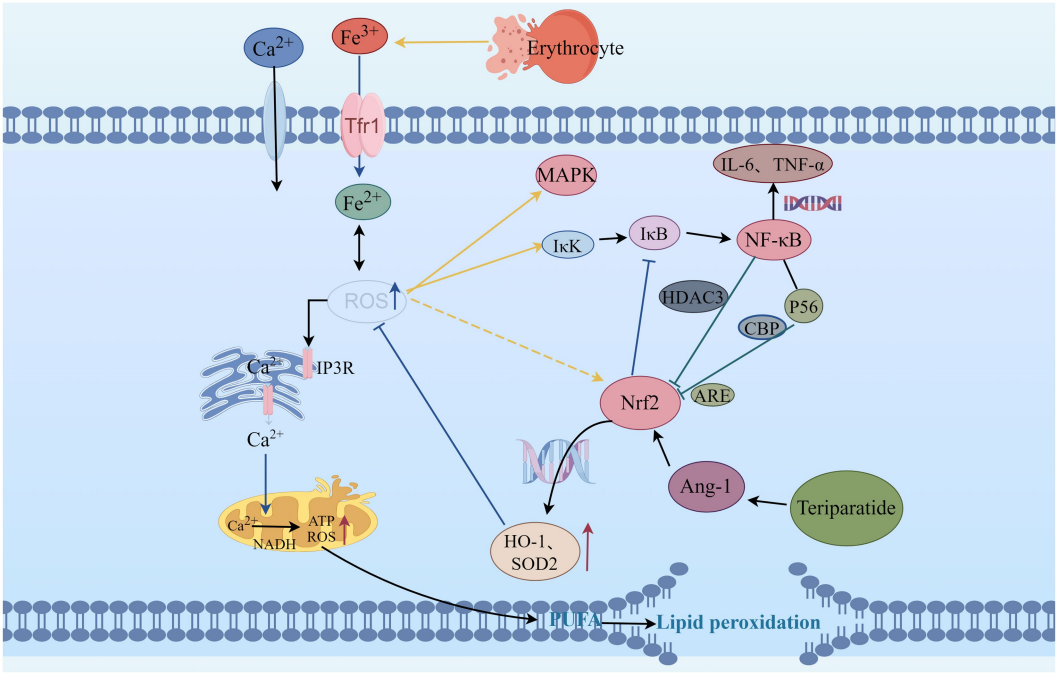

FIGURE 1
The relationship between Teriparatide and ROS. ROS, Reactive oxygen species; IP3R, inositol 1,4,5-trisphosphate receptors; MAPK, mitogen-activated protein kinase; Nrf2, Nuclear factor erythroid 2-related factor 2; HO-1, Heme Oxygenase-1; SOD2, Superoxide Dismutase 2; Trf1, Transferrin 1; NADH, Nicotinamide adenine dinucleotide; ATP, Adenosine Triphosphate; ARE, Antioxidant response elements; NF-κB, Nuclear factor kappa-B; IκB, inhibitor of NF-κB; IκK, activate IκB kinase; HDAC3, histone deacetylase 3; CBP, Cyclic-AMP response element-binding protein; P56, subunit of NF-κB; IL-6, Interleukin-6; TNF-α, Tumor necrosis factor-α; Ang-1, Angiopoietin-1; PUFA, Polyunsaturated fatty acids.

Due to the high content of polyunsaturated fatty acids in the spinal cord, oxygen free radicals can promote the generation of peroxidation intermediates such as 4-hydroxynonenal and malondialdehyde during SCI, leading to lipid oxidation degradation and disruption of the lipid bilayer structure of cell membranes (27, 28). The oxidative phospholipid markers in the core region of spinal cord lesions are significantly increased, it exacerbates the pathological process of SCI (29). The ROS scavengers can reduce lipid peroxidation induced by SCI, mitigate tissue damage, and improve neurological function (30). Moreover, the internal environment after SCI is in an acidic state, mechanical forces cause blood vessel rupture and bleeding, erythrocyte rupture, consequently free iron is increased (31). Neurons take up iron through transferrin and transferrin receptor-mediated iron uptake, leading to intracellular iron overload (32). Ferrous ions can participate in the aforementioned lipid peroxidation through Fenton reaction, generating a large amount of ROS, thereby causing secondary lipid peroxidation and further exacerbating oxidative stress (33). ROS can also react with C-H, S-H, N-H, or O-H in proteins, mediating the cleavage of peptide chains and modification of amino acid side chains, leading to protein misfolding, altered protein function, and increased susceptibility to hydrolysis and degradation (34). Experimental study (35) have shown that after SCI, proteins in the spinal cord are easily oxidized by oxidants to form advanced oxidation protein products. It can induce the expression of ROS through nicotinamide adenine dinucleotide phosphate oxidase, and excessive ROS can activate mitogen-activated protein kinase (MAPK) and nuclear factor kappa-B (NF-κB), inducing neuronal apoptosis.

Nuclear factor E2-related factor 2 (Nrf2)/Antioxidant Response Element (ARE) is an endogenous antioxidant defense mechanism of the body. It not only regulates oxidative stress but also participates in the regulation of inflammatory signaling pathways such as NF-κB and MAPK (36). Under normal physiological conditions, Nrf2 can form a dimer with Kelch-like ECH-associated protein 1 (Keap1) in the cytoplasm, resulting in the inhibition of Nrf2 activity (37). The Nrf2/ARE signaling pathway plays an important neuroprotective role in the early stage of SCI (38). After being activated by ROS, the Nrf2-Keap1 dimer dissociates, leading to Nrf2 phosphorylation and translocation into the cell nucleus, inducing the expression of a series of antioxidant enzyme genes such as heme oxygenase-1 (HO-1), NAD(P) H quinone oxidoreductase 1 (NQO1), and superoxide dismutase (SOD), directly or indirectly clearing free radicals, thus reducing or eliminating ROS, reducing cell oxidative stress (39). When the Keap1 gene is knocked out (40), Nrf2 is persistently activated in SCI astrocytes, which can increase the expression of NQO1, inhibit oxidative stress responses, reduce the damage to myelin and myelin-associated proteins, effectively protect neurons, and improve neurological functions. Study have shown (41) that upregulating Nrf2 expression and promoting HO-1 generation with polysaccharides effectively inhibits ROS production, suppresses oxidative stress response after SCI, and reduces neuronal apoptosis. This phenomenon can be reversed when siRNA silences Nrf2 expression.

Under physiological conditions, Nrf2 and nuclear factor kappa-B (NF-κB) signaling pathways are mutually coordinated to maintain cellular homeostasis (42). Under pathological conditions, oxidative stress can mediate the occurrence of inflammatory reactions, and excessive ROS can activate IκB kinase (IκK), inducing phosphorylation of its inhibitor IκB and leading to proteasomal degradation of IκB protein. This results in nuclear translocation of NF-κB and activation of downstream genes such as IL-6 and TNF-α (43). Nrf2 can inhibit the degradation of IκB-α, thereby blocking NF-κB nuclear translocation and the transcription of pro-inflammatory genes (42). Conversely, NF-κB can enhance the recruitment of histone deacetylase 3 to the antioxidant response element region, leading to inhibition of Nrf2 activity and hindrance of ARE gene transcription, thereby suppressing antioxidant responses (44). P65 is a subunit of NF-κB, and ARE is the gene binding site of Nrf2. p65 has the ability to inhibit the expression of ARE genes (45), and on the other hand, the p65 subunit can also bind with the CREB binding protein (CBP), a transcriptional co-activator of Nrf2, to jointly compete for the CH1-KIX domain of CBP, thereby inhibiting the Nrf2 signaling pathway (46). Research has found (47) that during SCI, experimental drug intervention can upregulate the expression of Nrf2 and inhibit the release of NF-κB-related mediators. When Nrf2 is suppressed, the expression of NF-κB-related factors increases, revealing that Nrf2 can be involved in regulating the NF-κB signaling pathway after SCI, thereby reducing neuronal death. Li et al. (48) found that inhibiting the expression of HO-1 can increase in NF-κB-related factors. Based on these findings, it is possible that Nrf2 and NF-κB may interact and influence each other in the oxidative stress response following SCI.

The correlation between PTH and SCI

Vaziri et al. (49) first reported the association between PTH and SCI. By examining various laboratory parameters in the serum of 40 SCI patients, they found a decrease in PTH levels after SCI, and significantly lower PTH levels in the SCI group compared to the control group, suggesting a potential correlation between PTH and SCI. Subsequently, Mechanick et al. (9) divided SCI patients into complete paralysis and incomplete paralysis groups according to the ASIA classification. They found a more pronounced decrease in PTH levels in the complete paralysis group, leading the authors to speculate that the severity of neural damage is related to the reduction of PTH. In recent years, Ouyang et al. (50) conducted further clinical research on the relationship between PTH and SCI, revealing a decrease in peripheral blood PTH levels in SCI patients and a significant correlation with the severity of SCI.

Similar phenomena have also been observed in animal models. Rouleau et al. (10) found that the levels of PTH in the serum of mice with SCI remained low throughout the entire animal experiment, with the most significant decrease occurring within 1 week after injury. This suggests that PTH synthesis and metabolism are related to the immune system after SCI. Del et al. (11) also found that PTH gradually decreased over time in mice with SCI, further demonstrating that PTH is one of the pathological and physiological factors affecting SCI. Subsequent studies (51, 52) have focused more on studying the effects of PTH on bone structure and bone density after SCI, as well as research related to osteoporosis and fracture healing involving PTH replacement therapies such as teriparatide (Table 1). However, they have not further explored whether it can promote the repair of neurological function after SCI. Recent study (8) have found that teriparatide can activate the Nrf2 pathway by inducing the production of angiogenin 1, which in turn increases the expression of its downstream antioxidant proteins HO-1 and SOD2, inhibit oxidative stress and improve nerve function. However, the exact mechanism of

TABLE 1 Correlation between PTH and spinal cord injury.

Study	Time	Research object	Results
Vaziri et al. (49)	1994	Human	SCI: decrease in PTH
Mechanick et al. (9)	1997	Human	PTH related to ASIA
Ouyang et al. (50)	2021	Human	PTH related to the degree of SCI
Rouleau et al. (10)	2007	Mouse	SCI: PTH decreased significantly within 1 week, and related to the immune system
Del et al. (11)	2016	Mouse	SCI: decrease in PTH
Sahbani et al. and Le et al. (51, 52)	2019 and 2021	Human	Decrease in PTH, teriparatide treat osteoporosis after SCI.

SCI, Spinal cord injury; PTH, Parathyroid hormone; ASIA, American Spinal Injury Association Impairment Scale, International Standards for Neurological Classification of Spinal Cord Injury.

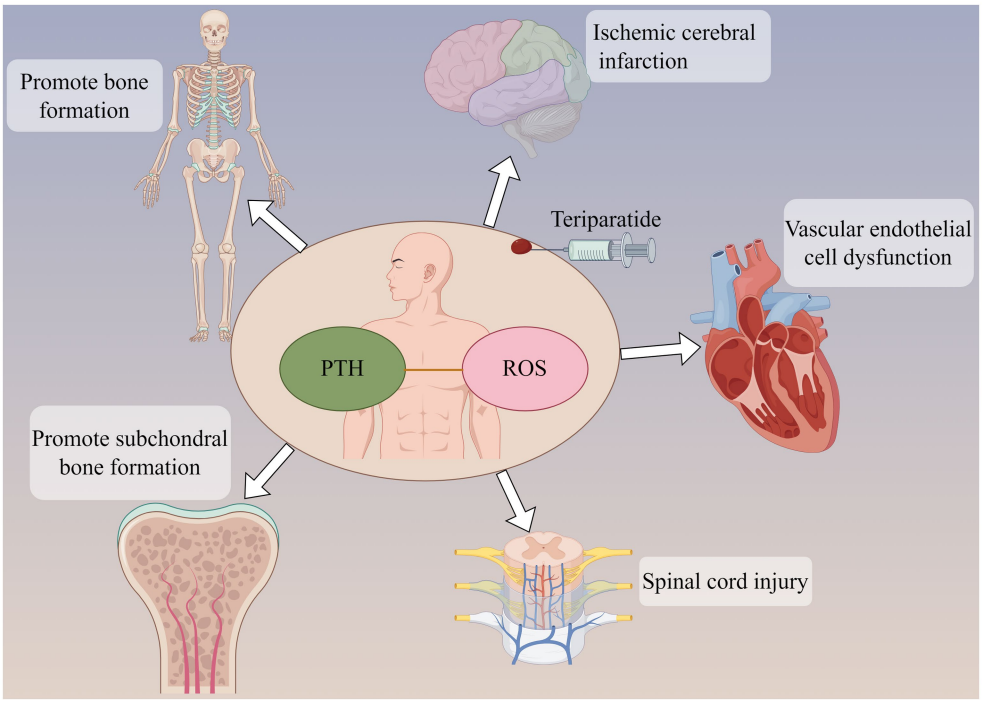

FIGURE 2
Parathyroid hormone (PTH) can not only promote bone formation and subchondral bone formation, but also act on ischemic cerebral infarction and reduce brain tissue injury. PTH may be involved in the pathological development of cardiovascular disease and spinal cord injury. The participation of PTH may be related to oxidative stress response in the above effects.

action has not been further studied by the authors. Therefore, in the early stages of SCI, teriparatide may exert its pharmacological effects by targeting neuronal cells.

The role of teriparatide in oxidative stress

The effects of PTH vary in different tissues. In endothelial cells, PTH acts on surface receptors to generate IP3, leading to an increase in intracellular Ca^{2+} concentration. Excessive calcium uptake by mitochondria subsequently increases the production of ROS, thereby inducing oxidative stress responses, which result in endothelial cell dysfunction (53). Research has discovered that PTH can activate DNA repair proteins (nuclear antigens) and FOXO transcription factor 3a, downregulate DNA damage protein 153, thereby enabling cells to avoid DNA damage caused by oxidative stress (54). Additionally, in osteoporosis induced by dexamethasone, dexamethasone can lead to an increase in ROS within bone cells. Concurrent use of teriparatide intervention while stimulating bone cells with dexamethasone can reduce the production of intracellular ROS, mitigate the harmful effects of dexamethasone on bone cells, promote the proliferation of bone cells, and prevent the occurrence of osteoporosis (7). Ardura (55) found that PTH analogs can increase the phosphorylation of Extracellular regulated protein kinases and Protein kinase B, regulate MAPK phosphatase-1 to activate MAPK dephosphorylation, enhance expression of peroxidase genes, reduce ROS production, suppress oxidative stress response, and decrease cell apoptosis (Figure 2).

Parathyroid hormone-related peptide (PTHrP) is a highly bioactive small molecule peptide that, in some respects, possesses superior functions to PTH (1–34). Its structure and mechanism of action are not entirely identical to those of PTH (1–34) (56). Study

TABLE 2 Relationship between PTH and oxidative stress in disease.

Disease	Effect	Main result	References
Cardiovascular disease	Negative	PTH: increases in ROS	(53)
Osteoporosis disease	Positive	Teriparatide: decrease in ROS	(7, 54)
	Positive	PTHrP: decrease in ROS	(55, 58)
Osteoarthritis	Positive	PTHrp: decrease in ROS	(57)
Ischemic cerebral infarction	Positive	Teriparatide: decrease in ROS	(8)

PTH, parathyroid hormone; ROS, Reactive oxygen species; PTHrP, PTH derivative; Teriparatide, new recombinant human parathyroid hormone.

(57) have shown that PTHrp can reduce ROS production in mesenchymal stem cells and stimulate cartilage formation. Wang et al. (58) discovered that PTHrP can attenuate the differentiation of osteoclast-like cells. Even under an oxidative stress environment, PTHrP is capable of protecting mesenchymal stem cells and human umbilical vein endothelial cells by reducing the production of ROS and mitochondrial damage, thereby promoting proliferation, migration, and angiogenesis. Therefore, PTH and its analogs play a role in regulating oxidative stress (Table 2).

Summary and perspective

In summary, SCI is associated with oxidative stress mediated by the Nrf2 and NF-κB cascades. As an Nrf2 activator, teriparatide may be used to treat SCI by targeting this pathway. However, current research on teriparatide in SCI mainly focuses on bone metabolism, and there are no reports on its effects on neurological function. Therefore, further validation is needed to determine whether teriparatide affects the pathological mechanisms of SCI through the Nrf2 signaling pathway.

Author contributions

GA: Conceptualization, Data curation, Formal analysis, Investigation, Methodology, Software, Writing – original draft. MX: Conceptualization, Methodology, Software, Supervision, Writing – review & editing. LD: Methodology, Software, Supervision, Validation, Writing – review & editing. JZ: Investigation, Resources, Supervision, Visualization, Writing – review & editing. QX: Conceptualization, Project administration, Resources, Validation, Writing – review & editing.

Funding

The author(s) declare that financial support was received for the research, authorship, and/or publication of this article. This work was funded by the Jiangxi Provincial Health Commission Science and Technology Program (no. SKJP202210016).

Conflict of interest

The authors declare that the research was conducted in the absence of any commercial or financial relationships that could be construed as a potential conflict of interest.

Publisher's note

References

1. McDonald JW, Sadowsky C. Spinal-cord injury. *Lancet*. (2002) 359:417–25. doi: 10.1016/S0140-6736(02)07603-1

2. Li Z, Zhao T, Ding J, Gu H, Wang Q, Wang Y, et al. A reactive oxygen species-responsive hydrogel encapsulated with bone marrow derived stem cells promotes repair and regeneration of spinal cord injury. *Bioact Mater*. (2023) 19:550–68. doi: 10.1016/j.bioactmat.2022.04.029

3. Schwab JM, Maas A, Hsieh J, Curt A. Raising awareness for spinal cord injury research. *Lancet Neurol*. (2018) 17:581–2. doi: 10.1016/S1474-4422(18)30206-0

4. Lambrechts MJ, Issa TZ, Hilibrand AS. Updates in the early Management of Acute Spinal Cord Injury. *J Am Acad Orthop Surg*. (2023) 31:e619–32. doi: 10.5435/JAAOS-D-23-00281

5. Leder BZ, Tsai JN, Uihlein AV, Wallace PM, Lee H, Neer RM, et al. Denosumab and teriparatide transitions in postmenopausal osteoporosis (the DATA-switch study): extension of a randomised controlled trial. *Lancet*. (2015) 386:1147–55. doi: 10.1016/S0140-6736(15)61120-5

6. Bashutski JD, Eber RM, Kinney JS, Benavides E, Maitra S, Braun TM, et al. Teriparatide and osseous regeneration in the oral cavity. *N Engl J Med*. (2010) 363:2396–405. doi: 10.1056/NEJMoa1005361

7. Wang T, Han C, Tian P, Li PF, Ma XL. Role of Teriparatide in glucocorticoid-induced osteoporosis through regulating cellular reactive oxygen species. *Orthop Surg*. (2018) 10:152–9. doi: 10.1111/os.12369

8. Xiong M, Feng Y, Huang S, Lv S, Deng Y, Li M, et al. Teriparatide induces angiogenesis in ischemic cerebral infarction zones of rats through AC/PKA signaling and reduces ischemia-reperfusion injury. *Biomed Pharmacother*. (2022) 148:112728. doi: 10.1016/j.biopha.2022.112728

9. Mechanick JI, Pomerantz F, Flanagan S, Stein A, Gordon WA, Ragnarsson KT. Parathyroid hormone suppression in spinal cord injury patients is associated with the degree of neurologic impairment and not the level of injury. *Arch Phys Med Rehabil*. (1997) 78:692–6. doi: 10.1016/S0003-9993(97)90075-7

10. Rouleau P, Ung RV, Lapointe NP, Guertin PA. Hormonal and immunological changes in mice after spinal cord injury. *J Neurotrauma*. (2007) 24:367–78. doi: 10.1089/neu.2006.0117

11. Del RT, Bethea JR. The effects of spinal cord injury on bone loss and dysregulation of the calcium/parathyroid hormone loop in mice. *Osteoporos Sarcopenia*. (2016) 2:164–9. doi: 10.1016/j.afos.2016.06.003

12. Forman HJ, Zhang H. Targeting oxidative stress in disease: promise and limitations of antioxidant therapy. *Nat Rev Drug Discov*. (2021) 20:689–709. doi: 10.1038/s41573-021-00233-1

13. Sies H. Oxidative eustress: on constant alert for redox homeostasis. *Redox Biol*. (2021) 41:101867. doi: 10.1016/j.redox.2021.101867

14. Foo J, Bellot G, Pervaiz S, Alonso S. Mitochondria-mediated oxidative stress during viral infection. *Trends Microbiol*. (2022) 30:679–92. doi: 10.1016/j.tim.2021.12.011

15. Nolfi-Donegan D, Braganza A, Shiva S. Mitochondrial electron transport chain: oxidative phosphorylation, oxidant production, and methods of measurement. *Redox Biol*. (2020) 37:101674. doi: 10.1016/j.redox.2020.101674

16. Visavadiya NP, Patel SP, VanRooyen JL, Sullivan PG, Rabchevsky AG. Cellular and subcellular oxidative stress parameters following severe spinal cord injury. *Redox Biol*. (2016) 8:59–67. doi: 10.1016/j.redox.2015.12.011

17. Zhou K, Zheng Z, Li Y, Han W, Zhang J, Mao Y, et al. TFE3, a potential therapeutic target for spinal cord injury via augmenting autophagy flux and alleviating ER stress. *Theranostics*. (2020) 10:9280–302. doi: 10.7150/thno.46566

18. Nukolova NV, Aleksashkin AD, Morozova AY, Gubskiy IL, Kirzhanova EA, Abakumov MA, et al. Multilayer polyion complex nanoformulations of superoxide dismutase 1 for acute spinal cord injury. *J Control Release*. (2018) 270:226–36. doi: 10.1016/j.jconrel.2017.11.044

19. Ji ZS, Gao GB, Ma YM, Luo JX, Zhang GW, Yang H, et al. Highly bioactive iridium metal-complex alleviates spinal cord injury via ROS scavenging and inflammation reduction. *Biomaterials*. (2022) 284:121481. doi: 10.1016/j.biomaterials.2022.121481

20. Andrabi SS, Yang J, Gao Y, Kuang Y, Labhasetwar V. Nanoparticles with antioxidant enzymes protect injured spinal cord from neuronal cell apoptosis by attenuating mitochondrial dysfunction. *J Control Release*. (2020) 317:300–11. doi: 10.1016/j.jconrel.2019.12.001

21. Liu X, Jiang X, Yu Q, Shen W, Tian H, Mei X, et al. Sodium alginate and naloxone loaded macrophage-derived nanovesicles for the treatment of spinal cord injury. *Asian J Pharm Sci*. (2022) 17:87–101. doi: 10.1016/j.ajps.2021.11.001

22. Huang Y, Wang J, Yue C, Wang R, Guo Q, Wang T, et al. An in situ assembled trapping gel repairs spinal cord injury by capturing glutamate and free calcium ions. *Small*. (2023) 19:e2206229. doi: 10.1002/smll.202206229

23. Neves D, Salazar IL, Almeida RD, Silva RM. Molecular mechanisms of ischemia and glutamate excitotoxicity. *Life Sci*. (2023) 328:121814. doi: 10.1016/j.lfs.2023.121814

24. Slater PG, Dominguez-Romero ME, Villarreal M, Eisner V, Larrain J. Mitochondrial function in spinal cord injury and regeneration. *Cell Mol Life Sci*. (2022) 79:239. doi: 10.1007/s00018-022-04261-x

25. Han Q, Xie Y, Ordaz JD, Huh AJ, Huang N, Wu W, et al. Restoring cellular energetics promotes axonal regeneration and functional recovery after spinal cord injury. *Cell Metab*. (2020) 31:623–641.e8. doi: 10.1016/j.cmet.2020.02.002

26. Xu X, Wang X, Yang Y, Ares I, Martinez M, Lopez-Torres B, et al. Neonicotinoids: mechanisms of systemic toxicity based on oxidative stress-mitochondrial damage. *Arch Toxicol*. (2022) 96:1493–520. doi: 10.1007/s00204-022-03267-5

27. Dong Y, Yong VW. Oxidized phospholipids as novel mediators of neurodegeneration. *Trends Neurosci*. (2022) 45:419–29. doi: 10.1016/j.tins.2022.03.002

28. Hill RL, Singh IN, Wang JA, Kulbe JR, Hall ED. Protective effects of phenelzine administration on synaptic and non-synaptic cortical mitochondrial function and lipid peroxidation-mediated oxidative damage following TBI in young adult male rats. *Exp Neurol*. (2020) 330:113322. doi: 10.1016/j.expneurol.2020.113322

29. Zrzavy T, Schwaiger C, Wimmer I, Berger T, Bauer J, Butovsky O, et al. Acute and non-resolving inflammation associate with oxidative injury after human spinal cord injury. *Brain*. (2021) 144:144–61. doi: 10.1093/brain/awaa360

30. Gao L, Zhang Z, Xu W, Li T, Ying G, Qin B, et al. Natrium benzoate alleviates neuronal apoptosis via the DJ-1-related anti-oxidative stress pathway involving Akt phosphorylation in a rat model of traumatic spinal cord injury. *Front Mol Neurosci*. (2019) 12:42. doi: 10.3389/fnmol.2019.00042

31. Chio J, Xu KJ, Popovich P, David S, Fehlings MG. Neuroimmunological therapies for treating spinal cord injury: evidence and future perspectives. *Exp Neurol*. (2021) 341:113704. doi: 10.1016/j.expneurol.2021.113704

32. Hu X, Xu Y, Xu H, Jin C, Zhang H, Su H, et al. Progress in understanding Ferroptosis and its targeting for therapeutic benefits in traumatic brain and spinal cord injuries. *Front Cell Dev Biol*. (2021) 9:705786. doi: 10.3389/fcell.2021.705786

33. Anjum A, Yazid MD, Fauzi DM, Idris J, Ng A, Selvi NA, et al. Spinal cord injury: pathophysiology, multimolecular interactions, and underlying recovery mechanisms. *Int J Mol Sci*. (2020) 21:533. doi: 10.3390/ijms21207533

34. Yu M, Wang Z, Wang D, Aierxi M, Ma Z, Wang Y. Oxidative stress following spinal cord injury: from molecular mechanisms to therapeutic targets. *J Neurosci Res*. (2023) 101:1538–54. doi: 10.1002/jnr.25221

35. Liu Z, Yao X, Jiang W, Li W, Zhu S, Liao C, et al. Advanced oxidation protein products induce microglia-mediated neuroinflammation via MAPKs-NF-kappaB signaling pathway and pyroptosis after secondary spinal cord injury. *J Neuroinflammation*. (2020) 17:90. doi: 10.1186/s12974-020-01751-2

36. Guo X, Kang J, Wang Z, Wang Y, Liu M, Zhu D, et al. Nrf2 signaling in the oxidative stress response after spinal cord injury. *Neuroscience*. (2022) 498:311–24. doi: 10.1016/j.neuroscience.2022.06.007

37. Cano M, Datta S, Wang L, Liu T, Flores-Bellver M, Sachdeva M, et al. Nrf2 deficiency decreases NADPH from impaired IDH shuttle and pentose phosphate pathway in retinal pigmented epithelial cells to magnify oxidative stress-induced mitochondrial dysfunction. *Aging Cell*. (2021) 20:e13444. doi: 10.1111/acel.13444

38. Ebrahimy N, Gasterich N, Behrens V, Amini J, Fragoulis A, Beyer C, et al. Neuroprotective effect of the Nrf2/ARE/miRNA145-5p signaling pathway in the early phase of spinal cord injury. *Life Sci*. (2022) 304:120726. doi: 10.1016/j.lfs.2022.120726

39. Jiang T, He Y. Recent advances in the role of nuclear factor Erythroid-2-related factor 2 in spinal cord injury: regulatory mechanisms and therapeutic options. *Front Aging Neurosci*. (2022) 14:851257. doi: 10.3389/fnagi.2022.851257

40. Zhao W, Gasterich N, Clarner T, Voelz C, Behrens V, Beyer C, et al. Astrocytic Nrf2 expression protects spinal cord from oxidative stress following spinal cord injury in a male mouse model. *J Neuroinflammation*. (2022) 19:134. doi: 10.1186/s12974-022-02491-1

41. Lv R, Du L, Zhang L, Zhang Z. Polydatin attenuates spinal cord injury in rats by inhibiting oxidative stress and microglia apoptosis via Nrf2/HO-1 pathway. *Life Sci*. (2019) 217:119–27. doi: 10.1016/j.lfs.2018.11.053

42. Casper E. The crosstalk between Nrf2 and NF-kappaB pathways in coronary artery disease: can it be regulated by SIRT6? *Life Sci*. (2023) 330:122007. doi: 10.1016/j.lfs.2023.122007

43. Sivandzade F, Prasad S, Bhalerao A, Cucullo L. NRF2 and NF-κB interplay in cerebrovascular and neurodegenerative disorders: molecular mechanisms and possible therapeutic approaches. *Redox Biol*. (2019) 21:101059. doi: 10.1016/j.redox.2018.11.017

44. Hayes JD, Dinkova-Kostova AT, Tew KD. Oxidative stress in Cancer. *Cancer Cell*. (2020) 38:167–97. doi: 10.1016/j.ccell.2020.06.001

45. Atalay ES, Gegotek A, Skrzydlewska E. The molecular activity of cannabidiol in the regulation of Nrf2 system interacting with NF-kappaB pathway under oxidative stress. *Redox Biol*. (2022) 57:102489. doi: 10.1016/j.redox.2022.102489

46. Gao W, Guo L, Yang Y, Wang Y, Xia S, Gong H, et al. Dissecting the crosstalk between Nrf2 and NF-kappaB response pathways in drug-induced toxicity. *Front Cell Dev Biol*. (2021) 9:809952. doi: 10.3389/fcell.2021.809952

47. Xia M, Zhang Y, Wu H, Zhang Q, Liu Q, Li G, et al. Forsythoside B attenuates neuro-inflammation and neuronal apoptosis by inhibition of NF-kappaB and p38-MAPK signaling pathways through activating Nrf2 post spinal cord injury. *Int Immunopharmacol*. (2022) 111:109120. doi: 10.1016/j.intimp.2022.109120

48. Li Z, Wu F, Xu D, Zhi Z, Xu G. Inhibition of TREM1 reduces inflammation and oxidative stress after spinal cord injury (SCI) associated with HO-1 expressions. *Biomed Pharmacother*. (2019) 109:2014–21. doi: 10.1016/j.biopha.2018.08.159

49. Vaziri ND, Pandian MR, Segal JL, Winer RL, Eltorai I, Brunnemann S. Vitamin D, parathormone, and calcitonin profiles in persons with long-standing spinal cord injury. *Arch Phys Med Rehabil*. (1994) 75:766–9. doi: 10.1016/0003-9993(94)90133-3

50. Ouyang YF, Su J, Guo X, Wang LR, He MR, Yuan CY. Correlation analysis of pNF-H, S100B, bone gamma-carboxyglutamic-acid-containing proteins, parathyroid hormone and bone-specific alkaline phosphatase expression in peripheral blood of patients with spinal fracture and spinal cord injury and their degree of disease. *Chinese J Exp Surg*. (2021) 38:2044. doi: 10.3760/cma.j.cn421213-20210618-00475

51. Sahbani K, Cardozo CP, Bauman WA, Tawfeek HA. Abaloparatide exhibits greater osteoanabolic response and higher cAMP stimulation and beta-arrestin recruitment than teriparatide. *Physiol Rep*. (2019) 7:e14225. doi: 10.14814/phy2.14225

52. Le B, Ray C, Gonzalez B, Miskevics S, Weaver FM, Priebe M, et al. Reasons for initiation and discontinuation of pharmacological therapies for osteoporosis in veterans with spinal cord injury and disorders. *J Clin Densitom*. (2021) 24:67–77. doi: 10.1016/j.jocd.2019.06.003

53. Gambardella J, De Rosa M, Sorriento D, Prevete N, Fiordelisi A, Ciccarelli M, et al. Parathyroid hormone causes endothelial dysfunction by inducing mitochondrial ROS and Specific oxidative signal transduction modifications. *Oxidative Med Cell Longev*. (2018) 2018:9582319. doi: 10.1155/2018/9582319

54. Schnoke M, Midura SB, Midura RJ. Parathyroid hormone suppresses osteoblast apoptosis by augmenting DNA repair. *Bone*. (2009) 45:590–602. doi: 10.1016/j.bone.2009.05.006

55. Ardura JA, Portal-Nunez S, Castelbon-Calvo I, Martinez DTI, De la Fuente M, Esbrit P. Parathyroid hormone-related protein protects osteoblastic cells from oxidative stress by activation of MKP1 phosphatase. *J Cell Physiol*. (2017) 232:785–96. doi: 10.1002/jcp.25473

56. Martin TJ, Sims NA, Seeman E. Physiological and pharmacological roles of PTH and PTHrP in bone using their shared receptor, PTH1R. *Endocr Rev*. (2021) 42:383–406. doi: 10.1210/endrev/bnab005

57. Yang Y, Lei H, Wang B. Effect of the PTHrP(1-34) analog abaloparatide on inducing chondrogenesis involves inhibition of intracellular reactive oxygen species production. *Biochem Biophys Res Commun*. (2019) 509:960–5. doi: 10.1016/j.bbrc.2019.01.049

58. Wang J, Chen R, Ren B, Feng Q, Li B, Hao Z, et al. A novel PTH-related peptide combined with 3D printed macroporous titanium alloy scaffold enhances osteoporotic Osseointegration. *Adv Healthc Mater*. (2023) 12:e2301604. doi: 10.1002/adhm.202301604

frontiers | Frontiers in Neurology

TYPE Systematic Review
PUBLISHED 06 May 2024
DOI 10.3389/fneur.2024.1405773

OPEN ACCESS

EDITED BY
Qingchun Mu,
Second Affiliated Hospital of Soochow University, China

REVIEWED BY
Yue Lv,
First Affiliated Hospital of Harbin Medical University, China
Ning Li,
Southeast University, China

*CORRESPONDENCE
Lingping Ma
malp@enzemed.com
Chengxin Xie
chengxin_xie@163.com

†These authors have contributed equally to this work

RECEIVED 23 March 2024
ACCEPTED 25 April 2024
PUBLISHED 06 May 2024

CITATION
Luo H, Yang Y, Wang Z, Ma L and Xie C (2024) Efficacy and safety of tranexamic acid in cervical spine surgery: a systematic review and meta-analysis.
Front. Neurol. 15:1405773.
doi: 10.3389/fneur.2024.1405773

Efficacy and safety of tranexamic acid in cervical spine surgery: a systematic review and meta-analysis

Hua Luo[1†], Yu Yang[1†], Zhitao Wang[2†], Lingping Ma[3*] and Chengxin Xie[1*]

[1]Department of Orthopedic, Taizhou Hospital of Zhejiang Province Affiliated to Wenzhou Medical University, Taizhou, Zhejiang, China, [2]Department of Pharmacy, Taizhou Hospital of Zhejiang Province Affiliated to Wenzhou Medical University, Taizhou, Zhejiang, China, [3]Department of Operation Room, Taizhou Hospital of Zhejiang Province Affiliated to Wenzhou Medical University, Taizhou, Zhejiang, China

Background: Tranexamic acid (TXA) is an antifibrinolytic drug associated with reduced blood loss in a range of surgical specialties. This meta-analysis aimed to compare the efficacy and safety of TXA in cervical surgery, focusing on its effects on intraoperative blood loss and related outcomes.

Methods: We searched the PubMed, EMBASE, Medline, and Cochrane Library databases to identify all literature related to TXA used in cervical spinal surgery. Intraoperative blood loss, postoperative drainage volume, total blood loss, postoperative hematological variables, and complications were analyzed.

Results: Eight trials met the inclusion criteria. The pooled results showed that intraoperative blood loss, total blood loss, and postoperative drainage volume were significantly lower in the TXA group than in the control group. The hemoglobin and hematocrit on postoperative day 1 was significantly higher in the TXA group than in the control group. There was no significant difference in complications between the two groups.

Conclusion: The available evidence indicates that TXA effectively reduces blood loss in cervical spinal surgery while maintaining a favorable safety profile, without increasing associated risks.

Systematic review registration: https://www.crd.york.ac.uk/prospero/, identifier CRD42023459652.

KEYWORDS

tranexamic acid, blood loss, cervical, complications, meta-analysis

Introduction

Tranexamic acid (TXA) is a well-established antifibrinolytic agent that has been shown to reduce blood loss during joint replacement, cardiac surgery, and spine surgery (1–3). In spine surgery, perioperative bleeding can have serious consequences, including spinal cord injury and compression of the esophagus and trachea by hematoma (4). To reduce surgical blood loss and the associated morbidity and mortality, researchers have been exploring a variety of strategies, including administration of erythropoietin to promote preoperative hematocrit, intraoperative autologous transfusion, controlled hypotension, and isovolumetric hemodilution (5). However, these methods are not without risks and

complications, and in some cases may not meet the requirements for cost-effectiveness. Therefore, there has been a focus on the potential of hemostatic agents, such as desmopressin, aprotinin, and others, to reduce blood loss and the need for transfusions (6). Unfortunately, desmopressin has not been shown to be effective, and aprotinin has not been cost-effective. Furthermore, the safety of antifibrinolytic agents remains uncertain, and previous studies have found that they are associated with an increased incidence of thromboembolic events (7). For these reasons, TXA is being studied as an alternative antifibrinolytic agent as one of the attempts to reduce blood loss during spinal surgery. In the normal fibrinolytic pathway, plasmin binds to fibrin through its lysine binding site and then undergoes fibrin degradation through its serine protease activity. TXA is a lysine analog that significantly reduces lysis of fibrin by competitively blocking lysine binding sites and inhibiting the activity of tissue plasminogen activator, plasminogen (a plasmin precursor), and plasmin (8). Therefore, TXA reduces degradation of platelets and promotes clot formation, thereby reducing the amount of blood lost during surgery. Previous systematic reviews and meta-analyses have shown that TXA can reduce blood loss in a variety of spine surgeries, including posterior lumbar interbody fusion, correction of spinal deformities in adults, and multilevel spine surgery (2, 9–13). However, to the best of our knowledge, there have been no meta-analyses of the efficacy of TXA in cervical surgery. In this meta-analysis and review, we present data from eight studies that investigated the safety and value of TXA in patients undergoing cervical surgery. The aim of this research was to further evaluate the effect of TXA on perioperative blood loss and complications, to update the medical evidence base, and to further clarify the specific role of TXA in cervical surgery so as to provide a reference for clinical work and accelerate the recovery of patients.

Methods

According to the PRISMA (Preferred Reporting Items for Systematic Reviews and Meta-Analyses) statement, this meta-analysis was performed in agreement (14). The protocol for this meta-analysis was registered on PROSPERO (Registration No: CRD 42023459652).

Inclusion criteria

Study type: randomized controlled trial (RCT), cohort study or case–control study. Study population: patients undergoing cervical surgery. Intervention and control: TXA used in the treatment group, no-TXA in the control group. Outcome index: intraoperative blood loss (IBL), postoperative drainage, total blood loss (TBL), postoperative hemoglobin (HB) and hematocrit (HCT) 1 day after surgery, and complications.

Exclusion criteria

Letters, case reports, meeting, reviews, animal trials, or republished studies; TXA wasn't used topically and intravenously in the treatment group; Studies lacking a control group; Patients with a past medical history of coagulopathy, bleeding disorders, seizures, blood clots.

Search strategy

One of the authors performed the search in PubMed, EMBASE, Web of Science (Medline), and the Cochrane Central Register of Controlled Trials from the inception dates to 30 October 2023, using the keywords "(tranexamic acid or transexamic acid or TXA or Ttxa or t-amcha or amcha or cyklokapron or transamine) and (cervical or spinal or spine or vertebra or vertebrae) and (blood loss or complication or drainage or hemoglobin or HB or hematocrit or HCT)." No language restrictions were applied during the search.

Study selection

Two researchers individually screened the retrieved literature strictly against inclusion and exclusion criteria. First, the documents that meet the inclusion criteria are read in full by reading the title and abstract, and the included papers are finally confirmed. If two researchers do not agree during the literature screening process, it will be left to the senior researcher.

Data collection process

Data on relevant outcome measures that met the inclusion criteria were extracted from the literature, including author year, study design type, country, sample size, participants, TXA treatment, age, outcomes, etc.

Assessment of risk of bias and quality of evidence

Two researchers independently assessed the quality of all included trials based on Cochrane risk-of-bias criteria (15). The Newcastle–Ottawa scale (NOS) was used to evaluate the literature quality of the retrospective studies (16).

Data synthesis

The Meta-analysis was performed using Stata (version 17; StataCorp, 2021) software. The heterogeneity was assessed by using the Q test and I^2 value calculation. The random effects model was used. The odds ratio (OR) and their associated 95% confidence interval (CI) were used to assess outcomes for dichotomous outcomes. Continuous outcomes were analyzed using mean, SD, and sample size to provide a mean difference (MD) between the TXA and control groups. A p-value less than 0.05 suggested that the difference was statistically significant.

Sensitivity analyses

We performed a sensitivity analysis by excluding the largest trial, excluding trials with a high risk of bias.

Results

The literature search yielded a total of 450 studies, 88 of which were duplicate publications and 341 were found to be irrelevant based on the titles and abstracts. After these articles were excluded, the full-text versions of 21 articles were read. Thirteen further articles were eliminated, including six trials that did not present results and five that were reports of meetings. Two trials included surgery of the spine, and it was not possible to extract data on the cervical spine, so we only included them in the review (17, 18). Finally, eight trials (two RCT and six retrospective studies including a total of 932 patients) (19–26) were included in the meta-analysis. The literature screening process is shown in Figure 1.

Characteristics of included studies

The basic characteristics of the included studies are shown in Table 1. These studies were published between 2011 and 2023. Three studies originate from China, one from Hong Kong, two from the USA, one from Japan, and one from Iran. As illustrated in Table 2, Ma et al. (23) exhibited some bias overall due to unclear detection bias. Tsutsumimoto et al. (20) demonstrated high bias overall as a consequence of employing medical record numbers in the randomization process. All non-randomized studies received NOS of 8 points or higher, indicating high-quality research (see Table 3).

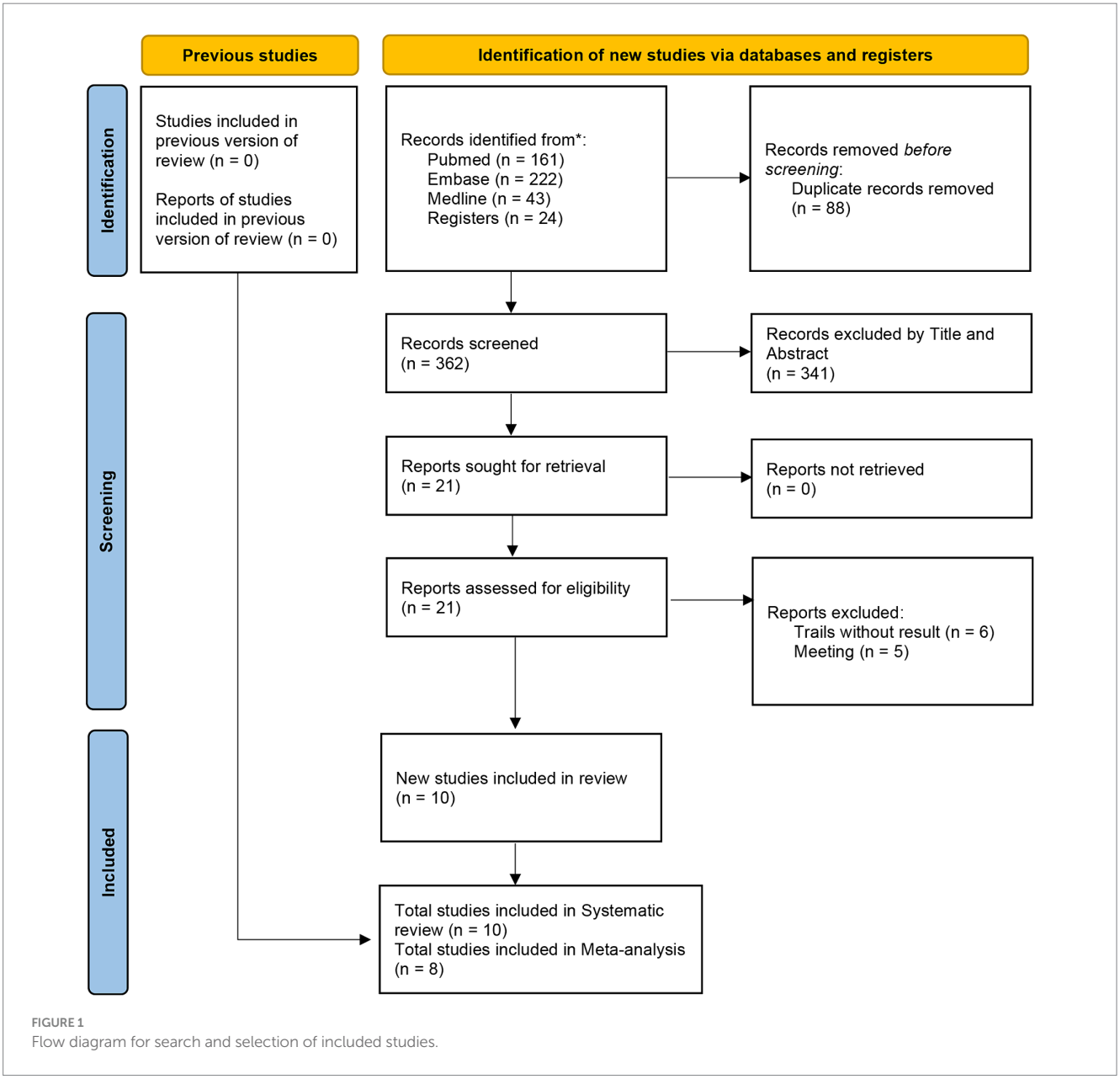

FIGURE 1
Flow diagram for search and selection of included studies.

TABLE 1 Characteristics of included studies.

Study	Country	Participants	Treatment with TXA	Design	Age		Sex (F/M)		BMI		Outcomes	No. of subject	
					TXA	Control	TXA	Control	TXA	Control		TXA	Control
Chen, 2022	China	Degenerative cervical myelopathy	Gelfoam soaked with 1 g TXA	Retrospective cohort	64.4 ± 8.68	65.12 ± 8.72	11/33	9/36	22.14 ± 1.90	21.37 ± 2.27	IBL, volume and length of drainage, transfusions rate, length of hospital stay, hematological parameters, complications	44	45
			1 g TXA injected into the wound		63.8 ± 9.43		9/35		21.44 ± 2.18			44	
Ho, 2020	Hong Kong	Multilevel compressive cervical myelopathy	10 mg/kg iv TXA + maintenance 1 mg/kg/h iv TXA	Retrospective cohort	61 ± 9	63 ± 10	12/18	15/17	NA	NA	IBL, volume of drainage, hematological parameters, complications	30	32
Khadivi, 2023	Iran	Posterior cervical laminectomy and lateral mass screw fixation	3 g TXA irrigated	Retrospective cohort	51.1 ± 11.0	53.5 ± 13.7	23/25	18/22	28.3 ± 5.3	28.6 ± 5.7	IBL, volume of drainage, length of postoperative hospital, complication	48	40
Ma, 2022	China	Cervical spondylotic myelopathy	15 mg/kg iv TXA	RCT	62.76 ± 5.83	63.65 ± 7.45	19/36	18/37	25.39(22.58, 27.39)	26.21 (23.05, 28.08)	IBL, hematological parameters, volume and length of drainage, length of hospital stay, complication	55	55
			30 mg/kg iv TXA		62.34 ± 7.02		19/36		25.95(22.98, 27.85)			55	
Perez-Roman, 2019	USA	Cervical stenosis	10 mg/kg iv TXA + 1 mg/kg/h iv TXA	Retrospective cohort	60 ± 12	65 ± 12	7/12	13/7	NA	NA	TBL, IBL, complication	19	20
Steinle, 2023	USA	Anterior cervical discectomy and fusion	30 mg/kg iv TXA+ 3 mg/kg/h iv TXA	Retrospective cohort	54.25 ± 11.28	52.53 ± 11	52/44	89/101	30.25 ± 6.5	31.36 ± 7.63	IBL, volume and length of drainage, hematological parameters, transfusions rate, complications	96	190
Tsutsumimoto, 2011	Japan	Cervical multilevel compressive myelopathy	15 mg/kg iv TXA	RCT	68.0 ± 11.0	65.8 ± 11.8	4/16	5/15	23.7 ± 2.5	23.1 ± 2.4	IBL, TBL, volume of drainage, complication	20	20
Yu, 2017	China	Multilevel cervical spondylotic myelopathy	15 mg/kg iv TXA + 100 mg/h iv TXA	Retrospective cohort	64.4 ± 9.13	63.7 ± 8.85	11/62	9/37	21.42 ± 1.92	21.35 ± 2.3	IBL, TBL, hematological parameters, complication	73	46

RCT, randomized controlled trial; TXA tranexamic acid; IBL, intraoperative blood loss; TBL, total blood loss; NA, not applicable.

10.3389/fneur.2024.1405773

TABLE 2 Risk of bias assessment with the Cochrane assessment tool.

Author	Bias from randomization	Bias from allocation	Bias from performance	Bias from detection	Bias from attrition	Bias from reporting	Bias from other	Overall risk of bias
Ma, 2022	Low	Low	Low	Some	Low	Low	Low	Some
Tsutsumimoto, 2011	High	Some	Some	Some	Low	Low	Low	High

TABLE 3 New Castle–Ottawa scale ratings.

Study	Selection	Comparability	Exposure/ outcome	Total score
Chen, 2022	****	**	***	9
Ho, 2020	****	**	***	9
Khadivi, 2023	****	**	***	9
Perez-Roman, 2019	****	**	***	9
Steinle, 2023	****	**	***	9
Yu, 2017	****	*	***	8

One * means score 1.

Intraoperative blood loss

Eight studies included intraoperative blood loss as the primary outcome (19–26). The pooled results showed a significant reduction in intraoperative blood loss in the TXA group (MD-48.81, 95% CI-82.01, −15.61, $I^2 = 90.0\%$, $p = 0.004$; Figure 2).

Total blood loss

Four studies reported total blood loss (19, 20, 22, 26). In a random-effects model, the total amount of blood loss was significantly lower in the TXA group than in the control group (MD −122.29, 95% CI -157.90, −86.69, $I^2 = 52.3\%$, $p < 0.0001$; Figure 3).

Postoperative drainage

Five studies reported on postoperative drainage (22–26). Use of TXA in cervical spine surgery significantly reduced postoperative drainage (MD −125.18, 95% CI -180.44, −69.92, $I^2 = 89.0\%$, $p < 0.0001$; Figure 4).

Postoperative hematological parameters on postoperative day 1

The four studies that reported the hemoglobin level on postoperative day 1 (19–21, 26) showed that it was significantly higher in the TXA group than in the control group (MD 0.46, 95% CI 0.21–0.72, $I^2 = 0.0\%$, $p < 0.0001$; Figure 5). Three of these studies also reported the hematocrit level on postoperative day 1 (19–21). The hematocrit level was significantly higher in the TXA group than in the control group (MD 1.06, 95% CI 0.28–1.84, $I^2 = 0.0\%$, $p < 0.0001$; Figure 6).

Complications

Eight studies reported complications (19–26). Six of these studies found no drug-related adverse events in either study group (19, 20, 22, 24–26). The pooled results showed no statistically significant difference in postoperative complications between the groups (OR 0.71, 95% CI 0.23–2.19, $I^2 = 0\%$, $p = 0.55$; Figure 7).

Sensitivity analysis

The remaining studies were combined when any individual study was excluded. No individual study had a significant effect on the results.

Risk of bias

Given that fewer than 10 trials were included, no publication bias assessment by funnel plots was performed.

Discussion

Many individual studies and meta-analyses have highlighted the antifibrinolytic and hemostatic properties of TXA in patients undergoing spinal surgery (27–30). TXA is often associated with reduced intraoperative and postoperative blood loss and may even reduce the need for blood transfusions. However, there have been no meta-analyses of the use of TXA in cervical spine surgery. In this study, we conducted a meta-analysis of eight studies that included a total of 932 patients to estimate the effect of TXA in cervical surgery. Only two of these studies were RCTs that provided high-quality evidence. The main advantages of RCTs are their ability to minimize bias and make stronger causal inferences. The studies randomly assigned participants and controlled for confounding factors, which makes their conclusions more reliable. However, our study also included six trials that were not randomized or controlled. Cumulatively, our inclusion of non-RCT, each achieving NOS scores of 8 or higher, underscores their high research quality. This, in turn, bolsters our ability to furnish robust and trustworthy evidence to substantiate our

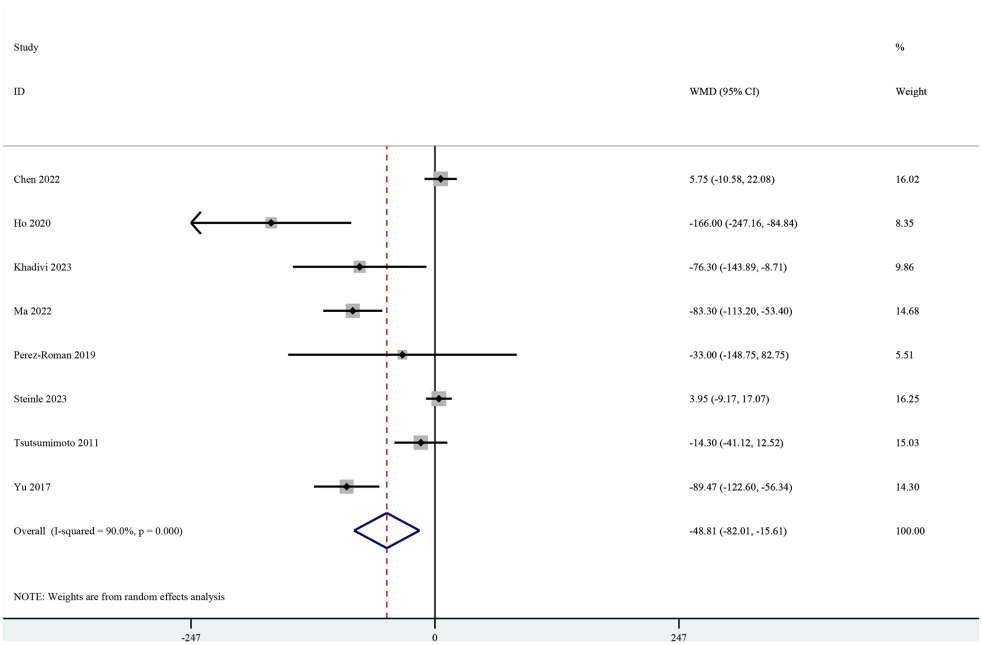

FIGURE 2
Forest plot of comparison: TXA vs. no-TXA; outcome: Intraoperative blood loss.

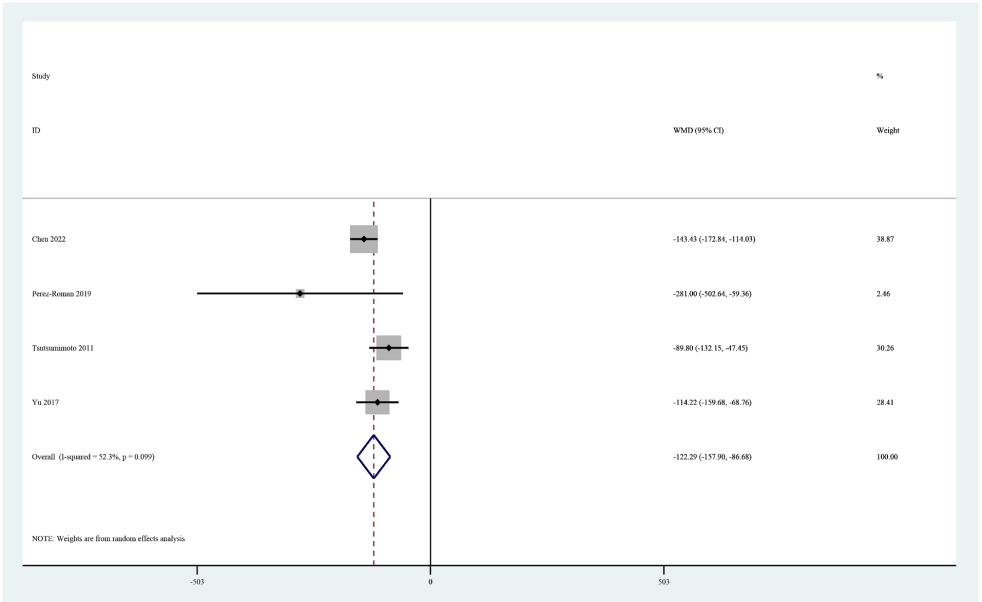

FIGURE 3
Forest plot of comparison: TXA vs. no-TXA; outcome: Total blood loss.

conclusions. The pooled results showed significant reductions in intraoperative blood loss, total blood loss, postoperative drainage, and loss of hemoglobin and hematocrit on the first postoperative day in comparison with the control group. When patients undergo surgery, there is a transient increase in fibrinolysis, which is thought to be a precipitating factor for blood loss during spinal surgery (31). TXA functions as a competitive antagonist of lysine binding sites on plasminogen, plasmin, and tissue plasminogen. This reversible blockade hinders fibrinolysis and degradation of blood clots and is activated intraoperatively and immediately after surgery, thereby reducing bleeding (32, 33). A study of 7,331 trauma patients by Knowlton et al. (34), a study of 168 knee arthroplasty procedures by Xue et al. (35), and a posterior spinal surgery study by Luan et al. (10) showed that use of TXA did not increase the risk of venous thrombosis in the lower extremities. In our pooled results, there were five cases of thrombosis-related

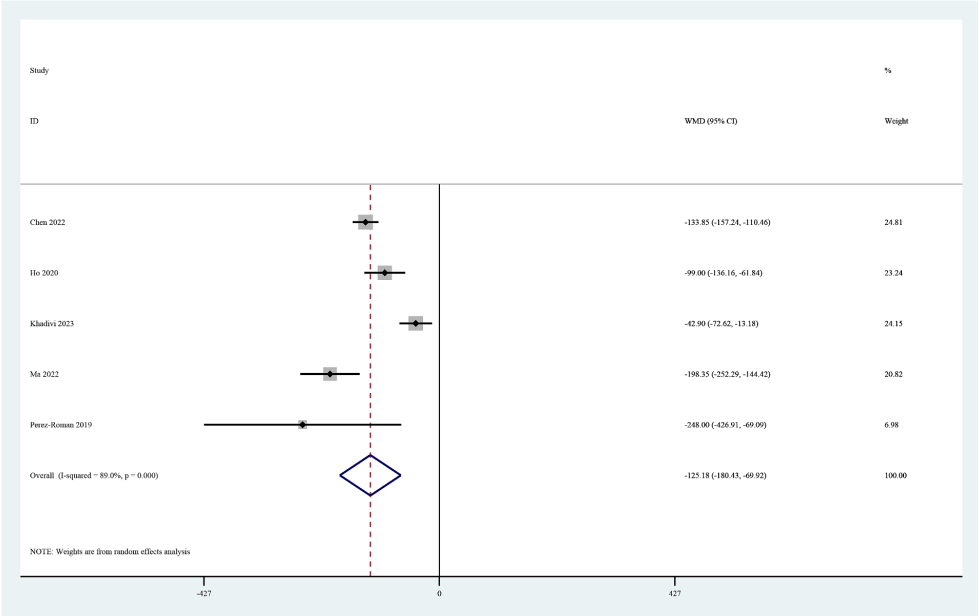

FIGURE 4
Forest plot of comparison: TXA vs. no-TXA; outcome: Postoperative drainage.

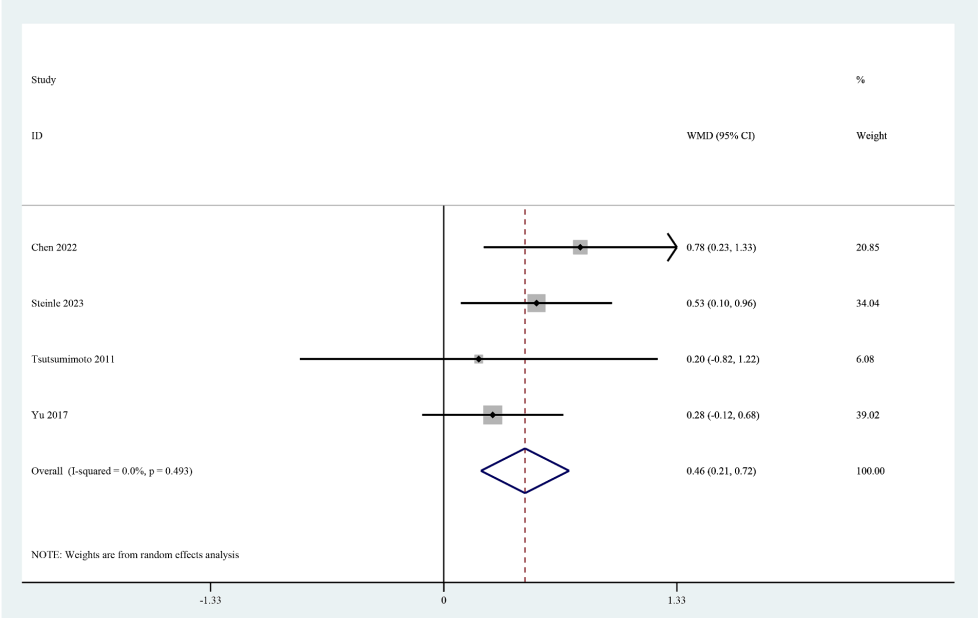

FIGURE 5
Forest plot of comparison: TXA vs. no-TXA; outcome: Hemoglobin levels on the first postoperative day.

complications in the TXA group and nine in the control group, with no marked difference between the two groups. Luo et al. found that use of TXA in spine surgery may induce epilepsy (36), and the incidence of convulsions increased from 0.5–1.0% to 6.4–7.3% with administration of TXA 50–100 mg/kg in cardiac surgery (37). No convulsion-related complications were reported in the studies included in our meta-analysis and review.

Limitations

This research had some limitations. First, most of the results were obtained under conditions of high heterogeneity, suggesting that there may be significant differences between studies, possibly owing to differences in patient populations, surgical procedures performed, doses of TXA, route of administration, publication

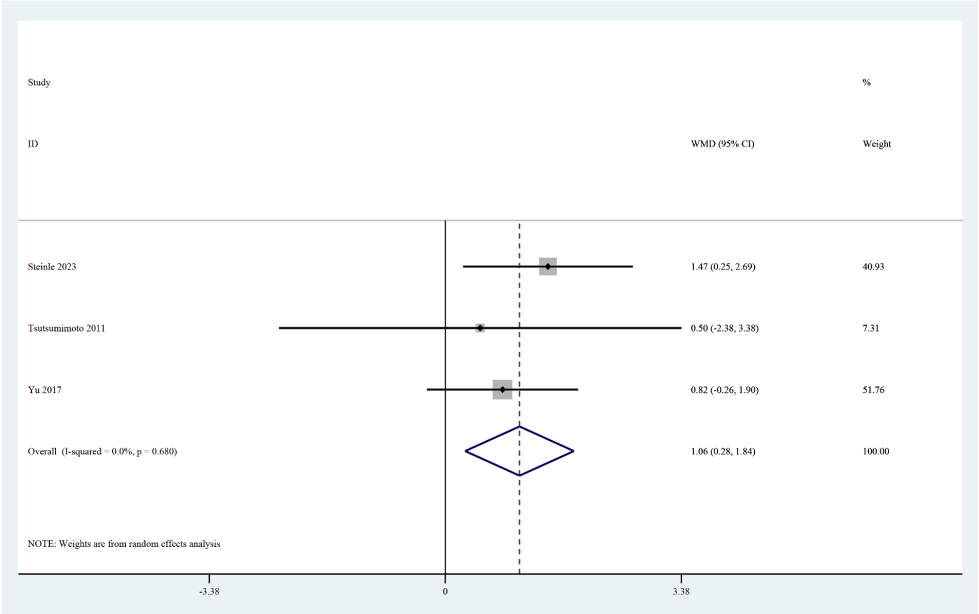

FIGURE 6
Forest plot of comparison: TXA vs. no-TXA; outcome: HCT levels on the first postoperative day.

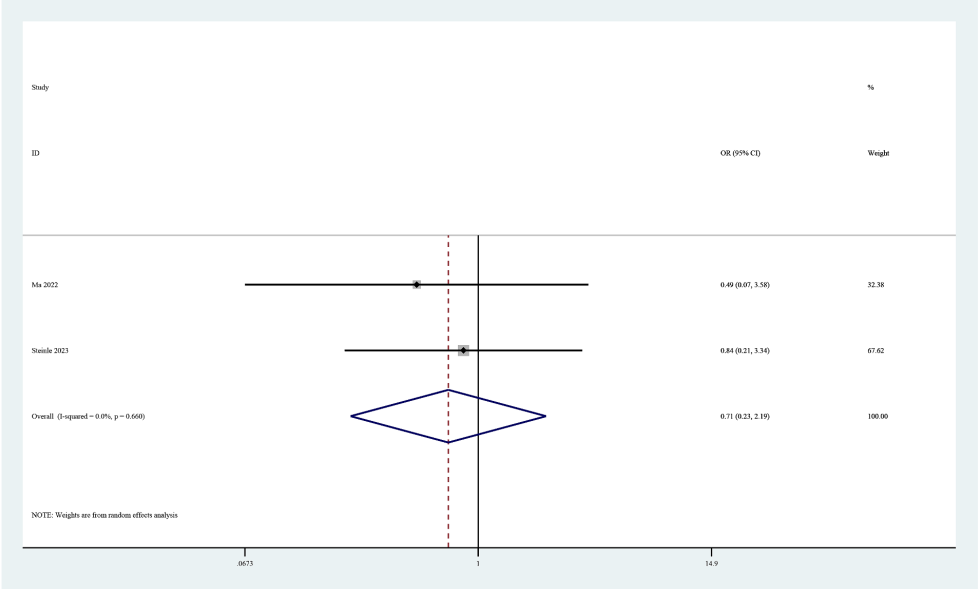

FIGURE 7
Forest plot of comparison: TXA vs. no-TXA; outcome: Complications.

bias, and potentially other unknown factors. Second, there were differences in the dose of TXA and its route of administration in the different studies. For example, Chen et al. injected 1 g of TXA around the wound while Ho et al. administered 10 mg/kg of TXA intravenously (25). Other studies applied topical TXA by irrigation, while others used soaked sponges, and some used local injection (24, 26). Therefore, the consistency and interpretability of our results may be affected by multiple TXA doses and regimens. Third, there were differences between the participants in the different studies, which may have introduced limitations in terms of heterogeneity, bias, and generalization. Again, these differences may affect the interpretation and applicability of the results of pooled analyses, so more rigorous statistical analysis and interpretation are needed to ensure confidence and clinical utility. Despite these limitations, our study provides strong evidence for the role of TXA in cervical surgery. However, more research is needed to address these limitations and confirm our findings.

Conclusion

The current evidence indicates that TXA significantly reduces blood loss in cervical surgery. Furthermore, TXA was confirmed not to increase the risk of complications. However, there was heterogeneity between studies and some outcomes differed across the different studies. Therefore, there is a need for future studies to examine the effects of TXA in different populations and types of surgery in greater detail to gain a more complete understanding of the role and applicability of TXA in cervical surgery.

Data availability statement

The original contributions presented in the study are included in the article/supplementary material, further inquiries can be directed to the corresponding author.

Author contributions

HL: Conceptualization, Data curation, Formal analysis, Funding acquisition, Investigation, Methodology, Validation, Visualization, Writing – original draft. YY: Data curation, Formal analysis, Writing – original draft. ZW: Supervision, Validation, Writing – original draft. LM: Supervision, Writing – review & editing. CX: Conceptualization, Data curation, Formal analysis, Investigation, Methodology, Writing – review & editing.

Funding

The author(s) declare that financial support was received for the research, authorship, and/or publication of this article. This work was supported by the Enze Medical Center (Group) Scientific Research (no. 23EZA04) and Zhejiang Medicine and Health Scientific Research Project (no. 2024KY531).

Conflict of interest

The authors declare that the research was conducted in the absence of any commercial or financial relationships that could be construed as a potential conflict of interest.

Publisher's note

References

1. Lin PS, Yao YT, Tian LJ, Jiang JJ, Zhang Y, He LX, et al. The efficacy and safety of intravenous administration of tranexamic acid in patients undergoing cardiac surgery: evidence from a single cardiovascular center. *Medicine*. (2023) 102:e33819. doi: 10.1097/md.0000000000033819

2. Luo H, Yan X, Ren Y, Zhang H, Pan W. The efficacy and safety of tranexamic acid in transforaminal lumbar interbody fusion: a systematic review and meta-analysis. *EFORT Open Rev*. (2023) 8:919–25. doi: 10.1530/eor-23-0168

3. Yang YZ, Cheng QH, Zhang AR, Yang X, Zhang ZZ, Guo HZ. Efficacy and safety of single- and double-dose intravenous tranexamic acid in hip and knee arthroplasty: a systematic review and meta-analysis. *J Orthop Surg Res*. (2023) 18:593. doi: 10.1186/s13018-023-03929-9

4. Le Huec JC, AlEissa S, Bowey AJ, Debono B, El-Shawarbi A, Fernández-Baillo N, et al. Hemostats in spine surgery: literature review and expert panel recommendations. *Neurospine*. (2022) 19:1–12. doi: 10.14245/ns.2143196.598

5. Lee SH, Cho KY, Khurana S, Kim KI. Less blood loss under concomitant administration of tranexamic acid and indirect factor Xa inhibitor following total knee arthroplasty: a prospective randomized controlled trial. *Knee Surg Sports Traumatol Arthrosc*. (2013) 21:2611–7. doi: 10.1007/s00167-012-2213-1

6. Mannucci PM, Levi M. Prevention and treatment of major blood loss. *N Engl J Med*. (2007) 356:2301–11. doi: 10.1056/NEJMra067742

7. Bryant-Smith AC, Lethaby A, Farquhar C, Hickey M. Antifibrinolytics for heavy menstrual bleeding. *Cochrane Database Syst Rev*. (2018) 2018:CD000249. doi: 10.1002/14651858.CD000249.pub2

8. Picetti R, Shakur-Still H, Medcalf RL, Standing JF, Roberts I. What concentration of tranexamic acid is needed to inhibit fibrinolysis? A systematic review of pharmacodynamics studies. *Blood Coagul Fibrinolysis*. (2019) 30:1–10. doi: 10.1097/mbc.0000000000000789

9. Hui S, Xu D, Ren Z, Chen X, Sheng L, Zhuang Q, et al. Can tranexamic acid conserve blood and save operative time in spinal surgeries? A meta-analysis. *Spine J*. (2018) 18:1325–37. doi: 10.1016/j.spinee.2017.11.017

10. Luan H, Liu K, Peng C, Tian Q, Song X. Efficacy and safety of tranexamic acid in posterior lumbar interbody fusion: a meta-analysis of randomized controlled trials. *J Orthop Surg Res*. (2023) 18:14. doi: 10.1186/s13018-022-03493-8

11. Luo W, Sun RX, Jiang H, Ma XL. The efficacy and safety of topical administration of tranexamic acid in spine surgery: a meta-analysis. *J Orthop Surg Res*. (2018) 13:96. doi: 10.1186/s13018-018-0815-0

12. Rahmani R, Singleton A, Fulton Z, Pederson JM, Andreshak T. Tranexamic acid dosing strategies and blood loss reduction in multilevel spine surgery: a systematic review and network meta-analysis: tranexamic acid for multilevel spine surgery. *N Am Spine Soc J*. (2021) 8:100086. doi: 10.1016/j.xnsj.2021.100086

13. Xiao K, Zhuo X, Peng X, Wu Z, Li B. The efficacy and safety of tranexamic acid in lumbar surgery: a meta-analysis of randomized-controlled trials. *Jt Dis Relat Surg*. (2022) 33:57–85. doi: 10.52312/jdrs.2022.432

14. Liberati A, Altman DG, Tetzlaff J, Mulrow C, Gøtzsche PC, Ioannidis JP, et al. The PRISMA statement for reporting systematic reviews and meta-analyses of studies that evaluate health care interventions: explanation and elaboration. *PLoS Med*. (2009) 6:e1000100. doi: 10.1371/journal.pmed.1000100

15. Cumpston M, Li T, Page MJ, Chandler J, Welch VA, Higgins JP, et al. Updated guidance for trusted systematic reviews: a new edition of the Cochrane handbook for systematic reviews of interventions. *Cochrane Database Syst Rev*. (2019) 10:Ed000142. doi: 10.1002/14651858.Ed000142

16. Wells G, Shea B, O'Connell J. *The Newcastle-Ottawa scale (NOS) for assessing the quality of nonrandomised studies in Meta-analyses* Ottawa Health Research Institute (2014). 7 p. Available at: https://www.ohri.ca/programs/clinical_epidemiology/oxford.asp

17. Honda A, Iizuka Y, Michihata N, Uda K, Mieda T, Takasawa E, et al. Effect of intraoperative tranexamic acid on perioperative major hemorrhage requiring transfusion in patients undergoing elective spine surgery: a propensity score-matched analysis using a National Inpatient Database. *Global Spine J*. (2022) 14:804–11. doi: 10.1177/21925682221123317

18. Elwatidy S, Jamjoom Z, Elgamal E, Zakaria A, Turkistani A, El-Dawlatly A. Efficacy and safety of prophylactic large dose of tranexamic acid in spine surgery: a prospective, randomized, double-blind, placebo-controlled study. *Spine*. (2008) 33:2577–80. doi: 10.1097/BRS.0b013e318188b9c5

19. Yu C-C, Gao W-J, Yang J-S, Gu H, Md MZ, Sun K, et al. Can tranexamic acid reduce blood loss in cervical laminectomy with lateral mass screw fixation and bone grafting: a retrospective observational study. *Medicine*. (2017) 96:e6043. doi: 10.1097/md.0000000000006043

20. Tsutsumimoto T, Shimogata M, Ohta H, Yui M, Yoda I, Misawa H. Tranexamic acid reduces perioperative blood loss in cervical laminoplasty: a prospective randomized study. *Spine*. (2011) 36:1913–8. doi: 10.1097/BRS.0b013e3181fb3a42

21. Steinle AM, Fogel JD, Chen JW, Chanbour H, Vaughan WE, Karwandyar A, et al. Determining the effect of intraoperative TXA on postoperative blood loss in ACDF. *Clin Spine Surg*. (2023) 37:E18–23. doi: 10.1097/bsd.0000000000001508

22. Perez-Roman RJ, Lugo-Pico JG, Burks JD, Madhavan K, Sheinberg D, Green BA, et al. Short-term safety of tranexamic acid use in posterior cervical decompression and fusion surgery. *J Clin Neurosci*. (2019) 66:41–4. doi: 10.1016/j.jocn.2019.05.029

23. Ma S, Sun X, Li L, Tan Y, Xia Y. Safety and efficacy of different doses of tranexamic acid in posterior cervical laminectomy with lateral mass screw fixation and bone graft fusion. *Zhongguo Xiu Fu Chong Jian Wai Ke Za Zhi*. (2022) 36:1506–11. doi: 10.7507/1002-1892.202208057

24. Khadivi M, Saghebdoust S, Moghadam N, Zarei M, Moosavi M, Ataei H, et al. Effect of topical Administration of Tranexamic Acid on intraoperative and postoperative blood loss during posterior cervical laminectomy and fusion surgery: a retrospective study. *Turk Neurosurg*. (2023) 33:94–100. doi: 10.5137/1019-5149.Jtn.37389-21.2

25. Ho CH, Wong RNM. Effectiveness of tranexamic acid in reducing blood loss in cervical laminoplasty: a retrospective observational study [article]. *J Orthopaed Trauma Rehabilit*. (2020) 27:162–5. doi: 10.1177/2210491720941872

26. Chen C, Ye Y-Y, Chen Y-F, Yang X-X, Liang J-Q, Liang G-Y, et al. Comparison of blood loss between tranexamic acid-soaked absorbable Gelfoam and topical retrograde injection via drainage catheter plus clamping in cervical laminoplasty surgery. *BMC Musculoskelet Disord*. (2022) 23:668. doi: 10.1186/s12891-022-05626-w

27. Ivasyk I, Chatterjee A, Jordan C, Geiselmann MT, Chang PS, Kamel H, et al. Evaluation of the safety of tranexamic acid use in pediatric patients undergoing spinal fusion surgery: a retrospective comparative cohort study. *BMC Musculoskelet Disord*. (2022) 23:651. doi: 10.1186/s12891-022-05604-2

28. Izima C, Sampath SG, Tang AJ, Ambati VS, Chou D, Chan AK. Systematic review and meta-analysis of topical tranexamic acid in spine surgery. *Neurosurg Focus*. (2023) 55:E18. doi: 10.3171/2023.7.Focus23363

29. Liu ZG, Yang F, Zhu YH, Liu GC, Zhu QS, Zhang BY. Is tranexamic acid beneficial in open spine surgery? And its effects vary by dosage, age, sites, and locations: a Meta-analysis of randomized controlled trials. *World Neurosurg*. (2022) 166:141–52. doi: 10.1016/j.wneu.2022.07.044

30. Lotan R, Lengenova S, Rijini N, Hershkovich O. Intravenous tranexamic acid reduces blood loss in multilevel spine surgeries. *J Am Acad Orthop Surg*. (2023) 31:e226–30. doi: 10.5435/jaaos-d-22-00738

31. Murray DJ, Pennell BJ, Weinstein SL, Olson JD. Packed red cells in acute blood loss: dilutional coagulopathy as a cause of surgical bleeding. *Anesth Analg*. (1995) 80:336–42. doi: 10.1097/00000539-199502000-00022

32. Zheng C, Ma J, Xu J, Li M, Wu L, Wu Y, et al. The optimal dose, efficacy and safety of tranexamic acid and epsilon-Aminocaproic acid to reduce bleeding in TKA: a systematic review and Bayesian network Meta-analysis. *Orthop Surg*. (2023) 15:930–46. doi: 10.1111/os.13678

33. Hardy JF, Desroches J. Natural and synthetic antifibrinolytics in cardiac surgery. *Can J Anaesth*. (1992) 39:353–65. doi: 10.1007/bf03009046

34. Knowlton LM, Arnow K, Trickey AW, Sauaia A, Knudson MM. Does tranexamic acid increase venous thromboembolism risk among trauma patients? A prospective multicenter analysis across 17 level I trauma centers. *Injury*. (2023) 54:111008. doi: 10.1016/j.injury.2023.111008

35. Xue CX, Yao YF, Lv H, Cheng L, Jing JH. Efficacy and safety of postoperative intravenous tranexamic acid in Total knee arthroplasty: a prospective randomized controlled study. *Orthop Surg*. (2021) 13:2227–35. doi: 10.1111/os.13045

36. Luo H, Shen C, Qu T, Chen L, Sun Y, Ren Y. Tranexamic acid-induced focal convulsions after spinal surgery: a rare case report and literature review on side effects of accidental spinal administration of tranexamic acid. *EFORT Open Rev*. (2023) 8:482–8. doi: 10.1530/eor-23-0016

37. Keyl C, Uhl R, Beyersdorf F, Stampf S, Lehane C, Wiesenack C, et al. High-dose tranexamic acid is related to increased risk of generalized seizures after aortic valve replacement. *Eur J Cardiothorac Surg*. (2011) 39:e114–21. doi: 10.1016/j.ejcts.2010.12.030

frontiers | Frontiers in Oncology

TYPE Original Research
PUBLISHED 10 May 2024
DOI 10.3389/fonc.2024.1412430

OPEN ACCESS

EDITED BY
Qingchun Mu,
Second Affiliated Hospital of Soochow University, China

REVIEWED BY
Ji Huaiyu,
The Fourth Hospital of Harbin Medical University, China
Xiaofeng Chen,
Harbin Medical University, China

*CORRESPONDENCE
Hakeem J. Shakir
Hakeem-Shakir@ouhsc.edu

RECEIVED 04 April 2024
ACCEPTED 29 April 2024
PUBLISHED 10 May 2024

CITATION
Evans AR, Harris DM, Gumerlock MK and Shakir HJ (2024) The safety and efficacy of the Stryker OptaBlate™ Bone Tumor Ablation system for vertebral body metastases. *Front. Oncol.* 14:1412430. doi: 10.3389/fonc.2024.1412430

The safety and efficacy of the Stryker OptaBlate™ Bone Tumor Ablation system for vertebral body metastases

Alexander R. Evans, Danielle M. Harris, Mary K. Gumerlock and Hakeem J. Shakir*

Department of Neurosurgery, University of Oklahoma, Oklahoma City, OK, United States

Background: Metastatic spinal lesions are a significant cause of morbidity and decreased quality of life in those with a high tumor burden. Despite treatment modalities such as medical therapy (e.g., chemotherapy, steroids), spinal augmentation procedures, and radiation therapy, many patients still experience refractory back pain due to neoplastic infiltration of the vertebral body and/or pathologic compression fractures. With the aim to address refractory pain in patients who have exhausted conventional treatment options, Stryker developed the OptablateTM Bone Tumor Ablation system (BTA; Stryker Corporation, Kalamazoo, MI), which delivers radiofrequency energy to pathologic vertebral body lesions. In this preliminary single-institution study, we characterize the use of the BTA system in 11 patients undergoing kyphoplasty for pathologic spinal lesions with the goal to demonstrate the impact of this novel technology on refractory pain in this challenging clinical setting.

Methods: A single-center retrospective chart review was performed on all patients identified as those receiving tumor ablation/kyphoplasty for spinal neoplasms using the OptablateTM BTA system performed by a single surgeon at the University of Oklahoma Medical Center. Sex, age, primary lesion type, presenting symptomatology, spinal level, time of follow-up, and outcome were obtained from the electronic medical record (EMR).

Results: Eleven patients (4 males, 7 females) with a mean age of 62 (range, 38–82) years had an average follow-up time of 6 months. Presenting symptoms attributed to spinal pathology included back pain (n = 11, 100%), pathologic fracture (n = 6, 55%), and lower extremity weakness (n = 3, 27%). A total of 20 lesions were ablated at 12 vertebral levels. Eight patients (73%) had improved pain. No complications were reported.

Conclusion: This preliminary study documents the safety of the BTA system, in addition to its diverse use across many levels. The majority of patients reported improvement in their pain. Further study is required to fully characterize the use of the BTA system in those with neoplastic spinal pathology.

KEYWORDS

Stryker, OptaBlate, spinal metastasis, radiofrequency ablation, kyphoplasty

Introduction

The metastasis of primary neoplasms to the spinal column is a widely prevalent phenomenon that markedly increases the risk for morbidity in patients already experiencing baseline pain secondary to a high tumor burden (1). Although metastases to the vertebral body may be asymptomatic, these lesions often present with focal back pain and/or pathologic vertebral body fractures. Current management of extradural vertebral body tumors includes medication, spinal augmentation procedures (vertebroplasty, kyphoplasty), and radiation therapy in efforts to control disease, preserve neurologic function, stabilize compression fractures, and reduce pain (2–4). Although spinal augmentation significantly decreases pain levels with minimal complications compared to open surgery (2), pain continues to be one of the most debilitating symptoms of vertebral body metastases.

To address the treatment needs of this patient population, Stryker's OptaBlate™ Bone Tumor Ablation system (BTA; Stryker Corporation, Kalamazoo, MI) emerged with the Food and Drug Administration's approval in 2022 (5). By ablating painful metastatic lesions to the spinal column, the BTA system now plays a role in vertebral augmentation procedures to further optimize pain control and restore vertebral body height. Further, the development of this technology offers a unique advantage of coupling bone lesion ablation with conventional augmentation procedures. In this preliminary single-institution study, we characterize the use of the Bone Tumor Ablation system in 11 patients undergoing kyphoplasty for pathologic vertebral body lesions.

Materials and methods

A single-center retrospective chart review was performed on all patients identified as receiving tumor ablation for vertebral body neoplasms using the Optablate™ BTA system between January 12, 2023 and October 26, 2023. All procedures were performed by a single surgeon at the University of Oklahoma Medical Center Adult Patient Tower, with follow-up through March 13, 2024.

The Bone Tumor Ablation system

The BTA system provides two probes for the delivery of radiofrequency ablation, depending on tumor size (Figure 1). Under fluoroscopic guidance, access cannulas are inserted and advanced to the area of pathology. Biopsies may then be taken for pathologic analysis. Subsequently, the cannulas are advanced to the posterior one-third of the vertebral body. A hand drill is inserted into the anterior third of the vertebral body to create a pathway through which bilateral probes are then inserted and connected to a microinfuser, allowing for the flow of sterile saline to the lesion site, thus preventing excess charring. The ablation is conducted, with surrounding tissue receiving radiofrequency energy according to prescribed regimens. Patients with lesions measuring 15mm in width receive 95°C ablation for 9 minutes, whereas patients with lesions measuring 20mm in width receive ablation at 95°C for 12 minutes (Figure 1) (5).

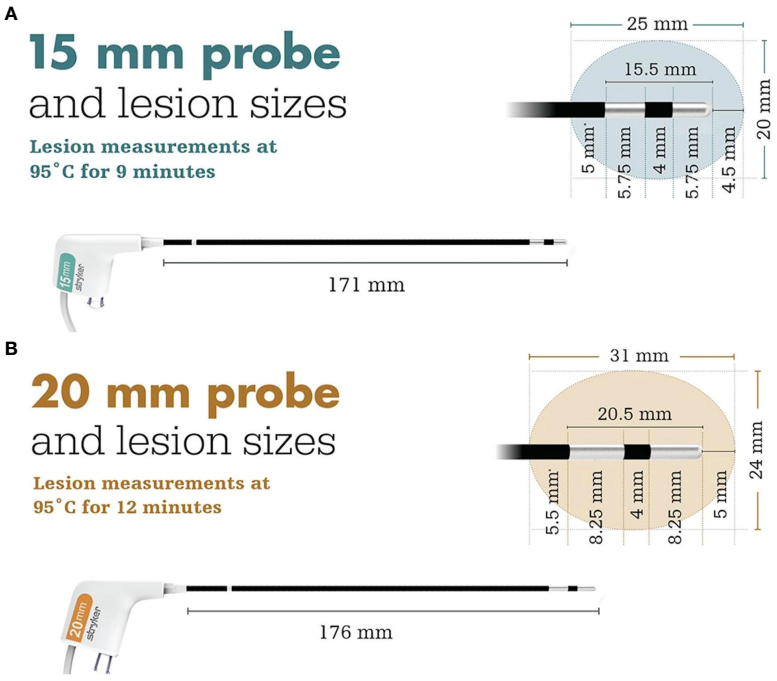

FIGURE 1
Ablation regimens and treatment area of the **(A)** 15 mm and **(B)** 20 mm probes reprinted with permission from Stryker (5).

Patient selection

Patients were selected for treatment having presented with back pain and at least one of the following: a diagnosis of focal neoplastic vertebral body lesion(s) or fracture (presumed pathologic). Exclusionary criteria included any contraindication to kyphoplasty, bleeding disorders, allergy to bone cement, or tumor mass involving the spinal canal. Patients with asymptomatic vertebral body fractures were excluded.

Data collection and analysis

Data collection obtained from the electronic medical record (EMR) included sex, age, primary lesion type, presenting symptomatology, spinal levels treated, outcome, and time to last follow-up. Pain was assessed via direct patient questioning at follow-up, in which improvement in pain was defined as partial or complete resolution of pain symptoms. Time to follow-up was determined from procedure date to time of most recent documented hospital or clinic visit as of March 13, 2024.

Results

Illustrative case example

A 38-year-old woman (Table 1, case 6) initially presenting to the emergency department (ED) with dyspnea was found to have a distal colon mass. Upon extensive workup, she was diagnosed with primary adenocarcinoma and widespread metastases. Decision was made to pursue palliative chemotherapy for the widespread metastases and zoledronic acid therapy for bony lesions. Upon the development of midline lumbar and left hip pain, she received radiation therapy, which did not adequately control her pain despite maximum medical therapy.

Approximately one year following the patient's initial diagnosis, she presented to the neurosurgery clinic for the evaluation of

TABLE 1 Summary of consecutive procedures utilizing the OptaBlate™ Bone Tumor Ablation System at our institution.

Case Number	Sex	Age	Primary Lesion Type	Presenting Symptom(s)	Spinal Level of Procedure	Outcome	Time to Follow-Up (Months)
1	F	52	SCC of the larynx	Midline lumbar pain, pathologic fracture	*L4	†Biopsy-confirmed metastatic SCC; alive at follow-up	14
2	M	52	Prostate adenocarcinoma	Lumbar pain, bowel and bladder incontinence, bilateral lower extremity weakness	L2	Died 6 months postoperatively; reported significant improvement in pain following treatment	5
3	F	72	Invasive ductal carcinoma of the breast	Lumbar pain, pathologic fracture, bilateral lower extremity weakness	T12 and L3	Died 3 months postoperatively; reported improvement in strength and pain	1
4	M	58	Renal cell carcinoma	Back/leg pain, left lower extremity weakness	L3	Alive at follow-up; reported significant improvement in pain	10
5	M	61	Multiple myeloma	Back pain with multiple pathologic fractures and lytic lesions at T7 and T9	*T7 and T9	Biopsy-confirmed plasma cell neoplasm, kappa-restricted; alive at follow-up; back pain resolved	8
6	F	38	Colorectal adenocarcinoma	Midline lumbar pain with T9/T12 lesions on imaging	T9 and T12	Died 33 days following procedure; reported immediate decrease in pain postoperatively	1 week
7	F	76	Retroperitoneal leiomyosarcoma	Midline back pain, pathologic fracture	T4	Alive at follow-up; reported resolution of pain	5
8	M	50	Colorectal adenocarcinoma	Back pain, pathologic fracture of T2, T6, T9, and T10	T9–11, L1	†Died 15 days following procedure	1 week
9	F	82	Lung, unspecified	Midline lower back pain with numerous enhancing spine lesions	T12 and L1	Died 32 days following procedure; reported a decrease in pain immediately postoperatively	2 days
10	F	64	Pancreatic adenocarcinoma	Lumbar pain	T11	Alive at follow-up; reported resolution of pain	5
11	F	78	Lung adenocarcinoma	Pathologic fracture, chronic intractable back pain	T6-T8	†Alive at follow-up	4

*Also received intraoperative biopsy.
†Pain not addressed or recorded in the patient chart.
M, male; F, female; SCC, squamous cell carcinoma.

refractory back pain. At that time, MRI of the spine revealed new metastatic infiltration and compression of the T9 and T12 vertebral bodies (Figure 2). Given her extensive history of pain, the decision was made to perform radiofrequency ablation and kyphoplasty of these neoplastic lesions with the goal of palliation.

The procedure was conducted under general anesthesia. Following localization at the proper spinal levels, stab incisions were made over the lateral pedicles. Trocars (11 gauge) provided pedicular access to the vertebral bodies. A hand drill was then used to enter the vertebral body near the anterior cortex. The OptaBlate™ 15mm radiofrequency ablation probe, inserted through the bilateral T9 and T12 pedicles to the lesions in the vertebral bodies (Figure 3A), delivered 95°C for 9 minutes at each site. Following ablation, kyphoplasty balloons were placed at each site and inflated to create a cavity. Bone cement was then placed into each vertebral body in 0.5ml aliquots (Figures 3B, C), thus concluding the kyphoplasty portion of the procedure. No postoperative complications were observed. The patient recovered well and was discharged home on the same day. She reported a noticeable improvement of pain symptoms at 7 days post-procedure and was comfortable until her death 33 days later.

Study results

Eleven patients (4 males, 7 females) with a mean age of 62 (range, 38–82) years had an average follow up of 6 months. All patients had vertebral body metastases from a primary neoplastic process, including retroperitoneal leiomyosarcoma, pancreatic adenocarcinoma, prostate adenocarcinoma, invasive ductal carcinoma of the breast, renal cell carcinoma, lung adenocarcinoma, squamous cell carcinoma (SCC) of the oropharynx, lung carcinoma, multiple myeloma, and colorectal adenocarcinoma (Table 1). Presenting symptoms attributed to vertebral pathology included back pain (n = 11, 100%), pathologic fracture (n = 6, 55%), and lower extremity weakness (n = 3, 27%).

A total of 20 lesions were ablated in 11 patients (Figure 4). Two patients had concurrent biopsy and all patients received ablation followed by kyphoplasty with the use of Stryker kyphoplasty balloons and Stryker bone cement. Eight patients (73%) had improved pain as documented on chart review. No complications were reported (Table 1).

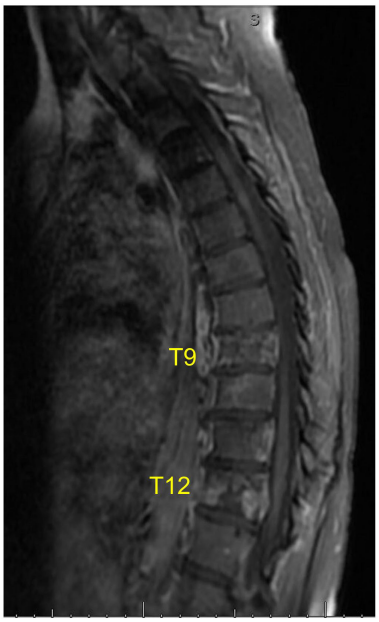

FIGURE 2
Preoperative sagittal MRI (T2-weighted) shows lesions at the T9 and T12 vertebral bodies.

Discussion

In this pilot study, a total of 20 vertebral body lesions in 11 patients were treated across 12 spinal levels, ranging from T4 to L4. The majority of patients (73%) had improvement of pain following ablation and kyphoplasty, as documented at follow-up. In addition, the Optablate Bone Tumor Ablation System provided technical success in 100% of patients, with no complications observed. Within the context of extensive malignant pathology, the safety and diverse application of the BTA system in conjunction with spinal augmentation procedures significantly improved pain management in those with disease.

Historically, palliative radiation has demonstrated significant pain control in patients with painful vertebral body lesions (4). In addition, corticosteroids have been established as an effective method of decreasing pain while preserving neurological function (3). In cases of refractory pain, tricyclic antidepressant and anticonvulsant medications are often utilized, with opioids now used more frequently for breakthrough pain (3). In light of the ongoing opioid epidemic in the United States and continued lack of pain control in this patient population, novel treatment options are needed for this therapeutically challenging clinical scenario.

A multi-modal approach to vertebral body metastases is emphasized in the present study, as the majority of patients had decreased pain following the combination of ablation with vertebral augmentation. Alternatively, cases of spinal instability and cord compression more frequently necessitate surgical intervention (6). If pain is related to instability, ablation with kyphoplasty may be advantageous by eliminating underlying pathology while restoring the structural integrity of the vertebral body.

In clinical circumstances where pain control is the predominant goal, the combination of steroids and radiotherapy is often the initial therapeutic strategy, with surgical augmentation reserved for cases of metastasis-related vertebral body fractures (4, 7). Interestingly, novel stereotactic radiosurgery has emerged as an initial treatment in those with metastatic cord compression, and has shown lower rates of failure than the combination of augmentative surgery followed by radiosurgery (8). Despite the evolving therapeutic landscape of surgical and/or medical management of vertebral metastases, refractory back pain remains as one of the most prevalent and debilitating symptoms of lesions in the spinal column.

Stryker's BTA system offers an innovative method of decreasing pain in this patient population. Whereas the boundaries of surgical

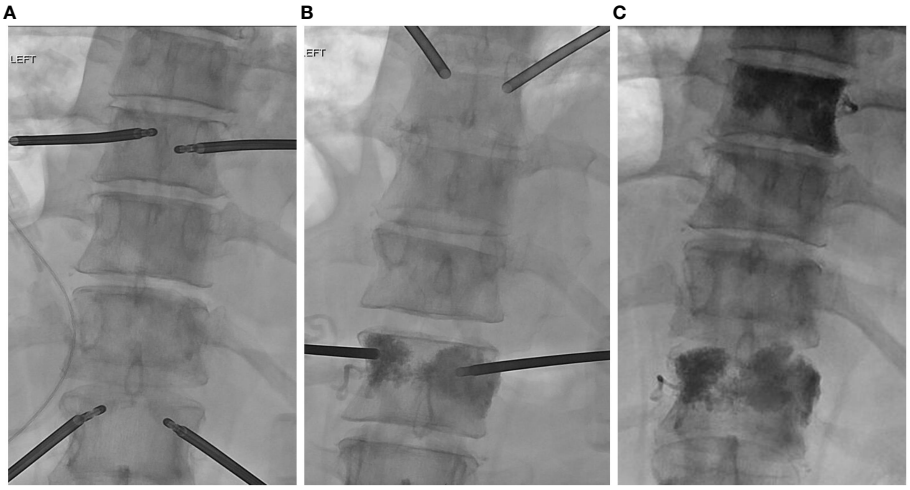

FIGURE 3
(A) Insertion of transpedicular ablation probes prior to bone tumor ablation and **(B, C)** bone cement placement following ablation at the T9 and T12 spinal levels.

augmentation, radiation therapy, and medical management have been explored, the novel BTA system couples lesion ablation with spinal augmentation. With the absence of complications in this pilot study, the BTA system appears to provide excellent pain control while maintaining a high level of safety when used in concordance with kyphoplasty. Although prior methods of analgesia have proved beneficial, the BTA system may be employed as an alternative or adjunct option for cases of particularly refractory or debilitating spinal pain. In addition, maintaining vertebral body height with kyphoplasty may place patients at a lower risk for the subsequent development of neurological deficits. Potential complications must be acknowledged, encompassing those observed in general radiofrequency ablation and kyphoplasty procedures. These include postablation radicular pain (secondary to heat-induced nerve damage), nerve root injury, cement embolism or extravasation, and infection (9–11). Selection of the proper ablation probe and adherence to the predetermined time and temperature regimen based on tumor size is critical in preventing ablation-related damage to the surrounding anatomy. We select a transpedicular route rather than a posterolateral one, to avoid nerve root injury (10). Regarding the prevention of cement embolism or extravasation, the use of high quality fluoroscopy may be advantageous by allowing clear visualization of cement progression and avoidance of venous structures in real time (10, 11). In the context of infection, polymerase chain reaction (PCR) may be used to promptly identify the infectious organism for tailored antibiotic management, in which surgical debridement may also be indicated (11).

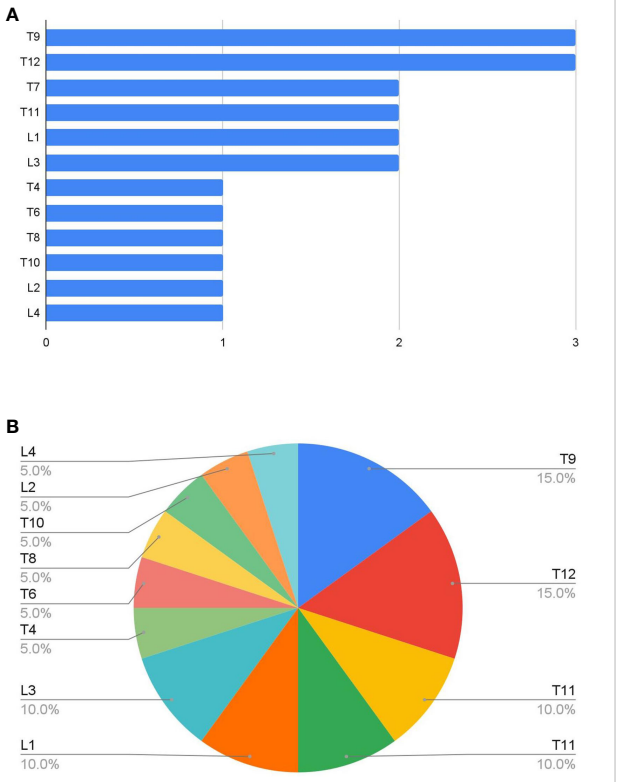

FIGURE 4
(A) Number and **(B)** proportion of lesions ablated at each vertebral level. T9, T12, L1, and L3 spinal levels were the most frequent sites treated.

This preliminary retrospective study has multiple limitations, including small sample size (n=11) and follow-up. Due to the progressive nature of metastatic disease, shortened follow-up time was a significant source of bias, as three patients died shortly following the procedure. Bias was also introduced from the subjective reporting of decreased pain in each patient's record. Ideally, numerical scoring methods would have been collected in order to quantify pain relief; however, the retrospective nature of this study revealed inconsistencies in the reporting of pain and quality of life scores. For example, seven patients had Numeric Rating Scale measurements, two had Karnofsky Performance

Status, and seven had Eastern Cooperative Oncology Group (ECOG) scores reported pre- and postoperatively in the medical record. In addition, our conclusions are limited to patients undergoing concurrent kyphoplasty, in which the prior treatment of metastatic neoplasms were widely variable between patients (three patients received spinal radiation, and many others received a diverse range of chemotherapeutic agents). Considering that kyphoplasty significantly improves pain in those with painful vertebral body metastases, future works may consider comparing pain outcomes in those receiving ablation with kyphoplasty versus those undergoing kyphoplasty alone.

Quality of life in patients with painful pathologic lesions and/or vertebral body compression fractures is significantly decreased. Current adjunct treatment of vertebral metastases includes radiation and spinal augmentation procedures, often without complete resolution of symptoms. In this preliminary study, we have documented the safety of the BTA system in treating pain across frequently-involved vertebral levels often the site of metastatic disease. Overall, the combination of lesion ablation and kyphoplasty is safe and can result in significant quality of life improvement in patients with pathologic vertebral body lesions. Future directions should include standardized prospective studies to more definitively establish the impact of the BTA system on pain in those with vertebral lesions.

Data availability statement

The raw data supporting the conclusions of this article will be made available by the authors, without undue reservation.

Ethics statement

The studies involving humans were approved by The University of Oklahoma Health Sciences Center Institutional Review Board. The studies were conducted in accordance with the local legislation and institutional requirements. The participants provided their written informed consent to participate in this study.

Author contributions

AE: Data curation, Writing – original draft, Writing – review & editing. DH: Writing – original draft. MG: Writing – review & editing. HS: Conceptualization, Investigation, Writing – review & editing.

Funding

The author(s) declare that no financial support was received for the research, authorship, and/or publication of this article.

Conflict of interest

The corresponding author of this work has a business relationship with Stryker.

The remaining authors declare that the research was conducted in the absence of any commercial or financial relationships that could be construed as a potential conflict of interest.

Publisher's note

References

1. Wewel JT, O'Toole JE. Epidemiology of spinal cord and column tumors. *Neuro-Oncol Pract* (2020) 7:i5–9. doi: 10.1093/nop/npaa046

2. Mossa-Basha M, Gerszten PC, Myrehaug S, Mayr NA, Yuh WT, Jabehdar Maralani P, et al. Spinal metastasis: diagnosis, management and follow-up. *Br J Radiol* (2019) 92:20190211. doi: 10.1259/bjr.20190211

3. Lawton AJ, Lee KA, Cheville AL, Ferrone ML, Rades D, Balboni TA, et al. Assessment and management of patients with metastatic spinal cord compression: A multidisciplinary review. *J Clin Oncol* (2019) 37:61–71. doi: 10.1200/JCO.2018.78.1211

4. Lutz S, Balboni T, Jones J, Lo S, Petit J, Rich SE, et al. Palliative radiation therapy for bone metastases: Update of an ASTRO Evidence-Based Guideline. *Pract Radiat Oncol* (2017) 7:4–12. doi: 10.1016/j.prro.2016.08.001

5. Digital Resources(2024). Available online at: https://providers.strykerivs.com/physician-resources/hcp-resources/digital-resources.

6. Hussain I, Hartley BR, McLaughlin L, Reiner AS, Laufer I, Bilsky MH, et al. Surgery for metastatic spinal disease in octogenarians and above: analysis of 78 patients. *Glob Spine J* (2023) 13:1481–9. doi: 10.1177/21925682211037936

7. George R, Sundararaj JJ, Govindaraj R, Chacko AG, Tharyan P. Interventions for the treatment of metastatic extradural spinal cord compression in adults. *Cochrane Database Syst Rev* (2015) 2018:29–30. doi: 10.1002/14651858.CD006716.pub3

8. Bate BG, Khan NR, Kimball BY, Gabrick K, Weaver J. Stereotactic radiosurgery for spinal metastases with or without separation surgery. *J Neurosurg Spine* (2015) 22:409–15. doi: 10.3171/2014.10.SPINE14252

9. Tomasian A, Marlow J, Hillen TJ, Jennings JW. Complications of percutaneous radiofrequency ablation of spinal osseous metastases: an 8-year single-center experience. *Am J Roentgenol* (2021) 216:1607–13. doi: 10.2214/AJR.20.23494

10. Laredo JD, Hamze B. Complications of percutaneous vertebroplasty and their prevention. *Semin Ultrasound CT MRI* (2005) 26:65–80. doi: 10.1053/j.sult.2005.02.003

11. Hu YC, Hart DJ. Complications of vertebroplasty and kyphoplasty. *Tech Reg Anesth Pain Manage* (2007) 11:164–70. doi: 10.1053/j.trap.2007.05.010

frontiers | Frontiers in Neurology

TYPE Review
PUBLISHED 10 May 2024
DOI 10.3389/fneur.2024.1341371

OPEN ACCESS

EDITED BY
Qingchun Mu,
Second Affiliated Hospital of Soochow University, China

REVIEWED BY
Longfei Shu,
Wuxi Clinical College of Anhui Medical University, China
Xiaofeng Chen,
Harbin Medical University, China

*CORRESPONDENCE
Eva Vlckova
✉ vlckova.eva@fnbrno.cz

RECEIVED 20 November 2023
ACCEPTED 18 April 2024
PUBLISHED 10 May 2024

CITATION
Horak T, Horakova M, Kerkovsky M, Dostal M, Hlustik P, Valosek J, Svatkova A, Bednarik P, Vlckova E and Bednarik J (2024) Evidence-based commentary on the diagnosis, management, and further research of degenerative cervical spinal cord compression in the absence of clinical symptoms of myelopathy.
Front. Neurol. 15:1341371.
doi: 10.3389/fneur.2024.1341371

Evidence-based commentary on the diagnosis, management, and further research of degenerative cervical spinal cord compression in the absence of clinical symptoms of myelopathy

Tomas Horak[1,2], Magda Horakova[1,2], Milos Kerkovsky[1,3], Marek Dostal[3,4], Petr Hlustik[5,6], Jan Valosek[5,7,8,9], Alena Svatkova[10,11], Petr Bednarik[10,11], Eva Vlckova[1,2]* and Josef Bednarik[1,2]

[1]Faculty of Medicine, Masaryk University, Brno, Czechia, [2]Department of Neurology, University Hospital Brno, Brno, Czechia, [3]Department of Radiology and Nuclear Medicine, University Hospital Brno, Brno, Czechia, [4]Department of Biophysics, Faculty of Medicine, Masaryk University, Brno, Czechia, [5]Department of Neurology, Faculty of Medicine and Dentistry, Palacký University Olomouc, Olomouc, Czechia, [6]Department of Neurology, University Hospital Olomouc, Olomouc, Czechia, [7]Department of Neurosurgery, Faculty of Medicine and Dentistry, Palacký University Olomouc, Olomouc, Czechia, [8]NeuroPoly Lab, Institute of Biomedical Engineering, Polytechnique Montreal, Montreal, QC, Canada, [9]Mila—Quebec AI Institute, Montreal, QC, Canada, [10]Danish Research Center for Magnetic Resonance, Center for Functional and Diagnostic Imaging and Research, Copenhagen University Hospital Amager and Hvidovre, Copenhagen, Denmark, [11]Department of Radiology, Center for Functional and Diagnostic Imaging and Research, Copenhagen University Hospital Amager and Hvidovre, Copenhagen, Denmark

Degenerative cervical myelopathy (DCM) represents the final consequence of a series of degenerative changes in the cervical spine, resulting in cervical spinal canal stenosis and mechanical stress on the cervical spinal cord. This process leads to subsequent pathophysiological processes in the spinal cord tissues. The primary mechanism of injury is degenerative compression of the cervical spinal cord, detectable by magnetic resonance imaging (MRI), serving as a hallmark for diagnosing DCM. However, the relative resilience of the cervical spinal cord to mechanical compression leads to clinical-radiological discordance, i.e., some individuals may exhibit MRI findings of DCC without the clinical signs and symptoms of myelopathy. This degenerative compression of the cervical spinal cord without clinical signs of myelopathy, potentially serving as a precursor to the development of DCM, remains a somewhat controversial topic. In this review article, we elaborate on and provide commentary on the terminology, epidemiology, natural course, diagnosis, predictive value, risks, and practical management of this condition—all of which are subjects of ongoing debate.

KEYWORDS

degenerative cervical cord compression, degenerative cervical myelopathy, cervical spinal canal stenosis, magnetic resonance imaging, subclinical myelopathy

1 Introduction

Degenerative changes in the cervical spine, primarily involving spondylosis and discopathy, lead to the narrowing of the cervical spinal canal, known as cervical spinal canal stenosis (CS). These changes are considered a common aspect of the aging process and are prevalent among the elderly population (1). The most serious and disabling consequence of CS is degenerative cervical myelopathy (DCM). DCM is an umbrella term used to describe progressive compression of the cervical spinal cord due to age-related changes in the spinal axis (2). Mechanical degenerative cervical spinal cord compression (DCC) is a key mechanism in the development of DCM, which together with complex pathophysiological mechanisms (e.g., necrosis, inflammation, gliosis, edema, demyelination, ischemia, and axonal and neuronal loss) leads to a variety of myelopathic symptoms. Current pathobiological and mechanistic knowledge does not adequately explain the disease phenotype, why only a subset of patients with identified spinal cord compression have clinical myelopathy, or why the degree of spinal cord compression correlates poorly with clinical disability. It has been proposed that DCM is better described as a function of multiple interacting mechanical forces, such as shear, traction, and compression, together with an individual's susceptibility to spinal cord injury, influenced by factors such as age, genetics, cardiovascular, gastrointestinal, and nervous system status, and time (3). Unlike compression, which can be visualized by MRI, the other mechanical forces are difficult to document or quantify. MRI evidence of spinal cord compression is therefore a key element in the diagnosis of DCM, along with clinical signs and symptoms of myelopathy (4, 5). Using the presence of clinical signs and symptoms of myelopathy as the main diagnostic criterion for the diagnosis of DCM can be difficult and sometimes misleading, as clinical signs of myelopathy can be present in a wide range of other diseases (2). Furthermore, the relative resilience of the cervical spinal cord to mechanical compression leads to a relatively high prevalence of clinical-radiological discordance, i.e., some individuals may exhibit MRI findings of DCC without the clinical signs and symptoms of myelopathy (Figures 1, 2). This condition may eventually progress to symptomatic DCM and should be considered as a precursor to DCM.

Several aspects of this condition need clarification and should be addressed in further research. First, there needs to be a general agreement on its definition and terminology, possibly encouraging further research into the subject. Second, the prevalence and natural history should be known. Third, as this probably common condition may precede the development of the much rarer DCM, it would be appropriate to identify biomarkers of the higher risk of progression to promote optimal management of high-risk individuals. Finally, the risk of developing symptomatic myelopathy after minor trauma, a risk that may eventually lead to a recommendation for surgery, should be disclosed.

2 Definition and terminology

Proper clinical management and even research into DCC without symptomatic myelopathy is hampered by its inconsistent definition and terminology, partly due to overlap with CS on the one hand and DCM on the other.

Cervical spinal stenosis is undoubtedly a key element leading to the eventual development of symptomatic radiculopathy or myelopathy. However, it is primarily defined as an anatomical narrowing of the cervical spinal canal that may lead to DCM but can and usually does remain completely asymptomatic for a long time or throughout life. Several measures are used to define both "developmental" and "degenerative" CS. Anteroposterior canal diameter < 10 mm or a Torg-Pavlov ratio < 0.82, as measures of narrowing of the bony cervical canal, tend to reflect congenital stenosis (6–8). Several more sophisticated measures have been proposed to define and quantify degenerative CS, such as "osseous spinal canal area," "dural sac area" (7), "space available for cord," and "canal to cord ratio" (9). However, the degree of CS correlates only weakly with the development of DCM, as we discuss later. CS is often presented as interchangeable with DCC (10, 11), which can be somewhat misleading. It seems logical to keep the term CS as an anatomical signature of the narrowing of the cervical spinal canal. Subjects with CS may have cervical spinal cord compression and clinical signs and symptoms of clinically symptomatic DCM,

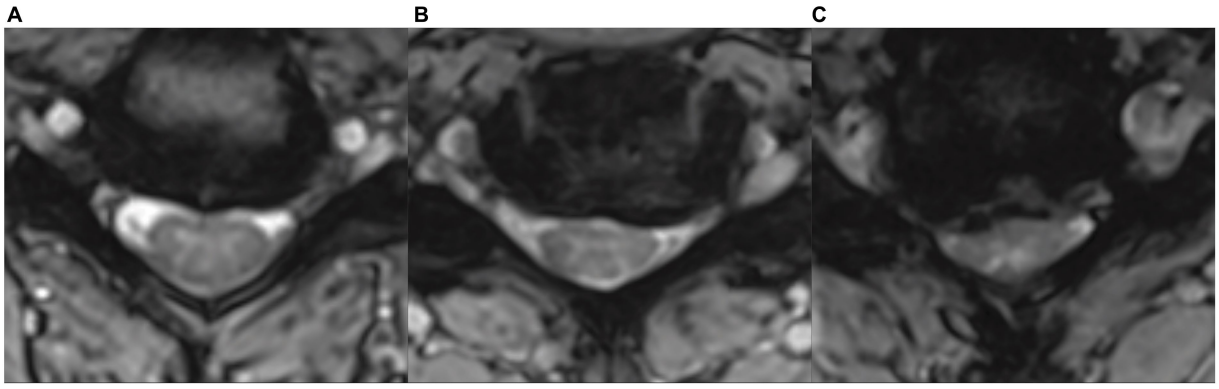

FIGURE 1
Examples of different types and severities of cervical spinal cord compression in axial MRI images in asymptomatic degenerative cervical cord compression subjects, illustrating the weak correlation between the severity of compression and the development of clinical myelopathic symptoms and signs. **(A)** Small ventral focal compression („impingement") with preserved cerebrospinal fluid space. **(B)** Flat ventral compression with flattened spinal cord and partially reduced ventral cerebrospinal fluid space. **(C)** Severe circular asymmetrical compression with flattening of the spinal cord and almost complete loss of cerebrospinal fluid space.

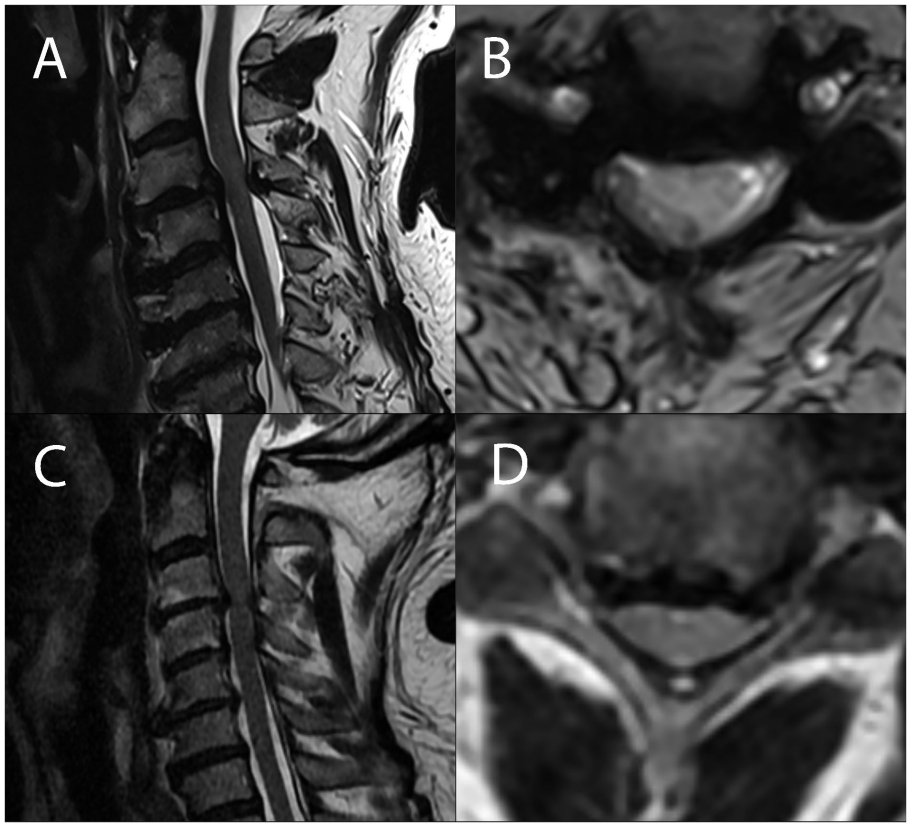

FIGURE 2
Sagittal and axial MRI sections of the cervical spinal cord showing degenerative compression in a patient with symptomatic degenerative cervical myelopathy **(A,B)** and in a patient without any myelopathic signs and symptoms **(C,D)**, showing no visible difference in the severity of compression between DCM and ADCC subjects.

radiculopathy, cervical pain, and limited range of neck motion, or they may remain completely asymptomatic.

A recent review of the literature found 118 articles on the pathology preceding DCM (12). The most common term found was asymptomatic (88%), followed by non-myelopathic (26%), presymptomatic (11%), subclinical (5%), and silent (2%). The greatest inconsistency was in the use and definition of "asymptomatic," with some papers using the term synonymously with healthy controls; the majority used it to describe patients with radiological evidence of degenerative spinal compression or other pathology, but without clinical symptoms of myelopathy. There was a further discrepancy between patients with and without symptoms and/or signs of radiculopathy (12).

The key question remains which conditions precede DCM and should be distinguished, defined, and appropriately named. It seems useful not to confuse simple CS with cases of radiologically proven DCC. Both of the most commonly used terms have some disadvantages. The term "asymptomatic" refers to the absence of clinical signs or symptoms of clinically symptomatic myelopathy, but some cases may have symptoms of radiculopathy or cervical pain and are therefore not completely asymptomatic. The term "non-myelopathic" may resolve this discrepancy, but it may also lead to the false assumption that there is no spinal cord injury.

It seems useful to coin the term asymptomatic degenerative cervical cord compression (ADCC) to describe individuals with radiological evidence of degenerative compression of the spinal cord, and to further stratify this group with respect to the presence or absence of symptomatic radiculopathy (13) or the presence of spinal cord dysfunction (detected by electrophysiological methods) or microstructural or metabolic myelopathy (detected by advanced MRI techniques, as we discuss later)—Figure 3.

2.1 Recommendation

The term "asymptomatic degenerative cervical cord compression" (ADCC) should preferably be used to describe individuals with MRI evidence of degenerative cervical cord compression without clinical signs and symptoms of myelopathy. The term "non-myelopathic degenerative cervical cord compression" should be considered synonymous with ADCC. The term cervical spinal stenosis (CS) should be reserved for describing anatomical narrowing of the cervical spinal canal, both developmental and degenerative.

3 Epidemiology and natural history

Degenerative cervical myelopathy, despite its low prevalence, cannot be categorized as a rare disease, as it is the most common cause of non-traumatic cervical spinal cord injury and lower limb paraparesis in individuals aged 55 and above (14). In North America, the published annual incidence is 41 per 1 million, and the prevalence is 605 per 1

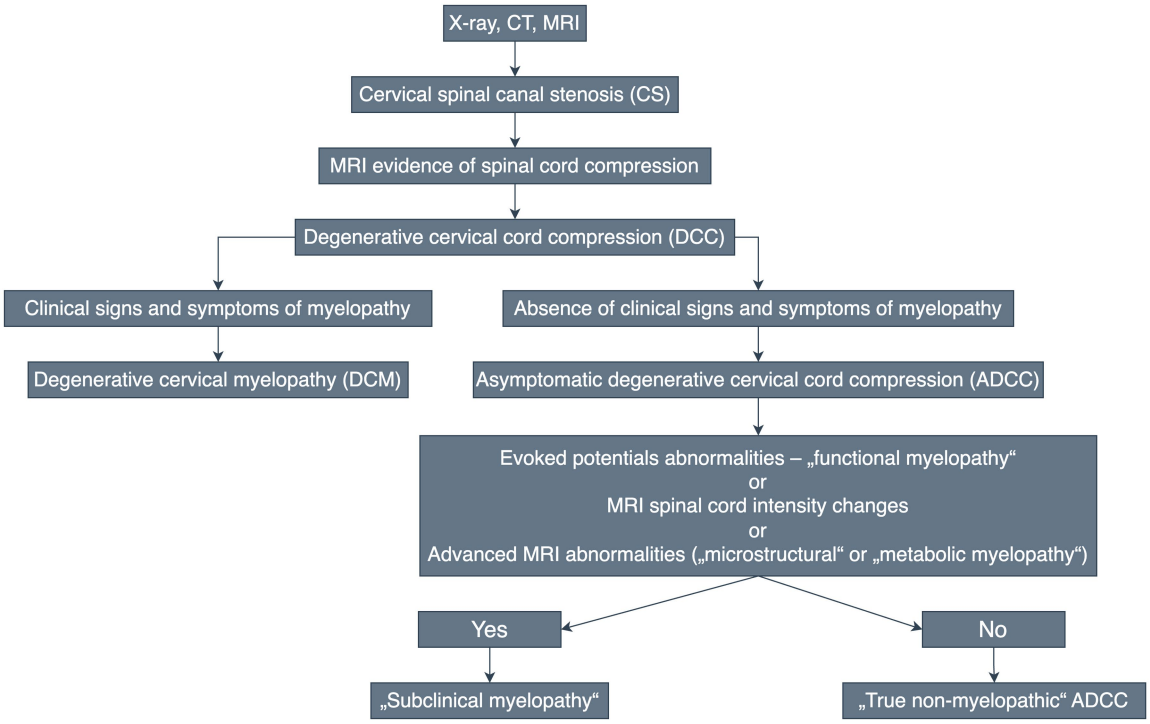

FIGURE 3
Diagram of the diagnosis and terminology of degenerative cervical spinal canal stenosis and subsequent cervical spinal cord compression.

million (15, 16). Nonetheless, a systematic review estimated the prevalence of DCM in the population to be as high as 2.3% (17).

The estimated prevalence of ADCC in a healthy population is much higher. A meta-analysis and systematic review demonstrated an estimated prevalence of 24.2%, with a significantly higher prevalence of ADCC in older populations and in North American/European populations as compared to Asian populations. In White European/North American populations aged over 60, the prevalence has risen as high as 40% (17, 18). A recent study of 267 young adult volunteers (with a mean age of 28.7 ± 5.6) identified the presence of mild spinal cord compression in 24% of the participants (19). ADCC is therefore a very common condition and a possible precursor of DCM, which increases the importance of its clinical management.

The natural history of ADCC is a key factor in assessing the risk of developing DCM and the influence of potential factors that increase this risk. In a small imaging study of 20 ADCC individuals, 2 (10%) eventually developed symptoms of myelopathy at a median follow-up of 21 months (20). In the largest prospective study performed to date on this topic, of 199 patients enrolled with ADCC, 8% developed symptoms of myelopathy at 12 months and 22.6% developed symptoms of myelopathy at a median follow-up of 44 months (range 12–24 months) (21). In another study by the same group in 2017, 13.4% of patients (15/112) developed DCM at a median follow-up of 36 months (22).

3.1 Recommendation

Asymptomatic degenerative cervical cord compression should be considered a very common condition, especially in an elderly White population. The rate of progression to DCM in the short and medium term is likely to be relatively low, not exceeding a few percent per year.

4 Detecting degenerative cervical cord compression

Magnetic resonance imaging is the reference imaging modality for assessing the extent of spinal cord compromise or injury, and typical features include visible spinal cord compression, altered spinal cord signal intensity, CS, altered sagittal spinal alignment, and ligamentous changes. Various quantitative measures of spinal cord compromise have been described, including “transverse area,” “compression ratio,” “maximum spinal cord compression,” and “spinal cord occupation ratio.” Despite years of research, no standard MRI features have been found to consistently represent disease severity in DCM (23). Even the extent of degenerative cervical cord compression, considered a hallmark of cervical cord injury in DCM, correlates poorly with the severity of clinical involvement (23, 24) (Figure 1). Nevertheless, the detection of DCC is critical to the current correct definition and diagnosis of both DCM and ADCC, and non-specialists, in particular, need information based on a reliable and consistent definition of MRI evidence of DCC, optimally provided by routine MRI.

The imaging definitions of DCC based on both quantitative and qualitative methods are vague, with no generally accepted quantitative parameter as a hallmark of DCC. The criteria used for DCC vary between studies, leading to bias in meta-analyses and making multicenter studies difficult (17, 25). Additionally, repeated MRI in longitudinal follow-up of mild DCM and ADCC requires reliable quantitative measures to assess the potential progression of radiological outcomes. Manual assessment of these quantitative measures is time-consuming and prone to inter-rater variability, making it unsuitable for large longitudinal studies. In 2014, the Spinal Cord Toolbox (SCT), an open-source software package for the analysis of spinal cord MRI data was introduced (26). Among its many

functionalities, the SCT offers automatic spinal cord segmentation and morphometric analysis tools (26, 27) enabling automatic extraction of common radiological measures such as transverse diameter, anterior–posterior diameter, and cross-sectional area (CSA), as well as parameters reflecting cord indentation and torsion. Martin et al. (20) recently compared the automatic shape analysis of morphometric measures calculated by SCT with expert assessments and reported promising results. They also proposed an objective definition of DCC as a deviation from normal in one of three quantitative parameters reflecting flattening, indentation, and torsion. Morphometric measures semi-automatically derived from two MRI scans using the SCT demonstrated the ability to detect spinal cord compression based on four parameters (CSA, solidity, compression ratio, and torsion) with lower inter-trial variability than a manual assessment by three experts (25). Despite the promising results, additional studies are needed to verify the generalization of the proposed methodologies across different MRI scanners, sequence settings, and population cohorts. The recently released *spine-generic* MRI acquisition protocol (28, 29) and morphometric measure normalization (19) can be employed to standardize both the MRI data acquisition and morphometry analysis in future multicenter and longitudinal studies.

4.1 Recommendation

The terminology used to describe spinal cord compression in radiological reports should be standardized. An automatic quantitative method of detecting spinal cord compression based on routine MRI sequences and freely available software may be helpful and potentially facilitate the practical management of both ADCC and DCM.

5 "Subclinical myelopathy" identified by imaging techniques in patients with DCC

A key diagnostic criterion for DCM (in addition to MRI evidence of cervical cord compression) is the presence of clinical symptoms and signs of myelopathy (4, 5). The use of this criterion can be difficult and sometimes misleading, as symptoms of DCM can also be present in a wide range of other conditions (2). However, the development of clinical myelopathic symptoms or signs can be a rather insensitive and late marker of spinal cord injury. Moreover, in quite a significant proportion of individuals with DCC but without clinical signs and symptoms of myelopathy, it is possible to detect subclinical functional, metabolic, and microstructural abnormalities using advanced or even routine diagnostic methods.

Electrophysiological methods, in particular, somatosensory evoked potentials (SEPs) and motor evoked potentials (MEPs) and electromyography can detect functional abnormalities of the spinal cord pathways or anterior horn cells in ADCC subjects (21, 30). Contact heat evoked potentials (CHEPs) have been shown to be more sensitive in detecting sensory pathway abnormalities in DCM (31) but have not been systematically studied in individuals with ADCC.

In addition to routine MRI showing "macrostructural" T2 or T1 hyper/hypointensities in the spinal cord, several novel quantitative MRI techniques are able to detect evidence of microstructural or metabolic myelopathy in patients with ADCC (32) using diffusion MRI (dMRI) (20, 33–37), T2*-weighted white/gray matter signal intensity ratio (38, 39), voxel-based volumetry demonstrating spinal cord degeneration (40–42), or proton (1H) magnetic resonance spectroscopy (MRS) (43) in comparison with healthy controls. While dMRI in ADCC patients consistently detected lower fractional anisotropy and higher mean diffusivity at compressed levels, caused by demyelination and axonal injury (20, 33, 34), magnetization transfer and 1H-MRS, along with advanced and tract-specific dMRI, recently revealed microstructural alterations, also rostrally pointing to Wallerian degeneration (19, 20, 36, 43). Recent studies also disclosed a significant relationship between microstructural damage and functional deficits, as assessed by quantitative MRI and electrophysiology, respectively (36, 43). Thus, tract-specific quantitative MRI, in combination with electrophysiology, critically extends our understanding of the underlying pathophysiology of degenerative spinal cord compression and may provide predictive markers of DCM development for accurate patient management. However, the prognostic value must be validated in longitudinal studies. The increased availability of 3 T MRI machines has facilitated the practical use of these techniques.

5.1 Recommendation

It seems reasonable to refer to ADCC patients with the evidence of "microstructural," "metabolic," or "functional" cervical cord impairment as ADCC with "subclinical myelopathy," whereas those with no other MRI abnormality (other than spinal cord compression) and no evidence of electrophysiological spinal cord dysfunction can be referred to as "true non-myelopathic" ADCC subjects (Figure 1). The predictive value of the presence of subclinical myelopathy detected by imaging techniques in ADCC subjects for progression to DCM should be established.

6 Which ADCC individuals have a higher risk of developing DCM?

The presence of radiculopathy and dysfunction of spinal cord pathways detected by evoked potentials have been repeatedly reported to predict a higher risk of progression to symptomatic DCM (21, 22, 30), but practical recommendations for the management of ADCC subjects are still debated (11, 13).

As for the imaging (mostly MRI) predictors of progression to the symptomatic myelopathy stage, many of these parameters have been studied, but with inconsistent results (24).

Older criteria for defining a narrow spinal canal, also known as "congenital canal stenosis" or "developmental canal stenosis," based on radiographic and cadaveric studies, used a sagittal width of <12–13 mm or a Torg-Pavlov ratio of <0.80–0.82 for diagnosis (44, 45), but evidence supporting a clear association between congenital stenosis and the development of myelopathy remains sparse (46). Recently, the relative size of the canal and spinal cord has been assessed, with the assumption that both a narrow canal and a large spinal cord may predispose patients to cervical spinal cord compression and potential myelopathy development (47, 48). This knowledge has led to the development of relative parameters based on MRI data that incorporate the size of the spinal cord, including space available for the cord (SAC) and spinal cord occupation ratio (SCOR). Depending on the technique, a cord-canal mismatch can be defined

as a SCOR ≥70% when measured on the midsagittal plane (49), ≥80% in the axial plane (50), or < 5 mm of SAC (51). In the subanalysis of the international and multicenter AOSpine studies of surgically treated patients with DCM, the prevalence of a cord-canal mismatch using a sagittal SCOR ≥70% was 8.4%, and patients diagnosed with a cord-canal mismatch at non-compressed sites were 5.4 years younger and had reduced baseline neurological function and quality of life (49). While both the large cord and the smaller canal have been shown to be risk factors for DCM, the predictive value of these parameters describing cord-canal mismatch and measured outside the level of compression for the development of DCM has not been investigated in the ADCC population.

Measures of the severity of cervical cord compression, such as compression ratio and CSA, have primarily been used to define and detect cord compression itself but have only exceptionally been studied as predictors of the development of DCM in ADCC individuals (22). In a 36-month longitudinal follow-up study of 112 ADCC individuals, multivariate analysis showed that radiculopathy, axial CSA ≤ 70.1 mm^2, and compression ratio ≤ 0.4 were predictive of the development of DCM.

Intramedullary signal changes in the spinal cord are commonly observed in patients with DCC, and the prevalence of T2 hyperintensity has been reported to range from 58 to 85% in patients with clinical symptoms of myelopathy (52). There appears to be a graded increase in neurological impairment when comparing patients with no signal changes, T2 hyperintensity, and both T2 hyperintensity and T1 hypointensity (53, 54). However, similar hyperintensity may also be an incidental finding. It was observed that 2.3% of 1,211 asymptomatic subjects had evidence of compressive cervical spine pathology with associated T2 hyperintensity (47). A few studies have investigated the predictive value of intramedullary signal changes on MR imaging in patients with mild DCM treated conservatively. Shimomura et al. found that T2 hyperintensity was not predictive of clinical progression as measured by worsening Japanese Orthopedic Association (JOA) score in patients with mild myelopathy (Shimomura). The predictive value of T2 hyperintensity in ADCC subjects has not been systematically studied. According to a review by Wilson et al. (11), hyperintensity on a T2-weighted MRI is a significant predictor of myelopathy development.

Several novel quantitative MRI techniques are able to detect evidence of microstructural or metabolic myelopathy in ADCC subjects, as discussed above, but their predictive value for progression to DCM has not been systematically investigated.

There are potential or established risk factors (including genetic and environmental) for the development of DCM, which have recently been summarized (3, 24). However, these are general risk factors for the development of DCM, but it is not known whether these risk factors, if assessed, could predict further outcome scenarios in pre-existing asymptomatic degenerative cervical cord compression.

6.1 Recommendation

It is reasonable to evaluate the contribution of both established clinical and electrophysiological predictors (i.e., radiculopathy and electrophysiological abnormalities) together with the new promising potential imaging predictors reflecting the severity of compression or subclinical microstructural or metabolic myelopathy in future longitudinal studies.

We propose that ADCC patients with identified high-level risk factors for developing DCM (including radiculopathy) be referred to as "presymptomatic myelopathy" subjects.

7 Risk of traumatic injury in ADCC

It is not uncommon for patients with ADCC, or even those with radiographic cervical spinal stenosis, to be recommended for surgery to reduce a perceived increased risk of neurological injury from a traumatic event (55). This problem is even more pressing in athletes or people accustomed to high-risk activities. However, the current literature addressing this issue is controversial.

A prospective cohort of 199 patients with ADCC was reviewed to specifically assess whether trauma is a risk factor for the development of neurological impairment (56). Fourteen traumatic events were identified during a mean follow-up period of 44 months, and only three minor traumatic events without cervical spine fracture were found among the symptomatic myelopathy cases, with no chronological relationship between trauma and myelopathy. The authors concluded that the risk of spinal cord injury is likely to be low, especially if a restriction on high-risk activities is implemented. This finding was supported by Chang et al. (57), who found that in a cohort of 55 prospectively followed asymptomatic or mildly symptomatic patients with CS, 18% experienced a traumatic event, but none of these had evidence of a spinal cord injury.

In another study, Ruegg et al. (50) used a retrospective case control methodology to address this question. A consecutive cohort of 52 patients presenting to a single center with traumatic quadriplegia or quadriparesis following a minor event over a 10-year period was compared with controls with similar minor injuries but no associated neurological compromise. They found that patients at risk of acute spinal cord injury after mild trauma can be reliably identified using the cord-canal-area ratio (>0.8) or the space available for the cord (<1.2 mm) measured on MRI. However, caution should be exercised before extrapolating these findings to all people with asymptomatic ADCC. No details are given, but the authors suggest that they excluded people with preexisting neurological symptoms. It is possible that some patients with post-traumatic neurological injury may have had preexisting symptoms of myelopathy that were not identified, given the retrospective nature of this study. It is noteworthy that falls were the precipitating mechanism in almost twice as many cases with neurological injury as in the controls (48% of cases vs. 27% of controls), which may indicate preexisting, yet unrecognized symptoms of myelopathy (55).

In a recent review article, a Torg-Pavlov ratio < 0.7, a minimal disk-level canal diameter < 8 mm, a cord-to-canal area ratio > 0.8, or space available for the cord <1.2 mm, were suggested as markers of higher risk for cervical spinal injury due to a traumatic event in patients with "asymptomatic cervical canal stenosis." These criteria were thought to be particularly useful in advising people who play either contact or collision sports (10).

7.1 Recommendation

Counseling ADCC subjects to avoid high-risk activities should be considered.

A high-quality prospective controlled study should be conducted to clarify the potential increased risk of spinal cord injury after minor injury

in the ADCC population. If such a risk is documented, the subsequent benefit of surgery to reduce this risk should be demonstrated.

8 Practical management of ADCC

In the first comprehensive systematic review and survey on patients with ADCC (11), a series of recommendations were made regarding the frequency, timing, and predictors of myelopathy development in asymptomatic patients with ADCC based on five articles that met most of the inclusion criteria of the review. They suggested that patients with ADCC who have clinical or electrophysiological evidence of cervical radicular dysfunction or central conduction deficits appear to be at higher risk for developing myelopathy and should be counseled to consider surgical treatment.

In subsequent AO Spine guidelines (13), this recommendation was further elaborated and modified. Patients with ADCC with clinical evidence of radiculopathy, with or without electrophysiological confirmation, are considered to be at a higher risk of developing myelopathy and should be counseled about this risk. These patients should be offered either surgical intervention or non-operative management consisting of close serial follow-up or a supervised trial of structured rehabilitation.

An evidence-based commentary (55) confirmed the lack of evidence to support surgery in asymptomatic individuals with ADCC who have no risk factors for progression. For these patients, the authors suggest nonoperative management, including education on the symptoms of myelopathy, clinical follow-up within 6–12 months, and avoidance of high-risk activities.

There is no clear recommendation on the extent of follow up, including the use of electrophysiological assessment or advanced MRI techniques to detect subclinical myelopathy, or repeated MRI to document the progression of DCC.

8.1 Recommendation

Patients with ADCC should be educated about the symptoms associated with myelopathy and should have follow-up visits on a regular basis, at least at 1-year intervals.

Patients with ADCC at higher risk of developing DCM (those currently with clinically symptomatic radiculopathy) should be offered surgery with counseling on both the risk of progression and the risk of surgery. The higher risk of developing DCM in "subclinical myelopathy" needs to be confirmed.

The optimal practical management of patients with ADCC, including the frequency, duration, and extent of clinical surveillance, additional testing, and avoidance of high-risk activities, should be further discussed and reviewed.

9 Conclusion

Asymptomatic degenerative cervical cord compression is a very common condition, particularly in the elderly population. A proportion of ADCC subjects may have some clinical non-myelopathic symptoms and signs of radiculopathy or cervical pain, or may have evidence of subclinical "microstructural," "metabolic," or "functional" cervical cord impairment detected by electrophysiological or advanced MRI techniques, while a large proportion may remain free of any clinical signs and symptoms, any MRI abnormality (other than spinal cord compression) and any evidence of electrophysiological spinal cord dysfunction ("true non-myelopathic" ADCC subjects). Further research is necessary to enhance the understanding of the natural history and the rates of deterioration of ADCC. This includes identifying important biomarkers (such as clinical, imaging, and electrophysiological factors) that predict clinical outcomes, improving clinical communication, facilitating treatment decisions, and determining the optimal duration and frequency of follow-up. The advancement of standardized classification and terminology, the standardization of MRI analysis and processing, and a critical analysis of the somewhat controversial existing evidence, are crucial for guiding both research and clinical recommendations in the significant yet sometimes overlooked area of ADCC, which acts as a precursor to DCM.

Author contributions

TH: Project administration, Writing – original draft. MH: Writing – review & editing. MK: Writing – review & editing, Methodology. MD: Writing – review & editing. PH: Supervision, Writing – review & editing. JV: Methodology, Writing – review & editing. AS: Supervision, Writing – review & editing, Methodology. PB: Methodology, Supervision, Writing – review & editing. EV: Supervision, Writing – review & editing. JB: Conceptualization, Funding acquisition, Methodology, Project administration, Supervision, Writing – original draft.

Funding

The author(s) declare financial support was received for the research, authorship, and/or publication of this article. This research was funded by the Czech Health Research Council grant NU22-04-00024, and also supported by Ministry of Health, Czech Republic—conceptual development of research organizations (FNBr, 65269705) and (FNOl, 00098892). JV has received funding from the European Union's Horizon Europe Research and Innovation program under the Marie Sklodowska-Curie grant agreement no. 101107932.

Conflict of interest

The authors declare that the research was conducted in the absence of any commercial or financial relationships that could be construed as a potential conflict of interest.

The author(s) declared that they were an editorial board member of Frontiers, at the time of submission. This had no impact on the peer review process and the final decision.

Publisher's note

References

1. Gore DR, Sepic SB, Gardner GM. Roentgenographic findings of the cervical spine in asymptomatic people. *Spine*. (1986) 11:521–4. doi: 10.1097/00007632-198607000-00003

2. Tetreault L, Kalsi-Ryan S, Benjamin Davies , Nanna-Lohkamp L, Garwood P, Martin AR, et al. Degenerative cervical myelopathy: a practical approach to diagnosis. Global. *Spine J*. (2022) 12:1881–93. doi: 10.1177/21925682211072847

3. Davies BM, Mowforth O, Gharooni A-A, Tetreault L, Nouri A, Dhillon RS, et al. A new framework for investigating the biological basis of degenerative cervical myelopathy [AO spine RECODE-DCM research priority number 5]: mechanical stress, vulnerability and time. *Glob Spine J*. (2022) 12:78S–96S. doi: 10.1177/21925682211057546

4. Kalsi-Ryan S, Karadimas SK, Fehlings MG. Cervical spondylotic myelopathy: the clinical phenomenon and the current pathobiology of an increasingly prevalent and devastating disorder. *Neuroscientist*. (2013) 19:409–21. doi: 10.1177/1073858412467377

5. Badhiwala JH, Ahuja CS, Akbar MA, Witiw CD, Nassiri F, Furlan JC, et al. Degenerative cervical myelopathy—update and future directions. *Nat Rev Neurol*. (2020) 16:108–24. doi: 10.1038/s41582-019-0303-0

6. Edwards WC, LaRocca H. The developmental segmental sagittal diameter of the cervical spinal canal in patients with cervical spondylosis. *Spine*. (1983) 8:20–7. doi: 10.1097/00007632-198301000-00003

7. Miyazaki M, Takita C, Yoshiiwa T, Itonaga I, Tsumura H. Morphological analysis of the cervical pedicles, lateral masses, and laminae in developmental canal stenosis. *Spine*. (2010) 35:E1381–5. doi: 10.1097/BRS.0b013e3181e8958f

8. Pavlov H, Torg JS, Robie B, Jahre C. Cervical spinal stenosis: determination with vertebral body ratio method. *Radiology*. (1987) 164:771–5. doi: 10.1148/radiology.164.3.3615879

9. Aebli N, Rüegg TB, Wicki AG, Petrou N, Krebs J. Predicting the risk and severity of acute spinal cord injury after a minor trauma to the cervical spine. *Spine J*. (2013) 13:597–604. doi: 10.1016/j.spinee.2013.02.006

10. Lee Y, Selverian S, Hsu WK, Watkins RG, Vaccaro AR, Hecht AC. Asymptomatic spinal cord compression: is surgery necessary to return to play. *Neurosurgery*. (2021) 88:955–60. doi: 10.1093/neuros/nyaa554

11. Wilson JR, Barry S, Fischer DJ, Skelly AC, Arnold PM, Riew KD, et al. Frequency, timing, and predictors of neurological dysfunction in the nonmyelopathic patient with cervical spinal cord compression, canal stenosis, and/or ossification of the posterior longitudinal ligament. *Spine*. (2013) 38:S37–54. doi: 10.1097/BRS.0b013e3182a7f2e7

12. Agrawal V, Yasin F, Yurac R, Kumar V, Murphy R, Tessitore E, et al. A systematic review of current terminology for conditions preceding degenerative cervical myelopathy: evidence to inform an AO spine expert opinion statement. *Brain Spine*. (2023) 3:102076. doi: 10.1016/j.bas.2023.102076

13. Fehlings MG, Tetreault LA, Riew KD, Middleton JW, Aarabi B, Arnold PM, et al. A clinical practice guideline for the management of patients with degenerative cervical myelopathy: recommendations for patients with mild, moderate, and severe disease and nonmyelopathic patients with evidence of cord compression. *Glob Spine J*. (2017) 7:70S–83S. doi: 10.1177/2192568217701914

14. Montgomery DM, Brower RS. Cervical spondylotic myelopathy. Clinical syndrome and natural history. *Orthop Clin North Am*. (1992) 23:487–93. doi: 10.1016/S0030-5898(20)31760-0

15. Yamaguchi S, Mitsuhara T, Abiko M, Takeda M, Kurisu K. Epidemiology and overview of the clinical spectrum of degenerative cervical myelopathy. *Neurosurg Clin N Am*. (2018) 29:1–12. doi: 10.1016/j.nec.2017.09.001

16. Nouri A, Tetreault L, Singh A, Karadimas SK, Fehlings MG. Degenerative cervical myelopathy: epidemiology, genetics, and pathogenesis. *Spine*. (2015) 40:E675–93. doi: 10.1097/BRS.0000000000000913

17. Smith SS, Stewart ME, Davies BM, Kotter MRN. The prevalence of asymptomatic and symptomatic spinal cord compression on magnetic resonance imaging: a systematic review and meta-analysis. *Glob Spine J*. (2021) 11:597–607. doi: 10.1177/2192568220934496

18. Kovalova I, Kerkovsky M, Kadanka Z, Kadanka Z, Nemec M, Jurova B, et al. Prevalence and imaging characteristics of nonmyelopathic and myelopathic spondylotic cervical cord compression. *Spine*. (2016) 41:1908–16. doi: 10.1097/BRS.0000000000001842

19. Valošek J, Bédard S, Keřkovský M, Rohan T, Cohen-Adad J (2023). A database of the healthy human spinal cord morphometry in the PAM50 template space.

20. Martin AR, De Leener B, Cohen-Adad J, Cadotte DW, Nouri A, Wilson JR, et al. Can microstructural MRI detect subclinical tissue injury in subjects with asymptomatic cervical spinal cord compression? A prospective cohort study. *BMJ Open*. (2018) 8:e019809. doi: 10.1136/bmjopen-2017-019809

21. Bednarik J, Kadanka Z, Dusek L, Kerkovsky M, Vohanka S, Novotny O, et al. Presymptomatic spondylotic cervical myelopathy: an updated predictive model. *Eur Spine J*. (2008) 17:421–31. doi: 10.1007/s00586-008-0585-1

22. Kadanka Z, Adamova B, Kerkovsky M, Kadanka Z, Dusek L, Jurova B, et al. Predictors of symptomatic myelopathy in degenerative cervical spinal cord compression. *Brain Behav*. (2017) 7:e00797. doi: 10.1002/brb3.797

23. Tempest-Mitchell J, Hilton B, Davies BM, Nouri A, Hutchinson PJ, Scoffings DJ, et al. A comparison of radiological descriptions of spinal cord compression with quantitative measures, and their role in non-specialist clinical management. *PLoS One*. (2019) 14:e0219380. doi: 10.1371/journal.pone.0219380

24. Nouri A, Tessitore E, Molliqaj G, Meling T, Schaller K, Nakashima H, et al. Degenerative cervical myelopathy: development and natural history [AO spine RECODE-DCM research priority number 2]. *Glob Spine J*. (2022) 12:39S–54S. doi: 10.1177/21925682211036071

25. Horáková M, Horák T, Valošek J, Rohan T, Koriťáková E, Dostál M, et al. Semi-automated detection of cervical spinal cord compression with the spinal cord toolbox. *Quantat Imag Med Surg*. (2022) 12:2261–79. doi: 10.21037/qims-21-782

26. De Leener B, Lévy S, Dupont SM, Fonov VS, Stikov N, Louis Collins D, et al. SCT: spinal cord toolbox, an open-source software for processing spinal cord MRI data. *NeuroImage*. (2017) 145:24–43. doi: 10.1016/j.neuroimage.2016.10.009

27. Gros C, De Leener B, Badji A, Maranzano J, Eden D, Dupont SM, et al. Automatic segmentation of the spinal cord and intramedullary multiple sclerosis lesions with convolutional neural networks. *NeuroImage*. (2019) 184:901–15. doi: 10.1016/j.neuroimage.2018.09.081

28. Cohen-Adad J, Alonso-Ortiz E, Abramovic M, Arneitz C, Atcheson N, Barlow L, et al. Open-access quantitative MRI data of the spinal cord and reproducibility across participants, sites and manufacturers. *Sci Data*. (2021) 8:219. doi: 10.1038/s41597-021-00941-8

29. Cohen-Adad J, Alonso-Ortiz E, Abramovic M, Arneitz C, Atcheson N, Barlow L, et al. Generic acquisition protocol for quantitative MRI of the spinal cord. *Nat Protoc*. (2021) 16:4611–32. doi: 10.1038/s41596-021-00588-0

30. Bednarik J, Kadanka Z, Dusek L, Novotny O, Surelova D, Urbanek I, et al. Presymptomatic spondylotic cervical cord compression. *Spine*. (2004) 29:2260–9. doi: 10.1097/01.brs.0000142434.02579.84

31. Jutzeler CR, Ulrich A, Huber B, Rosner J, Kramer JLK, Curt A. Improved diagnosis of cervical Spondylotic myelopathy with contact heat evoked potentials. *J Neurotrauma*. (2017) 34:2045–53. doi: 10.1089/neu.2016.4891

32. Valošek J, Bednařík P, Keřkovský M, Hluštík P, Bednařík J, Svatkova A. Quantitative MR markers in non-Myelopathic spinal cord compression: a narrative review. *J Clin Med*. (2022) 11:2301. doi: 10.3390/jcm11092301

33. Kerkovský M, Bednarík J, Dušek L, Šprláková-Puková A, Urbánek I, Mechl M, et al. Magnetic resonance diffusion tensor imaging in patients with cervical spondylotic spinal cord compression; correlations between clinical and electrophysiological findings. *Spine*. (2012) 37:48–56. doi: 10.1097/brs.0b013e31820e6c35

34. Keřkovský M, Bednařík J, Jurová B, Dušek L, Kadaňka Z, Kadaňka Z, et al. Spinal cord MR diffusion properties in patients with degenerative cervical cord compression. *J Neuroimaging*. (2017) 27:149–57. doi: 10.1111/jon.12372

35. Labounek R, Valošek J, Horák T, Svátková A, Bednařík P, Vojtíšek L, et al. HARDI-ZOOMit protocol improves specificity to microstructural changes in presymptomatic myelopathy. *Sci Rep*. (2020) 10:17529. doi: 10.1038/s41598-020-70297-3

36. Valošek J, Labounek R, Horák T, Horáková M, Bednařík P, Keřkovský M, et al. Diffusion magnetic resonance imaging reveals tract-specific microstructural correlates of electrophysiological impairments in non-myelopathic and myelopathic spinal cord compression. *Eur J Neurol*. (2021) 28:3784–97. doi: 10.1111/ene.15027

37. Dostál M, Keřkovský M, Staffa E, Bednařík J, Šprláková-Puková A, Mechl M. Voxelwise analysis of diffusion MRI of cervical spinal cord using tract-based spatial statistics. *Magn Reson Imaging*. (2020) 73:23–30. doi: 10.1016/j.mri.2020.07.008

38. Martin AR, De Leener B, Cohen-Adad J, Kalsi-Ryan S, Cadotte DW, Wilson JR, et al. Monitoring for myelopathic progression with multiparametric quantitative MRI. *PLoS One*. (2018) 13:e0195733. doi: 10.1371/journal.pone.0195733

39. Martin AR, De Leener B, Cohen-Adad J, Cadotte DW, Kalsi-Ryan S, Lange SF, et al. A novel MRI biomarker of spinal cord white matter injury: T2*-weighted white matter to gray matter signal intensity ratio. *AJNR Am J Neuroradiol*. (2017) 38:1266–73. doi: 10.3174/ajnr.A5162

40. Grabher P, Mohammadi S, Trachsler A, Friedl S, David G, Sutter R, et al. Voxel-based analysis of grey and white matter degeneration in cervical spondylotic myelopathy. *Sci Rep*. (2016) 6:24636. doi: 10.1038/srep24636

41. Grabher P, Mohammadi S, David G, Freund P. Neurodegeneration in the spinal ventral horn prior to motor impairment in cervical Spondylotic myelopathy. *J Neurotrauma*. (2017) 34:2329–34. doi: 10.1089/neu.2017.4980

42. Valošek J, Bednařík P, Horák T, Horáková M, Svátková A, Labounek R, et al. (2020). "Cervical spinal cord atrophy above level of asymptomatic degenerative cervical cord compression" in *Proceedings of the 26th Annual Meeting of the Organization for Human Brain Mapping, Virtual*. p. 3136.

43. Horak T, Horakova M, Svatkova A, Kadanka Z, Kudlicka P, Valosek J, et al. In vivo molecular signatures of cervical spinal cord pathology in degenerative compression. *J Neurotrauma*. (2021) 38:2999–3010. doi: 10.1089/neu.2021.0151

44. Torg JS, Naranja RJ, Pavlov H, Galinat BJ, Warren R, Stine RA. The relationship of developmental narrowing of the cervical spinal canal to reversible and irreversible injury

of the cervical spinal cord in football players. *J Bone Joint Surg Am*. (1996) 78:1308–14. doi: 10.2106/00004623-199609000-00003

45. Bajwa NS, Toy JO, Young EY, Ahn NU. Establishment of parameters for congenital stenosis of the cervical spine: an anatomic descriptive analysis of 1,066 cadaveric specimens. *Eur Spine J*. (2012) 21:2467–74. doi: 10.1007/s00586-012-2437-2

46. Singh A, Tetreault L, Fehlings MG, Fischer DJ, Skelly AC. Risk factors for development of cervical spondylotic myelopathy: results of a systematic review. *Evid Spine Care J*. (2012) 3:35–42. doi: 10.1055/s-0032-1327808

47. Nakashima H, Yukawa Y, Suda K, Yamagata M, Ueta T, Kato F. Relatively large cervical spinal cord for spinal canal is a risk factor for development of cervical spinal cord compression: a cross-sectional study of 1211 subjects. *Spine*. (2016) 41:E342–8. doi: 10.1097/BRS.0000000000001255

48. Nouri A, Montejo J, Sun X, Virojanapa J, Kolb LE, Abbed KM, et al. Cervical Cord-Canal mismatch: a new method for identifying predisposition to spinal cord injury. *World Neurosurg*. (2017) 108:112–7. doi: 10.1016/j.wneu.2017.08.018

49. Nouri A, Tetreault L, Nori S, Martin AR, Nater A, Fehlings MG. Congenital cervical spine stenosis in a multicenter global cohort of patients with degenerative cervical myelopathy: an Ambispective report based on a magnetic resonance imaging diagnostic criterion. *Neurosurgery*. (2018) 83:521–8. doi: 10.1093/neuros/nyx521

50. Rüegg TB, Wicki AG, Aebli N, Wisianowsky C, Krebs J. The diagnostic value of magnetic resonance imaging measurements for assessing cervical spinal canal stenosis. *J Neurosurg Spine*. (2015) 22:230–6. doi: 10.3171/2014.10.SPINE14346

51. Presciutti SM, DeLuca P, Marchetto P, Wilsey JT, Shaffrey C, Vaccaro AR. Mean subaxial space available for the cord index as a novel method of measuring cervical spine geometry to predict the chronic stinger syndrome in American football players. *J Neurosurg Spine*. (2009) 11:264–71. doi: 10.3171/2009.3.SPINE08642

52. Nouri A, Martin AR, Mikulis D, Fehlings MG. Magnetic resonance imaging assessment of degenerative cervical myelopathy: a review of structural changes and measurement techniques. *Neurosurg Focus*. (2016) 40:E5. doi: 10.3171/2016.3.FOCUS1667

53. Harrop JS, Naroji S, Maltenfort M, Anderson DG, Albert T, Ratliff JK, et al. Cervical myelopathy: a clinical and radiographic evaluation and correlation to cervical spondylotic myelopathy. *Spine*. (2010) 35:620–4. doi: 10.1097/BRS.0b013e3181b723af

54. Nouri A, Martin AR, Kato S, Reihani-Kermani H, Riehm LE, Fehlings MG. The relationship between MRI signal intensity changes, clinical presentation, and surgical outcome in degenerative cervical myelopathy: analysis of a global cohort. *Spine*. (2017) 42:1851–8. doi: 10.1097/BRS.0000000000002234

55. Witiw CD, Mathieu F, Nouri A, Fehlings MG. Clinico-radiographic discordance: an evidence-based commentary on the Management of Degenerative Cervical Spinal Cord Compression in the absence of symptoms or with only mild symptoms of myelopathy. *Glob Spine J*. (2018) 8:527–34. doi: 10.1177/2192568217745519

56. Bednařík J, Sládková D, Kadaňka Z, Dušek L, Keřkovský M, Voháňka S, et al. Are subjects with spondylotic cervical cord encroachment at increased risk of cervical spinal cord injury after minor trauma? *J Neurol Neurosurg Psychiatry*. (2011) 82:779–81. doi: 10.1136/jnnp.2009.198945

57. Chang V, Ellingson BM, Salamon N, Holly LT. The risk of acute spinal cord injury after minor trauma in patients with preexisting cervical stenosis. *Neurosurgery*. (2015) 77:561–5. doi: 10.1227/NEU.0000000000000888

frontiers | Frontiers in Oncology

TYPE Case Report
PUBLISHED 28 May 2024
DOI 10.3389/fonc.2024.1417268

OPEN ACCESS

EDITED BY
Qingchun Mu,
Second Affiliated Hospital of Soochow University, China

REVIEWED BY
Jinlu Yu,
First Affiliated Hospital of Jilin University, China
Xiangyi Meng,
First Affiliated Hospital of Harbin Medical University, China

*CORRESPONDENCE
Jungang Xue
xuejungang002@outlook.com
Wenyuan Wei
Xahhweiweny@outlook.com

RECEIVED 14 April 2024
ACCEPTED 07 May 2024
PUBLISHED 28 May 2024

CITATION
Dang Y, Du A, Wei W and Xue J (2024) Primary cervicothoracic melanoma of spinal cord: a case report and literature review. *Front. Oncol.* 14:1417268. doi: 10.3389/fonc.2024.1417268

Primary cervicothoracic melanoma of spinal cord: a case report and literature review

Ying Dang[1,2], Aichao Du[2], Wenyuan Wei[1]* and Jungang Xue[1]*

[1]Department of Neurosurgery, Honghui Hospital, Xi'an Jiaotong University, Xi'an, Shaanxi, China, [2]Department of Neurosurgery, The Second Hospital of Lanzhou University, Lanzhou, China

A 53-year-old male patient presented progressive numbness and weakness in the right limbs for a 2-year duration. Magnetic resonance imaging scans revealed an intramedullary lesion crossed over cervical and thoracic levels accompanied by syringomyelia at the proximal end of the lesion. The patient underwent subtotal resection of the neoplasm. The histological findings of the tumor were consistent with primary intramedullary malignant melanoma and not initial ependymoma after careful dermatologic and ophthalmologic re-examination. Primary melanoma of the spinal cord, particularly cervicothoracic localization with syringomyelia, is seldom reported in the literature. We report a case of this uncommon tumor and also discuss the clinical course, diagnosis, and treatment.

KEYWORDS

primary, cervicothoracic, spinal cord, electromyogram, CSEP, DSEP

Introduction

Malignant melanomas are rarely seen as aggressive tumors that arise from the pigment-producing melanocytes. The World Health Organization classifies primary melanocytic tumors of the central nervous system (CNS) into meningeal melanomatosis, meningeal melanocytoma, meningeal melanoma, and meningeal melanocytosis (1). Primary melanomas of the CNS are rare. The occurrence of primary spinal melanoma is extremely rare, and only <70 cases have been reported in the literature since Hirschberg first reported primary spinal cord melanoma in 1906 (2). Spinal cord melanoma usually shows signal hyperintensity on T1-weighted images and signal hypointensity on T2-weighted images (3), with mild contrast enhancement of the lesion (4). However, the mass of our case appeared iso- and hypointense on T1-weighted images and non-homogeneous hypointensity on T2-weighted images accompanied by syringomyelia at the proximal end of the lesion. Moreover, the intramedullary melanoma in the presented case crossed over cervical and thoracic levels, which is seldom reported in the literature. Here, we present this uncommon case to add variety to clinical databases and discuss the clinical course, diagnosis, and treatment for primary spinal melanomas.

Case description

History and examination

A 53-year-old man was admitted to the hospital for progressive numbness and weakness in the right limbs for a 2-year duration. The neurological examination revealed 3/5 strength in the right arm and right leg with no other neurological positive signs. An electromyogram (EMG) showed a decreased rate and lengthened latent period of the F-wave on the median nerve and ulnar nerve in the right. Cortical somatosensory evoked potential (CSEP) and dermatomal somatosensory evoked potential (DSEP) revealed the disappearance of P1-wave, suggesting handicap of somatosensory conduction pathways of the right dorsal spinocerebellar tract under the C5 level. Beyond an elevated C-reactive protein level (179.48 mg/L, 0–5 mg/L), the results of routine blood chemical analysis and serum carcinoembryonic antigen were normal.

Magnetic resonance imaging (MRI) of the spine revealed a mixture of iso- and hypointense intramedullary mass at the C6–T4 level on T1-weighted images and non-homogeneous hypointensity on T2-weighted images (Figures 1A, B). After administration of contrast material, slightly non-homogeneous enhancement of the focal lesion at the T2–T3 level was observed (Figure 1C). Moreover, long T1 and long T2 signals with the increased signal intensity of fat-suppressed images at the level between the medulla and C6 indicated syringomyelia at the proximal end of the lesion (Figures 1D–F). The appearance of the lesion on MRI was misdiagnosed as ependymoma initially in this case.

Operation and pathological examination

Operation

The patient underwent a C6–T4 laminectomy through a midline incision in the upper thoracic back. The epidural space was absolutely free of tumors with no pathological findings in the extravertebral soft tissues, spinous processes, or laminas. At the dural opening, a black tumor with multiple small satellite lesions under the pia was observed, and the main tumor was found to be apparently infiltrated with the parenchyma (Figure 2A). After the spinal cord incision, the coal cinder-like lesions were removed in piecemeal, and multiple biopsies were taken (Figures 2B, C). However, the lack of a clear cleavage plane between the tumor and normal tissue rendered surgical gross total resection (GTR)

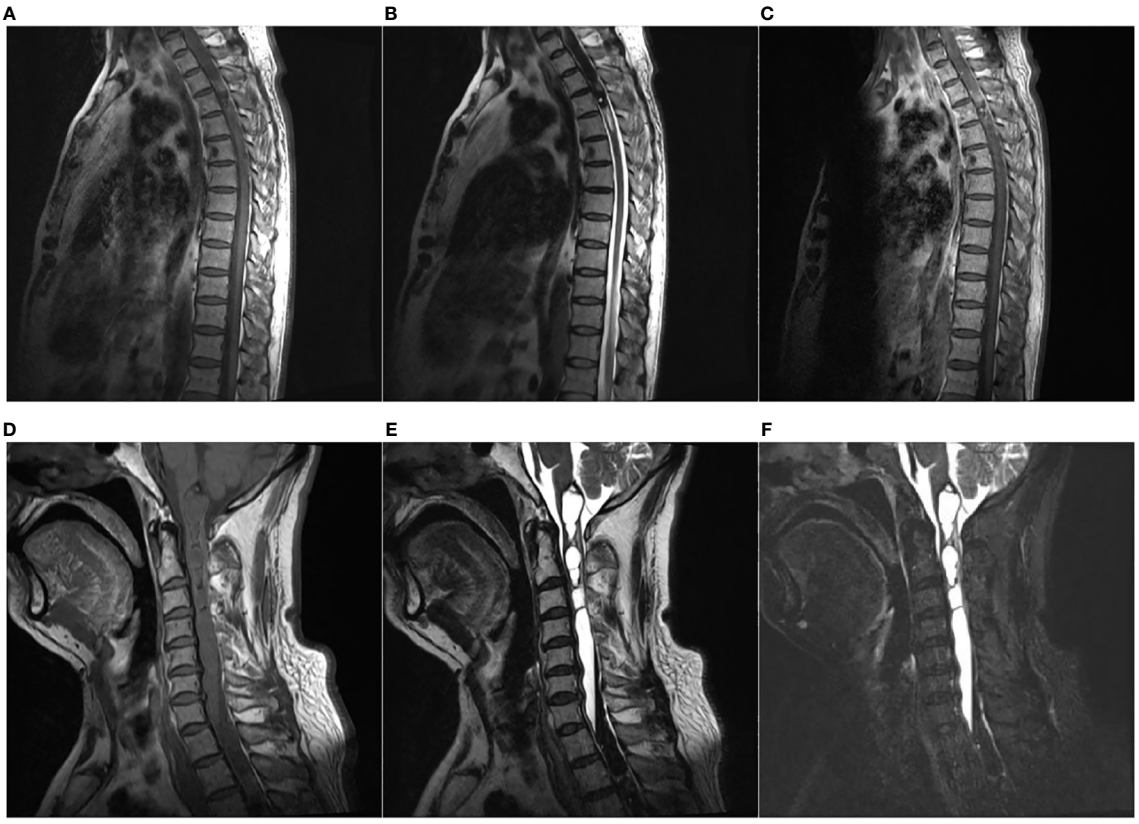

FIGURE 1
Magnetic resonance imaging (MRI). **(A–C)** An intramedullary tumor was located at C6–T4 with mixture of iso- and hypointensity on sagittal T1-weighted image (T1WI) **(A)**, non-homogeneous hypointensity on sagittal T2-weighted image (T2WI) **(B)**, and slightly non-homogeneous enhancement on sagittal T1WI with gadolinium **(C)**. **(D, E)** Long T1 [**(D)**, sagittal] and long T2 [**(E)**, sagittal] signals with increased signal intensity of fat-suppressed images [**(F)**, sagittal] at the level between medulla and C6 suggestive of syringomyelia at the proximal end of the lesion.

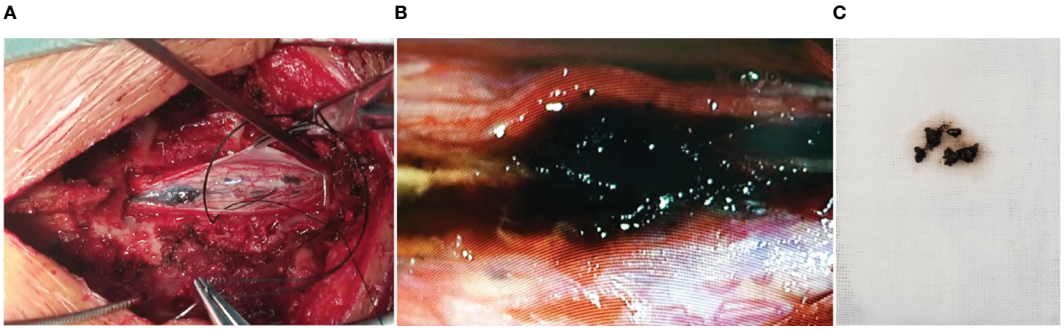

FIGURE 2
Intraoperative photograph showing the darkly pigmented intramedullary lesion with multiple small satellite lesions under the pia **(A)**. After spinal cord incision, the coal cinder-like lesions were removed in piecemeal, and multiple biopsies were taken **(B, C)**.

unachievable, and the tumor was debulked to the greatest possible extent.

Histopathological features

Microscopic examination revealed that the tumor consisted of an abundance of ovoid, spindle, or polygonal tumor cells and was arranged in nests and sheets accompanying the deposition of abundant melanin granules (Figure 3A). Higher magnification of the lesions showed significant cellular pleomorphism with nuclear atypia and enlargement and a high nuclear-to-cytoplasmic ratio (Figure 3B). Necrotic areas were also seen, but no evidence of hemorrhage or products of its degeneration was identified, and tumor cells with granular cytoplasmic pigmentation were arranged around the vascellum (Figures 3C, D). Immunohistochemical examination showed that the neoplastic cells stained strongly positive for antimelanoma antibody (HMB-45), S-100, and MelanA, and Ki-67 staining showed high proliferative index (50%), both pointing to malignant melanoma of the spinal cord (Figures 3E–H).

Postoperative course

Subsequent examinations, including dermatological physical examination and ophthalmologic fundoscopic examination, endoscopy of the gastrointestinal tract, contrast-enhanced thoracoabdominal computed tomography (CT), and cranial MRI revealed no evidence of primary origin of the melanoma in other parts of the body. The final diagnosis of primary spinal malignant melanoma was confirmed. The patient refused any further aggressive or adjuvant treatment and was discharged to a rehabilitation facility. Postoperative telephone follow-up was performed periodically. At the last follow-up assessment,

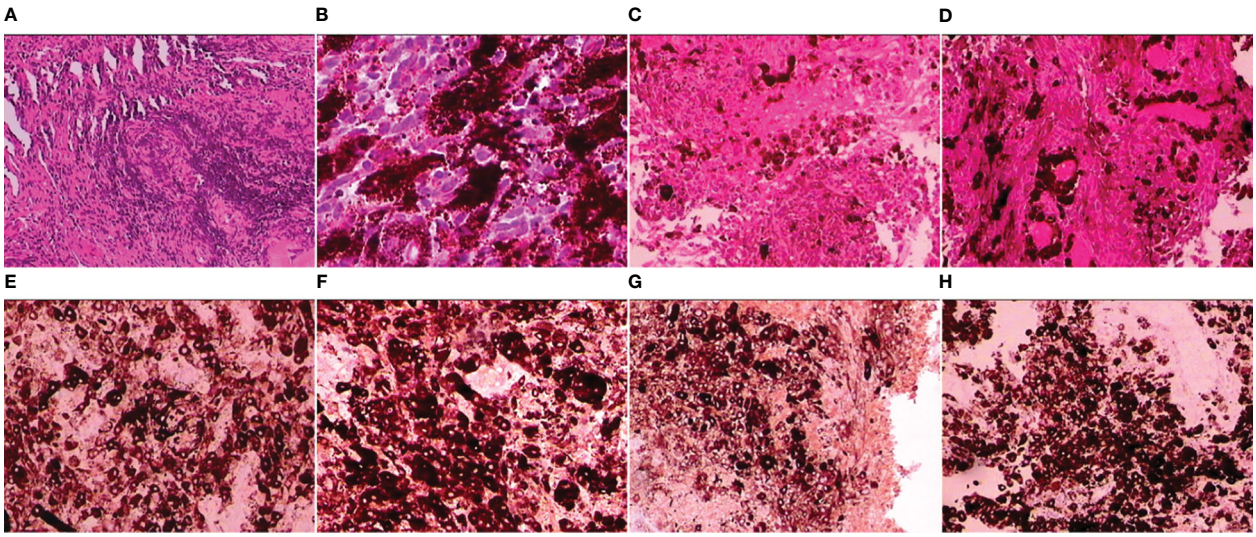

FIGURE 3
Neoplasm was densely cellular arranged in nests and sheets with deposition of abundant melanin pigment [**(A)**; hematoxylin and eosin (H&E), magnification ×100]; pleomorphic ovoid, spindle, or polygonal cells with significant nuclear atypia characterized by large nuclei, high nuclear-to-cytoplasmic ratio, and scattered mitosis [**(B)**; H&E, magnification ×200]; representative necrosis in the tumor [**(C)**; H&E, magnification ×200]; tumor cells with granular cytoplasmic pigmentation were arranged around the vascellum [**(D)**; H&E, magnification ×200]; positive staining for HMB-45, S-100, and MelanA [**(E–G)**; magnification ×200]; Ki-67 labeling indices counted more than 50% denoted pigmented cells that were mitotically active [**(H)**; magnification ×200].

the patient had an uneventful recovery with no clinical deterioration and no additional complications after postoperative 6 months.

Discussion

Although primary spinal melanoma is extremely rare, the high disability and mortality rate of this tumor have attracted more attention recently. Computer searches were performed on MEDLINE/PubMed (2018 to date), Embase (2018 to date), Cochrane Library, China National Knowledge Infrastructure (CNKI), Chinese Biomedical Database (CBM), and Wanfang databases. The search terms were as follows: spinal, Myelon, Cervical cord, Thoracic Cord, intramedullary, intra-medullary, and others. Here, recent literature on spinal cord melanoma was collected and systematically reviewed (Table 1), and a thorough review of the available literature was performed. There are some interesting points that need to be discussed, as follows.

1. Clinical features: The clinical symptoms and signs of primary spinal cord melanoma are often non-specific. The presenting symptoms are predominantly those of spinal cord compression and neurological deficits, which are dependent on tumor location. Some patients may present with elevated intracranial pressure due to obstruction of the cerebrospinal fluid (CSF) circulation, although the occurrence of this is rare (12). The mean symptom duration in previous cases was 15 months and ranged from 0.3 to 96 months (13). Primary spinal malignant melanoma most frequently presents as a middle or lower thoracic cord lesion (14), probably because of the normally higher density of melanocytes in these locations. Primary spinal melanomas are usually located in the intradural extramedullary or intramedullary compartment. Less commonly, these tumors are extradural or spread out along the nerve root sheaths to involve the extradural tissue (15, 16). M. Zhang et al. reported that across 60 cases of primary spinal melanomas, 30.51% of the tumors were cervical, 52.54% were thoracic, and 16.95% were lumbar; 37.74% of the tumors were located intramedullary, and 62.26% were located extramedullary (2). Primary spinal melanoma can also give rise to metastases or diffuse leptomeningeal dissemination, although the occurrence of this is rare (17, 18). In this case, the 53-year-old male patient presented progressive numbness and weakness in the right limbs for a 2-year duration, and the intramedullary lesion was located at the C6–T4 level. A spinal cord lesion is not usually suspected at the presentation of the first symptoms; therefore, the diagnosis of a primary spinal melanoma may be delayed, and leptomeningeal dissemination may progress before a definitive diagnosis.

2. Auxiliary examination:

2.1 MRI: Primary spinal melanoma should be suspected when T1-weighted images show signal hyperintensity and when T2-weighted images show signal iso- or hypointensity, with mild contrast enhancement of the lesion (3). MRI may offer some indication of a melanotic lesion, but the rarity of a primary melanotic lesion in the CNS most often precludes the preoperative radiological diagnosis of this lesion. However, primary malignant melanoma varies in its imaging features, based on the degree of melanocytic content and the presence of hemorrhage and fat (19). In our case, the appearance of the lesion on MRI images was partly in accordance with the reported findings in the literature. T1-weighted images of our case revealed signal iso- and hypointensity at the C6–T4 level, and T2-weighted images showed signal non-homogeneous hypointensity (Figures 1A, B). After administration of contrast material, mild and non-homogeneous enhancement was observed in the foci of the lesion (Figure 1C). Different from previous cases, MRI images of our case appeared long T1 and T2 signals with increased signal intensity of fat-suppressed images at the level between the medulla and C6, which indicated syringomyelia at the proximal end of the lesion (Figures 1D–F). These differences in MRI signal intensities are related to the degree of the paramagnetic effects of stable free radicals in melanin and/or hemorrhagic products (20). The syringomyelia in this case was probably caused by obstructing cerebrospinal drainage by the spinal cord lesion. Nevertheless, the MRI pattern may correspond to that of other pigmented tumors, such as meningeal melanocytoma, melanotic schwannoma, or a tumoral hemorrhagic lesion (21). MRI patterns can easily suggest an erroneous diagnosis. In our patient, although the signal pattern on MRI was partly in accordance with that usually seen in occupying melanotic neoplasm, the long duration of symptoms, the rounded borders of the tumor, and the presence of an associated intramedullary cyst on MRI suggested an initial diagnosis of ependymoma. The ultimate diagnosis must be made following histopathologic examination.

2.2 PET/CT: In addition to MRI, positron emission tomography/CT (PET/CT) has become a useful imaging modality for the auxiliary examination of malignant melanomas (22). Indeed, some authors have reported the accuracy of PET as being almost 91% when diagnosing the local and distant involvement of malignant melanoma (23). A primary origin outside the spinal cord can be excluded after PET scanning (24), which plays a more and more important role in distinguishing the primary from the metastatic spinal melanoma.

2.3 Gene examination: Gene analysis on genomic DNA to determine the presence of possible oncogenic somatic mutations has become a new tool for early discovery and further targeted therapy of malignant melanoma. Some authors have reported that characteristic mutations in BRAF, NRAS, and CDKN2A are frequently seen in cutaneous melanoma (25). G. Angelino et al. reported a case of primary leptomeningeal melanoma with the presence of an $NRAS^{Q61K}$ mutation (26).

3. Histopathological features: Histopathological analysis is indispensable for the confirmative diagnosis of primary spinal melanoma from other similar lesions. Malignant melanoma is characterized by positive immunohistochemical reaction to HMB-45, MelanA, and S-100 protein. Furthermore, the high Ki-67 labeling index indicates the high malignant potential of the lesions, which is a protein highly expressed in proliferating cells and encoded by the *MIB-1* gene. In addition, vimentin, Leu7, and epithelial membrane antigen (EMA) can be used to distinguish spinal melanoma from other different spinal tumors undergoing melanization, such as meningeal melanocytoma, meningioma, schwannoma, medulloblastoma, and gliomas (27). In our case,

TABLE 1 Literature review of primary malignant spinal cord melanoma.

Author (year)	Age	Sex	Location	Duration (months)	Symptoms	Treatment	EOR	Follow-up (months)	Outcome	Recurrence or metastases
Armocida D (5) (2018)	60	M	Thoracic	4	Radiating right side low back pain and paraesthesia	Surgery	GTR	1	Alive	No
Kohei Hironaka (6) (2019)	39	M	Lumbar and sacrum	—	Headache, papilledema, hydrocephalus, ventricular dilatation, aneurysm, progressive gait disturbance, dysuria	Surgery	Aneurysm clipping, ventriculoperitoneal (VP) shunt Codman	14	Died	No
Ritodhi (7) (2019)	78	M	Cervical and thoracic	2	Fatigue, increased right-side weakness, paresthesia, urinary incontinence	Surgery	GTR	18	Alive	No
Tang S (8) (2020)	55	M	Lumbar	36	Low back pain with toe paralysis and sensory disturbances	Surgery	GTR	5	Alive	Yes
Corrêa DG (9) (2020)	78	M	Thoracic	6	Progressive myasthenia was lower limb paralysis	Surgery +radiotherapy+chemotherapy	GTR	—	Alive	Yes
Akgun MY (10) (2020)	30	F	Cervical	Less than a month	Decreased sensation	Surgery	GTR	84	Alive	No
Hongbo Lv (11) (2021)	67	M	Thoracic	12	Progressive calf tremor and paroxysmal convulsions, numbness and weakness of the legs, paraplegia, and dysuria	Surgery	GTR	3	Alive	No
Our one	53	M	Cervical and thoracic	24	Progressive numbness and weakness of the limbs	Surgery	STR	12	Alive	No

M, male; F, female; EOR, extent of resection; GTR, gross total resection; STR, subtotal resection; —, unclear.

10.3389/fonc.2024.1417268

the immunohistochemical examination showed that the neoplastic cells stained strongly positive for HMB-45, S-100, and MelanA, and Ki-67 staining showed a high proliferative index (50%), pointing to a confirmative pathological diagnosis of malignant melanoma. Nevertheless, our immunohistochemical examination also showed positive EMA, cytokeratin pan (CK), and smooth muscle actin (SMA) staining, which suggested that the tumor may be heterologous (Supplementary Figures 1A–C). As far as we were able to determine, the strong positivity of characteristic markers such as HMB-45, S-100, and MelanA lent support to the pathological diagnosis of malignant melanoma because of the non-specificity of the markers EMA, CK, and SMA.

4. Differential diagnosis: According to Hayward's criteria, diagnosis of a primary melanoma must consider the following factors: 1) malignant melanoma outside the CNS was not detected, 2) absence of this lesion in other sites in the CNS, and 3) the intramedullary lesion was confirmed pathologically (16). Our case was in accordance with these criteria. However, preoperative diagnosis of primary spinal melanoma is often difficult since the gross pathological, histological, and radiological features of the many varied spinal lesions overlap. The differential diagnosis of spinal pigmented lesions includes meningeal melanocytoma, metastatic malignant melanoma, and other uncommon melanotic tumors such as neurocutaneous melanosis, leptomeningeal melanomatosis, and melanotic schwannoma.

4.1 Meningeal melanocytoma: According to Brat, meningeal melanocytoma and malignant melanoma both arising from the normal melanocytic cells in the leptomeninges are the two extremes of a spectrum of primary melanocytic neoplasms ranging from low-grade to high-grade in the CNS (28). Melanoma and melanocytoma may be distinguished from each other on the basis of pathological features and clinical behavior (19). Pathologically, melanocytomas are well-differentiated tumors with benign histological features, and the lack of mitotic activity, nuclear pleomorphism, and hyperchromaticity is a characteristic that indicates melanocytoma rather than melanoma (29). Nevertheless, distinguishing between malignant melanoma and well-differentiated melanocytoma remains a diagnostic challenge. Hoffmann et al. recently suggested that molecular analysis is the best method for distinguishing between melanocytoma and malignant melanoma (30). Moreover, melanocytomas were usually cured by gross total resection alone with lower levels of local recurrence and mortality than melanomas (28).

4.2 Metastatic malignant melanoma: Although the CNS is a common site of metastases from malignant melanoma, which is the third most common neoplasm to metastasize to the CNS, spinal metastatic melanoma is extremely rare with accompanying multiple lesions in other sites of the CNS (31). K.D. Barron et al. reported malignant melanoma metastatic to the spinal cord and coverings that occurred only once in a series of 127 metastatic lesions of the spinal cord verified by autopsy (32). In addition, Z. Gokaslan et al. also reported intramedullary spinal cord metastasis that unusually occurred in as few as 2% of autopsy cases of systemic cancers and usually signified a late-stage event for the patient (33). Patients with melanoma metastatic to the CNS have a poor prognosis, with a median survival of 113 days after discovery (34). It is obviously important to determine if the melanoma is primary or secondary. However, in some cases, the primary tumor remains undetectable, and thus, it is difficult to differentiate metastases from primary spinal melanoma. A thorough physical examination to search for a primary cutaneous, mucosal, or ocular melanoma is recommended and is usually sufficient to exclude evidence of systemic disease (31). However, this is all the more difficult when one considers that achromic cutaneous melanomas exist, that metastatic melanomas of the skin can appear following the complete disappearance of a primitive melanoma, and finally that authentic primary melanomas of the central nervous system can metastasize elsewhere (35, 36). Moreover, Bergdahl et al. concluded that primary malignant melanomas of the CNS may also metastasize inside and outside the CNS (37). Recently, some authors have applied non-invasive PET/CT scanning to search for primary concealed malignant melanoma outside the CNS to substantiate the diagnosis (24).

4.3 Other melanotic tumors

4.3.1 Neurocutaneous melanosis: Neurocutaneous melanosis is one of the most infrequent neoplastic lesions of the CNS, which is characterized by the presence of congenital melanocytic cutaneous nevi associated with intracranial leptomeningeal melanocytosis. Compared with primary melanoma, neurocutaneous melanosis is associated with large or multiple congenital nevi, and the age of patients is usually younger (37).

4.3.2 Leptomeningeal melanomatosis: Primary leptomeningeal melanomatosis is a rare, diffuse neoplasm of the CNS that arises from melanocytes within the leptomeninges. It is also referred to as a meningeal variant of primary malignant melanoma (38). However, the morphological characteristics of leptomeningeal melanomatosis are diffuse darkening and thickening of the leptomeninges in the gross specimen. The CT and MR imaging also reveal diffuse thickening of the leptomeninges, with abnormal enhancement on the postcontrast images.

4.3.3 Melanotic schwannoma: Melanotic schwannomas are rare primary lesions in the CNS that consist of neoplastic Schwann cells and proliferating melanocytes (39). These lesions are more typically intracranial, but they also occur within the spinal canal. When they develop within the spine, the tumors most often arise in the thoracic region, and they may be intramedullary (40). Compared with spinal melanoma, melanotic schwannoma is usually well-circumscribed, and the behavior of this neoplasm is typically benign. Moreover, results from immunohistochemical staining help secure differential diagnosis. Melanotic schwannomas stain positive for S-100 protein Leu7 and vimentin but stain variably with glial fibrillary acid protein, HMB-45, and other melanocytic markers.

Other melanotic tumors like melanocytic glioma and medulloblastoma are very rare and are usually distinguished from spinal melanoma by pathological and immunohistochemical characteristics.

5. Treatment: Because of the rarity of primary spinal melanomas, the development of a standard treatment protocol is difficult. As case reports have accumulated, most clinicians have generally accepted the view that treatment for primary spinal melanoma needs multidisciplinary management (41).

Surgical GTR offers patients the greatest chance for survival (13). Unfortunately, most patients with intramedullary melanoma have many or diffuse lesions with ill-demarcated neural tissue, and GTR is not feasible. In our case, subtotal resection (STR) of the intramedullary tumor was achieved.

The role of adjuvant radiotherapy and chemotherapy for primary spinal melanoma is still controversial. Some authors have suggested radiotherapy and chemotherapy for preventing local tumor recurrence and dissemination combined with GTR or even STR (41), but others have claimed that the procedure may be ineffective and produce radiation-induced toxicity (19). To the best of our knowledge, adjuvant radiotherapy and chemotherapy should be integrated with surgical resection, especially subtotal resection, though malignant melanomas are considered to be highly radio-resistant tumors (42). Liang Wu et al. performed adjuvant radiotherapy in four STR patients, and three of them showed no recurrence during follow-up (24). Chemotherapy, including intrathecal administration, has been attempted. B.C. Bae et al. reported a favorable outcome of primary spinal melanoma with chemotherapy including vincristine, bleomycin, and cisplatin. Intrathecal methotrexate, interleukin-2, and dacarbazine (DTIC) have been reported for primary CNS melanomas and may be effective in controlling tumor progression for a certain period (43). However, there is little evidence that radiotherapy and chemotherapy are effective for primary spinal melanoma, and the efficacy remains to be assessed in a larger series.

Immunotherapies such as interferon-α, interferon-γ, and lymphokine-activated killer (LAK) cells have been applied to other melanomas (43). Additionally, polyvalent melanoma vaccine has also been tried in malignant melanoma patients with minimal residual disease after resection of the tumor, which shows encouraging results with prolonged survival of several years (44). Newly emerged targeted immunotherapy has shown some positive effects. Ganesh et al. reported a series of metastatic spinal melanoma patients who underwent regular immunotherapy and acquired longer median survival (45). Zhang et al. reported that the use of PD-1 or PD-L1 antibodies has some effect in preventing tumor local recurrence of spinal malignant melanomas (46). This new management can be attempted in primary CNS melanomas.

6. Prognosis: In general, the prognosis of primary spinal melanoma varies depending on the site of the initial primary and the presence or absence of other visceral involvement (31). The survival duration of patients with primary spinal melanoma ranged from 3 to 156 months (12, 14). The mean survival time of patients who have undergone surgical excision of spinal cord melanoma with or without additional treatment is 6 years 7 months after the onset of symptoms (41). According to a retrospective study, the 12-month survival was 89.6% and the 72-month survival was 39.6% (2). These tumors are potentially malignant and liable to recurrences locally, or at a distance within the CNS (47), and they rarely metastasize to outside or inside the central nervous system. Leptomeningeal seeding and hydrocephalus are poor prognostic factors in melanomas, which means disease progression and difficulty in archiving total removal of the melanoma (48). Beyhan et al. suggested that the prognosis for dural melanoma is better than that for leptomeningeal melanoma because of no involvement of the leptomeninges (49).

7. Conclusion: In conclusion, although primary spinal melanomas are rare, we should suspect this tumor if the MRI depicts a spinal cord tumor with paramagnetic properties. Surgical removal with multidisciplinary management is recommended. To the best of our knowledge, the presented report is unique in that the intramedullary lesion crossed between cervical and thoracic levels and showed iso- and hypointense on T1-weighted images accompanying syringomyelia at the proximal end of the lesion. The final diagnosis was primary spinal melanoma based on the results of pathological examination. Further studies with larger sample sizes are required to collect more imaging data and establish well-defined diagnostic criteria and treatment strategies.

Data availability statement

The datasets presented in this study can be found in online repositories. The names of the repository/repositories and accession number(s) can be found in the article/Supplementary Material.

Ethics statement

The studies involving humans were approved by Ethics Committee of Xi'an Honghui Hospital. The studies were conducted in accordance with the local legislation and institutional requirements. The participants provided their written informed consent to participate in this study. Written informed consent was obtained from the individual(s) for the publication of any potentially identifiable images or data included in this article.

Author contributions

YD: Investigation, Writing – original draft, Writing – review & editing. AD: Writing – review & editing. WW: Supervision, Writing – review & editing. JX: Supervision, Writing – review & editing.

Funding

The author(s) declare financial support was received for the research, authorship, and/or publication of this article. This work was supported by the Natural Science Foundation of Shaanxi Province (Clinical Application of Preoperative Magnetic Resonance Tomography Angiography for Evaluating Assisted Microvascular Decompression in the Treatment of Cranial Nerve Diseases; Project No. 2023-YBSF-088).

Acknowledgments

We thank the patient for permitting us to use his data to complete this article.

Conflict of interest

The authors declare that the research was conducted in the absence of any commercial or financial relationships that could be construed as a potential conflict of interest.

Publisher's note

All claims expressed in this article are solely those of the authors and do not necessarily represent those of their affiliated organizations, or those of the publisher, the editors and the reviewers. Any product that may be evaluated in this article, or claim that may be made by its manufacturer, is not guaranteed or endorsed by the publisher.

Supplementary material

The Supplementary Material for this article can be found online at: https://www.frontiersin.org/articles/10.3389/fonc.2024.1417268/full#supplementary-material

SUPPLEMENTARY FIGURE 1
Positive staining for epithelial membrane antigen (EMA), cytokeratin pan (CK), smooth muscle actin (SMA) [**(A–C)**, magnification: 200×].

References

1. Louis DN, Perry A, Reifenberger G, von Deimling A, Figarella-Branger D, Cavenee WK, et al. The 2016 world health organization classification of tumors of the central nervous system: a summary. *Acta Neuropathol*. (2016) 131:803–20. doi: 10.1007/s00401–016-1545–1

2. Zhang M, Liu R, Xiang Y, Mao J, Li G, Ma R, et al. Primary spinal cord melanoma: A case report and a systemic review of overall survival. *World Neurosurg*. (2018) 114:408–20. doi: 10.1016/j.wneu.2018.03.169

3. Farrokh D, Fransen P, Faverly D. MR findings of a primary intramedullary Malignant melanoma: case report and literature review. *AJNR Am J neuroradiology*. (2001) 22:1864–6.

4. Yamasaki T, Kikuchi H, Yamashita J, Asato R, Fujita M. Primary spinal intramedullary Malignant melanoma: case report. *Neurosurgery*. (1989) 25:117–21. doi: 10.1097/00006123–198907000–00023

5. Armocida D, Pesce A, Berra LV, Marzetti F, Antonelli M, Santoro A. Intradural extramidullary dorsal melanocytoma in the adult: Case report and review of the literature. *J Clin neuroscience: Off J Neurosurgical Soc Australasia*. (2019) 62:248–53. doi: 10.1016/j.jocn.2018.12.004

6. Hironaka K, Tateyama K, Tsukiyama A, Adachi K, Morita A. Hydrocephalus secondary to intradural extramedullary Malignant melanoma of spinal cord. *World neurosurgery*. (2019) 130:222–6. doi: 10.1016/j.wneu.2019.07.046

7. Chatterjee R, Nascimento FA, Heck KA, Ropper AE, Sabichi AL. Primary spinal cord melanoma - an uncommon entity. *Can J neurological Sci Le J canadien Des Sci neurologiques*. (2019) 46:348–50. doi: 10.1017/cjn.2019.28

8. Tang S, Zuo J, Zhang H, Wu Z, Liang B. Spinal metastatic melanoma with unknown primary lesions presenting as radiculopathy: Case report and literature review. *World neurosurgery*. (2020) 140:320–4. doi: 10.1016/j.wneu.2020.05.067

9. Corrêa DG, Dos Santos RQ, Hygino da Cruz LC Jr. Primary intramedullary Malignant melanoma: can imaging lead to the correct diagnosis? *J Int Med Res*. (2020) 48:300060520966152. doi: 10.1177/0300060520966152

10. Akgun MY, Isler C, Ulu MO. C6-T1 intradural extramedullary ventral meningeal melanocytoma resected via anterior corpectomy with reconstruction. *World neurosurgery*. (2020) 138:457–60. doi: 10.1016/j.wneu.2020.03.122

11. Lv H, Song C, Li W, Liu Y. Orthostatic tremor secondary to primary Malignant melanoma of the spinal cord: A case report. *Eur J neurology*. (2022) 29:942–6. doi: 10.1111/ene.15208

12. Kounin GK, Romansky KV, Traykov LD, Shotekov PM, Stoilova DZ. Primary spinal melanoma with bilateral papilledema. *Clin Neurol neurosurgery*. (2005) 107:525–7. doi: 10.1016/j.clineuro.2004.10.013

13. Kim MS, Yoon DH, Shin DA. Primary spinal cord melanoma. *J Korean Neurosurgical Society*. (2010) 48:157–61. doi: 10.3340/jkns.2010.48.2.157

14. Larson TC 3rd, Houser OW, Onofrio BM, Piepgras DG. Primary spinal melanoma. *J neurosurgery*. (1987) 66:47–9. doi: 10.3171/jns.1987.66.1.0047

15. Naing A, Messina JL, Vrionis FR, Daud AI. Uncommon manifestations of common Malignancies: case 3. Malignant melanoma arising from a spinal nerve root. *J Clin oncology: Off J Am Soc Clin Oncol*. (2004) 22:3194–5. doi: 10.1200/jco.2004.09.021

16. Hayward RD. Malignant melanoma and the central nervous system. A guide for classification based on the clinical findings. *J neurology neurosurgery Psychiatry*. (1976) 39:526–30. doi: 10.1136/jnnp.39.6.526

17. King AB, Chambers JW, Garey J. Primary Malignant melanoma of the spinal cord. *AMA Arch Neurol Psychiatry*. (1952) 68:266–75. doi: 10.1001/archneurpsyc.1952.02320200104012

18. Salpietro FM, Alafaci C, Gervasio O, La Rosa G, Baio A, Francolini DC, et al. Primary cervical melanoma with brain metastases. Case report and review of the literature. *J neurosurgery*. (1998) 89:659–66. doi: 10.3171/jns.1998.89.4.0659

19. Salame K, Merimsky O, Yosipov J, Reider-Groswasser I, Chaitchik S, Ouaknine GE. Primary intramedullary spinal melanoma: diagnostic and treatment problems. *J neuro-oncology*. (1998) 36:79–83. doi: 10.1023/a:1005770929074

20. Kashiwagi N, Hirabuki N, Morino H, Taki T, Yoshida W, Nakamura H. Primary solitary intracranial melanoma in the sylvian fissure: MR demonstration. *Eur radiology*. (2002) 12 Suppl 3:S7–10. doi: 10.1007/s00330–002-1372–8

21. Woodruff WW Jr., Djang WT, McLendon RE, Heinz ER, Voorhees DR. Intracerebral Malignant melanoma: high-field-strength MR imaging. *Radiology*. (1987) 165:209–13. doi: 10.1148/radiology.165.1.3628773

22. Lee NK, Lee BH, Hwang YJ, Sohn MJ, Chang S, Kim YH, et al. Findings from CT, MRI, and PET/CT of a primary Malignant melanoma arising in a spinal nerve root. *Eur Spine journal: Off Publ Eur Spine Society Eur Spinal Deformity Society Eur Section Cervical Spine Res Society*. (2010) 19 Suppl 2:S174–8. doi: 10.1007/s00586–010-1285–1

23. Schöder H, Larson SM, Yeung HW. PET/CT in oncology: integration into clinical management of lymphoma, melanoma, and gastrointestinal Malignancies. *J Nucl medicine: Off publication Soc Nucl Med*. (2004) 45 Suppl 1:72s–81s.

24. Wu L, Xu Y. Primary spinal intramedullary Malignant melanoma involving the medulla oblongata. *Spine journal: Off J North Am Spine Society*. (2016) 16:e499–500. doi: 10.1016/j.spinee.2016.01.079

25. Gray-Schopfer V, Wellbrock C, Marais R. Melanoma biology and new targeted therapy. *Nature*. (2007) 445:851–7. doi: 10.1038/nature05661

26. Angelino G, De Pasquale MD, De Sio L, Serra A, Massimi L, De Vito R, et al. NRAS(Q61K) mutated primary leptomeningeal melanoma in a child: case presentation and discussion on clinical and diagnostic implications. *BMC cancer*. (2016) 16:512. doi: 10.1186/s12885-016-2556-y

27. Lee CH, Moon KY, Chung CK, Kim HJ, Chang KH, Park SH, et al. Primary intradural extramedullary melanoma of the cervical spinal cord: case report. *Spine*. (2010) 35:E303–7. doi: 10.1097/BRS.0b013e3181ccb1b3

28. Brat DJ, Giannini C, Scheithauer BW, Burger PC. Primary melanocytic neoplasms of the central nervous systems. *Am J Surg pathology*. (1999) 23:745–54. doi: 10.1097/00000478–199907000–00001

29. Perrini P, Caniglia M, Pieroni M, Castagna M, Parenti GF. Malignant transformation of intramedullary melanocytoma: case report. *Neurosurgery*. (2010) 67:E867–9. doi: 10.1227/01.Neu.0000372919.96651.34

30. Hoffmann M, Koelsche C, Seiz-Rosenhagen M, Mai S, Lohr F, Reuss D, et al. The GNAQ in the haystack: intramedullary meningeal melanocytoma of intermediate grade at T9–10 in a 58-year-old woman. *J neurosurgery*. (2016) 125:53–6. doi: 10.3171/2015.5.Jns15233

31. Amer MH, Al-Sarraf M, Baker LH, Vaitkevicius VK. Malignant melanoma and central nervous system metastases: incidence, diagnosis, treatment and survival. *Cancer*. (1978) 42:660–8. doi: 10.1002/(ISSN)1097-0142

32. Barron KD, Hirano A, Araki S, Terry RD. Experiences with metastatic neoplasms involving the spinal cord. *Neurology*. (1959) 9:91–106. doi: 10.1212/wnl.9.2.91

33. Gokaslan ZL, Aladag MA, Ellerhorst JA. Melanoma metastatic to the spine: a review of 133 cases. *Melanoma Res*. (2000) 10:78–80. doi: 10.1097/00008390-200002000-00010

34. Sampson JH, Carter JH Jr., Friedman AH, Seigler HF. Demographics, prognosis, and therapy in 702 patients with brain metastases from Malignant melanoma. *J neurosurgery*. (1998) 88:11–20. doi: 10.3171/jns.1998.88.1.0011

35. Smith JL Jr., Stehlin JS Jr. Spontaneous regression of primary Malignant melanomas with regional metastases. *Cancer*. (1965) 18:1399–415. doi: 10.1002/(ISSN)1097-0142

36. Pasquier B, Couderc P, Pasquier D, Panh MH, Arnould JP. Primary Malignant melanoma of the cerebellum: a case with metastases outside the nervous system. *Cancer*. (1978) 41:344–51. doi: 10.1002/(ISSN)1097-0142

37. Bergdahl L, Boquist L, Liliequist B, Thulin CA, Tovi D. Primary Malignant melanoma of the central nervous system. A report of 10 cases. *Acta neurochirurgica*. (1972) 26:139–49. doi: 10.1007/bf01406550

38. Grant DN. Primary meningeal melanomatosis: limitations of current diagnostic techniques. *J neurology neurosurgery Psychiatry*. (1983) 46:874–5. doi: 10.1136/jnnp.46.9.874

39. Zhang HY, Yang GH, Chen HJ, Wei B, Ke Q, Guo H, et al. Clinicopathological, immunohistochemical, and ultrastructural study of 13 cases of melanotic schwannoma. *Chin Med J*. (2005) 118:1451–61.

40. Acciarri N, Padovani R, Riccioni L. Intramedullary melanotic schwannoma. Report of a case and review of the literature. *Br J Neurosurgery*. (1999) 13:322–5. doi: 10.1080/02688699943772

41. Nishihara M, Sasayama T, Kondoh T, Tanaka K, Kohmura E, Kudo H. Long-term survival after surgical resection of primary spinal Malignant melanoma. *Neurologia medico-chirurgica*. (2009) 49:546–8. doi: 10.2176/nmc.49.546

42. Beresford HR. Melanoma of the nervous system: treatment with corticosteroids and radiation. *Neurology*. (1968) 18:277–8.

43. Fuld AD, Speck ME, Harris BT, Simmons NE, Corless CL, Tsongalis GJ, et al. Primary melanoma of the spinal cord: a case report, molecular footprint, and review of the literature. *J Clin oncology: Off J Am Soc Clin Oncol*. (2011) 29:e499–502. doi: 10.1200/jco.2010.34.0695

44. Miller K, Abeles G, Oratz R, Zeleniuch-Jacquotte A, Cui J, Roses DF, et al. Improved survival of patients with melanoma with an antibody response to immunization to a polyvalent melanoma vaccine. *Cancer*. (1995) 75:495–502. doi: 10.1002/(ISSN)1097-0142

45. Shankar GM, Choi BD, Grannan BL, Oh K, Shin JH. Effect of immunotherapy status on outcomes in patients with metastatic melanoma to the spine. *Spine*. (2017) 42: E721–e5. doi: 10.1097/brs.0000000000001993

46. Zhang Z, Gong H, Zhao C, Wang D, Qian M, Wu Z, et al. Prognostic factors of patients with spinal Malignant melanoma after surgical intervention: a case series of 21 patients and literature review. *J neuro-oncology*. (2019) 142:119–27. doi: 10.1007/s11060–018-03071–1

47. Kiel FW, Starr LB, Hansen JL. Primary melanoma of the spinal cord. *J neurosurgery*. (1961) 18:616–29. doi: 10.3171/jns.1961.18.5.0616

48. Mirone G, Cinalli G, Spennato P, Ruggiero C, Aliberti F. Hydrocephalus and spinal cord tumors: a review. *Child's nervous system: ChNS: Off J Int Soc Pediatr Neurosurgery*. (2011) 27:1741–9. doi: 10.1007/s00381–011-1543–5

49. Ozden B, Barlas O, Hacihanefioğlu U. Primary dural melanomas: report of two cases and review of the literature. *Neurosurgery*. (1984) 15:104–7. doi: 10.1227/00006123–198407000–00020

frontiers | Frontiers in Neurology

TYPE Original Research
PUBLISHED 28 May 2024
DOI 10.3389/fneur.2024.1383980

OPEN ACCESS

EDITED BY
David Warren Newell,
Independent Researcher, Seattle,
United States

REVIEWED BY
Edoardo Mazzucchi,
Regina Elena National Cancer Institute
(IRCCS), Italy
Lukas Rasulić,
University of Belgrade, Serbia

*CORRESPONDENCE
Jiabin Wang
✉ wangjiabin2014@126.com
Qingchun Mu
✉ muq@suda.edu.cn
Liankun Wang
✉ Wangliankun1981@163.com

†These authors have contributed equally to this work

RECEIVED 23 February 2024
ACCEPTED 30 April 2024
PUBLISHED 28 May 2024

CITATION
Chen X, Han D, Mao T, Xu H, Guo H, Ge H, Meng X, Teng L, Wang L, Mu Q and Wang J (2024) Unilateral hemilaminectomy vs. laminoplasty for the resection of spinal schwannomas: an analysis of 100 patients. *Front. Neurol.* 15:1383980. doi: 10.3389/fneur.2024.1383980

Unilateral hemilaminectomy vs. laminoplasty for the resection of spinal schwannomas: an analysis of 100 patients

Xiaofeng Chen[1†], Dianhui Han[1†], Tie Mao[2†], Huilong Xu[3], Hua Guo[1], Haitao Ge[1], Xiangyi Meng[1], Lei Teng[1], Liankun Wang[4*], Qingchun Mu[5*] and Jiabin Wang[1*]

[1]Department of Neurosurgery, The First Affiliated Hospital of Harbin Medical University, Harbin, China, [2]Department of Neurosurgery, Heilongjiang Provincial Hospital, Harbin, Heilongjiang, China, [3]Department of Neurosurgery, The First Hospital of Sui Hua City, Suihua, Heilongjiang, China, [4]Department of Neurology, Heilongjiang Province Hospital, Harbin, China, [5]Department of Neurosurgery, Gaozhou People's Hospital, Guangdong Medical University, Guangdong, China

Objective: Spinal schwannomas are the most common intradural extramedullary tumors, and their complete removal is recommended to avoid tumor recurrence. Although laminoplasty provides a sufficient window for tumor resection, this approach may increase tissue trauma and cause postoperative instability compared with unilateral hemilaminectomy. This study aimed to compare the efficacy and clinical outcomes of the two approaches.

Materials and methods: We included 100 consecutive patients who underwent unilateral hemilaminectomy or laminoplasty for resection of spinal schwannomas between January 2015 and February 2023. The patients' baseline characteristics, including sex, age, tumor location, percentage of tumor occupying the intradural space, operative time, postoperative length of hospital stay, intraoperative bleeding volume, visual analog scale score, and neurologic results, were retrospectively analyzed.

Results: Hemilaminectomy patients who underwent unilateral hemilaminectomy had smaller intraoperative bleeding ($p = 0.020$) volume, shorter operative time ($p = 0.012$), and shorter postoperative length of hospital stay ($p = 0.044$). The mean VAS scores at the last follow-up were similar between the two groups ($p = 0.658$). Although the postoperative McCormick and Karnofsky Performance scores were not significantly different between the laminoplasty and unilateral hemilaminectomy groups ($p = 0.687$ and $p = 0.649$, respectively), there was a statistically significant improvement based on postoperative neurological results compared to preoperative neurological results for both groups. The incidence of postoperative complications was 5% and 11.7% in the unilateral hemilaminectomy and laminoplasty groups, respectively ($p = 0.308$).

Conclusions: For spinal schwannoma resection, unilateral hemilaminectomy has more advantages than laminoplasty, including a shorter postoperative hospital stay, faster procedure, and less intraoperative blood loss while achieving the same desired result.

KEYWORDS

unilateral hemilaminectomy, spinal schwannoma, laminoplasty, spine, surgery

Introduction

Spinal schwannomas are slow-growing benign WHO grade I nerve sheath neoplasm that arises from Schwann cells. Total resection of these tumors are the main goal of surgical treatment (1, 2). Although conventional surgical approaches such as laminoplasty provide an adequate window for tumor resection and restoration of the anatomical structure, they are associated with significant tissue trauma, postoperative deformities, pain, and spinal instability (3, 4).

Minimally invasive procedures, such as unilateral hemilaminectomy, minimize bony defects, reduce tissue trauma, and decrease the incidence of spinal instability (5, 6). However, it is unclear whether unilateral hemilaminectomy is safer and more effective than laminoplasty for the excision of intradural extramedullary schwannomas, and there have been no comparative studies on laminoplasty and hemilaminectomy approaches.

To the best of our knowledge, this is the first retrospective study to compare the clinical efficacy and outcomes of hemilaminectomy and laminoplasty for spinal schwannoma resection in 100 consecutive patients.

Materials and methods

We retrospectively reviewed the clinical data of 100 consecutive patients who were performed either unilateral hemilaminectomy or laminoplasty for spinal schwannoma resection between January 2015 and February 2023 at the First Affiliated Hospital of Harbin Medical University. The approach used for each patient was selected according to the surgeon's preference. The inclusion criteria were patients (1) with tumors occupying <3 motion segments of the spine, (2) operated on by the same surgeon, (3) operated on for >6 months, (4) with intact clinical data, (5) with tumor laterality, and (6) with intradural tumors. Exclusion criteria were as follows: patients with incomplete clinical data, those who were not followed up, those who were followed up for <6 months, those with recurrent tumors, those with tumors occupying ≥3 motion segments of the spine, those with multiple tumors, and with dumbbell-shaped tumors developing in the neural foramen and outside the canal. For each case, clinicopathological data were carefully extracted from the hospital database, including age at the time of surgery, sex, vertebral level location (cervical, thoracic, and lumbar), percentage of tumors occupying the intradural space, surgical approach, neurofunctional status according to McCormick grading, total operative time, postoperative length of hospital stay, intraoperative bleeding volume, visual analog scale (VAS) and Karnofsky performance score (KPS). The percentage of tumors occupying the intradural space was calculated on magnetic using image analysis software (Image J; Wayne Rasband, National Institutes of Health) as follows: (maximum tumor area in cm^2)/(intradural space area in the same section in cm^2) ×100 (%). The pathologic diagnosis of intradural schwannoma following surgery was confirmed by three qualified pathologists.

Operative technique

All patients underwent a posterior approach in the prone position. A small midline skin incision was made in accordance with the radiographic marker positioned on the spinous process where the lesion was located. In the unilateral hemilaminectomy group, the paravertebral muscles were retained to expose the laminae on one side. The supraspinal and interspinal ligaments and contralateral muscles were left undisturbed. Hemilaminectomy was performed with a combination of high-speed pneumatic drill round burrs and Kerrison rongeurs to resect the soft tissue and ligamentum flavum and create an adequate surgical corridor. For laminoplasty, paravertebral muscle dissection was bilateral, a high-speed pneumatic drill was used to resect the laminae, the supraspinal and interspinous ligaments were dissected, and the spinous process ligament complex was completely removed. Subsequently, the dura was opened and micro-neurosurgical techniques were used to resect the spinal schwannomas. The tumors were completely resected in all patients, and the affected nerve roots were cut.

Watertight spinal dural closure was performed running locked 6-0 Prolene (Ethicon Inc.). In laminoplasty, the incised laminae and spinous processes are installed and fixed using screws and connectors, and the supraspinal ligament is fixed with silk thread *in situ* sutures.

Statistical analysis

SAS9.4 software version (SAS Inc., Cary, NCSU, USA) was used for the statistical analyses. The incidences of postoperative complications were compared and evaluated using Fisher's exact test. Sex and tumor location were compared and evaluated between the two approaches using the chi-square test. The VAS score, age, KPS score, McCormick score, duration of surgery, postoperative length of hospital stay, and amount of intraoperative bleeding were compared and analyzed using the Kruskal–Wallis test. Results were considered statistically significant for p values < 0.05.

Result

Patient demographic data

The clinical data of the 100 patients were analyzed and discussed. Of these patients, 56 (56%) were women and the remaining 44 (44%) were men, with an average age of 51.2 ± 13.1 years (age range of 12–81 years). The main presenting symptoms were radiculopathy in 61 patients (61%), back pain in 14 (14%), motor deficits in 26 (26%), sensory changes in 41 (41%), and bladder/bowel dysfunction in 11 (11%). In the current study, 40 patients underwent unilateral hemilaminectomy (Figure 1), and 60 patients underwent laminoplasty (Figure 2). Age, sex, extent of tumor involvement, preoperative VAS score, preoperative McCormick score, and preoperative KPS score were not significantly different between the two groups ($p > 0.05$). In the laminoplasty group, the tumors were located in the thoracic (18.3%), cervical (38.3%), and

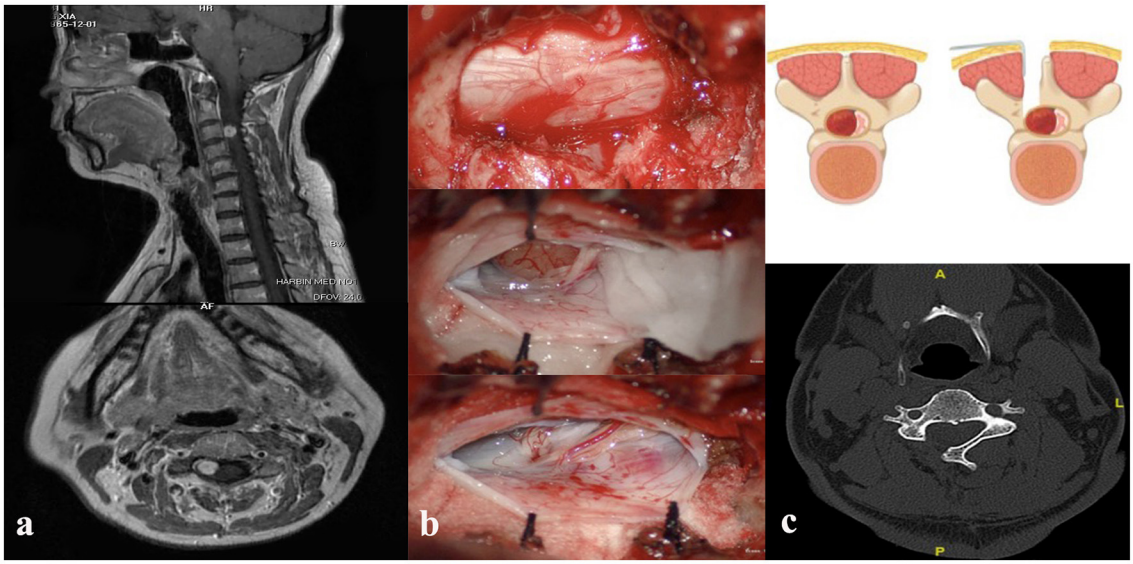

FIGURE 1
(a) Preoperative cervical magnetic resonance imaging T1-weighted sagittal (up) and axial (down) image with contrast showing heterogeneously enhancing intradural extramedullary lesion at the level of the C3 vertebrae. **(b)** Intraoperative unilateral hemilaminectomy with resection of the laminae (up), exposure of the tumor (middle), and removal of the lesion (down). **(c)** Demonstration of unilateral hemilaminectomy (up), postoperative computed tomography scan study (down).

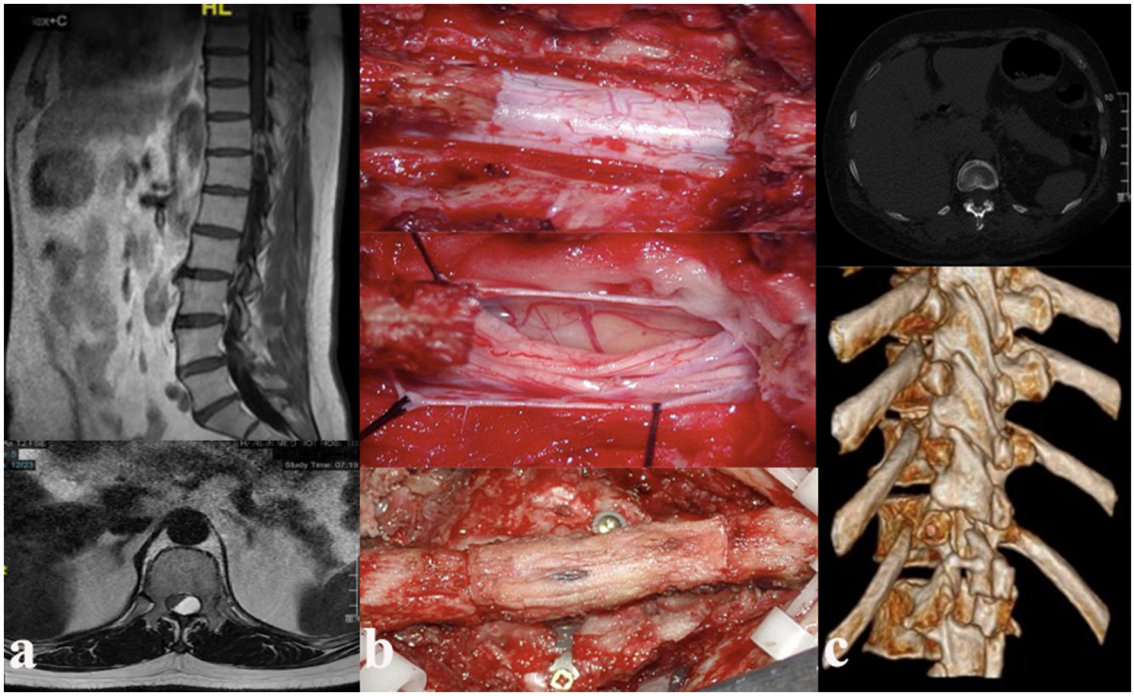

FIGURE 2
(a) Preoperative thoracic magnetic resonance imaging T1-weighted sagittal (up) and axial (down) image with contrast showing heterogeneously enhancing intradural extramedullary lesion at the level of the T11–12 vertebrae. **(b)** Intraoperative laminoplasty with resection of the laminae (up), exposure and resection of tumor (middle), and reduction of the resected lamina (down). **(c)** Postoperative computed tomography (CT) scan study.

lumbar (43.3%) spinal regions. Patients who underwent unilateral hemilaminectomy more commonly had tumors in the cervical region; 17 (42.5%) patients who underwent unilateral hemilaminectomy also had tumors in this region (Table 1). The percentage of tumors occupying the intradural space was 77.1% in the unilateral hemilaminectomy group and 82.3% in the laminoplasty group, respectively ($p = 0.080$) (Table 1).

TABLE 1 Comparison of the demographic and clinical data of patients treated for spinal schwannoma with unilateral hemilaminectomy and laminoplasty.

	Hemilaminectomy ($n = 40$)	Laminoplasty ($n = 60$)	p value
Age (years), mean ± SD	53 (46–59)	52 (40.5–59.5)	0.563
Sex			
Male	15 (37.5)	29 (48.33)	0.285
Female	25 (62.5)	31 (51.67)	
Site of surgery			
Cervical	17 (42.5)	23 (38.33)	0.15
Thoracic	10 (25)	16 (18.3)	
Lumbar	13 (32.5)	21 (43.3)	
Preoperative McCormick			
I	25 (62.5)	41 (68.33)	0.637
II	11 (27.5)	11 (18.33)	
III	2 (5)	8 (13.33)	
IV	2 (5)	0 (0)	
Preoperative KPS score	80 (70–80)	80 (70–80)	0.825
Preoperative VAS score	6 (3.5–7)	7 (4–7)	0.236
Occupying (%)	77.1 (67.6–80.65	82.3 (68.4–84.1)	0.08
Cranio-caudal tumor extension			0.328
1 level	23(57.5%)	32(53.3%)	
2 levels	17 (42.5%)	28 (46.7%)	

TABLE 2 Surgical outcomes according to the surgical intervention.

	Hemilaminectomy ($n = 40$)	Laminoplasty ($n = 60$)	p value
Postoperative complications			
No	38 (95)	53 (88.33)	0.308
Yes	2 (5)	7 (11.67)	
Follow-up McCormick score			
I	35 (87.5)	54 (90)	0.687
II	3 (7.5)	4 (6.67)	
III	2 (5)	2 (3.33)	
Follow-up KPS	90 (90–90)	90 (90–100)	0.649
Follow-up VAS	1 (0–1)	1 (0–1)	0.658
Operative time (min)	210 (172.5–247)	232.5 (205–270)	0.012
Hospitalization length (d)	7 (6–9)	9 (7–10)	0.044
Blood loss (ml)	50 (30–80)	70 (60–100)	0.02

TABLE 3 Comparison of VAS and KPS scores according to the surgical intervention type.

	Preoperative	Follow-up	p value
Hemilaminectomy ($n = 40$)			
VAS	6 (3.5–7)	1 (0–1)	0.005
KPS	80 (70–80)	90 (90–90)	0.03
Laminoplasty ($n = 60$)			
VAS	7 (4–7)	1 (0–1)	0.004
KPS	80 (70–80)	90 (90–100)	0.04

Surgical outcomes

In the current study, the operative time was significantly different between the two approaches (hemilaminectomy: 210 (172.5–247) min, laminoplasty: 232.5 (205–270) min; $p = 0.012$). Similarly, there were significant differences in intraoperative bleeding volume (hemilaminectomy: 50 (30–80) ml, laminoplasty: 70 (60–100); $p = 0.020$) and postoperative length of hospital stay (hemilaminectomy: 7 (6–9) days, laminoplasty: 9 (7–10) days; $p = 0.044$). The incidences of postoperative complications were 5% in the unilateral hemilaminectomy group and 11.67% in the laminoplasty group, respectively ($p = 0.308$) (Table 2).

Follow-up and functional outcome

The average follow-up time was 49.6 ± 30.0 months (range, 6–96 months) in the laminoplasty group and 48.0 ± 28.1 months (range, 6–96 months) in the unilateral hemilaminectomy group ($p > 0.05$).

The VAS scores were evaluated in both groups, and patients reported significantly less pain at the last follow-up than at admission ($p < 0.05$) (Table 3). Remarkably, all patients experienced pain relief; however, there was no statistically significant difference in the postoperative VAS between the laminoplasty patients and unilateral hemilaminectomy patients at the last follow-up ($p = 0.658$) (Table 2).

The KPS and McCormick scores reflect the patients' functional outcomes. In the unilateral hemilaminectomy group, the overall median KPS improved from an average of 80 (70–80) to 90 (90–100) ($p = 0.03$), whereas in the laminoplasty group, it improved from an average of 80 (70–80) to 90 (90–90) ($p = 0.040$) (Table 3). In terms of neurological recovery based on the McCormick grade, 11 (27.5%) patients in the unilateral hemilaminectomy group and 16 (26.7%) patients in the laminoplasty group showed improvement, while 29 (72.5%) patients in the unilateral hemilaminectomy group and 43 (71.7%) patients in the laminoplasty group showed no improvement (Table 4). In the laminoplasty group, 1 patient with McCormick grade II deteriorated to McCormick grade III. Although there was no statistically significant difference at the last follow up in the postoperative McCormick score between the laminoplasty group and unilateral hemilaminectomy group ($p = 0.687$), there

TABLE 4 Comparison of postoperative neurological outcomes between patients treated with hemilaminectomy or laminoplasty at the last follow-up.

	Hemilaminectomy ($n = 40$)	Laminoplasty ($n = 60$)	p value
Neurologically improved n (%)	11 (27.5)	16 (26.7)	0.824
Neurologically the same n (%)	29 (72.5)	43 (71.)	
Aggravated_ neurologically n (%)	0 (0)	1 (1.6)	

TABLE 5 Comparison of neurological outcomes according to surgical intervention type.

	Preoperative McCormick (n, %)	Follow-up McCormick (n, %)	p value
Hemilaminectomy ($n = 40$)			
I	25 (62.5)	35 (87.5)	0.0005
II	11 (27.5)	3 (7.5)	
III	2 (5)	2 (5)	
IV	2 (5)	0 (0)	
Laminoplasty ($n = 60$)			
I	41 (68.33)	54 (90)	0.0002
II	11 (18.33)	4 (6.67)	
III	8 (13.33)	2 (3.33)	
IV	0 (0)	0 (0)	

was a statistically significant difference in the postoperative McCormick score compared to the preoperative McCormick score in both groups (hemilaminectomy, $p = 0.0005$; laminoplasty, $p = 0.0002$) (Table 5), indicating that patients in both groups experienced significant improvement in neurological function. None of the patients developed iatrogenic kyphosis requiring fusion or instrumentation.

Discussion

Spinal schwannomas are slow-growing benign WHO grade I nerve sheath neoplasm arising from Schwann cells, accounting for 55% of all intraspinal tumors (7). The age of patients at the onset of spinal schwannoma symptoms was 60–70 years (8). In our study, the average age of our patients was consistent with that reported in previous literature. Total tumor excision is the gold standard treatment because it is associated with minimal morbidity and functional improvement (9). Several approaches have been accepted for the resection of spinal tumors, including laminectomy or laminoplasty. These approaches require bilateral dissection of the paraspinal muscles from the lamina (10).

Resection of the lamina and the interspinous ligaments may result in postoperative back pain and increase the risk of late-stage spinal instability or kyphosis. The incidence of post-laminectomy spinal deformities ranges from 33% to 100% (11, 12). Although laminoplasty, as an improved technique, may restore the spinal integrity of the posterior elements, both animal and clinical studies have reported a lower incidence of kyphotic deformities after laminoplasty (3).

As the main goal is complete resection, minimally invasive techniques are advantageous because they avoid iatrogenic trauma, prevent possible instability, and reduce the incidence of postoperative complications while achieving the same desired result. The unilateral hemilaminectomy has become the preferred surgical technique for the removal of intraspinal lesions (13, 14). Some authors have performed a unilateral hemilaminectomy approach for tumor resection and found the advantages of less intraoperative bleeding, fewer postoperative complications, and a shorter length of hospital stay (15, 16). In contrast, Iacoangeli et al. showed that the exposure generated by unilateral hemilaminectomy was limited, which may prolong the operative time and increase the amount of intraoperative blood loss (17). In the current study, 40% patients underwent tumor excision using unilateral hemilaminectomy. Consistent with previous studies, the present study revealed that unilateral hemilaminectomy was associated with significantly less blood loss, shorter operative time, and significantly shorter postoperative hospital stay. This may be owing to the minimal invasiveness of unilateral hemilaminectomy or its association with minimal iatrogenic trauma, including the preservation of the contralateral zygapophyseal joints, contralateral paraspinal musculature, supraspinous, and interspinous ligaments with the integrity of the "tension band" (18).

In unilateral hemilaminectomy, the narrow surgical corridor between the spinous process and the facet joint may increase the risks of inadequate closure of the dura mater and nerve injury, thereby leading to severe postoperative pain, postoperative infection, cerebrospinal fluid leak, and neurological dysfunction (19). Therefore, we compared the postoperative KPS and McCormick scores of the unilateral hemilaminectomy group with those of the laminoplasty group, and the findings revealed that there were no statistically significant in neuro-functional recovery. Moreover, in the current study, the incidence of postoperative cerebrospinal fluid leakage and infection was analyzed. The incidence of postoperative complications was 5% and 11.7% in the unilateral hemilaminectomy and laminoplasty groups, respectively. Our study revealed that compared with laminoplasty, unilateral hemilaminectomy was not associated with an increased risk of postoperative complications, which is consistent with the results of previous studies.

Previous studies have shown that compared with laminectomy, unilateral hemilaminectomy not only reduces the probability of postoperative pain but also relieves pre-existing pain (6). However, in the current study, there was no statistically significant difference in the postoperative VAS scores between the laminoplasty and unilateral hemilaminectomy groups at the last follow-up, which might have allowed anatomical reconstruction of the spinal posterior element and a longer follow-up.

Although the narrow surgical corridor was a disadvantage, the exposed operative field was adequate for microsurgery; in particular, undercutting of the spinous process base and

oblique tilting of the operating table allowed safe reversal of spinal schwannomas.

This study has some limitations, such as its retrospective nature, and the choice of approach for each case was based mainly on the operator's experience. Furthermore, the time for postoperative VAS measurement and postoperative neurological testing were not uniform for all patients. Therefore, further prospective randomized studies with large populations that include both unilateral hemilaminectomy and laminoplasty techniques to verify the results of the present study are needed.

However, compared to patients who underwent laminoplasty, those who underwent unilateral hemilaminectomy had a shorter operative time, less blood loss, and faster recovery. More importantly, the differences in complication rates and long-term functional outcomes between the two techniques were not statistically significant.

Conclusion

Unilateral hemilaminectomy is advantageous for the resection of spinal schwannomas. Our findings show that this procedure allows safe, effective, and complete removal of intradural tumors with satisfactory outcomes and many benefits, such as a shorter hospital stay, shorter operative time, and less blood loss.

Data availability statement

The original contributions presented in the study are included in the article/supplementary material, further inquiries can be directed to the corresponding authors.

Ethics statement

The studies involving humans were approved by the First Affiliated Hospital of Harbin Medical University. The studies were conducted in accordance with the local legislation and institutional requirements. The participants provided their written informed consent to participate in this study. Written informed consent was obtained from the individual(s) for the publication of any potentially identifiable images or data included in this article.

Author contributions

XC: Methodology, Writing – review & editing. DH: Formal analysis, Methodology, Writing – original draft. TM: Formal analysis, Investigation, Methodology, Writing – original draft. HX: Data curation, Formal analysis, Writing – review & editing. HGu: Formal analysis, Project administration, Resources, Writing – original draft, Writing – review & editing. HGe: Formal analysis, Writing – review & editing. XM: Formal analysis, Investigation, Writing – original draft, Writing – review & editing. LT: Methodology, Project administration, Writing – original draft. LW: Writing – review & editing, Funding acquisition. QM: Funding acquisition, Writing – review & editing. JW: Formal analysis, Funding acquisition, Writing – original draft, Writing – review & editing.

Funding

The author(s) declare financial support was received for the research, authorship, and/or publication of this article. This work was supported by the Postdoctoral Science Foundation of Heilongjiang Province (LBH-Z19076), the Heilongjiang Welfare Fund Organization of Disabled Persons (HJ2022-1and2023HX037), the National Natural Science Foundation of China (82360366), the Natural Science Foundation of Guangdong Province (2023A1515012969), and the Natural Science Foundation of Heilongjiang Province (LH2021H065).

Conflict of interest

The authors declare that the research was conducted in the absence of any commercial or financial relationships that could be construed as a potential conflict of interest.

Publisher's note

References

1. Tish S, Habboub G, Lang M, Ostrom QT, Kruchko C, Barnholtz-Sloan JS, et al. The epidemiology of spinal schwannoma in the United States between 2006 and 2014. *J Neurosurg Spine.* (2019) 32:661–6. doi: 10.3171/2019.10.SPINE191025

2. Hirano K, Imagama S, Sato K, Kato F, Yukawa Y, Yoshihara H, et al. Primary spinal cord tumors: review of 678 surgically treated patients in Japan. A multicenter study. *Eur Spine J Oct.* (2012) 21:2019–26. doi: 10.1007/s00586-012-2345-5

3. Fields MJ, Hoshijima K, Feng AH, Richardson WJ, Myers BS. A biomechanical, radiologic, and clinical comparison of outcome after multilevel cervical laminectomy or laminoplasty in the rabbit. *Spine.* (2000) 25:2925–31. doi: 10.1097/00007632-200011150-00015

4. Morio Y, Yamamoto K, Teshima R, Nagashima H, Hagino H. Clinicoradiologic study of cervical laminoplasty with posterolateral fusion or bone graft. *Spine.* (2000) 25:190–6. doi: 10.1097/00007632-200001150-00008

5. Mobbs RJ, Maharaj MM, Phan K, Rao PJ. Unilateral hemilaminectomy for intradural lesions. *Orthop Surg.* (2015) 7:244–9. doi: 10.1111/os.12184

6. Pompili A, Caroli F, Crispo F, Giovannetti M, Raus L, Vidiri A, et al. Unilateral laminectomy approach for the removal of spinal meningiomas and schwannomas: impact on pain, spinal stability, and neurologic results. *World Neurosurg.* (2016) 85:282–91. doi: 10.1016/j.wneu.2015.09.099

7. Ando K, Imagama S, Ito Z, Kobayashi K, Yagi H, Hida T, et al. How do spinal schwannomas progress? The natural progression of spinal schwannomas on MRI. *J Neurosurg Spine.* (2016) 24:155–9. doi: 10.3171/2015.3.SPINE141218

8. Traul DE, Shaffrey ME, Schiff D. Part I: spinal-cord neoplasms-intradural neoplasms. *Lancet Oncol.* (2007) 8:35–45. doi: 10.1016/S1470-2045(06)71009-9

9. Turel MK, D'Souza WP, Rajshekhar V. Hemilaminectomy approach for intradural extramedullary spinal tumors: an analysis of 164 patients. *Neurosurg Focus.* (2015) 39:E9. doi: 10.3171/2015.5.FOCUS15170

10. Kim CH, Chung CK. Surgical outcome of a posterior approach for large ventral intradural extramedullary spinal cord tumors. *Spine.* (2011) 36:E531–7. doi: 10.1097/BRS.0b013e3181dc8426

11. Hida S, Naito M, Arimizu J, Morishita Y, Nakamura A. The transverse placement laminoplasty using titanium miniplates for the reconstruction of the laminae in thoracic and lumbar lesion. *Eur Spine J.* (2006) 15:1292–7. doi: 10.1007/s00586-006-0099-7

12. Park SB, Jahng TA, Kim CH, Chung CK. Thoracic and lumbar laminoplasty using a translaminar screw: morphometric study and technique. *J Neurosurg Spine.* (2009) 10:603–9. doi: 10.3171/2009.2.SPINE08257

13. Oktem IS, Akdemir H, Kurtsoy A, Koc RK, Menku A, Tucer B. Hemilaminectomy for the removal of the spinal lesions. *Spinal Cord.* (2000) 38:92–6. doi: 10.1038/sj.sc.3100963

14. Xie T, Qian J, Lu Y, Chen B, Jiang Y, Luo C. Biomechanical comparison of laminectomy, hemilaminectomy and a new minimally invasive approach in the surgical treatment of multilevel cervical intradural tumour: a finite element analysis. *Eur Spine J.* (2013) 22:2719–30. doi: 10.1007/s00586-013-2992-1

15. Lei D, Zhou Y, Yao D, Zhang F, Wang X, Jiang X, et al. Efficacy of unilateral hemilaminectomy for intraspinal tumor resection: a systematic review and meta-analysis. *Ann Palliat Med.* (2021) 10:984–99. doi: 10.21037/apm-20-499

16. Chiou SM, Eggert HR, Laborde G, Seeger W. Microsurgical unilateral approaches for spinal tumour surgery: eight years' experience in 256 primary operated patients. *Acta Neurochir.* (1989) 100:127–33. doi: 10.1007/BF01403599

17. Iacoangeli M, Gladi M, Di Rienzo A, Dobran M, Alvaro L, Nocchi N, et al. Minimally invasive surgery for benign intradural extramedullary spinal meningiomas: experience of a single institution in a cohort of elderly patients and review of the literature. *Clin Interv Aging.* (2012) 7:557–64. doi: 10.2147/CIA.S38923

18. Sun CX, Meng XL, Xie SN Yu Y, Yang HJ, Wu B. Unilateral hemilaminectomy for patients with intradural extramedullary tumors. *J Zhejiang Univ Sci B.* (2011) 12:575–81. doi: 10.1631/jzus.B1000402

19. Dobran M, Paracino R, Nasi D, Aiudi D, Capece M, Carrassi E, et al. Laminectomy versus unilateral hemilaminectomy for the removal of intraspinal schwannoma: experience of a single institution and review of literature. *J Neurol Surg A Cent Eur Neurosurg.* (2021) 82:552–5. doi: 10.1055/s-0041-1722968

frontiers | Frontiers in Neurology

TYPE Original Research
PUBLISHED 02 July 2024
DOI 10.3389/fneur.2024.1300597

OPEN ACCESS

EDITED BY
Qingchun Mu,
Second Affiliated Hospital of Soochow University, China

REVIEWED BY
Fulvio Tartara,
University Hospital of Parma, Italy
Michael M. Reinert,
Hirslanden St. Anna, Switzerland

*CORRESPONDENCE
Zhenghua Hong
✉ hongzh@enzemed.com
Hua Luo
✉ 18732196660@163.com

†These authors have contributed equally to this work

RECEIVED 23 September 2023
ACCEPTED 18 June 2024
PUBLISHED 02 July 2024

CITATION
Chen W, Yang Y, Pan W, Lei X, Hong Z and Luo H (2024) Treatment of lower cervical spine fracture with ankylosing spondylitis by simple long anterior cervical plate: a retrospective study of 17 cases. *Front. Neurol.* 15:1300597. doi: 10.3389/fneur.2024.1300597

Treatment of lower cervical spine fracture with ankylosing spondylitis by simple long anterior cervical plate: a retrospective study of 17 cases

Weifu Chen†, Yu Yang†, Wenjun Pan†, Xinhuan Lei†, Zhenghua Hong* and Hua Luo*

Department of Orthopedics, Taizhou Hospital of Zhejiang Province Affiliated with Wenzhou Medical University, Taizhou, Zhejiang Province, China

Objective: Ankylosing spondylitis (AS), an autoimmune disease, often leads to lower cervical spine fractures, with the potential for severe spinal nerve damage even from low-energy injuries. The optimal treatment approach remains debated.

Methods: A retrospective study involved 17 AS patients with lower cervical spine fractures who received anterior cervical fixation. Most presented cervicothoracic or thoracolumbar kyphosis, with 11 exhibiting neurological deficits. Patient characteristics, clinical data, visual analog scale (VAS), complications, and nerve recovery were analyzed.

Results: No postoperative neurological deterioration occurred. All cases experienced complete fusion of fractures during the follow-up period. Preoperative VAS significantly decreased at 3 days and 3 months post-surgery. Of the 11 patients with preoperative neurological deficits, approximately 54.5% showed improvement post-surgery. No complications were reported, such as esophageal fistula, wound infection, or fixation failure.

Conclusion: Anterior internal fixation is a possible treatment for AS-related lower cervical fractures. This approach ensures satisfactory spinal stability and neurological recovery with proper cranial traction and external fixation post-surgery. Our findings demonstrate that this surgical method is safe and effective.

KEYWORDS

ankylosing spondylitis, fracture, cervical spinal cord injury, long anterior cervical plate, anterior approach

Introduction

Ankylosing spondylitis (AS) is an autoimmune disease that mainly affects axial bones, such as the spine and the sacroiliac joints, causing stiffness and rigidity of the sacroiliac joints and spine (1). The affected spine in AS is often unable to withstand relatively normal stress compared to a healthy spine because patients with AS often have varying degrees of decreased bone density or osteoporosis and are more likely to develop fragility fractures of the spine in response to violence. According to relevant literature reports (2, 3), the incidence of spinal fracture in AS patients is

four times that of ordinary people, with an incidence of 5–15%. Clinical studies have shown that the lower cervical vertebra is the most common fracture site of AS, and the fracture type has its unique characteristics. It is often a three-column fracture across the intervertebral space, similar to the "bamboo" long lever arm fracture, so this fracture is extremely unstable. According to statistics (4–6), about one-third of patients with AS have fatal injuries after cervical spine fractures and even low-energy injuries can cause severe spinal nerve injuries.

The fracture site of the cervical vertebra in AS is most likely at the lower cervical vertebra and the junction of the cervical-thoracic vertebra. This brings many difficulties to the clinical diagnosis and causes delayed or missed diagnosis. Therefore, it is suggested that a three-dimensional CT or MR Examination should be performed when a fracture is suspected in patients (7, 8). Timely and effective treatment of AS with cervical fracture is essential to restore normal neuromotor function and even save lives. At present, there are apparent disputes about the treatment (9–12): traditionally, doctors do not recommend surgery because of the high rate of surgical complications. However, with the update of the treatment concept in recent years, more and more doctors now recommend surgical internal fixation treatment. In addition, the choice of surgical approach is also controversial. Some surgeons recommend simple posterior cervical fixation, while others recommend anterior cervical fixation and fusion (13–15). However, the stability of anterior fixation has been questioned. Although the posterior approach has advantages in decompression and fixation, there are many problems in position placement, intraoperative fracture reduction, accurate nail placement, postoperative incision infection, etc. In contrast, the anterior approach can better avoid the above problems. The difficulty of the operation is relatively simple and fast. Long segmental steel plates can effectively compensate for the shortcomings in cervical stability after the anterior approach.

This study presents the preliminary clinical and imaging results of the anterior long segmental steel plate fixation treatment of AS with lower cervical fracture. It is intended to explore and analyze the injury characteristics of AS with lower cervical fracture through relevant research results, evaluate the efficacy of this technique in treating AS with cervical fracture, analyze and discuss the limitations and deficiencies of this technology.

Methods

Study design and patient population

This is a retrospective clinical study conducted through continuous retrospective analysis at Taizhou Enze Medical Center (Group) from June 2010 to December 2022, and it has been approved by the ethics committee under approval number NO. K20220609. In this study, patients who were not diagnosed with AS or patients who had lower cervical spine fractures in the early stage of disease progression but whose spines were still flexible or had no severe cervical kyphosis were excluded. Finally, 17 patients who received anterior long-segment steel plate (German Mediox) surgery for AS combined with lower cervical spine fractures were selected to be included in this study. Among the 17 patients, 11 were accompanied by spinal nerve dysfunction of varying degrees, and surgery was arranged for them as soon as possible after admission. The basic information, the condition of fracture injury, neurological function classification, and other perioperative details of the patients are shown in Table 1.

Data collection

The types of injuries seen on CT scans were determined based on the systems: Caron et al. (16) were evaluated and classified by two experienced surgeons above the deputy chief of spine surgery. The injury score of the American Spinal Injury Association (ASIA) was used to evaluate the degree of neurological injury (17). Evaluation of cervical healing status: Cervical spine anteroposterior and lateral X-ray and three-dimensional CT imaging data. Other clinical data include the Visual analog scale (VAS), intraoperative blood loss, length of hospital stay and complications (such as esophageal fistula, wound infection, failure of internal fixation, cerebrospinal fluid leakage, location loss after fracture reduction, further injury of spinal nerve function, respiratory and cardiac arrest or even death).

Treatment and surgical techniques

Preoperative management: patients were given stay-in-bed and neck brace immobilization immediately after admission. For those who cannot be fixed with a neck brace, use sandbags on both sides of the neck to improve the cervical spine. This group of patients did not receive traction therapy. After admission, patients with spinal cord injury were given symptomatic treatment such as dehydration, detumescence, nerve nutrition and analgesia, and surgery was performed as soon as possible after complete evaluation and exclusion of contraindications.

Surgical position

All patients were placed in the position in a fully awake state, supine position, with the head and neck naturally raised, cranial traction arch placed under local anesthesia, appropriate traction and neck flexion under the lateral monitoring of C-arm X-ray machine, to reduce the displaced cervical fracture as far as possible, while the displaced fracture position was kept in place, and the shoulders and head and neck were fixed. At this time, patients' heads tend to have a higher place, so lower the head and elevate the feet to meet the surgical position and avoid insufficient blood supply to the head during the operation. If necessary, the skull should be kept in 2–4 kg traction, and the position of the broken end of the fracture should be confirmed by fluoroscopy again to prepare for surgical treatment. Then, general anesthesia through nasal or oral tracheal intubation was used with the assistance of a fiber bronchoscope in an awake state.

Surgical methods

The anterior edge of the sternocleidomastoid approach was taken. Treatment of intervertebral fracture: Along the gap between the carotid sheath and the internal cervical viscera to the front of the vertebral body, explore and confirm the fracture location, properly stretch the injured intervertebral space, and clean the fracture fragments. If the fracture extends to the intervertebral disk, the disk is meticulously cleaned, followed by iliac bone grafting. Subsequently, a

TABLE 1 Clinical data of 17 patients managed by long anterior cervical plate.

Case No.	Age (Years)	Sex	D-AS (Y)	Mechanism	Level	Classification of fracture	ASIA grade	TBINS	Plate treatment	BL (mL)	HS (D)	Follow-up (Y)
1	54	M	NA	Hyperextension	C6	II	C	6 D	C4-7	50	12	5
2	35	M	10	Hyperextension	C6-7	I	D	2 M	C5-T1	100	34	9
3	45	M	16	Hyperflexion-Hyperextension	C6-7	I	D	4 D	C5-T1	50	13	7
4	48	M	10	Hyperextension	C5-6	I	D	3 D	C4-7	50	34	7
5	49	M	10	Hyperflexion-Hyperextension	C7	IV	E	3 D	C5-T1	50	37	7
6	45	M	20	Hyperextension	C7-T1	I	E	6 D	C6-T2	30	17	6
7	52	M	28	Hyperextension	C5-6	IV	C	2 D	C4-7	50	11	5
8	44	M	NA	Hyperextension	C7	II	E	3 D	C5-T1	40	32	5
9	49	M	20	Hyperextension	C5-6	I	E	6 D	C4-7	300	18	7
10	48	M	30	Hyperextension	C7-T1	I	D	3 D	C6-T2	100	25	4
11	67	F	10	Hyperextension	C6-7	I	C	2 D	C5-T1	50	43	4
12	58	M	10	Hyperextension	C5-6	I	E	3 D	C4-7	50	23	10
13	36	M	18	Hyperextension	C7	II	C	8 D	C5-T2	700	23	10
14	45	M	20	Hyperextension	C6-7	IV	E	6 D	C5-T1	20	23	1
15	34	M	12	Hyperextension	C6	IV	D	4 D	C5-T1	50	11	3
16	71	M	7	Hyperextension	C7	II	D	6 M	C5-T2	30	11	1
17	56	M	10	Hyperextension	C5-6	I	C	1 D	C4-7	100	18	3

M, Male; F, Female; D-AS, Duration of AS progression; NA, Not applicable; TBINS, Time between injury and surgery; OT, Operation time (minutes); BL, Blood loss (mL); HS, Hospital stay (days); D, Day; M, Month; and Y, Year.

long steel plate is delicately positioned at the front of the neck and secured with screws for stabilization. In cases where the fracture does not affect the intervertebral disk, only a long steel plate is used for fixation. The fractured end of the vertebral body usually does not require treatment and intervention, but if fracture fragments invade the spinal canal, they should be removed and decompressed. Other treatment methods of bone grafting and plate fixation are the same as those of intervertebral space fracture. Neurophysiological monitoring and protection were used throughout the operation.

Postoperative management

The skull traction was continued for 2 weeks after surgery, and the patient was allowed to turn over in bed. Then, the head, neck, and chest braces were fixed for 3 months. When the muscle strength of both lower limbs was equal to or greater than grade IV, the patient was allowed to walk on the ground. For patients with spinal cord injury, comprehensive rehabilitation therapy such as hyperbaric oxygen and limb function exercise should be started at an early stage.

Statistical analysis

The data statistics and analysis were performed using SPSS 25.0. ANOVA was used to compare VAS scores at different time points before and after surgery. And the comparison of ASIA scores before and after surgery was conducted using the Wilcoxon signed-rank test. p value<0.05 was identified as a significant difference.

Results

Visual analog scale

The average VAS score of patients before surgery was 6.88 ± 1.27 points, and the neck pain symptoms were relieved after surgery. The average VAS score of patients 3 days after surgery was 2.94 ± 0.97 points, significantly lower than the VAS score of patients before surgery, and the difference was statistically significant ($p < 0.05$). The average VAS score of patients 3 months after surgery was 1.47 ± 0.62 points, which was further reduced than the average VAS score of patients 3 days after surgery, and the difference was still statistically significant ($p < 0.05$).

The American spinal injury association grade

According to ASIA function rating criteria, 17 patients after treatment did not show any postoperative neurological dysfunction deterioration at the last follow-up, and 11 patients with neurological dysfunction before surgery showed improvement of neurological dysfunction in about 54.5% of them (Table 2). Comparison of neurological function between patients before surgery and the last follow-up showed that there was statistical significance ($p < 0.05$).

Fracture healing situation

The postoperative review showed that the internal fixation position was good, and the fracture fixation was firm. All cases exhibited fracture healing during the follow-up period, without occurrences of fracture displacement, non-union, or plate breakage. Typical case was shown in Figure 1.

Complications

In this group, there were no postoperative complications such as esophageal fistula, wound infection, failure of internal fixation (internal plant rupture, screw rupture, and internal plant loosening, etc.), cerebrospinal fluid leakage, position loss after fracture reduction, respiratory and cardiac arrest, or even death.

TABLE 2 ASIA grading for neurological function before operation and at the end of follow-up respectively among 17 patients.

Preoperative ASIA grade	Case lode	ASIA grade at the end of follow-up				
		A	B	C	D	E
A	0	0	0	0	0	0
B	0	0	0	0	0	0
C	5	0	0	2	2	1
D	6	0	0	0	3	3
E	6	0	0	0	0	6

Discussion

Although some earlier literature reported that surgical treatment of these fractures has a high mortality rate, it is clear that surgical treatment has been increasingly recommended (9, 18). Many surgeons recommend posterior surgery, which provides reasonable control and stability at the fracture end by fixing the cervical pedicle (18, 19). However, posterior surgery is also controversial; for example, pedicle nail placement is difficult, dural injury, cerebrospinal fluid leakage, incision infection, and internal fixation looseness are easy to occur, and in patients undergoing posterior surgery, the anterior angle of cervical fracture is not easy to be corrected, resulting in esophageal contusion and esophageal fistula (20, 21). Therefore, a few physicians recommend anterior approach fixation fusion for lower cervical spine fractures in patients with AS. Anterior surgery has the advantages of less trauma, relatively simple operation, thorough decompression, and a high fusion rate. However, the stability of anterior fixation has always been questioned, and it is mostly used in patients without obvious dislocation (2, 22). Internal fixation failure only occurred in simple anterior or posterior internal fixation, so combined anterior and posterior fixation was recommended for such

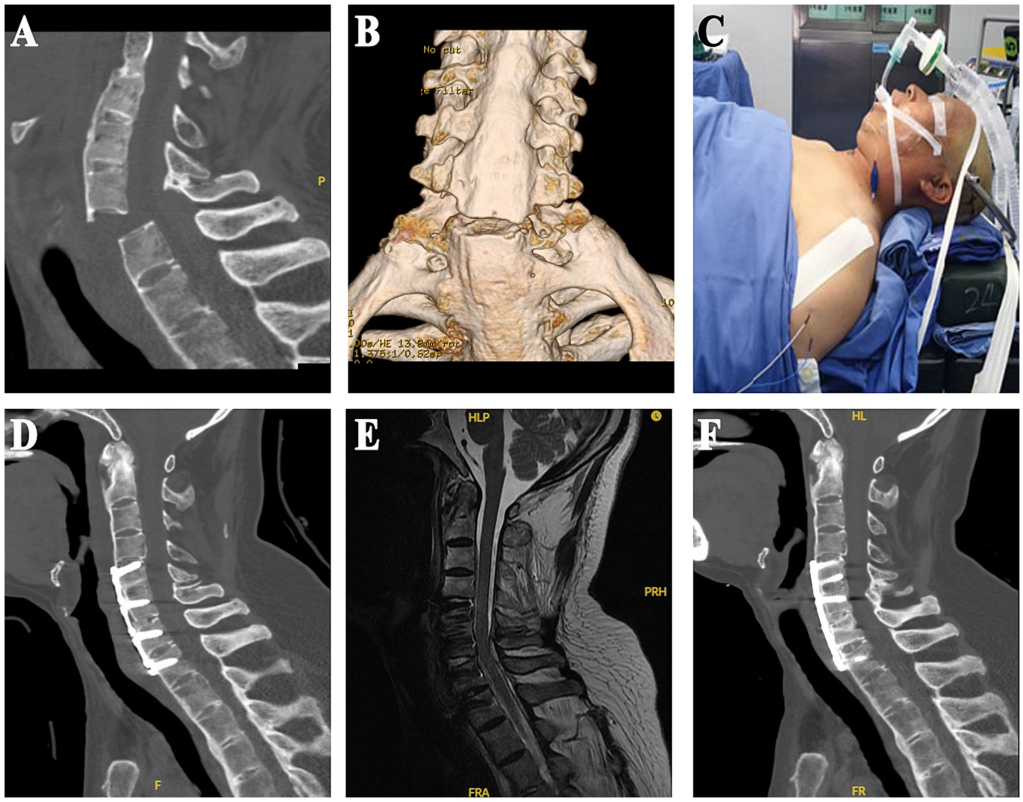

FIGURE 1
(A,B) Preoperative cervical spine CT sagittal and three-dimensional reconstruction images. **(C)** Special postures used by the patient during surgery. **(D,E)** Sagittal CT and MRI images within 1 week after surgery, CT indicated that the internal fixation position was good and stable, and the anatomical morphology of the spinal canal was restored to the maximum extent. **(F)** Sagittal CT images 6 months after surgery.

fractures. However, anterior and posterior fixation has higher surgical risks and more complex operations; surgical position placement is also challenging to ensure that it does not cause secondary nerve damage; at the same time, it has all the risks of anterior and posterior surgery because of the trauma and high risk. In anticipation of the heightened risk of esophageal injury during anterior neck surgery for cervical spine fractures in AS, our approach involves a meticulous preoperative assessment, encompassing imaging and clinical evaluation. Proactive measures to address challenges associated with soft tissue swelling include careful surgical planning and anatomical mapping. During surgery, we prioritize optimal exposure, delicate tissue handling, real-time monitoring, and utilize anatomical knowledge to minimize the risk of esophageal injury. This comprehensive strategy aims to enhance patient safety and mitigate potential complications in this challenging surgical context. In this study, we tried to use only the anterior method of cross-segment fixation of the cervical fracture with long segmental steel plates, combined with the process of postoperative skull traction and auxiliary fixation with the head, neck, and chest brace to overcome the shortcomings in the stability of anterior surgery; our research results show that this method has achieved excellent clinical effects in terms of fixation strength, neurological function recovery, surgical complications, and cervical fracture healing.

Our experience is as follows: (1) Before surgery, the patient's head and neck are positioned high while awake, followed by continuous skull traction under local anesthesia. Dynamic monitoring with fluoroscopy ensures the reduction of cervical fractures and dislocations until satisfactory results are achieved. (2) General anesthesia with endotracheal intubation through the nasal or oral cavity, assisted by a bronchoscope, is preferred. Throughout the procedure, movements of the head and neck are carefully avoided. (3) Comprehensive monitoring and protection of neuroelectrophysiology are maintained throughout the process. (4) Injury to the recurrent laryngeal nerve is minimized through the left neck approach. (5) Given the compression of the anterior column of the fractured vertebra in patients with AS, optimal reduction of the middle and posterior columns is achieved by meticulously removing and scraping the injured intervertebral disk endplate. This is performed without decompression to the posterior edge of the vertebral body, coupled with gentle and appropriate stretching. Autogenous tricortical iliac bone grafting is then implemented. (6) While many AS patients present with cervicothoracic kyphosis, sternotomy or sternoplasty is typically unnecessary for anterior cervical fixation and fusion, as fixation to the T2 vertebra suffices in most cases. Moreover, due to complete fusion of the cervical and thoracic vertebrae in AS patients, adjacent segment instability resulting from adjacent intervertebral disk injury is not a concern. With an adequately long anterior cervical fixation plate, sufficient stability is provided for the patient's cervical vertebrae. Cervical fractures in AS patients are treated akin to osteoporotic extremity fractures. We have found that using the longest anterior cervical plate (3 or 4 segments, with 4–6 locking screws at both ends) yields excellent fixation results. The screws penetrate the vertebral endplate for multi-cortical and multi-angle fixation, resembling the principle of AO limb internal fixation. Consequently, screw loosening and withdrawal are rare in our cases. Furthermore, to prevent potential internal fixation failure, each patient receives an autogenous iliac bone graft and continuous axial cranial traction protection postoperatively, allowing for axial movement and repositioning.

Regarding the necessity for orthopedic intervention, the consensus among most scholars is that cervical fractures in AS patients present an opportunity for kyphosis correction, as these fractures often involve all three columns and resemble surgical osteotomies (20). We assert that orthosis significantly heightens surgical risks in AS patients with lower cervical fractures, and we do not recommend excessive kyphosis correction via the anterior approach. Instead, following anterior decompression, a modest distraction and robust bone grafting to support the cervical anterior column, along with effective long-segment steel plate fixation, offer a simple, safe, and secure solution.

Regarding the rehabilitation of neurological function, postoperative rehabilitation of lower cervical fracture patients with spinal cord injury is arduous based on AS. Neurological recovery in these patients is often inferior to non-AS patients with lower cervical fractures due to the disease itself. Kouyoumdjian (23) reported that most of the deaths were due to quadriplegia patients with severe spinal cord injury before surgery (grade A or B according to ASIA). We excluded grade A cases from our analysis as there were none present in our study cohort. The operative time of our anterior treatment is relatively short, and early comprehensive treatment such as hyperbaric oxygen within 1 month after surgery is also one of the reasons for the better recovery of patients.

Limitations

This study also possesses several limitations. Retrospective analysis may introduce recall bias among patients. Additionally, the relatively small sample size and absence of a control group limit the generalizability of the study results. These constraints underscore the necessity for further enhancement through multicenter, prospective randomized controlled clinical trials to validate the findings of this study.

Conclusion

Anterior cervical long plate surgery is a possible treatment for AS combined with cervical spine fractures due to its simplicity, shorter operation time, and lower bleeding risk. This approach shows high success rates in fracture healing, providing satisfactory spinal stability and neurological function improvement. With the addition of cranial traction and external fixation postoperatively, it proves to be a simple, safe, and effective treatment, especially for surgeons or hospitals unable to master the posterior approach. In addition to surgical segment, the selection of surgical approach should also consider the patient's bone quality, oedema plane of spinal cord injury, and whether there are Andersson lesions.

Data availability statement

The original contributions presented in the study are included in the article/supplementary material; further inquiries can be directed to the corresponding authors.

Ethics statement

The studies involving humans were approved by Enze Hospital of Taizhou Enze Medical Center. The studies were conducted in accordance with the local legislation and institutional requirements. The participants provided their written informed consent to participate in this study.

Author contributions

WC: Conceptualization, Data curation, Funding acquisition, Investigation, Methodology, Project administration, Resources, Writing – original draft. YY: Project administration, Resources, Data curation, Formal analysis, Funding acquisition, Investigation, Writing – original draft. WP: Methodology, Project administration, Resources, Supervision, Validation, Visualization, Writing – review & editing. XL: Formal analysis, Funding acquisition, Project administration, Resources, Visualization, Writing – review & editing. ZH: Project administration, Writing – review & editing, Investigation, Supervision. HL: Supervision, Writing – review & editing, Formal analysis, Software.

Funding

The author(s) declare that financial support was received for the research, authorship, and/or publication of this article. This study was funded by the Zhejiang Province Medical Science and Technology Program of China (No. 2020PY088), the Taizhou City Science and Technology Program of Zhejiang China (No. 1901ky12), the Scientific Research of Enze Medical Center (Group) (No. 22EZC13), the Basic and Public Research Project of Zhejiang Province (LGF20H250004), the Taizhou City Key Discipline Construction Program of Zhejiang China (No. ZDXKQJJ12), Enze Medical Center (Group) Scientific Research (No. 23EZA04), and Zhejiang Medicine and Health Scientific Research Project (No. 2024KY531).

Conflict of interest

The authors declare that the research was conducted in the absence of any commercial or financial relationships that could be construed as a potential conflict of interest.

Publisher's note

All claims expressed in this article are solely those of the authors and do not necessarily represent those of their affiliated organizations, or those of the publisher, the editors and the reviewers. Any product that may be evaluated in this article, or claim that may be made by its manufacturer, is not guaranteed or endorsed by the publisher.

References

1. Braun J, Sieper J. Ankylosing spondylitis. *Lancet*. (2007) 369:1379–90. doi: 10.1016/s0140-6736(07)60635-7

2. Brown MA. Progress in spondylarthritis. Progress in studies of the genetics of ankylosing spondylitis. *Arthritis Res Ther*. (2009) 11:254. doi: 10.1186/ar2692

3. Masi AT. Might axial myofascial properties and biomechanical mechanisms be relevant to ankylosing spondylitis and axial spondyloarthritis? *Arthritis Res Ther*. (2014) 16:107. doi: 10.1186/ar4532

4. Jo DJ, Kim SM, Kim KT, Seo EM. Surgical experience of neglected lower cervical spine fracture in patient with ankylosing spondylitis. *J Kor Neurosurg Soc*. (2010) 48:66–9. doi: 10.3340/jkns.2010.48.1.66

5. Shen N, Wu X, Guo Z, Yang S, Liu C, Guo Z, et al. Classification and treatment for cervical spine fracture with ankylosing spondylitis: a clinical nomogram prediction study. *Pain Res Manag*. (2022) 2022:1–13. doi: 10.1155/2022/7769775

6. Bai H, Li Y, Huang X, Tan Q, Ma X, Wang Q, et al. Can a nomogram predict survival after treatment for an ankylosing spondylitis cervical fracture in a patient with neurologic impairment? A national. *Multicenter Study Clin Orthop Relat Res*. (2023) 481:1399–411. doi: 10.1097/corr.0000000000002542

7. Jo DJ, Kim SM, Kim KT, Seo EM. Erratum: surgical experience of neglected lower cervical spine fracture in patient with ankylosing spondylitis. *J Kor Neurosurg Soc*. (2010) 48:188. doi: 10.3340/jkns.2010.48.2.188

8. Williams AL, Gornet MF, Burkus JK. CT evaluation of lumbar interbody fusion: current concepts. *Am J Neuroradiol*. (2005) 26:2057–66.

9. Jacobs WB, Fehlings MG. Ankylosing spondylitis and spinal cord injury: origin, incidence, management, and avoidance. *Neurosurg Focus*. (2008) 24:E12. doi: 10.3171/foc/2008/24/1/e12

10. Longo UG, Loppini M, Petrillo S, Berton A, Maffulli N, Denaro V. Management of cervical fractures in ankylosing spondylitis: anterior, posterior or combined approach? *Br Med Bull*. (2015) 115:57–66. doi: 10.1093/bmb/ldv010

11. Bhattacharyya S, Kim M. Cervical spine fracture associated with ankylosing spondylitis. *Neurology*. (2014) 83:1297. doi: 10.1212/wnl.0000000000000833

12. He A, Xie D, Cai X, Qu B, Kong Q, Xu C, et al. One-stage surgical treatment of cervical spine fracture-dislocation in patients with ankylosing spondylitis via the combined anterior-posterior approach. *Medicine (Baltimore)*. (2017) 96:e7432. doi: 10.1097/md.0000000000007432

13. Guo Q, Cui Y, Wang L, Lu X, Ni B. Single anterior approach for cervical spine fractures at C5-T1 complicating ankylosing spondylitis. *Clin Neurol Neurosurg*. (2016) 147:1–5. doi: 10.1016/j.clineuro.2016.05.015

14. Ma J, Wang C, Zhou X, Zhou S, Jia L. Surgical therapy of cervical spine fracture in patients with ankylosing spondylitis. *Medicine (Baltimore)*. (2015) 94:e1663. doi: 10.1097/md.0000000000001663

15. Taggard DA, Traynelis VC. Management of cervical spinal fractures in ankylosing spondylitis with posterior fixation. *Spine (Phila Pa 1976)*. (2000) 25:2035–9. doi: 10.1097/00007632-200008150-00006

16. Caron T, Bransford R, Nguyen Q, Agel J, Chapman J, Bellabarba C. Spine fractures in patients with ankylosing spinal disorders. *Spine (Phila Pa 1976)*. (2010) 35:E458–64. doi: 10.1097/BRS.0b013e3181cc764f

17. APPENDIX a: American spinal injury association standard neurological classification of spinal cord injury. *Continuum*. (2011) 17:644–5. doi: 10.1212/01.CON.0000399078.30556.4a

18. Yang H, Wang H, Zhang B, Sun Y, Wang L, Lu X. Cervical spine fracture-dislocation in patients with ankylosing spondylitis and severe thoracic kyphosis: application of halo vest before and during surgical management. *Clin Neurol Neurosurg*. (2021) 207:106744. doi: 10.1016/j.clineuro.2021.106744

19. Liu B, Ji H, Zhang Z, Guo Y, Lv Y, Yang Z, et al. Surgical treatment for cervical spine fracture in patients with ankylosing spondylitis: single posterior approach or combined anterior-posterior approach? *Clin Spine Surg*. (2021) 34:E308–14. doi: 10.1097/bsd.0000000000001155

20. Heyde CE, Fakler JK, Hasenboehler E, Stahel PF, John T, Robinson Y, et al. Pitfalls and complications in the treatment of cervical spine fractures in patients with ankylosing spondylitis. *Patient Saf Surg*. (2008) 2:15. doi: 10.1186/1754-9493-2-15

21. Wang J, Shi L, Chen H, Yuan W. Esophageal perforation in a cervical fracture patient with progressed ankylosing spondylitis: case report and review of the literature. *Spine (Phila Pa 1976)*. (2016) 41:E1364–7. doi: 10.1097/brs.0000000000001885

22. Leone A, Marino M, Dell'Atti C, Zecchi V, Magarelli N, Colosimo C. Spinal fractures in patients with ankylosing spondylitis. *Rheumatol Int*. (2016) 36:1335–46. doi: 10.1007/s00296-016-3524-1

23. Kouyoumdjian P, Guerin P, Schaelderle C, Asencio G, Gille O. Fracture of the lower cervical spine in patients with ankylosing spondylitis: retrospective study of 19 cases. *Orthop Traumatol Surg Res*. (2012) 98:543–51. doi: 10.1016/j.otsr.2012.03.011

frontiers | Frontiers in Surgery

TYPE Original Research
PUBLISHED 03 July 2024
DOI 10.3389/fsurg.2024.1407484

OPEN ACCESS

EDITED BY
Qingchun Mu,
Second Affiliated Hospital of Soochow University, China

REVIEWED BY
Tao Li,
Shandong Provincial Hospital Affiliated to Shandong First Medical University, China
Jiaao Gu,
First Affiliated Hospital of Harbin Medical University, China

*CORRESPONDENCE
Chengxin Xie
✉ chengxin_xie@163.com
Xin Sun
✉ s1979x0739@126.com

†These authors have contributed equally to this work and share first authorship

RECEIVED 27 March 2024
ACCEPTED 17 June 2024
PUBLISHED 03 July 2024

CITATION
He Q, Yan Y, Mei J, Xie C and Sun X (2024) 3D-CT reconstruction for pedicle outer width assessment in patients with thoracolumbar spine fractures: a comparative analysis between age groups <60 years and ≥60 years. Front. Surg. 11:1407484.
doi: 10.3389/fsurg.2024.1407484

3D-CT reconstruction for pedicle outer width assessment in patients with thoracolumbar spine fractures: a comparative analysis between age groups <60 years and ≥60 years

Qiang He[1,2†], Yifeng Yan[3†], Jie Mei[1†], Chengxin Xie[4,5*] and Xin Sun[1*]

[1]Department of Orthopedics, Nanjing Hospital of Traditional Chinese Medicine Affiliated to Nanjing University of Chinese Medicine, Nanjing, China, [2]Department of Orthopedics, Shandong University of Traditional Chinese Medicine Affiliated Hospital, Jinan, China, [3]Department of Orthopedics, Jiangsu Province Second Hospital of Traditional Chinese Medicine, Nanjing, China, [4]Faculty of Graduate Studies, Shandong First Medical University, Jinan, China, [5]Department of Orthopedics, Taizhou Hospital of Zhejiang Province Affiliated to Wenzhou Medical University, Taizhou, China

Objective: This study aims to compare the utilization of 3D-CT reconstruction in measuring pedicle outer width (POW) between younger/middle-aged patients (<60 years) and older patients (≥60 years) with thoracolumbar spine fractures (TSF).
Methods: We conducted a retrospective study from January 2021 to December 2022, involving a total of 108 patients with TSF. The study population consisted of 62 patients aged ≥60 years (observation group) and 46 patients aged <60 years (control group). We compared the POW on both the right and left sides of the thoracolumbar spine between the two groups. Additionally, we analyzed the POW by gender within each group and calculated the incidence of patients falling below the critical values for arch root puncture (5 mm) and arch root nailing (7 mm) in both groups.
Results: There were no statistically significant differences observed in the POW between the two groups on both the left and right sides of each corresponding vertebra ($P > 0.05$). In the observation group, both male and female patients had significantly smaller POW compared to the control group ($P < 0.05$). However, no significant difference in POW was observed between the same-sex groups in the L4 to L5 vertebrae ($P > 0.05$). In the observation group, the POW was less than 5 mm in 9.33% (81/868) of cases and less than 7 mm in 49.88% (433/868) of cases, primarily observed from T11 to L3. In the control group, 4.81% (31/644) of cases had a POW of less than 5 mm, and 13.81% (88/644) had a POW of less than 7 mm.
Conclusion: Utilizing preoperative 3D-CT reconstruction to measure POW in patients with TSF not only facilitates the assessment of surgical feasibility but also aids in surgical pathway planning, thus potentially reducing the incidence of postoperative complications.

KEYWORDS

three-dimensional CT reconstruction, thoracolumbar spine fracture, pedicle outer width, osteoporosis vertebral fractures, vertebral pedicle

1 Introduction

Thoracolumbar spine fractures (TSF) are primarily caused by osteoporosis in elderly patients, often triggered by minor trauma. The severity of the disease can be exacerbated by significantly reduced bone strength and disrupted bone balance (1). With the society undergoing progressive aging, there has been a notable increase in the number of elderly patients seeking medical treatment. Surgical intervention currently remains the primary approach, with percutaneous kyphoplasty (PKP) being a commonly utilized procedure in clinical practice. PKP is renowned for its minimally invasive nature, effective pain relief, and ability to restore vertebral height, thereby serving as the cornerstone of surgical management for TSF (2, 3). However, the occurrence of postoperative complications, including pedicle wall fractures, spinal cord compression, and nerve root injuries, closely relates to the anatomical characteristics of the pedicle. Therefore, accurate measurement of pedicle morphology and dimensions becomes crucial (4).

This retrospective analysis comprises 108 TSF patients (T11 to L5) and aims to compare the changes and characteristics of POW measurements in two distinct age groups (age <60 years and ≥60 years), providing valuable insights for clinical surgical practice.

2 Methods

2.1 Study setting and subjects

This retrospective study utilized electronic medical records (EMR) from Nanjing Hospital of Traditional Chinese Medicine Affiliated to Nanjing University of Chinese Medicine to collect patient data who were received treatment between January 2021 and December 2022. Demographics data (i.e., age and sex), course of disease records, prescription drug dispensation records, bone mineral density (BMD) data, and fracture site records were captured.

The inclusion criteria were as follows: (1) age ≥ 18 years; (2) confirmed diagnosis of TSF, including osteoporotic vertebral compression fractures (OVCF) caused by minor trauma; (3) no history of spinal fractures before TSF; (4) a definite history of trauma. The exclusion criteria were as follows: (1) patients with vertebral tumors or tuberculosis; (2) patients with infectious diseases, coagulation disorders, or spinal cord nerve injuries; (3) patients with vertebral pedicle fractures or dislocations that hindered the measurement of POW; and (4) patients with poor adherence or who discontinued follow-up.

The study followed the Declaration of Helsinki (revised in 2013) and was approved by the ethics committee of Nanjing Hospital of Traditional Chinese Medicine Affiliated to Nanjing University of Chinese Medicine. All patients included in this study provided informed consent for the surgical protocol.

2.2 POW measurement

The POW measurements of thoracolumbar spine (T11 to L5) were measured by Revolution 256-row CT machine (General Electric, USA) with a dose of 120 kV and 250 mA. The acquired images were transferred to the ADW4.6 workstation for processing and storage. The images had a layer thickness and layer spacing of 0.625 mm, a window width of 1,300 Hu, a window position of 400 Hu, and a distance accuracy of 0.1 mm. Surface-masked images of T11 to L5 were generated using techniques such as stage limitation and regional clipping. Reconstruction parameters were adjusted, while the soft tissues surrounding the vertebral body were shielded, resulting in the acquisition of multidimensional images (Figure 1A). The center of the shortest distance from the top and bottom walls of the pedicles was selected to be O, and the axis of the pedicle was drawn as *P* (Figure 1B). The POW was defined as the distance between the medial and lateral bone cortex at the narrowest point of the pedicle, passing through *P* and parallel to the cross-sectional image of the upper endplate (Figure 1C).

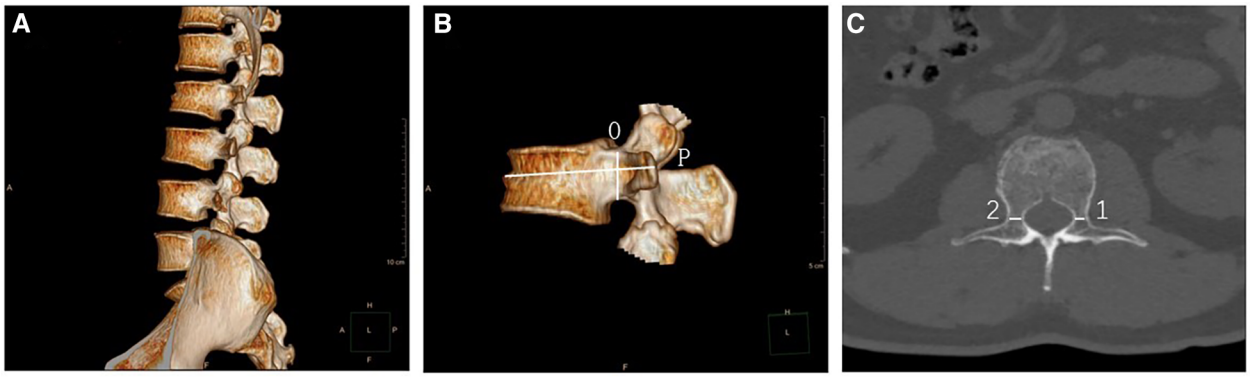

FIGURE 1
(**A**) A multidimensional image from T11 to L5, highlighting the significant wedge-shaped flattening of the L2 vertebral body. (**B**) A lateral image identifying the position of the pedicle axis (P). (**C**) A cross-sectional view used to measure the POW value.

2.3 Outcome indicators

We measured the POW of the thoracolumbar spine (T11 to L5) on the left and right sides of the corresponding vertebrae in the patients. Subsequently, we conducted a comparison of the POW measurements between the two groups. Furthermore, we analyzed and compared the POW measurements of the thoracolumbar spine between the two groups across different genders. To determine the incidence of patients falling below the threshold values for pedicle impingement (POW < 5 mm) and pedicle implantation (POW < 7 mm), we referenced the threshold values used in both domestic and international clinical settings and calculated the measurements accordingly in the two groups.

2.4 Statistical methods

All analyses were conducted with SPSS (version 24.0, IBM, Inc., New York, USA). Continuous variables were calculated using a t-test and presented as the mean ± standard deviation (mean ± SD). Categorical variables were calculated using a chi-square test and presented as frequencies (%). $P < 0.05$ was considered significant statistically.

3 Results

3.1 Baseline characteristics

A total of 108 patients meets the inclusion and exclusion criteria were included in this study. The observation group consisted of 62 elderly patients (age ≥60 years). Among these, 48 patients had a single vertebral compression fracture, and 14 patients had two or more fractures. The control group consisted of 46 young and middle-aged patients (age <60 years). Among these, 38 patients had a single vertebral fracture, while 8 patients had two or more fractures. The baseline characteristics of patients see Table 1.

3.2 Comparison of POW between the left and right sides of each corresponding vertebra

There was no statistically significant difference ($P > 0.05$) in POW measurements between the left and right sides of each corresponding vertebra (T11 to L5) within both groups (Table 2). Therefore, the average of the POW measurements from the left and right sides of each corresponding vertebra was calculated and used as the POW value for the respective pedicle.

3.3 Comparison of POW between the two groups

As shown in Table 3, in the observation group, the POW measurements of each corresponding vertebra from T11 to L3 were found to be smaller compared to those in the control group ($P < 0.05$). However, there was no statistically significant difference in POW measurements of L4 to L5 between the two groups ($P > 0.05$).

3.4 Comparison of POW between the genders

In both the observation and control groups, the POW measurements of male patients from T_{11} to L_3 were found to be greater than those of female patients ($P < 0.05$). However, there was no significant difference in the POW of L_4 to L_5 between males and females in two groups ($P > 0.05$). In the comparison of POW within the same gender between the two groups, the POW

TABLE 1 Baseline characteristics of patients.

Groups	Age (years)	Sex	BMD *T*-score (mean ± SD)	Disease duration (days)	Fracture sites (cases)						
					T11	T12	L1	L2	L3	L4	L5
Observation group ($n = 62$)	73.25 ± 6.67	44F/18M	−3.32 ± 0.71	21.09 ± 7.27	6	12	32	21	9	3	1
Control group ($n = 46$)	38.91 ± 8.54	17F/29M	Not measured	38.91 ± 8.54	3	8	29	16	5	2	1
t/x^2	10.294	6.289		8.278	1.089						
P	<0.001	<0.001		<0.001	>0.05						

TABLE 2 Comparison of POW between the right and left sides of each corresponding vertebra (mean ± SD, mm).

Groups		T_{11}	T_{12}	L_1	L_2	L_3	L_4	L_5
Observation group ($n = 62$)	Left side	6.20 ± 0.88	6.61 ± 0.96	5.61 ± 0.97	6.34 ± 0.91	7.31 ± 0.98	10.12 ± 1.58	12.46 ± 1.43
	Right side	6.29 ± 0.90	6.79 ± 0.97	5.71 ± 0.94	6.40 ± 0.92	7.36 ± 1.01	10.19 ± 1.54	12.58 ± 1.47
T		0.698	0.677	0.718	0.412	0.343	0.512	0.582
P		0.488	0.521	0.461	0.684	0.735	0.617	0.566
Control group ($n = 46$)	Left side	7.63 ± 1.16	8.22 ± 1.13	7.43 ± 1.17	7.83 ± 1.15	8.43 ± 1.12	10.49 ± 1.34	12.82 ± 1.14
	Right side	7.71 ± 1.41	8.29 ± 1.17	7.51 ± 1.22	7.92 ± 1.21	8.51 ± 1.18	10.54 ± 1.41	12.91 ± 1.23
t		0.724	0.511	0.691	0.688	1.218	0.917	0.617
P		0.425	0.621	0.476	0.491	0.114	0.282	0.502

TABLE 3 Comparison of POW between the two groups (mean ± SD, mm).

Groups		T_{11}	T_{12}	L_1	L_2	L_3	L_4	L_5
Observation group ($n = 62$)	Realm	4.21~9.03	4.14~9.45	3.45~8.66	4.42~9.36	4.82~10.48	6.12~14.18	8.56~16.25
	Average value	6.25 ± 0.88*	6.65 ± 0.98*	6.18 ± 1.31*	6.36 ± 0.93*	7.33 ± 1.01*	10.13 ± 1.52	12.53 ± 1.44
Control Group ($n = 46$)	Realm	5.11~9.98	4.88~10.70	4.47~10.24	5.02~10.88	5.67~11.38	7.02~13.94	9.77~15.89
	Average value	7.66 ± 1.08	8.26 ± 1.18	7.46 ± 1.19	7.87 ± 1.22	8.46 ± 1.18	10.31 ± 1.36	12.84 ± 1.21
t		0.724	0.511	0.691	0.688	1.218	0.917	0.617
P		0.425	0.621	0.476	0.491	0.114	0.282	0.502

Compared with the control group.
*$P < 0.05$.

TABLE 4 Comparison of POW between the genders (mean ± SD, mm).

Groups		T_{11}	T_{12}	L_1	L_2	L_3	L_4	L_5
Male	Observation group ($n = 62$)	6.65 ± 0.96*	7.14 ± 1.11*	6.41 ± 1.14*	6.79 ± 1.01*	7.77 ± 1.13*	11.53 ± 1.36	13.62 ± 1.41
	Control group ($n = 46$)	7.81 ± 1.13**	8.38 ± 1.47**	7.57 ± 1.21**	8.07 ± 1.22**	8.66 ± 1.20**	11.01 ± 1.22	13.08 ± 1.26
t		0.698	10.152	11.718	9.296	16.916	4.683	0.916
P		0.488	<0.001	<0.001	0.003	<0.001	0.033	0.163
Female	Observation group ($n = 62$)	6.09 ± 0.82	6.46 ± 0.83	6.11 ± 1.39	6.22 ± 0.88	7.21 ± 0.93	9.63 ± 1.26	12.12 ± 1.25
	Control group ($n = 46$)	7.45 ± 1.07	8.08 ± 1.16	7.27 ± 1.10	7.62 ± 1.09	8.18 ± 1.17	9.71 ± 1.19	12.45 ± 1.12
t		0.724	9.075	15.518	10.926	11.064	7.298	0.728
P		0.425	0.006	<0.001	<0.001	<0.001	0.015	0.342

Compared with the female in observation group.
*$P < 0.05$; Compared with the female in control group, **$P < 0.05$.

measurements in each corresponding vertebra of the T12 to L3 were smaller in the observation group compared to the control group ($P < 0.05$). However, there was no significant difference in the POW of L4 to L5 within the same gender between the two groups. ($P > 0.05$). See Table 4.

3.5 Occurrence of below the threshold for pedicle puncture and nail placement

In the observation group, a total of 868 pedicles were measured, and 9.33% (81/868) of them had a POW measurement below the critical value for pedicle puncture (<5 mm). The POW below the critical value for pedicle implantation (<7 mm) accounting for 49.88% (433/868), with the majority of these measurements observed from T11 to L3. In the control group, a total of 644 pedicles were measured. Among them, 4.81% (31/644) had a POW measurement below 5 mm and 13.66% (88/644) had a POW measurement below 7 mm. These measurements were primarily distributed from T11 to L3. See Table 5.

4 Discussion

TSF is a prevalent type of fracture observed in clinical spinal surgery, particularly among the elderly population (5, 6). It is often attributed to factors such as gastrointestinal dysfunction, impaired absorption of calcium, decreased bone formation, mineralization capacity, and reduced BMD. With the bone trabeculae becoming less dense and the bones becoming more brittle, TSF can occur even in the absence of apparent causal factors or with minimal external force exerted (7, 8).

The diameter of the vertebral pedicle gradually widens with age within certain age brackets, indicating a continuous alteration.

TABLE 5 Occurrence of POW below the threshold for pedicle puncture and nail placement.

	Observation group males($n = 36$)		Observation group females ($n = 88$)		Control group males ($n = 58$)		Control group females ($n = 34$)	
	<5 mm	<7 mm	<5 mm	<7 mm	<5 mm	<7 mm	<5 mm	<7 mm
T_{11}	1 (2.78)	16 (44.44)	16 (18.18)	81 (92.05)	0 (0)	11 (18.97)	7 (20.59)	12 (35.29)
T_{12}	1 (2.78)	12 (33.33)	12 (13.64)	74 (84.09)	0 (0)	8 (13.79)	3 (8.82)	4 (11.76)
L_1	6 (16.67)	28 (77.78)	22 (25.00)	84 (95.45)	5 (8.62)	14 (24.14)	9 (26.47)	11 (32.35)
L_2	2 (5.56)	13 (36.11)	14 (15.90)	73 (82.95)	0 (0)	9 (15.52)	5 (14.71)	9 (26.47)
L_3	1 (2.78)	4 (11.11)	6 (6.82)	41 (46.59)	0 (0)	5 (8.62)	2 (5.88)	5 (14.71)
L_4	0 (0)	0 (0)	0 (0)	7 (7.95)	0 (0)	0 (0)	0 (0)	0 (0)
L_5	0 (0)	0 (0)	0 (0)	0 (0)	0 (0)	0 (0)	0 (0)	0 (0)
total	11 (4.37)	73 (28.97)	70 (11.36)	360(58.44)	5(1.23)	47(11.58)	26(10.92)	41(17.23)

[n (%)].

Specifically, it widens progressively in adulthood, with females ceasing to show increases after the age of 50 and males after 60, thereafter exhibiting a diminishing trend (9, 10, 11). Our study findings revealed that older patients with TSF had smaller vertebral POW measurements compared to young and middle-aged individuals, specifically in the range from T11 to L3 ($P < 0.05$). In addition, our investigation revealed a gender disparity in the POW measurements of the thoracolumbar vertebrae (T11 to L3) within the same cohort. Specifically, males have exhibited larger POW measurements in contrast to females. Notably, there was a male-to-female ratio of 9:22 among elderly patients, indicating that female patients were more susceptible to TSF.

The strength of the lumbar extensor muscles decreases with age, this gradual weakening contributes to the development of stress changes in the spine, particularly affecting the vulnerability of the anterior spine to osteoporotic vertebral compression fractures. In addition, the age-related decline in the strength of the lumbar extensors leads to alterations in spinal stress distribution, further results in increased pressure on the anterior column of the spine, increased angle of thoracic kyphosis, decreased angle of lumbar lordosis, and a shift in the body's center of gravity. Consequently, these changes contribute to remodeling of the vertebral arches. It is noteworthy that while the T11 and T12 vertebrae are still connected to the ribs, they do not significantly contribute to the formation of the thoracic contour. Therefore, the stress concentration in the spinal region shifts from the thoracic to the lumbar anterior convexity. As a result, TSF most commonly occurs between the T11 vertebra and the L3 vertebra, with a particularly high prevalence at the L1 and L2 vertebrae. Furthermore, the significant hormonal changes that occur in elderly female patients after menopause make them more susceptible to osteoporosis, increasing their risk of fractures.

Currently, surgical treatment remains the preferred approach for achieving efficient recovery in patients with TSF. In particular, the pedicle plays an indispensable role in PKP, which is a commonly employed surgical procedure for treating TSF (12). The assessment of pedicle parameters, particularly POW, is crucial for the successful execution of surgical procedures. The reduction in POW significantly impacts intraoperative vertebral pedicle puncture procedures. A POW of less than 5 mm indicates a narrow vertebral pedicle, making it unsuitable for using standard-sized puncture catheters (13). As POW decreases, there arises a necessity to adjust the catheter diameter. Therefore, preoperative POW measurements can provide direct evidence for selecting the appropriate puncture catheter during the procedure. In addition, in patients presenting with severe spinal instability, spinal cord injury, spinal tumors, and similar conditions, vertebral pedicle screw insertion procedures are warranted (14). A diminutive POW may exacerbate the difficulty of screw insertion, potentially leading to complications such as fractures of the inner and outer walls of the pedicle (14).Therefore, when performing vertebral pedicle screw insertion procedures, it is imperative to calculate the appropriate critical value for pedicle screw placement based on preoperative POW measurements, aiming to mitigate postoperative complications.

POW, as one of the crucial parameters, serves as a valuable tool for clinicians to discern the anatomical characteristics of the vertebral pedicle (15). The critical values for pedicle puncture (POW < 5 mm) and pedicle nail placement (POW < 7 mm) have been established (16). When the POW falls below these critical values, it is not advisable to utilize conventional puncture instruments for the operation. Therefore, precise determination of the POW value is essential for procedural success.

5 Conclusion

In this study, we observed that the percentage of patients with POW measurements below the critical value for pedicle puncture (5 mm) and the critical value for pedicle nail placement (7 mm) in the observation group was higher than that of control group. In addition, in the observation group and the control group, the percentage of females with POW below 5 mm was higher than the males in the same group. The percentage of females with POW measurements below 7 mm was higher than the males in the same group. These findings indicate the importance of exercising additional caution when performing pedicle puncture, particularly in females, especially when the fracture involves the vertebral levels ranging from the T12 to L2 vertebrae.

Data availability statement

The original contributions presented in the study are included in the article/Supplementary Material, further inquiries can be directed to the corresponding authors.

Ethics statement

The studies involving humans were approved by The ethics committee of Nanjing Hospital of Traditional Chinese Medicine affiliated to Nanjing University of Chinese Medicine. The studies were conducted in accordance with the local legislation and institutional requirements. The participants provided their written informed consent to participate in this study.

Author contributions

QH: Writing – original draft, Visualization, Investigation, Formal Analysis, Data curation, Conceptualization. YY: Writing – original draft, Methodology, Investigation, Formal Analysis, Data curation. JM: Writing – original draft, Investigation, Formal Analysis, Data curation. CX: Writing – review & editing, Validation, Supervision, Resources, Investigation. XS: Writing – review & editing, Supervision, Conceptualization.

Funding

The author(s) declare financial support was received for the research, authorship, and/or publication of this article.

This research was funded by Science and Technology Project of Jiangsu Province (No. SBE2021740210).

Conflict of interest

The authors declare that the research was conducted in the absence of any commercial or financial relationships that could be construed as a potential conflict of interest.

Publisher's note

All claims expressed in this article are solely those of the authors and do not necessarily represent those of their affiliated organizations, or those of the publisher, the editors and the reviewers. Any product that may be evaluated in this article, or claim that may be made by its manufacturer, is not guaranteed or endorsed by the publisher.

References

1. Yu W, Zhang H, Yao Z, Zhong Y, Jiang X, Cai D. Prediction of subsequent vertebral compression fractures after thoracolumbar kyphoplasty: a multicenter retrospective analysis. *Pain Med.* (2023) 24(8):949–56. doi: 10.1093/pm/pnad044

2. Thapa BB, Shah RP. Functional and radiological outcome of short same segment instrumentation in thoracolumbar burst fracture. *J Nepal Health Res Counc.* (2023) 21 (1):15–8. doi: 10.33314/jnhrc.v21i1.4387

3. Zhuang M, Cai B, Wang F. Effectiveness and safety of percutaneous kyphoplasty combined with zoledronic acid in treatment of osteoporotic vertebral compression fractures: a meta-analysis. *Arch Orthop Trauma Surg.* (2022) 142(10):2435–43. doi: 10.1007/s00402-021-03858-4

4. Kim WJ, Ma SB, Shin HM, Song DG, Lee JW, Chang SH, et al. Correlation of sagittal imbalance and recollapse after percutaneous vertebroplasty for thoracolumbar osteoporotic vertebral compression fracture: a multivariate study of risk factors. *Asian Spine J.* (2022) 16(2):231–40. doi: 10.31616/asj.2021.0062

5. Wood KB, Li W, Lebl DR, Ploumis A. Management of thoracolumbar spine fractures. *Spine J.* (2014) 14(1):145–64. doi: 10.1016/j.spinee.2012.10.041

6. Kutsal FY, Ergin Ergani GO. Vertebral compression fractures: still an unpredictable aspect of osteoporosis. *Turk J Med Sci.* (2021) 51(2):393–9. doi: 10.3906/sag-2005-315

7. Imamudeen N, Basheer A, Iqbal AM, Manjila N, Haroon NN, Manjila S. Management of osteoporosis and spinal fractures: contemporary guidelines and evolving paradigms. *Clin Med Res.* (2022) 20(2):95–106. doi: 10.3121/cmr.2021.1612

8. Wang B, Cao J, Chang J, Yin G, Cai W, Li Q, et al. Effectiveness of tirobot-assisted vertebroplasty in treating thoracolumbar osteoporotic compression fracture. *J Orthop Surg Res.* (2021) 16(1):65. doi: 10.1186/s13018-021-02211-0

9. Imagama S, Matsuyama Y, Hasegawa Y, Sakai Y, Ito Z, Ishiguro N, et al. Back muscle strength and spinal mobility are predictors of quality of life in middle-aged and elderly males. *Eur Spine J.* (2011) 20(6):954–61. doi: 10.1007/s00586-010-1606-4

10. Kasukawa Y, Miyakoshi N, Hongo M, Ishikawa Y, Kudo D, Suzuki M, et al. Age-related changes in muscle strength and spinal kyphosis angles in an elderly Japanese population. *Clin Interv Aging.* (2017) 12:413–20. doi: 10.2147/CIA.S113352

11. Liang C, Sun J, Cui X, Jiang Z, Zhang W, Li T. Spinal sagittal imbalance in patients with lumbar disc herniation: its spinopelvic characteristics, strength changes of the spinal musculature and natural history after lumbar discectomy. *BMC Musculoskelet Disord.* (2016) 17:305. doi: 10.1186/s12891-016-1164-y

12. Luo Y, Jiang T, Guo H, Lv F, Hu Y, Zhang L. Osteoporotic vertebral compression fracture accompanied with thoracolumbar fascial injury: risk factors and the association with residual pain after percutaneous vertebroplasty. *BMC Musculoskelet Disord.* (2022) 23(1):343. doi: 10.1186/s12891-022-05308-7

13. Kalemci O, Kizmazoglu C, Ozyoruk S, Uzunoglu I, Husemoglu B, Atar M, et al. What is the effect of pedicle screw reinsertion through the same trajectory on pullout strength? *Turk Neurosurg.* (2022) 32(4):635–40. doi: 10.5137/1019-5149.JTN.35526-21.3

14. Mandelka E, Gierse J, Zimmermann F, Gruetzner PA, Franke J, Vetter SY. Implications of navigation in thoracolumbar pedicle screw placement on screw accuracy and screw diameter/pedicle width ratio. *Brain Spine.* (2023) 3:101780. doi: 10.1016/j.bas.2023.101780

15. Chazono M, Soshi S, Inoue T, Kida Y, Ushiku C. Anatomical considerations for cervical pedicle screw insertion: the use of multiplanar computerized tomography reconstruction measurements. *J Neurosurg Spine.* (2006) 4(6):472–7. doi: 10.3171/spi.2006.4.6.472

16. Hu H, Lin X, Tan L. Thoracolumbar osteoporotic vertebral compression fracture treatment by unilateral percutaneous vertebroplasty using curved diffusion needle. *Indian J Orthop.* (2023) 57(6):899–906. doi: 10.1007/s43465-023-00848-z

frontiers | Frontiers in Neurology

TYPE Original Research
PUBLISHED 16 July 2024
DOI 10.3389/fneur.2024.1422357

OPEN ACCESS

EDITED BY
Qingchun Mu,
Second Affiliated Hospital of Soochow University, China

REVIEWED BY
Andrea J. Santamaria,
The Miami Project to Cure Paralysis, United States
Xiaofeng Chen,
Harbin Medical University, China
Hongzhi Gao,
The Second Affiliated Hospital of Fujian Medical University, China

*CORRESPONDENCE
Sean M. Barber
✉ sbarber@houstonmethodist.org

RECEIVED 24 April 2024
ACCEPTED 28 June 2024
PUBLISHED 16 July 2024

CITATION
Barber SM, Wolfe T, Steele AG, Hoffman K, Hogan MK, Frazier A, Tang X, Sayenko DG and Horner PJ (2024) A novel minimally invasive and versatile kyphoplasty balloon-based model of porcine spinal cord injury. *Front. Neurol.* 15:1422357. doi: 10.3389/fneur.2024.1422357

A novel minimally invasive and versatile kyphoplasty balloon-based model of porcine spinal cord injury

Sean M. Barber[1,2]*, Tatiana Wolfe[2,3], Alexander G. Steele[2], Kris Hoffman[2], Matthew K. Hogan[2], Allison Frazier[2], Xiufeng Tang[2], Dimitry G. Sayenko[2] and Philip J. Horner[2]

[1]Department of Neurosurgery, Houston Methodist Neurological Institute, Houston, TX, United States, [2]Center for Neuroregeneration, Houston Methodist Research Institute, Houston, TX, United States, [3]University of Arkansas for Medical Sciences, Psychiatric Research Institute, Brain Imaging Research Center, Little Rock, AR, United States

Introduction: Spinal cord injury (SCI) animal models often utilize an open surgical laminectomy, which results in animal morbidity and also leads to changes in spinal canal diameter, spinal cord perfusion, cerebrospinal fluid flow dynamics, and spinal stability which may confound SCI research. Moreover, the use of open surgical laminectomy for injury creation lacks realism when considering human SCI scenarios.

Methods: We developed a novel, image-guided, minimally invasive, large animal model of SCI which utilizes a kyphoplasty balloon inserted into the epidural space via an interlaminar approach without the need for open surgery.

Results: The model was validated in 5 Yucatán pigs with imaging, neurofunctional, histologic, and electrophysiologic findings consistent with a mild compression injury.

Discussion: Few large animal models exist that have the potential to reproduce the mechanisms of spinal cord injury (SCI) commonly seen in humans, which in turn limits the relevance and applicability of SCI translational research. SCI research relies heavily on animal models, which typically involve an open surgical, dorsal laminectomy which is inherently invasive and may have untoward consequences on animal morbidity and spinal physiology that limit translational impact. We developed a minimally invasive, large animal model of spinal cord injury which utilizes a kyphoplasty balloon inserted percutaneously into the spinal epidural space. Balloon inflation results in a targeted, compressive spinal cord injury with histological and electrophysiological features directly relevant to human spinal cord injury cases without the need for invasive surgery. Balloon inflation pressure, length of time that balloon remains inflated, and speed of inflation may be modified to achieve variations in injury severity and subtype.

KEYWORDS

spinal cord injury, animal model, minimally invasive surgery, kyphoplasty, spinal cord contusion injury

Introduction

The annual incidence of spinal cord injury (SCI) in the United States is estimated at 54 cases per one million people, totaling around 18,000 new cases annually (1). SCI can result in enduring sensory and motor alterations, causing partial or complete paralysis, sensory loss, autonomic dysreflexia, bowel and bladder changes, and pain (2). These impairments significantly impact an individual's quality of life, necessitating continuous rehabilitation efforts to maintain the ability to perform daily tasks. The occurrence and severity of post-injury impairments vary based on the level and extent of the injury. The precise pathophysiological mechanisms at work in SCI and their relationship to the clinical phenotype of a patient with SCI are currently underexplored. Despite a clinical diagnosis of "complete loss" of sensorimotor function in some patients with SCI, evidence suggests that many sub-functional neural connections between the brain and spinal cord remain intact across the injury site (3–5). These connections are not robust enough to drive clinically detectable function; however, they are capable of influencing the excitability of spinal sensorimotor networks below the lesion (6–8). Crucially, the decrease of descending pathways' integrity and cortical grey matter volume is directly correlated with spinal cord atrophy, suggesting that trauma-induced spinal degenerative processes spread towards the brain. These changes appear to be dynamic and influenced by the level, completeness, and time after injury, as well as the extent of clinical recovery (9). These findings are critically relevant to our study, as they indicate that (1) brain networks involved in different demands of motor control remain responsive even in chronic paralysis, (2) therapeutic strategies aimed at restoring spinal cord function, even in individuals with chronic SCI, can build on preserved competent descending control, and (3) the heterogeneity in residual motor function associated with SCI and individual response to a therapy can be addressed using mechanistic neurophysiology studies.

Research into the pathophysiology of SCI and therapeutics to spur regeneration of the injured spinal cord has drawn in large part from animal studies. The development of animal models for SCI that reliably and accurately reproduce the sequelae of SCI in humans is thus crucial to our progress towards effective treatments. The large majority of contemporary animal models for SCI rely on an invasive surgical procedure (i.e., laminectomy) for access to - and reproducible mechanical deformation of - spinal tissue (10). While laminectomy is useful in that it allows direct visualization and manipulation of the spinal cord, the procedure itself also imparts some degree of animal morbidity, may impact animal recovery/functional status, and demonstrates limited clinical correlation to the closed, compressive SCIs commonly seen in humans. Furthermore, though the effect of laminectomy itself on the injury and recovery pattern itself after SCI has not been well studied, laminectomy is often indicated as a surgical treatment in patients with spinal cord injury who are found to have persistent spinal cord compression, and as such, laminectomy could conceivably have an effect on functional recovery after injury creation. Additionally, laminectomy may lead to changes in spinal cord perfusion, cerebrospinal fluid (CSF) flow dynamics, and spinal stability that may confound the results of a study evaluating novel therapeutics or interventions even in the absence of ongoing spinal cord compression (11–14).

A variety of minimally invasive animal models for spinal cord injury have been developed, including models wherein a small laminectomy or hemilaminectomy is utilized to minimize bony removal (15, 16), and models involving microscopic dissection and/or operating techniques intended to minimize collateral tissue trauma (17). Each of these, however, still requires muscle dissection and removal of bone over the site of injury. Other models have utilized a balloon compression device inserted into the epidural or subdural space via a small hemilaminectomy performed caudal to the site of injury (18–20), which may mitigate the effect of laminectomy on CSF and vascular dynamics at the site of injury, but the methods utilized in these models nevertheless require muscular dissection, bony removal, and other collateral tissue damage that impact animal recovery and well-being in the post-injury phase.

We aimed to develop a minimally invasive large animal model of thoracic spinal cord injury that requires no muscle dissection or bony removal and can be performed safely and reproducibly in a large animal. The primary incentives for development of this new model were to minimize procedure-related animal morbidity, alleviate the confounding influence of bony removal on injury-site dynamics and maximize animal recovery after injury surgery. Subsequently, we conducted a thorough investigation into the pathophysiology of this injury model, employing comprehensive assessments such as imaging, neurophysiology, neurofunctional and histology results in five representative pigs.

Results

Four of the five animals tolerated the procedure well. One animal expired on the day of injury while awakening from anesthesia. The precise cause of death was unclear, but was theorized to be related to spinal shock resulting from a relatively severe spinal cord injury. The animal was the youngest of the pigs included (3 months and 21 days at surgery, weighing 18 kg) and developed respiratory failure 2 h after extubation while in post-operative recovery, expiring as a result. Post-mortem examination revealed a relatively severe spinal cord injury with associated intradural and intramedullary hemorrhage, but no other systemic abnormalities to explain the respiratory failure and subsequent death.

MRI

Immediate post-injury 1.5 T MRI demonstrated a T2-hyperintense focus within the spinal cord parenchyma at the site of injury in each animal consistent with a mild contusion injury. Endpoint T1w, T2w, T2-FLAIR, and myelin SHIFT MRI in all animals demonstrated signal changes within the spinal cord consistent with a mild contusion injury and a trend towards increase myelin SHIFT T2 signal, consistent with mildly injured myelin.

Electrophysiology

After the balloon implantation but before inflation, spinally evoked potentials were evident in recorded hindlimb muscles. Transcranial electrical stimulation (TES) induced motor-evoked potentials (MEPs) in both forelimb and hindlimb muscles. Once the balloon reached 100 pounds per square inch (PSI) and during the subsequent 10 min, MEPs in hindlimb muscles were universally abolished in all animals, while spinally evoked potentials remained

unchanged. This suggests that the injury caused damage to descending motor pathways without affecting the spinal reflex circuitry below the level of compression. The MEPs in hindlimb muscles recovered 8 days post-surgery (Figure 1).

Neurofunctional testing

All animals exhibited normal gait function at baseline (BBB score 21). After injury, neurophysiological data was available for 3 of the 5 animals (due to 1 animal expiring and 1 animal not having undergone video recording). Of the 3 animals for which neurophysiological data was available, immediate post-injury BBB scores ranged from 4–17 (mean 9), with endpoint BBB scores ranging from 9–20 (mean 16.3). In animal #4, post-operative functional deficits were relatively mild, whereas in animals #3 and #5, post-operative deficits were more severe. Both animals #4 and #5 experienced considerable recovery of function by endpoint testing. Animal #3 experienced only modest recovery of function by endpoint testing, although this animal's endpoint was relatively soon after injury (8 days) (Table 1).

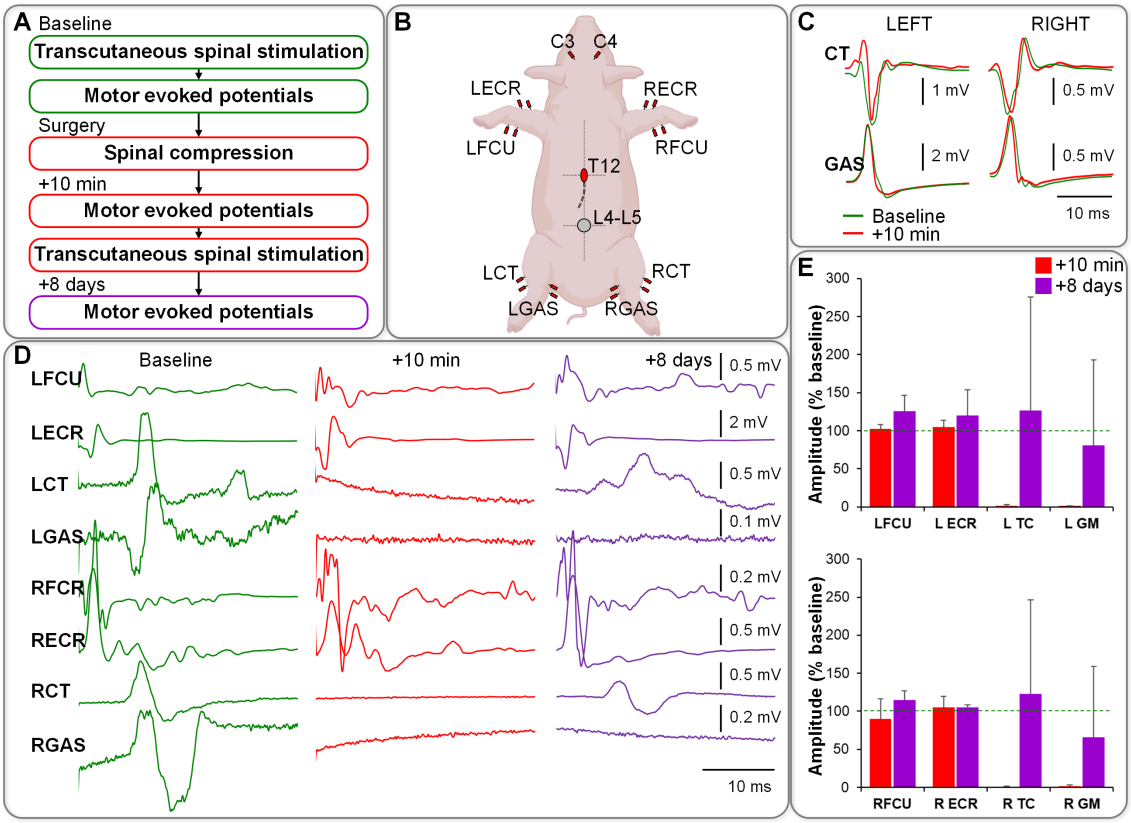

FIGURE 1
(A) Electrophysiology protocol/order. **(B)** Setup of stimulating and recording electrodes. **(C)** Responses elicited in hindlimb muscles during transcutaneous spinal stimulation at L4-L5 (no changes observed between baseline and post-compression). **(D)** Motor evoked responses induced during transcranial stimulation over the motor cortex (responses in hindlimb muscles were abolished immediately post-compression and partially restored on day 8 post-surgery). **(E)** Group data from $n = 4$, normalized to the baseline.

TABLE 1 **Neurofunctional outcomes.**

Neurofunctional outcomes (BBB)			
Animal #	Preop	Postop	Final
1	ND (not recorded)	ND (not recorded)	ND (not recorded)
2	21	ND (expired)	ND (expired)
3	21	4 (POD 2)	9 (day 8)
4	21	17 (POD2)	20 (day 8)
5	21	6 (POD0)	20 (day 14)

Neurofunctional Scores (BBB) for 5 pigs undergoing experimental balloon-based thoracic spinal cord injury.
Preop, pre-operative; Postop, post-operative.

Histology

Post-mortem examination did not demonstrate any systemic (e.g., cardiopulmonary) pathologies in any animal. Endpoint spinal cord histology in each case demonstrated multilobular cystic cavitation at the site of injury, which was typically unilateral (Figures 2A–C). Sparse axonal sparing was seen within each cavitation perimeter along with signs of inflammation (Figures 2B,C). Significant axonal loss was observed in the dorsal and lateral funiculi producing damage to the anatomical location of descending motor corticospinal, rubrospinal and vestibulospinal tracts as well as ascending sensory tracts. Gray matter damage was limited to the ipsilateral dorsal horn and the superficial contralateral dorsal horn. In some cases, contralateral injury and/or ischemic infarcts were seen in the ventral horn with neuronal cell loss (Figure 2D).

Discussion

The ideal animal model for SCI would closely and reproducibly mimic the scale and physiological consequences of SCI seen in humans. Large animal models hold significant advantages to model the scale and physiological consequences of spinal trauma but are limited in use due to expense, limited injury technology and the complexity of surgery and recovery. Here we have generated an innovative, minimally invasive spinal compression model in a large animal that is reproducible and mimics much of the pathophysiology of human spinal cord injury while maintaining the integrity of the spinal column and related structures. This model is well-suited for conducting quantitative assessments of sensorimotor physiology and imaging to evaluate lesion severity and is a potential tool for exploratory research and translational testing of surgical, neuromodulatory, and molecular repair approaches in the context of spinal injuries.

The first documented spinal cord injury animal model was a canine laminectomy and weight-drop model published by Alfred Allen in 1911 (21), and although advances in technology and understanding of spinal cord injury have led to improvements in this model, a large number of modern SCI animal models continue to utilize a contusion performed via an open surgical laminectomy (10). While contusion models do effectively reproduce a mechanism of SCI seen frequently in humans (22, 23), several limitations to the use of open laminectomy in animal models of SCI exist. Firstly, an open surgical laminectomy is an invasive procedure that requires muscle dissection and bony removal and leads to post-operative pain and morbidity. Laminectomy also carries risks such as durotomy, CSF leakage (1–15% in humans) (24), epidural hematoma (1% in humans) (25) and post-operative spinal instability (seen in 4.1–12% in humans) (12). Finally, laminectomy results in structural changes to the spinal

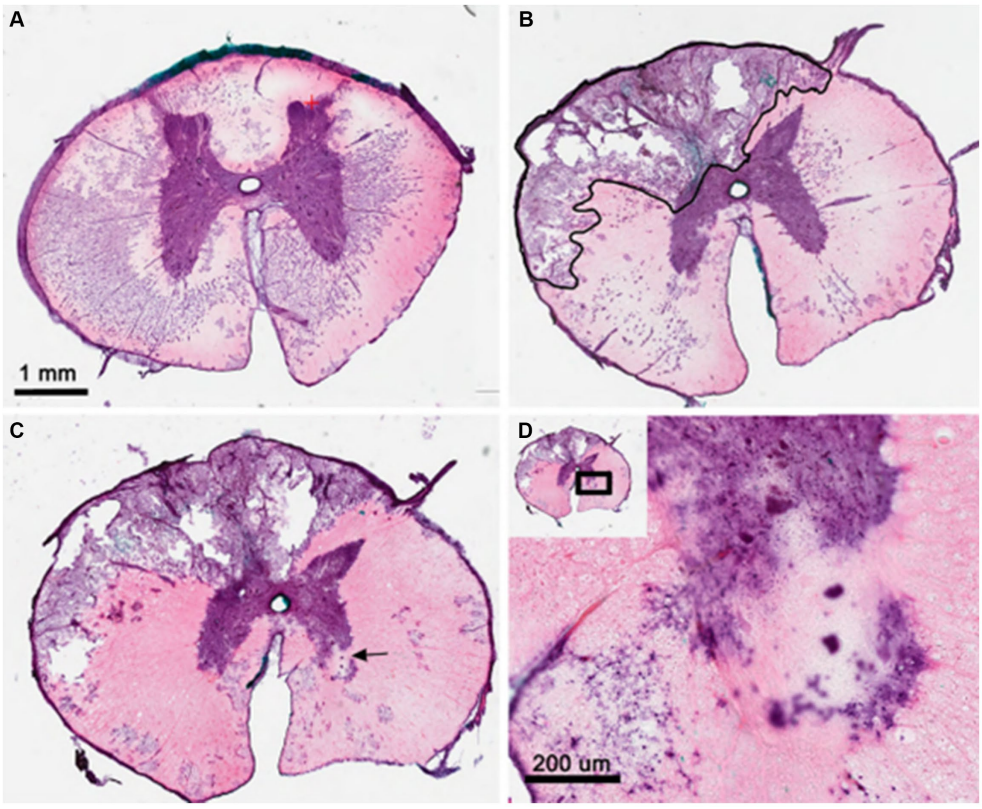

FIGURE 2
Histologic analysis of dorsolateral compression injury of the thoracic spinal cord from pig #4. **(A)** H&E staining of T10 spinal segment showing normal thoracic gray and white matter structures. **(B)** T12 segment at site of balloon compression shows cystic cavitation in the dorsolateral white matter and ipsilateral dorsal horn. Black outline indicates early cavitation perimeter with sparse axonal sparing and inflammation. **(C)** 100 mm caudal to lesion epicenter showing multi-lobular nature of cystic cavity and evidence of contralateral gray matter stroke (arrow). **(D)** High magnification of contralateral ventral horn showing evidence of both ventral horn motor loss and scarring as well as neighboring white matter damage. H&E, hematoxylin and eosin; mm, millimeters.

canal which impact spinal cord perfusion pressure (14) and CSF flow dynamics (11) in ways that confound the investigation of spinal cord injury pathophysiology and therapeutics in an animal model.

Minimally invasive models of SCI

Previously described minimally invasive animal models of spinal cord injury include models that minimize the amount of bone removed during the laminectomy portion of the injury surgery (15, 16), models involving microscopic dissection and/or operating techniques intended to minimize collateral tissue trauma (17), and models wherein a balloon compression device is inserted into the epidural or subdural space via a small hemilaminectomy defect (18–20). While each of these are less invasive than a typical open surgical laminectomy, they each still involve muscle dissection and bony removal, and are subject to the limitations of laminectomy in a spinal cord injury model discussed previously.

A canine SCI model described by Purdy et al. (26) utilizes an angioplasty balloon inserted percutaneously into the spinal subarachnoid space to induce a compression injury. This method foregoes the need for laminectomy or open surgery, and the histological and imaging results provided by the investigators are consistent with those seen in the currently described model but limited to 4 hours post-lesion. The authors utilized a balloon inflation pressure of 10 atmospheres (atm) in the majority of animals and left the balloon inflated for a period of 30 min. The authors' description of the model is limited to the acute period and does not include neurofunctional assessments, electrophysiologic assessments, or myelin-based MRI imaging assessments, as were performed in our study. Dynamic, intraoperative electrophysiologic assessments were particularly important in our described model, as balloon inflation pressure was tailored to each animal (i.e., inflation was stopped at such time that transcranial MEPs were found to be absent in the lower extremities) in an attempt to create a reproducible, titratable injury and mitigate variance in canal and spinal cord size between animals. Additionally, the post-injury histology in our study frequently demonstrated cystic cavitation and loss of descending and ascending white matter tracts as well as limited motor neuron loss within the ventral horn ipsilateral to injury, which was not seen in the model described by Purdy et al.

Applications for balloon-based SCI animal models

Animal models for SCI would ideally recapitulate forms of SCI seen in humans, and traumatic SCI in humans often involves high-speed ballistic injury with forces exceeding those attainable through the relatively slow inflation of a balloon, as was utilized in our study. Balloon inflation models may, however, appropriately reproduce the underlying mechanisms of spinal cord contusion seen in patients with gradually developing compressive pathologies such as epidural hematoma, epidural abscess, or degenerative stenosis. Additionally, pathologies such as cervical myelopathy (wherein spinal cord injury occurs due to very slowly progressive spinal cord compression) or spinal cord compression via a spinal tumor with epidural extension could theoretically be modeled with the use of slow and prolonged balloon expansion (27). The model developed here would also allow the redirection of the balloon to achieve either the midline, dorsolateral or even ventral compression.

Limitations and future approaches

Our study possesses several limitations. Firstly, the sample size of the study was relatively small (5 animals). In addition, the method of neurofunctional testing used (BBB score via recorded video) is subject to bias. Furthermore, while the balloon inflation pressure utilized was governed by electrophysiologic loss of motor potentials in the lower extremities, the balloon inflation time utilized (15 min) was arbitrarily chosen, and balloon inflation was performed manually while a mechanical inflation may be more rigorous. Insertion of a kyphoplasty needle into the epidural space of a pig is technically challenging, as the Jamshidi needle used for insertion is of relatively large bore, and very little subarachnoid space is present in the thoracic spine of Yucatán pigs. The technique could possibly be improved upon with the use of CT-guided navigation, or experimentation with a transforaminal - rather than interlaminar - insertional approach. Moreover, the neurofunctional outcomes in the study were evaluated using the Basso, Beattie and Bresnahan (BBB) score, which is designed for use in rodents. While efforts have been made by other investigators to create a scale to characterize gait in pigs, no real consensus exists regarding gait outcomes scoring in pigs. Given this, the authors utilized the BBB score, which is widely utilized to evaluate gait function after spinal cord injury in rodents, but its relevance to gait function outcomes in pigs is unclear. Finally, the injury observed in the majority of animals was clinically, radiographically and histologically very mild, and as a result additional titration of injury severity may be necessary in order to achieve injury magnitudes bearing greater clinical relevance for therapeutic studies. Additional work is also necessary to better define differences in injury severity and morphology findings that will undoubtedly occur with variation in the time that the balloon is left inflated, the circumferential position of the catheter or variation in the speed of its inflation. The expense of performing these experiments may limit the utility of the model but the potential exists to produce distinct models that closely mimic a variety of common human SCI pathologies.

Materials and methods

Institutional approval

All animal experiments were performed with the approval of the institutional animal care and use committee (IACUC).

Animals

Five healthy femaleYucatán pigs were utilized for the model. Mean pig age was 8 months at the time of surgery (range 3 months – 21 months). Mean weight was 44.4 kg (range 18–103 kg). Animal demographics are described in Table 2. Animals were sourced by the veterinary staff of our institutional Comparative Medicine Program. Prior to the injury surgery, all animals underwent baseline MRI, baseline neurofunctional testing and baseline neurophysiological testing. A diagram depicting the overall experimental protocol is seen

TABLE 2 Animal age, weight and other demographic characteristics.

Pig number	Strain	Age at surgery	Weight at surgery (kg)	Surgery to euthanasia timespan (days)
1	Yucatán	21 m 14d	103	5
2	Yucatán	3 m 21d	18	0
3	Yucatán	4 m 9d	25	8
4	Yucatán	6 m 5d	40	29
5	Yucatán	6 m 24d	35.8	27

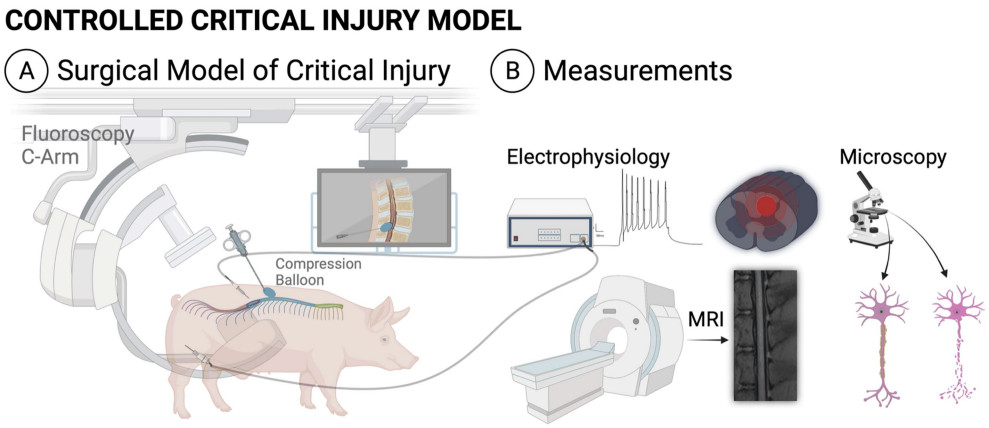

FIGURE 3
Illustration of the experimental protocol, including the surgical model **(A)** and experimental measurements **(B)**. All animals underwent pre-injury MRI, electrophysiologic testing and neurofunctional testing as well as immediate post-injury MRI and electrophysiologic testing. At endpoint, each animal underwent final neurofunctional testing, MRI and histology. MRI, magnetic resonance imaging.

in Figure 3. Post-operatively, animals were monitored by veterinary staff and received frequent direct observations and analgesia administration, as needed.

Injury surgery

All animals received pre-operative penicillin and underwent general anesthesia via total intravenous technique (TIVA) using propofol in order to allow for testing of evoked potentials. Animals were placed prone on an operating table and were affixed to the table with straps. The T6 level was localized in each animal using fluoroscopy. A small incision was made in the left paramedian T10 area (4–6 cm lateral to the midline) and a Jamshidi needle was introduced into the T8/9 interlaminar space using fluoroscopy. From here, a kyphoplasty balloon (Kyphon, Medtronic, Inc., 8 gauge catheters, 15 mm diameter, 5 cc full inflation volume, 700 psi-rated) was introduced through the Jamshidi needle into the epidural space. The kyphoplasty balloon was advanced until the balloon was seen to be present laterally at the T6 level in order to create a lateralized injury. From here, the balloon was slowly inflated while running continuous motor-evoked potentials (MEPs). Once the MEPs in the lower extremities were seen to be absent, balloon inflation was stopped and the balloon was maintained at its current pressure for 15 min, after which time, the balloon was deflated and the balloon and Jamshidi needle were removed. Balloon inflation pressure amounted to roughly 15 psi in most cases, although inflation volume was not stopped according to balloon pressure, but rather according to the pressure at which MEPs in the lower extremities were abolished. The wound was closed in standard layered fashion. Final skin closure was with a topical skin adhesive. The animal was maintained under anesthesia for a post-injury MRI as well as post-injury neurophysiologic testing, after which time the animal was awoken from anesthesia. Fluoroscopy images depicting the kyphoplasty balloon deployment and inflation within the epidural space are seen in Figure 4.

MRI

Each animal underwent baseline 3 T MRI on the day of injury, prior to the injury surgery, under general anesthesia. Traditional MRI sequences (T1, T2, STIR) images were acquired as well as myelin SHIFT MRI, which is a protocol intended to evaluate for the presence and character of myelin within the spinal cord and has been described in detail elsewhere (28). After the injury surgery, while still under general anesthesia, the animals underwent post-injury 1.5 T MRI, again with standard sequences as well as a myelin SHIFT protocol. Finally, at each animal's endpoint, animals underwent final endpoint 3 T MRI under general anesthesia utilizing standard sequences and myelin SHIFT protocols.

Electrophysiology

Baseline electrophysiology tests were performed for each animal on the day of injury, prior to injury, while the animal was under

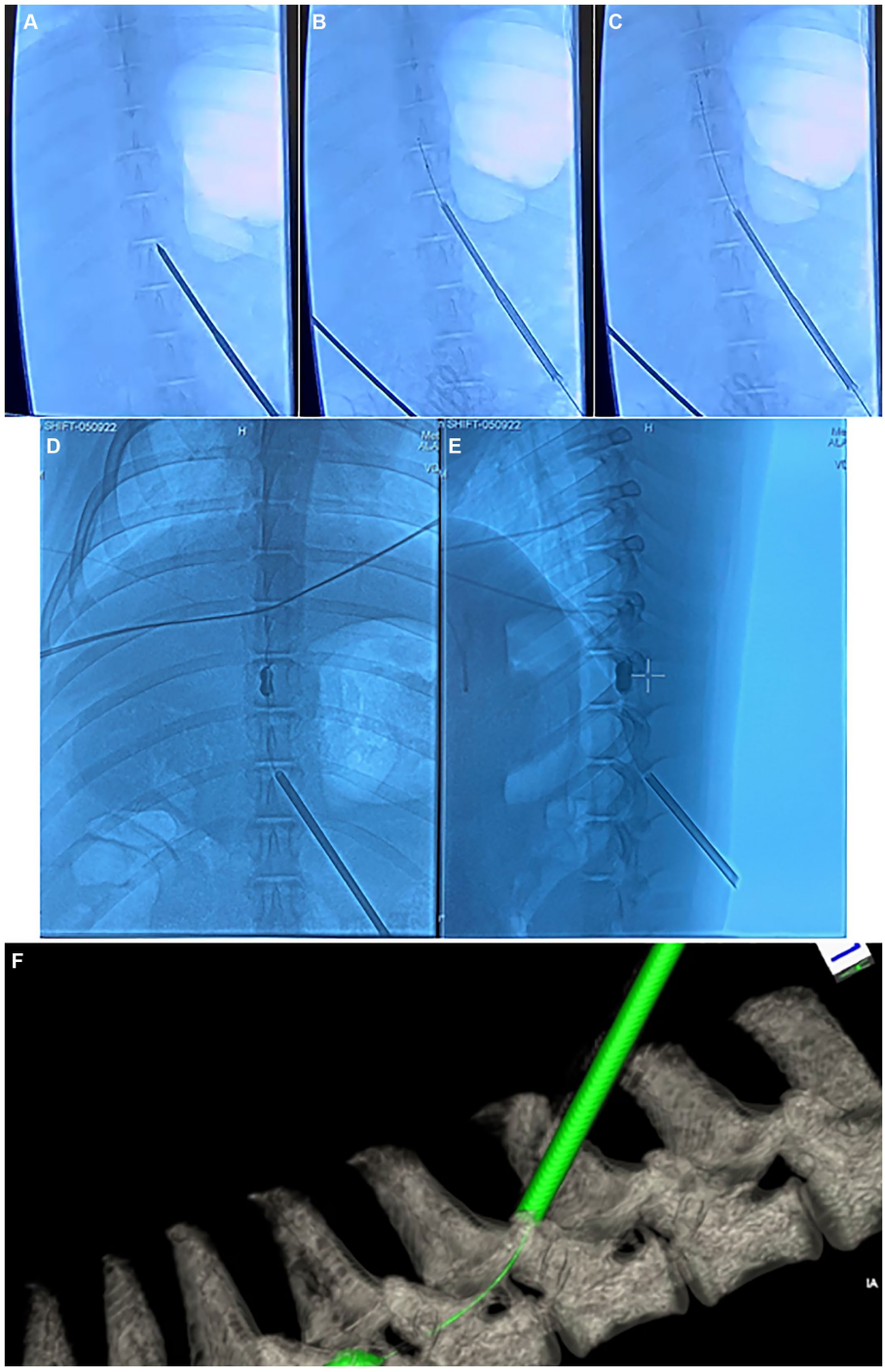

FIGURE 4
Fluoroscopy and computed tomography (CT) images depicting the injury surgery. **(A–C)** anterior–posterior (AP) fluoroscopy images depicting the insertion of the Jamshidi needle into the interlaminar epidural space in the thoracic spine, along with deployment of the kyphoplasty cannula into the epidural space. **(D)** AP and **(E)** lateral fluoroscopy images depicting inflation of the kyphoplasty balloon within the epidural space. **(F)** Dyna-CT depicting the kyphoplasty catheter and inflated balloon within the epidural space.

general anesthesia. Electrophysiology tests were also performed during the injury surgery, immediately after the injury surgery, and at animal endpoint.

Electromyography (EMG): Subdermal 20 mm needle electrodes (Rhythmlink Columbia, SC, United States) were applied bilaterally to the left and right extensor carpi radialis (ECR), flexor carpi ulnaris (FCU), cranial tibial (CT), and gastrocnemius (GAS) muscles. A differential amplifier Octal Bio Amp (ADInstruments, Australia; gain: 100, range: ± 200 μV, resolution: 100 nV, common-mode rejection ratio: > 60 dB, input impedance: > 1 GOhm, < 100 pF) was used to amplify the recorded signals. Data were sampled at 10,000 Hz using a

PowerLab data acquisition system (ADInstruments) and recorded using LabChart ADInstruments (version 8.1.24). The reference for the amplifier was a subdermal needle electrode positioned over the right calcaneal tuberosity.

Transcutaneous spinal stimulation (TSS) was delivered to the skin over the approximate location of the lumbosacral spinal enlargement (29) using an electronically controlled constant-current stimulator DS8R (Digitimer Ltd., United Kingdom). The physiologic state of motor pools and interneuronal networks in the lumbosacral enlargement was evaluated for each animal using this non-invasive approach, assessing the magnitude of spinally evoked motor potentials (SEMP) in the hindlimb muscles. Stimulation was administered using a self-adhesive cathode (diameter 5 cm; PALS, Axelgaard Manufacturing Co. Ltd., United States) placed along the midline of the spine between the L4 and L5 spinous processes. One oval anode (size 7.5 cm x 13 cm; PALS, Axelgaard Manufacturing Co. Ltd., United States) was placed on the abdomen. TSS was administered using single 500 μs monophasic square-wave pulses every 5 s. TSS started at 10 mA, increasing incrementally by 5 mA, reaching a maximum of 150 mA or until the magnitude of the somatosensory evoked potentials (SMEP) reached a plateau.

Transcranial electrical stimulation was administered through a constant-current stimulator (DS8R, Digitimer Ltd., United Kingdom). Two self-adhesive electrodes (diameter 3.2 cm; PALS, Axelgaard Manufacturing Co. Ltd., United States) were positioned along an imaginary line between the ears and approximately 3–4 cm toward the eyes, targeting the motor cortex (specifically referring to the C3/C4 position in the international 10–20 system of human EEG) (30, 31). Motor evoked potentials (MEPs) in the forelimb and hindlimb muscles were elicited using five pulses of 500 μs width, with interstimulus intervals of 1 ms (31), commencing at 30 mA and increasing in 10 mA increments, reaching up to 200 mA or until MEP magnitude plateaued. The supra-motor threshold MEP monitoring in the hindlimb muscles was conducted intraoperatively during the surgery as a means of determining the injury occurrence and severity through signal attenuation.

Neurofunctional testing

Neurofunctional testing was performed for each animal immediately prior to the injury surgery, after recovery from the injury surgery (no greater than 1 week post-operatively), and once weekly after the injury surgery until animal endpoint. An "open field" behavioral observation method was utilized to gauge the animal's neurological function. Each pig's cadence up and down a secluded section of the animal vivarium hallway was recorded for 5–15 min each instance. Recording was performed via a wireless camcorder with a small tripod. Gait function was scored post-hoc via an independent observer utilizing the Basso, Beattie and Bresnahan (BBB) score (32).

Endpoint and histology

At each animal endpoint, each animal underwent final neurofunctional assessment and was then once again placed under general anesthesia, after which time they underwent endpoint neurophysiological testing and endpoint MRI followed by euthanasia with barbiturate overdose. Transcardial perfusion was performed under general anesthesia using 4% paraformaldehyde. After euthanasia, tissues were harvested from each animal and histology was performed. Spinal cords were embedded in optimal-cutting-temperature (OCT) compound. A Microm HM450 microtome was used to cut spinal cord sections (20um each). Frozen sections were air dried overnight for staining.

Hematoxylin and eosin stains were performed as follows: Xylene bath for 1 min, Xylene bath for 2 min, additional Xylene bath for 2 min; 100% Ethanol bath for 30 s, second 100% Ethanol bath for 30 s; 95% Ethanol for 30 s; ddH2O bath for 30 s, Hematoxylin staining for 3 min, tap water rinse, acid alcohol (3 dips), tap water rinse, bluing Reagent for 1 min, tap water rinse, 95% Ethanol for 30 s, Eosin staining for 30 s, 95% Ethanol for 1 min, 100% Ethanol for 2 min, 100% Ethanol for an additional 2 min, Xylene for 2 min, Xylene for an additional 2 min, Xylene for a final 2 min, coverslip application.

Significance statement

Few large animal models exist that have the potential to reproduce the mechanisms of spinal cord injury (SCI) commonly seen in humans, which in turn limits the relevance and applicability of SCI translational research. SCI research relies heavily on animal models, which typically involve an open surgical, dorsal laminectomy which is inherently invasive and may have untoward consequences on animal morbidity and spinal physiology that limit translational impact. We developed a minimally invasive, large animal model of spinal cord injury which utilizes a kyphoplasty balloon inserted percutaneously into the spinal epidural space. Balloon inflation results in a targeted, compressive spinal cord injury with histological and electrophysiological features directly relevant to human spinal cord injury cases without the need for invasive surgery.

Data availability statement

The original contributions presented in the study are included in the article/supplementary material, further inquiries can be directed to the corresponding author.

Ethics statement

The animal study was approved by Houston Methodist Institutional Animal Care and Use Committee. The study was conducted in accordance with the local legislation and institutional requirements.

Author contributions

SB: Conceptualization, Data curation, Formal analysis, Investigation, Methodology, Validation, Writing – original draft, Writing – review & editing. TW: Conceptualization, Data curation, Investigation, Methodology, Software, Writing – review & editing. AS: Data curation, Investigation, Methodology, Writing – review & editing. KH: Data curation, Investigation, Methodology, Writing

– review & editing. MH: Data curation, Investigation, Methodology, Writing – review & editing. AF: Data curation, Investigation, Methodology, Writing – review & editing. XT: Data curation, Investigation, Methodology, Writing – review & editing. DS: Conceptualization, Data curation, Formal analysis, Investigation, Methodology, Supervision, Writing – review & editing. PH: Funding acquisition, Investigation, Supervision, Writing – review & editing.

Funding

The author(s) declare financial support was received for the research, authorship, and/or publication of this article. This work was in part supported by the National Institutes of Health (NIH) 1R01NS119587-01A grant, the Walter Neurological Restoration Initiative sponsored by The Paula and J. C. "Rusty" Walter III and the Walter Oil & Gas Corporation, and the Wings for Life Foundation (268). The funders were not involved in the design of the study, the collection, analysis, and interpretation of the experimental data, the writing of this article, or the decision to submit this article for publication.

Acknowledgments

The authors acknowledge Houston Methodist Research Institute, Houston Methodist Neurological Institute, and Doris (Dee) Loftin, for their contributions to this research.

Conflict of interest

The authors declare that the research was conducted in the absence of any commercial or financial relationships that could be construed as a potential conflict of interest.

Publisher's note

References

1. National Spinal Cord Injury Statistical Center (2023) 'Traumatic spinal cord injury facts and figures at a glance', Birmingham, AL: University of Alabama at Birmingham. 1–2.

2. Silva NA, Sousa N, Reis RL, Salgado AJ. From basics to clinical: a comprehensive review on spinal cord injury. *Prog Neurobiol.* (2014) 114:25–57. doi: 10.1016/j.pneurobio.2013.11.002

3. Dimitrijevic M. Residual motor functions in spinal cord injury. *Adv Neurol.* (1988) 47:138–55.

4. Dobkin BH, Havton LA. Basic advances and new avenues in therapy of spinal cord injury. *Annu Rev Med.* (2004) 55:255–82. doi: 10.1146/annurev.med.55.091902.104338

5. Kakulas BA. Pathology of spinal injuries. *Cent Nerv Syst Trauma.* (1984) 1:117–26. doi: 10.1089/cns.1984.1.117

6. Mayr W, Krenn M, Dimitrijevic MR. Motor control of human spinal cord disconnected from the brain and under external movement. *Adv Exp Med Biol.* (2016) 957:159–71. doi: 10.1007/978-3-319-47313-0_9

7. McKay WB, Lim HK, Priebe MM, Stokic DS, Sherwood AM. Clinical neurophysiological assessment of residual motor control in post-spinal cord injury paralysis. *Neurorehabil Neural Repair.* (2004) 18:144–53. doi: 10.1177/0888439004267674

8. Taccola G, Sayenko D, Gad P, Gerasimenko Y, Edgerton VR. And yet it moves: recovery of volitional control after spinal cord injury. *Prog Neurobiol.* (2018) 160:64–81. doi: 10.1016/j.pneurobio.2017.10.004

9. Kokotilo KJ, Eng JJ, Curt A. Reorganization and preservation of motor control of the brain in spinal cord injury: a systematic review. *J Neurotrauma.* (2009) 26:2113–26. doi: 10.1089/neu.2008.0688

10. Sharif-Alhoseini M, Khormali M, Rezaei M, Safdarian M, Hajighadery A, Khalatbari MM, et al. Animal models of spinal cord injury: a systematic review. *Spinal Cord.* (2017) 55:714–21. doi: 10.1038/sc.2016.187

11. Haughton V, Mardal KA. Spinal fluid biomechanics and imaging: an update for neuroradiologists. *Am J Neuroradiol.* (2014) 35:1864–9. doi: 10.3174/ajnr.A4023

12. Mosenthal WP, Dickherber JL, Saitta BH, Lee MJ. Post laminectomy instability In: Seminars in Spine Surgery: W.B. Saunders (2019) 31:100713.

13. Schwartz ED, Himes BT. New model of minimally invasive experimental spinal cord injury. *Am J Neuroradiol.* (2003) 24:166–8.

14. Werndle MC, Saadoun S, Phang I, Czosnyka M, Varsos GV, Czosnyka ZH, et al. Monitoring of spinal cord perfusion pressure in acute spinal cord injury: initial findings of the injured spinal cord pressure evaluation study*. *Crit Care Med.* (2014) 42:646–55. doi: 10.1097/CCM.0000000000000028

15. Baydin A, Cokluk C, Aydin K. A new minimally invasive experimental spinal cord injury model in rabbits. *Minim Invasive Neurosurg.* (2007) 50:170–2. doi: 10.1055/s-2007-985375

16. Duan H, Pang Y, Zhao C, Zhou T, Sun C, Hou M, et al. A novel, minimally invasive technique to establish the animal model of spinal cord injury. *Ann Transl Med.* (2021) 9:881–1. doi: 10.21037/atm-21-2063

17. Elzat EYY, Fan X, Yang Z, Yuan Z, Pang Y, Feng S. Establishing a mouse contusion spinal cord injury model based on a minimally invasive technique. *J Vis Exp.* (2022) 187:1–17. doi: 10.3791/64538

18. Aslan A, Cemek M, Eser O, Altunbaş K, Buyukokuroglu ME, Cosar M, et al. Does dexmedetomidine reduce secondary damage after spinal cord injury? An experimental study. *Eur Spine J.* (2009) 18:336–44. doi: 10.1007/s00586-008-0872-x

19. Lim JH, Jung CS, Byeon YE, Kim WH, Yoon JH, Kang KS, et al. Establishment of a canine spinal cord injury model induced by epidural balloon compression. *J Vet Sci.* (2007) 8:89–94. doi: 10.4142/jvs.2007.8.1.89

20. Nesathurai S, Graham WA, Mansfield K, Magill D, Sehgal P, Westmoreland SV, et al. Model of traumatic spinal cord injury in *Macaca fascicularis*: similarity of experimental lesions created by epidural catheter to human spinal cord injury. *J Med Primatol.* (2006) 35:401–4. doi: 10.1111/j.1600-0684.2006.00162.x

21. Allen AR. Surgery of experimental lesion of spinal cord equivalent to crush injury of fracture dislocation of spinal column. *J Am Med Assoc.* (1908) 57:878–80. doi: 10.1001/jama.1911.04260090100008

22. David G, Mohammadi S, Martin AR, Cohen-Adad J, Weiskopf N, Thompson A, et al. Traumatic and nontraumatic spinal cord injury: pathological insights from neuroimaging. *Nat Rev Neurol.* (2019) 15:718–31. doi: 10.1038/s41582-019-0270-5

23. Mataliotakis GI, Tsirikos AI. Spinal cord trauma: pathophysiology, classification of spinal cord injury syndromes, treatment principles and controversies. *Orthop Trauma.* (2016) 30:440–9. doi: 10.1016/j.mporth.2016.07.006

24. Jin JY, Yu M, Xu RF, Sun Y, Li BH, Zhou FF. Risk factors for cerebrospinal fluid leakage after extradural spine surgery: a meta-analysis and systematic review. *World Neurosurg.* (2023) 179:e269–80. doi: 10.1016/j.wneu.2023.08.075

25. Glotzbecker MP, Bono CM, Wood KB, Harris MB. Postoperative spinal epidural hematoma: a systematic review. *Spine.* (2010) 35:E413–20. doi: 10.1097/BRS.0b013e3181d9bb77

26. Purdy PD, Duong RT, White CL 3rd , Baer DL, Reichard RR, Pride GL Jr , et al. Percutaneous translumbar spinal cord compression injury in a dog model that uses angioplasty balloons: MR imaging and histopathologic findings. *Am J Neuroradiol.* (2003) 24:177–84.

27. Karadimas SK, Erwin WM, Ely CG, Dettori JR, Fehlings MG. Pathophysiology and natural history of cervical spondylotic myelopathy. *Spine.* (2013) 38:S21–36. doi: 10.1097/brs.0b013e3182a7f2c3

28. Wolfe T, Hoffman K, Hogan MK, Salazar B, Tang X, Chaboub L, et al. Quantification of myelinated nerve fraction and degeneration in spinal cord neuropil by SHIFT MRI. *J Magn Reson Imaging.* (2021) 53:1162–74. doi: 10.1002/jmri.27397

29. Toossi A, Bergin B, Marefatallah M, Parhizi B, Tyreman N, Everaert DG, et al. Comparative neuroanatomy of the lumbosacral spinal cord of the rat, cat, pig, monkey, and human. *Sci Rep*. (2021) 11:1955. doi: 10.1038/s41598-021-81371-9

30. Benavides FD, Santamaria AJ, Bodoukhin N, Guada LG, Solano JP, Guest JD. Characterization of motor and somatosensory evoked potentials in the Yucatan micropig using transcranial and epidural stimulation. *J Neurotrauma*. (2017) 34:2595–608. doi: 10.1089/neu.2016.4511

31. Maier S, Goebel U, Krause S, Benk C, Schick MA, Buerkle H, et al. Somatosensory and transcranial motor evoked potential monitoring in a porcine model for experimental procedures. *PLoS One*. (2018) 13:e0205410. doi: 10.1371/journal.pone.0205410

32. Basso DM, Beattie MS, Bresnahan JC. A sensitive and reliable locomotor rating scale for open field testing in rats. *J Neurotrauma*. (1995) 12:1–21. doi: 10.1089/neu.1995.12.1

frontiers | Frontiers in Cardiovascular Medicine

TYPE Original Research
PUBLISHED 01 August 2024
DOI 10.3389/fcvm.2024.1459062

OPEN ACCESS

EDITED BY
Qingchun Mu,
Second Affiliated Hospital of Soochow University, China

REVIEWED BY
Sanjeev Nirala,
Tribhuvan University Teaching Hospital, Nepal
Madiha Zahra Syeda,
Zhejiang University, China

*CORRESPONDENCE
Hua Luo
✉ luoh5367@enzemed.com

†These authors have contributed equally to this work and share first authorship

RECEIVED 09 July 2024
ACCEPTED 23 July 2024
PUBLISHED 01 August 2024

CITATION
Xie C, Ren Y, He Q, Wang C and Luo H (2024) Association between arteriosclerosis index and lumbar bone mineral density in U.S adults: a cross-sectional study from the NHANES 2011–2018.
Front. Cardiovasc. Med. 11:1459062.
doi: 10.3389/fcvm.2024.1459062

Association between arteriosclerosis index and lumbar bone mineral density in U.S adults: a cross-sectional study from the NHANES 2011–2018

Chengxin Xie[1,2†], Yu Ren[3†], Qiang He[4†], Chenglong Wang[1] and Hua Luo[1*]

[1]Department of Orthopedics, Taizhou Hospital of Zhejiang Province Affiliated to Wenzhou Medical University, Taizhou, China, [2]Key Laboratory of Endocrine Glucose & Lipids Metabolism and Brain Aging, Ministry of Education, Department of Endocrinology, Shandong Provincial Hospital Affiliated to Shandong First Medical University, Jinan, China, [3]Department of Pharmacy, Taizhou Hospital of Zhejiang Province Affiliated to Wenzhou Medical University, Taizhou, China, [4]Department of Orthopedics, Shandong University of Traditional Chinese Medicine Affiliated Hospital, Jinan, China

Background: The arteriosclerosis index, defined as the ratio of non-high density lipoprotein cholesterol to high density lipoprotein cholesterol (NHHR), has emerged as a novel biomarker for various diseases. The relationship between NHHR and lumbar bone mineral density (BMD) has not been previously examined.

Methods: This cross-sectional study analyzed data from the National Health and Nutrition Examination Survey (NHANES) 2011–2018. NHHR was calculated as (total cholesterol—high-density lipoprotein cholesterol)/high-density lipoprotein cholesterol. Lumbar BMD was calculated to *Z* scores. Weighted multivariate linear regression, subgroup analysis, interaction analysis, generalized additive model, and two-piecewise linear regression were used.

Results: A total of 8,602 participants were included. The negative association between NHHR and lumbar BMD was consistent and significant (Model 1: $\beta = -0.039$, 95% CI: −0.055, −0.023, $p < 0.001$; Model 2: $\beta = -0.045$, 95% CI: −0.062, −0.027, $p < 0.001$; Model 3: $\beta = -0.042$, 95% CI: −0.061, −0.023, $p < 0.001$). The linear relationship between NHHR and lumbar BMD was significantly influenced by body mass index (p for interaction = 0.012) and hypertension (p for interaction = 0.047). Non-linear associations between NHHR and lumbar BMD *Z* scores were observed in specific populations, including U-shaped, reverse U-shaped, L-shaped, reverse L-shaped, and U-shaped relationships among menopausal females, underweight participants, those with impaired glucose tolerance, those with diabetes mellitus and those taking anti-hyperlipidemic drugs, respectively.

Conclusions: NHHR exhibited a negative association with lumbar BMD, but varying across specific populations. These findings suggest that NHHR should be tailored to individual levels to mitigate bone loss through a personalized approach. Individuals at heightened risk of cardiovascular disease should focus on their bone health.

KEYWORDS

arteriosclerosis index, NHHR, lipid ratio, bone mineral density, adult, NHANES

1 Introduction

Osteoporosis is the most common metabolic bone disorder, characterized by diminished bone mineral density (BMD) and deteriorated bone microarchitecture, resulting in increased bone fragility and fracture susceptibility (1). Fractures can occur in any bone, but hip and spinal fractures predominate, encompassing 42% of all osteoporotic fractures (2). Approximately 10.2 million individuals aged 50 and older in the U.S. are affected by osteoporosis, with over 40% of older adults exhibiting low bone mass, posing a heightened risk of progressing to osteoporosis (2). Reduced BMD is utilized as a diagnostic marker for osteoporosis, with the lumbar spine being a commonly measured site (3).

Dyslipidemia and osteoporosis are common diseases encountered globally. Emerging evidence suggests a positive correlation between cardiovascular diseases and osteoporosis, with lipid metabolism identified as a potential link (4, 5). Numerous studies have investigated the relationship between lipid profiles and BMD, yet the findings remain inconsistent and contentious (6–11). For instance, a cross-sectional study involving 10,039 U.S. adults revealed an inverse relationship between total cholesterol (TC) levels and BMD (6). Conversely, another study found a positive association between TC levels and lumbar BMD in Chinese males (7). The relationship between high-density lipoprotein cholesterol (HDL-C) and BMD also remains inconsistent. A meta-analysis study reported an elevated HDL-C levels were associated with osteoporosis (10), whereas another study reported a positive association between HDL-C and lumbar BMD (11). Current studies also failed to conclusively establish a clear relationship between low-density lipoprotein cholesterol (LDL-C) and BMD. These inconsistencies underscore the necessity of a comprehensive lipid index to determine its correlation with BMD accurately.

In recent years, the arteriosclerosis index has garnered increased attention as a superior biomarker compared to conventional lipid indicators for predicting cardiovascular risk (12–14). This index, calculated as the ratio of non-HDL-C to HDL-C (NHHR), reflects the balance between atherogenic and protective lipoproteins in the blood. It integrates all atherogenic cholesterol components, including LDL-C, very LDL-C, intermediate-density lipoprotein cholesterol, and lipoprotein (a), with HDL-C, which functions as an anti-atherogenic factor. The heterogeneity among various forms of non-HDL cholesterol might influence its association with BMD. In addition, other lipoprotein ratios, such as apolipoprotein B/apolipoprotein A1, are not typically included in standard testing and exhibit limited predictive performance (15). As a novel lipid indicator, NHHR accounts for the dual influence of non-HDL-C and HDL-C overcoming the limitations of single-lipid indicators. Encouragingly, NHHR has proven valuable for predicting various disease, including metabolic syndrome (15), diabetes (16), chronic kidney disease (17), kidney stones (18), nonalcoholic fatty liver disease (19), periodontitis (20), and depression (21). However, the relationship between the NHHR and bone health has yet to be investigated. Herein, this study explores this relationship in adults through a cross-sectional analysis, aiming to identify a clinically accessible indicator for BMD evaluation.

2 Methods

2.1 Data source

The National Health and Nutrition Examination Survey (NHANES) captures nationally representative statistics of the U.S. non-institutionalized civilian population biennially, employing a complex survey design and population-specific sample weights. Briefly, a series of household interviews were conducted, along with standardized physical examinations and laboratory tests in designated mobile examination centers (MEC) arranged across the country. The NHANES protocol was approved by the Ethics Review Committee of the National Center for Health Statistics, with all participants providing written informed consent. Detailed information can be accessed from the NHANES website (https://www.cdc.gov/nchs/nhanes/).

2.2 Population selection

The population data were sourced from the NHANES database across four consecutive cycles (2011–2012, 2013–2014, 2015–2016, and 2017–2018), compassing a total of 39,156 participants (11). Initially, 20,384 individuals with incomplete lumbar BMD data were excluded. The dual-energy x-ray absorptiometry (DXA) examination was limited to participants aged 8 to 59 years, and pregnant females were ineligible. Individuals under 20 years old and those with missing data in NHHR and covariate variables were further removed. Participants with cancer or malignancy, taking glucocorticoids, and thyroid hormones were excluded. Finally, individuals with abnormal NHHR values [exceeding three times standard deviation (SD)] were excluded, leaving 8,707 participants (weighted $n = 207,456,466$) for analysis (Figure 1).

2.3 Exposure variable and outcome variables

The exposure variable was the NHHR, calculated as (TC–HDL-C)/HDL-C (12). TC and HDL-C were measured from the fasting serum samples. Participants were stratified based on the NHHR quartiles, including group Q1 (0.36,1.90), group Q2 (1.91, 2.65), group Q3 (2.66, 3.64), and group Q4 (3.65, 7.53).

The outcome variable was the lumbar spine BMD Z scores, representing the number of SDs by which an individual's BMD differs from the expected mean for the same age, gender, and race group (22). BMD values were evaluated via DXA during participants' visits to the MEC. The mean BMD for the scanned anteroposterior length from L1 to L4 was calculated and utilized for lumbar spine BMD reporting.

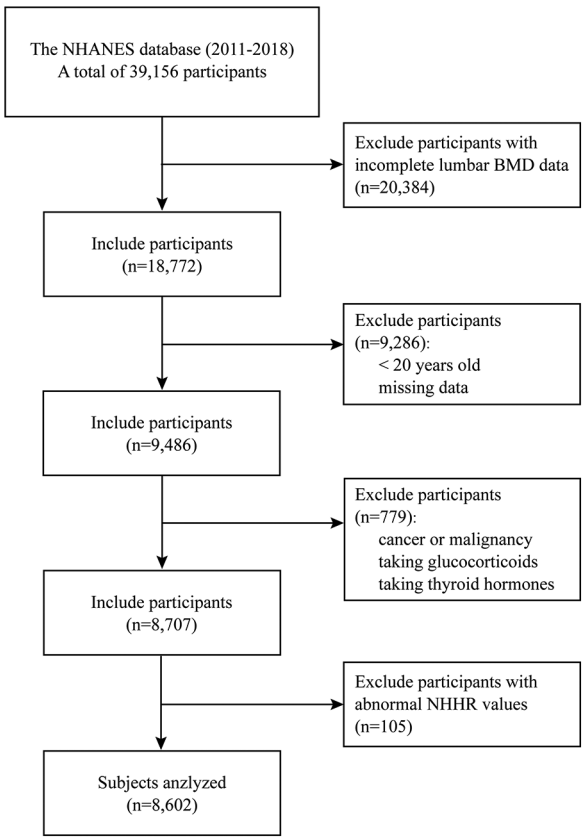

FIGURE 1
Flow chart of participants selection from the NHANES 2011–2018.

2.4 Covariates

Demographic data and variables potentially affecting NHHR and BMD were included as covariates: age, sex, race, education level, marital status, income, body mass index (BMI), waist circumference, smoking status, alcohol intake, hypertension, type 2 diabetes mellitus (DM) status, vigorous/moderate work activity (V/MWA), anti-hyperlipidemic drugs usage, alanine aminotransferase (ALT), aspartate aminotransferase (AST), alkaline phosphatase (ALP), albumin, serum calcium, serum phosphorus, serum 25-hydroxyvitamin D2 + D3 (25OHD2 + D3), and triglyceride (TG).

Age groups were stratified using a threshold of 35 years, given that bone mass gradually increases during early life, reaching its peak around ages 20 to 35 years (23). BMI was classified as underweight (< 18.5 kg/m^2), normal weight (18.5 kg/m^2 ≤ BMI <25 kg/m^2), overweight (25 kg/m^2 ≤ BMI <30 kg/m^2) and obese (≥30 kg/m^2) (24). Waist circumference was stratified into two groups based on the definition of central obesity (25): > 102 cm for males or >88 cm for females. Smoking status was divided into never (smoked less than 100 cigarettes in life), former (smoking >100 cigarettes in life but does not smoke now), and now (smoking ≥1 cigarette every day). V/MWA was defined as having done at least 10 min of V/MWA in a typical week. Hypertension was defined as systolic blood pressure ≥ 140 mmHg and/or diastolic blood pressure ≥ 90 mmHg, or self-reported hypertension along with the use of anti-hypertensive medication (26). DM status was classified into categories of no, impaired fasting glucose/glycemia (IFG), impaired glucose tolerance (IGT), and DM according to the standards set by the American Diabetes Association (27).

2.5 Statistical analysis

Appropriate weighting methodologies were employed to accommodate the complex sampling design in accordance with NHANES guidelines (28). Initially, the NHHR was divided into quartiles, with the lowest quartile (Q1) designated as the reference group. The basic characteristics of categorical variables were expressed as percentages (%) and continuous variables were described by means and standard error. Chi-square tests were employed to examine disparities among categorical variables, and analysis of variance (ANOVA) was utilized to analyze differences among continuous variables.

The association between the NHHR and lumbar BMD *Z* scores was investigated using a multiple linear regression model. According to the STROBE statement (29), Model 1 was unadjusted, Model 2 was minimally adjusted (adjusted for age, sex, and race), and Model 3 was fully adjusted (adjust for age, sex, race, education level, marital status, income, BMI, waist circumference, smoking status, hypertension, DM status, V/MWA, anti-hyperlipidemic drugs usage, alcohol intake, ALT, AST, ALP, albumin, serum calcium, serum phosphorus, serum 25OHD2 + D3, and TG). Based on Model 3, a multivariate linear regression model was applied to perform subgroup analyses of the linear association between NHHR and lumbar BMD *Z* scores across different subgroups. Interaction testing was performed to explore the potential effects of covariates on the association between NHHR and lumbar BMD *Z* scores.

The potential nonlinear association between NHHR and lumbar BMD *Z* scores was identified by generalized additive model (GAM) based on smooth curve fitting. When non-linearity was detected, a recursive algorithm was used to determine the significant inflection points, and a threshold effect analysis was conducted to assess the difference between the standard linear regression model and the segmented linear regression model.

All statistical analysis was performed using R software (version 4.3.3, http://www.R-project.org) and EmpowerStats (version 2.0, www.empowerstats.com). Statistical significance was defined as $p < 0.05$.

3 Results

3.1 Baseline characteristics of the participants

A total of 8,602 individuals were analyzed, comprising 4,517 male, 3,431 premenopausal female, and 654 menopausal female. The distribution of participants based on NHHR values is visualized in Figure 2. The median NHHR was higher among the

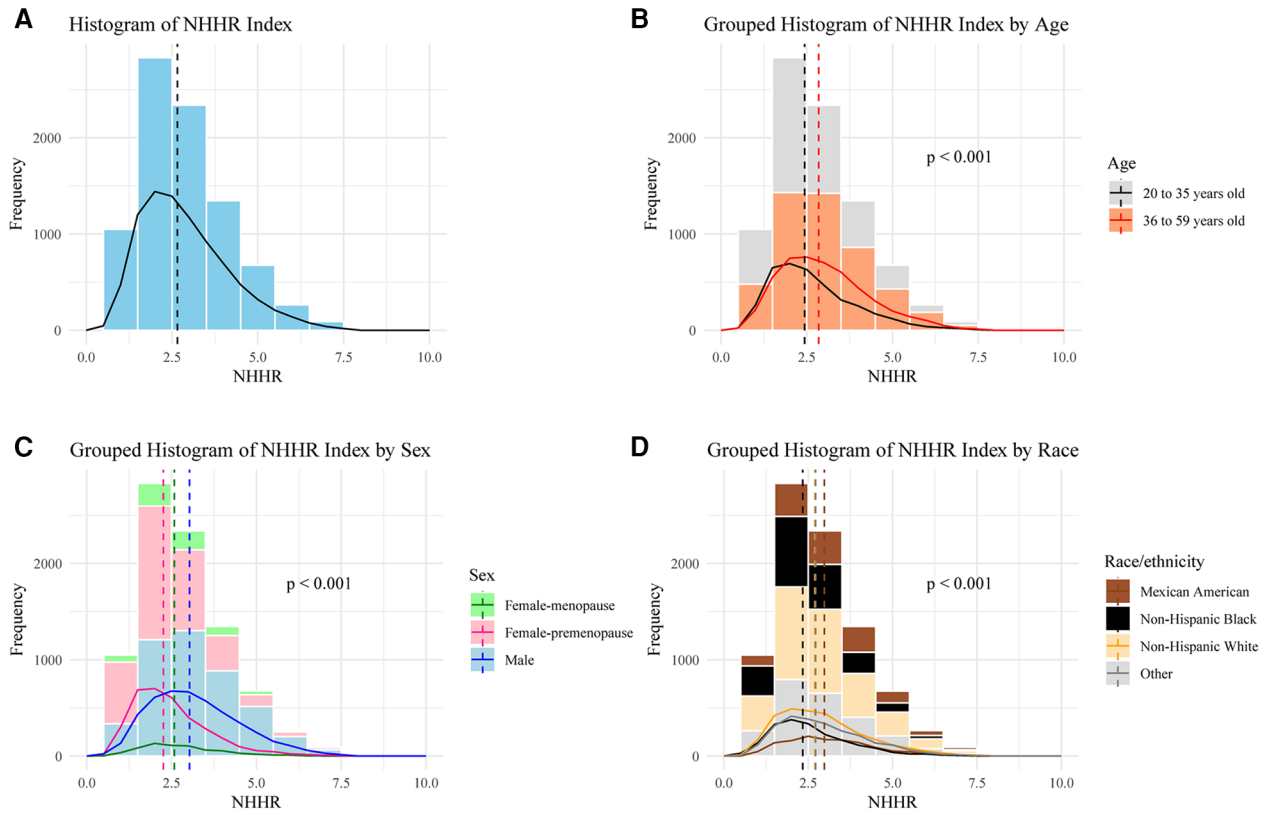

FIGURE 2
Frequency distribution of participants based on NHHR. (**A**) Overall, (**B**) Stratified by age, (**C**) Stratified by sex, (**D**) Stratified by race/ethnicity. One-way ANOVA was used to evaluate whether there are significant differences in NHHR values among different groups.

males, Mexican Americans, and those aged over 35 years. The baseline characteristics of the included participants according to NHHR quartile are shown in Table 1. Compared to participants in the lower NHHR group, those in the NHHR Q4 group showed significantly lower lumbar BMD values and its *Z* scores ($p < 0.001$).

3.2 Association between NHHR and lumbar BMD

The association between NHHR and lumbar BMD *Z* scores was assessed by three multivariate linear regression models (Table 2). The association between NHHR and lumbar BMD *Z* scores was consistently and significantly negative across all models (Model 1: $\beta = -0.039$, 95% CI: −0.055, −0.023, $p < 0.001$; Model 2: $\beta = -0.045$, 95% CI: −0.062, −0.027, $p < 0.001$; Model 3: $\beta = -0.042$, 95% CI: −0.061, −0.023, $p < 0.001$). The trend remained statistical significance among the NHHR quartile groups (all p for trend <0.001), with participants in Q3 and Q4 having progressively lower lumbar BMD *Z* scores compared to those in Q1 (all $p < 0.01$). The smooth curve fits and GAM showed a linear association between NHHR and lumbar BMD *Z* scores based on the Model 3 (Figure 3).

3.3 Subgroup analysis and interaction test

To determined whether the association between NHHR and lumbar BMD *Z* scores persists across specific populations, subgroups were stratified by age, sex, race, marital status, education level, BMI, waist circumference, smoking status, hypertension, DM status, V/MWA, and anti-hyperlipidemic drugs usage. A consistently negative association was observed across age, marital status, waist circumference, and V/MWA subgroups, suggesting that differences in covariates such as sex, race, education level, BMI, smoking status, hypertension, DM status, and the usage of anti-hyperlipidemic drugs may influence the linear relationship between NHHR and lumbar BMD *Z* scores (Supplementary Table S1). Interaction tests confirmed that the linear relationship between NHHR and lumbar BMD *Z* scores was significantly influenced by BMI (p for interaction = 0.012) and hypertension (p for interaction = 0.047).

3.4 Non-linear relationships

To detect the non-linear relationships of NHHR and lumbar BMD *Z* scores in the subgroups and further confirm the results, a GAM and smooth curve fitting based on the fully adjusted

10.3389/fcvm.2024.1459062

TABLE 1 Characteristics of the study population from NHANES 2011–2018.

Variable	Total	NHHR quartile				*p*-value
		Q1 (0.36–1.90)	Q2 (1.91–2.65)	Q3 (2.66–3.64)	Q4 (3.65–7.53)	
Age (years)	38.688 (0.252)	36.280 (0.456)	37.752 (0.365)	39.985 (0.383)	40.784 (0.368)	<0.001
Age-stratified (%)						<0.001
20–35 years old	43.485	52.962	47.800	37.881	35.132	
36–59 years old	56.515	47.038	52.200	62.119	64.868	
Sex (%)						<0.001
Male	54.039	34.837	47.712	59.513	74.861	
Female-premenopause	38.026	56.483	42.941	32.725	19.265	
Female-menopause	7.934	8.681	9.348	7.762	5.874	
Race/ethnicity (%)						<0.001
Non-Hispanic white	61.729	63.225	60.454	63.365	59.690	
Non-Hispanic black	11.505	14.670	13.316	9.692	8.267	
Mexican American	10.322	7.620	9.415	10.940	13.435	
Other	16.445	14.484	16.816	16.003	18.608	
Married (%)						< 0.001
No	49.243	56.892	50.556	45.625	43.762	
Yes	50.757	43.108	49.444	54.375	56.238	
Education (%)						<0.001
<High school	12.328	8.919	11.131	13.081	16.341	
High school	21.881	18.584	20.866	23.577	24.561	
>High school	65.790	72.498	68.003	63.342	59.098	
Smoke (%)						<0.001
Never	60.090	65.188	62.347	60.337	52.119	
Former	19.119	15.955	17.064	21.186	22.331	
Now	20.790	18.857	20.589	18.477	25.550	
Hypertension (%)						<0.001
No	73.733	83.011	76.486	70.620	64.499	
Yes	26.267	16.989	23.514	29.380	35.501	
DM (%)						<0.001
No	84.899	91.620	86.861	83.109	77.734	
IFG	4.474	2.146	4.185	4.651	7.033	
IGT	2.388	1.736	2.036	2.779	3.015	
DM	8.239	4.497	6.918	9.461	12.219	
V/MWA (%)						0.003
No	49.545	53.349	50.576	50.176	43.784	
Yes	50.455	46.651	49.424	49.824	56.216	
Anti-hyperlipidemic drugs (%)						0.21
No	56.718	58.233	54.874	55.293	58.579	
Yes	7.836	6.513	8.950	8.650	7.194	
Other	35.445	35.254	36.176	36.057	34.226	
Income to poverty ratio	2.945 (0.052)	3.018 (0.069)	2.980 (0.071)	2.979 (0.058)	2.795 (0.069)	0.019
BMI (kg/m^2)	28.849 (0.143)	25.612 (0.173)	28.466 (0.185)	30.040 (0.202)	31.360 (0.213)	<0.001
Waistline (cm)	97.988 (0.353)	88.527 (0.417)	96.305 (0.433)	101.450 (0.478)	105.931 (0.512)	<0.001
ALT (U/L)	26.144 (0.254)	21.790 (0.521)	23.433 (0.324)	26.572 (0.417)	33.070 (0.637)	<0.001
AST (U/L)	25.041 (0.187)	24.567 (0.419)	23.951 (0.390)	24.899 (0.318)	26.823 (0.465)	<0.001
ALP (U/L)	66.665 (0.439)	61.887 (0.702)	64.408 (0.607)	68.556 (0.689)	71.974 (0.692)	<0.001
Serum phosphorus (mg/dl)	3.706 (0.010)	3.744 (0.019)	3.722 (0.017)	3.676 (0.017)	3.681 (0.019)	0.036
Serum calcium (mg/dl)	9.375 (0.007)	9.356 (0.011)	9.362 (0.010)	9.374 (0.011)	9.410 (0.010)	<0.001
Albumin (g/dl)	4.328 (0.007)	4.331 (0.011)	4.314 (0.012)	4.323 (0.010)	4.345 (0.010)	0.085
TG (mg/dl)	143.108 (1.902)	79.490 (0.749)	107.630 (1.334)	149.898 (2.118)	239.432 (3.945)	<0.001
TC (mg/dl)	189.928 (0.731)	167.498 (1.054)	179.286 (0.951)	195.128 (1.216)	218.907 (1.209)	<0.001
HDL-C (mg/dl)	52.774 (0.330)	68.902 (0.525)	54.938 (0.294)	47.675 (0.298)	39.089 (0.254)	<0.001
Alcohol intake (g)	14.494 (0.650)	18.855 (1.030)	13.906 (0.895)	12.357 (1.108)	12.830 (1.218)	<0.001
Serum 25OHD2 + D3 (nmol/L)	65.931 (0.790)	68.771 (1.151)	66.760 (1.030)	66.315 (1.073)	61.662 (0.885)	<0.001
Lumbar spine BMD (g/cm^2)	1.039 (0.002)	1.059 (0.004)	1.045 (0.004)	1.033 (0.005)	1.018 (0.004)	<0.001
Lumbar spine BMD *Z* scores	0.025 (0.017)	0.094 (0.032)	0.045 (0.030)	0.012 (0.029)	−0.054 (0.031)	<0.001

Categorical variables were expressed as percentages (%).
Continuous variables were described by means and standard error.

10.3389/fcvm.2024.1459062

TABLE 2 The association between NHHR and lumbar spine BMD *Z*-scores.

Exposure	Model 1, β (95% CI)	Model 2, β (95% CI)	Model 3, β (95% CI)
	p-value	*p*-value	*p*-value
NHHR	−0.039 (−0.055, −0.023)	−0.045 (−0.062, −0.027)	−0.042 (−0.061, −0.023)
	< 0.001	< 0.001	< 0.001
NHHR Quartile			
Q1 (0.36–1.90)	Reference	Reference	Reference
Q2 (1.91–2.65)	−0.046 (−0.105, 0.012)	−0.049 (−0.108, 0.010)	−0.054 (−0.114, 0.006)
	0.121	0.102	0.076
Q3 (2.66–3.64)	−0.081 (−0.139, −0.023)	−0.094 (−0.153, −0.034)	−0.094 (−0.156, −0.033)
	0.006	0.002	0.003
Q4 (3.65–7.53)	−0.147 (−0.206, −0.088)	−0.165 (−0.228, −0.103)	−0.156 (−0.223, −0.088)
	< 0.001	< 0.001	< 0.001
p for trend	<0.001	<0.001	<0.001

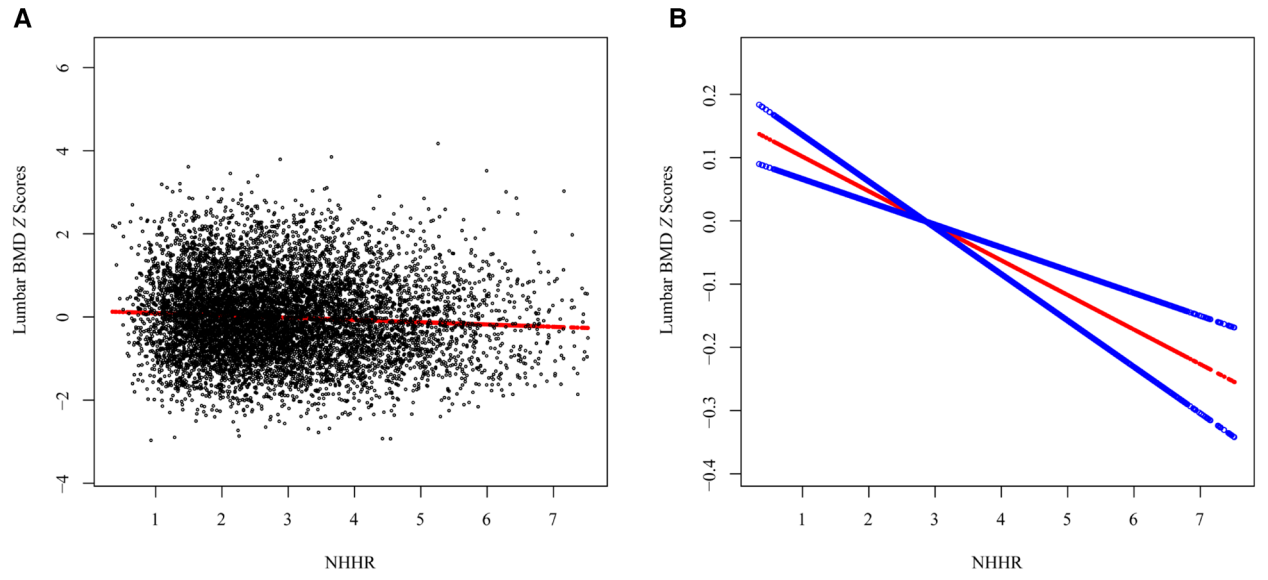

FIGURE 3
The association between the NHHR and lumbar spine BMD *Z* scores. (**A**) Each black point represents a sample, (**B**) Smooth curve fitting using GAM. The red line represents the smooth curve fit, and the blue line represents its 95% CI.

model (Model 3) were conducted. In addition to the significant interaction of BMI and hypertension, several potential demographic and comorbidity factors were explored (Figure 4).

A U-shaped association between NHHR and lumbar BMD *Z* scores in menopause females was identified (Figure 4A), with an inflection point at 4.891 (Table 3). Threshold effect analysis revealed a significant negative correlation before the inflection point ($\beta = -0.096$, 95% CI: −0.188, −0.005, $p = 0.038$) and a significant positive correlation afterward ($\beta = 0.715$, 95% CI: 0.245, 1.185, $p = 0.003$).

A reverse U-shaped association between NHHR and lumbar BMD *Z* scores was found in underweight participants (Figure 4B), with an inflection point at 1.4 (Table 3). Threshold effect analysis revealed a significant positive correlation before the inflection point ($\beta = 1.899$, 95% CI: 0.597, 3.201, $p = 0.005$), and a significant negative correlation afterward ($\beta = -0.256$, 95% CI: −0.498, −0.014, $p = 0.041$).

An L-shaped association between NHHR and lumbar BMD *Z* scores was detected in participants with IGT (Figure 4C), with an inflection point at 3.163 (Table 3). A significant negative correlation was present before the inflection point ($\beta = -0.311$, 95% CI: −0.560, −0.063, $p = 0.015$), while no significant correlation was found after the inflection point ($\beta = 0.081$, 95% CI: −0.102, 0.263, $p = 0.387$).

A reverse L-shaped relationship was observed between NHHR and lumbar BMD *Z* scores in participants with DM (Figure 4C), with an inflection point at 1.6 (Table 3). A significant positive correlation was observed before the inflection point ($\beta = 0.915$, 95% CI: 0.207, 1.623, $p = 0.012$), with no significant correlation afterward ($\beta = -0.046$, 95% CI: −0.099, 0.007, $p = 0.092$).

Among participants using anti-hyperlipidemic drugs, a U-shaped association between NHHR and lumbar BMD *Z* scores was observed (Figure 4D, Table 3). Before the inflection point at 2.16, a negative correlation was evident ($\beta = -0.321$, 95% CI: −0.636, −0.006, $p = 0.046$), followed by a significant positive correlation after the inflection point ($\beta = 0.089$, 95% CI: 0.006, 0.173, $p = 0.037$).

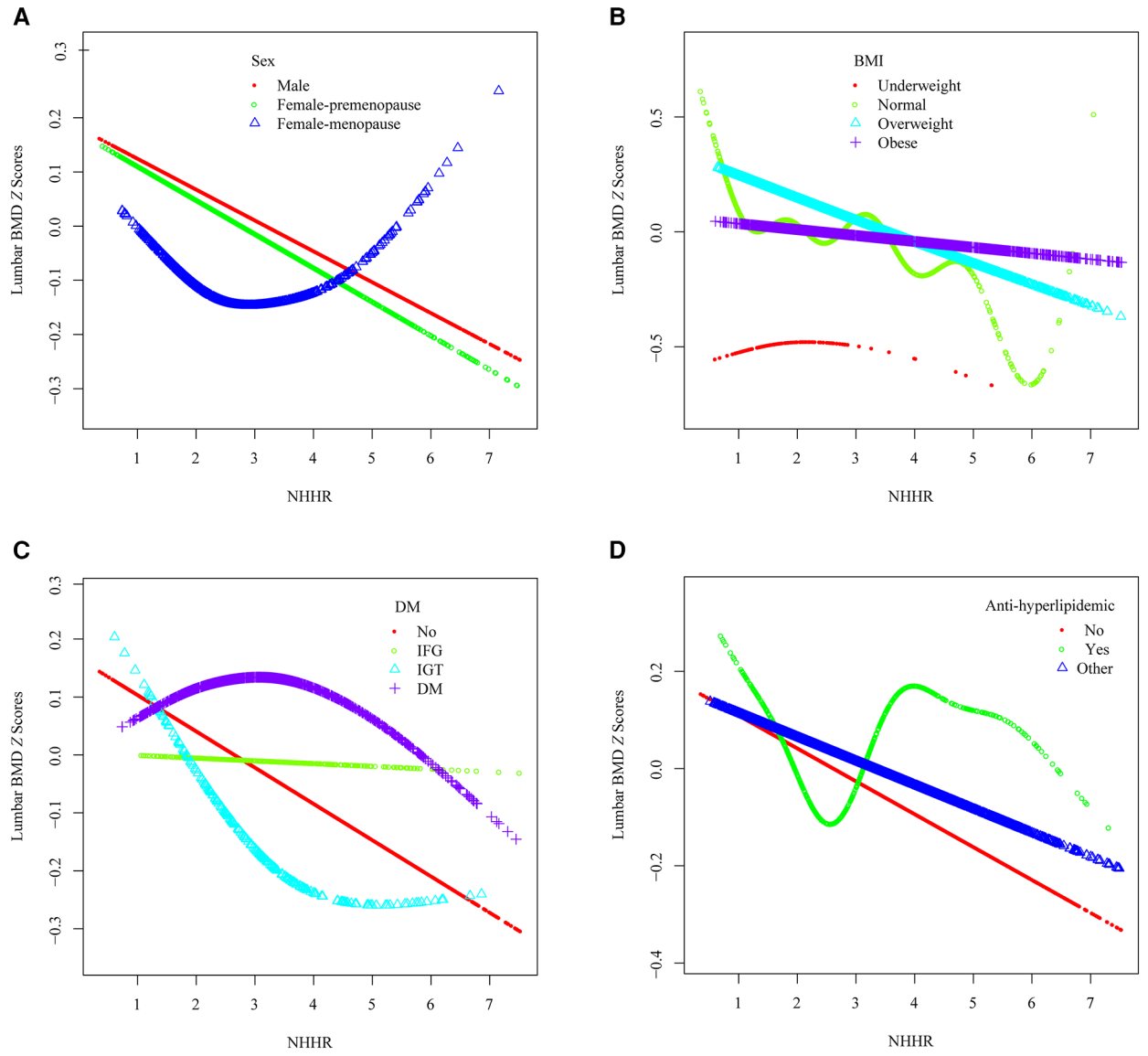

FIGURE 4
The association between the NHHR and lumbar spine BMD *Z* scores within specific populations. (**A**) Stratified by sex, (**B**) Stratified by BMI, (**C**) Stratified by DM, (**D**) Stratified by anti-hyperlipidemic drugs usage.

4 Discussion

To our knowledge, this is the first study to investigate the association between arteriosclerosis index and lumbar BMD in a population-based setting. Despite initially statistically significant negative associations were observed between NHHR and lumbar BMD *Z* scores in the multivariate linear regression models, these associations varied within specific populations identified through subgroup analyses.

It is important to note that a non-linear and U-shaped association was seen among menopause females. In this population, an NHHR value greater than 4.891 appeared to be a protective factor against bone mass loss. Menopause is linked to dyslipidemia and an elevated risk of cardiovascular disease and osteoporosis due to a deterioration in lipid profile during the transition to postmenopausal status, characterized by increases in TC, LDL-C and TG along with a net reduction in HDL-C (30). A multi-center study reported that a high HDL-C level is an independent risk factor for bone loss in both males and females (31). However, other studies have demonstrated a positive correlation between HDL-C and lumbar BMD in females (11) or postmenopausal females (8). In addition, the association between LDL-C and BMD among postmenopausal females remains uncertain (8, 32, 33). Explanations for the above controversial results may be attributed to differences in participants and assessment of BMD. To our knowledge, there is no evidence of a U-shaped relationship between TC and BMD or between HDL-C and BMD. This study identified the optimal inflection point of NHHR in specific populations, providing a beneficial range for regulating lipid levels. NHHR was regarded as a novel instrument for elucidating the relationship between lipids and

TABLE 3 Threshold effect analysis of NHHR on lumbar spine BMD *Z* scores within specific populations.

NHHR	*β* (95%CI) *p* value				
	Female-menopause	Underweight	IGT	DM	Anti-hyperlipidemic drugs taken
Fitting by the standard linear model					
	−0.020 (−0.098, 0.058) 0.616	−0.091 (−0.316, 0.135) 0.432	−0.073 (−0.187, 0.040) 0.207	−0.022 (−0.072, 0.028) 0.395	0.034 (−0.035, 0.103) 0.333
Fitting by the two-piecewise linear model					
Inflection point (K)	4.891	1.4	3.163	1.6	2.16
NHHR < K	−0.096 (−0.188, −0.005) 0.038	1.899 (0.597, 3.201) 0.005	−0.311 (−0.560, −0.063) 0.015	0.915 (0.207, 1.623) 0.012	−0.321 (−0.636, −0.006) 0.046
NHHR > K	0.715 (0.245, 1.185) 0.003	−0.256 (−0.498, −0.014) 0.041	0.081 (−0.102, 0.263) 0.387	−0.046 (−0.099, 0.007) 0.092	0.089 (0.006, 0.173) 0.037
Log likelihood ratio	0.002	<0.001	0.027	0.009	0.021

lumbar BMD, emphasizing the importance of other atherogenic cholesterols in bone metabolism.

Notably, the detrimental effect of NHHR on lumbar BMD is most pronounced among the overweight population. Conversely, NHHR exhibits a positive association with lumbar BMD among the underweight cohort when NHHR values are below 1.4. Obesity can have significant consequences on various organs and systems, with its effects on bone being particularly controversial (34). Lower BMI has been associated with an increased risk of osteoporosis, and higher body weight is believed to provide protection against fractures (35). However, obesity and its comorbidities such as dyslipidemia, type 2 diabetes, and metabolic syndrome, may contribute to affect bone health (36). Elevated NHHR within eutrophic ranges poses a greater risk for bone loss; however, this effect diminishes with progression toward morbid obesity, where other comorbidities exert a more substantial influence on BMD.

The negative association between NHHR and lumbar BMD was more likely to be seen among the population without overt health issues (hypertension, IFG, IGT, or DM). Hypertension has been identified as being associated with decreased BMD (37). In addition, prolonged usage of non-thiazide diuretics among hypertensive individuals might contribute to diminished BMD due to increased urinary calcium excretion, which decreases calcium availability for bone formation (38). Conversely, thiazide diuretics reduce renal calcium excretion by promoting calcium reabsorption in the distal convoluted tubules, reduce bone turnover by lowering parathyroid hormone levels, and may stimulate osteoblast differentiation while inhibiting osteoclast formation (38, 39). The correlation between DM and bone health is intricate. Most studies suggest normal or superior trabecular bone structure in patients with DM, although some have reported a decreased lumbar spine trabecular bone score and an increased risk of spine fracture (40). Importantly, both hypertension and DM are acknowledged risk factors for cardiovascular disease, exerting direct or indirect influences on lipid metabolism. Therefore, the relationship between NHHR and lumbar BMD is further complicated by the interference of diabetes or hypertension.

Lipid-lowering therapy, such as commonly prescribed statin medications, undeniably influences the linear association between NHHR and lumbar BMD. Preclinical studies have demonstrated that statins mitigate bone loss by inhibiting osteoclastogenesis and promoting osteoblast development, potentially exerting an additional favorable impact on BMD (41, 42). Statins upregulate the expression of key mediators in bone metabolism, including ALP, bone morphogenetic protein-2, transforming growth factor-beta, type I collagen, collagenase-1, and glucocorticoids (42). Upon excluding individuals taking glucocorticoids and thyroid hormones, no significant influence of medications other than lipid-lowering drugs was found on the relationship between NHHR and lumbar BMD.

This study possesses several notable strengths. Firstly, utilizing *Z* scores provides greater precision in predicting fracture risk, benefiting from a standardized reference across age, gender, and race (43). Second, two critical time-frames of bone loss were examined: 35 years old, marking the onset of bone aging, and menopause, when bone loss accelerates. Third, the liner association between NHHR and lumbar BMD was observed in an ostensibly healthy population, enhancing the relevance of the findings to the general population.

However, several limitations must be acknowledged. First, the cross-sectional design of the NHANES dataset precludes establishing causality between NHHR and lumbar BMD. Second, BMD scans in the NHANES 2011–2018 were conducted on adults up to age 59 years, whereas routine BMD measurements are clinically recommended around age 65 years, potentially leading to a failure to capture the period of highest risk for osteoporosis (44). Third, serum estradiol data from the NHANES 2011-2012 and NHANES 2017–2018 were unavailable. Fourth, despite adjustments for numerous confounding variables, the influence of unmeasured or unknown confounders on the results cannot be entirely ruled out such as diet quality, nutritional supplements, exercise types. Finally, our study focuses solely on lumbar BMD and does not consider other sites like the thoracic spine, hip, or forearm. We will conduct further studies to provide a more comprehensive understanding of this relationship.

5 Conclusion

This study revealed a negative association between NHHR and lumbar BMD. In population with specific condition or statuses, NHHR should be tailored to individual levels to mitigate bone loss. Individuals at heightened risk of cardiovascular disease are encouraged to prioritize their bone health. This study introduces a novel tool for monitoring lipid levels and mitigating bone loss, with notable clinical implications.

Data availability statement

Publicly available datasets were analyzed in this study. This data can be found here: https://www.cdc.gov/nchs/nhanes/.

Ethics statement

The studies involving human participants were reviewed and approved by the ethics review board of the National Center for Health Statistics. The studies were conducted in accordance with the local legislation and institutional requirements. The participants provided their written informed consent to participate in this study.

Author contributions

CX: Conceptualization, Data curation, Formal Analysis, Investigation, Methodology, Software, Writing – original draft, Writing – review & editing. YR: Formal Analysis, Investigation, Methodology, Validation, Writing – original draft, Writing – review & editing. QH: Investigation, Methodology, Validation, Writing – original draft, Writing – review & editing. CW: Data curation, Software, Visualization, Writing – review & editing. HL: Funding acquisition, Supervision, Writing – review & editing.

Funding

The author(s) declare financial support was received for the research, authorship, and/or publication of this article.

This research was funded by Enze Medical Center (Group) Scientific Research (No. 23EZA04) and Zhejiang Medicine and Health Scientific Research Project (No. 2024KY531).

Acknowledgments

We express our gratitude to NHANES for providing the data and to all the participants involved.

Conflict of interest

The authors declare that the research was conducted in the absence of any commercial or financial relationships that could be construed as a potential conflict of interest.

Publisher's note

All claims expressed in this article are solely those of the authors and do not necessarily represent those of their affiliated organizations, or those of the publisher, the editors and the reviewers. Any product that may be evaluated in this article, or claim that may be made by its manufacturer, is not guaranteed or endorsed by the publisher.

Supplementary material

The Supplementary Material for this article can be found online at: https://www.frontiersin.org/articles/10.3389/fcvm.2024.1459062/full#supplementary-material

References

1. Compston JE, McClung MR, Leslie WD. Osteoporosis. *Lancet*. (2019) 393 (10169):364–76. doi: 10.1016/S0140-6736(18)32112-3

2. Qaseem A, Hicks LA, Etxeandia-Ikobaltzeta I, Shamliyan T, Cooney TG. Pharmacologic treatment of primary osteoporosis or low bone mass to prevent fractures in adults: a living clinical guideline from the American College of Physicians. *Ann Intern Med*. (2023) 176(2):224–38. doi: 10.7326/M22-1034

3. Yang TL, Shen H, Liu A, Dong SS, Zhang L, Deng FY, et al. A road map for understanding molecular and genetic determinants of osteoporosis. *Nat Rev Endocrinol*. (2020) 16(2):91–103. doi: 10.1038/s41574-019-0282-7

4. Hofbauer LC, Schoppet M. Osteoprotegerin: a link between osteoporosis and arterial calcification? *Lancet*. (2001) 358(9278):257–9. doi: 10.1016/S0140-6736(01)05494-0

5. Azeez TA. Osteoporosis and cardiovascular disease: a review. *Mol Biol Rep*. (2023) 50(2):1753–63. doi: 10.1007/s11033-022-08088-4

6. Cao L, Wu W, Deng X, Guo H, Pu F, Shao Z. Association between total cholesterol and total bone mineral density in US adults: National Health and Nutrition Examination Survey (NHANES), 2011–2018. *J Orthop Surg Res*. (2023) 18 (1):40. doi: 10.1186/s13018-022-03485-8

7. Sun Y, Qi X, Lin X, Zhou Y, Lv X, Zhou J, et al. Association between total cholesterol and lumbar bone density in Chinese: a study of physical examination data from 2018 to 2023. *Lipids Health Dis*. (2023) 22(1):180. doi: 10.1186/s12944-023-01946-5

8. Zolfaroli I, Ortiz E, García-Pérez M, Hidalgo-Mora JJ, Tarín JJ, Cano A. Positive association of high-density lipoprotein cholesterol with lumbar and femoral neck bone mineral density in postmenopausal women. *Maturitas*. (2021) 147:41–6. doi: 10.1016/j.maturitas.2021.03.001

9. Tang Y, Wang S, Yi Q, Xia Y, Geng B. High-density lipoprotein cholesterol is negatively correlated with bone mineral density and has potential predictive value for bone loss. *Lipids Health Dis*. (2021) 20(1):75. doi: 10.1186/s12944-021-01497-7

10. Zhao H, Li Y, Zhang M, Qi L, Tang Y. Blood lipid levels in patients with osteopenia and osteoporosis:a systematic review and meta-analysis. *J Bone and Miner Metab*. (2021) 39(3):510–20. doi: 10.1007/s00774-020-01189-9

11. Xie R, Huang X, Liu Q, Liu M. Positive association between high-density lipoprotein cholesterol and bone mineral density in U.S. Adults: the NHANES 2011–2018. *J Orthop Surg Res*. (2022) 17(1):92. doi: 10.1186/s13018-022-02986-w

12. Yamano Y, Miyakawa S, Nakadate T. Association of arteriosclerosis index and oxidative stress markers in school children. *Pediatr Int*. (2015) 57(3):449–54. doi: 10.1111/ped.12545

13. Lin W, Luo S, Li W, Liu J, Zhou T, Yang F, et al. Association between the non-HDL-cholesterol to HDL- cholesterol ratio and abdominal aortic aneurysm from a Chinese screening program. *Lipids Health Dis*. (2023) 22(1):187. doi: 10.1186/s12944-023-01939-4

14. Wang A, Li Y, Zhou L, Liu K, Li S, Zong C, et al. Non-HDL-C/HDL-C ratio is associated with carotid plaque stability in general population: a cross-sectional study. *Front Neurol*. (2022) 13:875134. doi: 10.3389/fneur.2022.875134

15. Kim SW, Jee JH, Kim HJ, Jin SM, Suh S, Bae JC, et al. Non-HDL-cholesterol/HDL-cholesterol is a better predictor of metabolic syndrome and insulin resistance than apolipoprotein B/apolipoprotein A1. *Int J Cardiol*. (2013) 168(3):2678–83. doi: 10.1016/j.ijcard.2013.03.027

16. Sheng G, Liu D, Kuang M, Zhong Y, Zhang S, Zou Y. Utility of non-high-density lipoprotein cholesterol to high-density lipoprotein cholesterol ratio in evaluating incident diabetes risk. *Diabetes Metab Syndr Obes*. (2022) 15:1677–86. doi: 10.2147/DMSO.S355980

17. Zuo PY, Chen XL, Liu YW, Zhang R, He XX, Liu CY. Non-HDL-cholesterol to HDL-cholesterol ratio as an independent risk factor for the development of chronic kidney disease. *Nutr Metab Cardiovasc Dis*. (2015) 25(6):582–7. doi: 10.1016/j.numecd.2015.03.003

18. Hong H, He Y, Gong Z, Feng J, Qu Y. The association between non-high-density lipoprotein cholesterol to high-density lipoprotein cholesterol ratio (NHHR) and kidney stones: a cross-sectional study. *Lipids Health Dis*. (2024) 23(1):102. doi: 10.1186/s12944-024-02089-x

19. Yang S, Zhong J, Ye M, Miao L, Lu G, Xu C, et al. Association between the non-HDL-cholesterol to HDL-cholesterol ratio and non-alcoholic fatty liver disease in Chinese children and adolescents: a large single-center cross-sectional study. *Lipids Health Dis*. (2020) 19(1):242. doi: 10.1186/s12944-020-01421-5

20. Hou K, Song W, He J, Ma Z. The association between non-high-density lipoprotein cholesterol to high-density lipoprotein cholesterol ratio (NHHR) and prevalence of periodontitis among US adults: a cross-sectional NHANES study. *Sci Rep*. (2024) 14(1):5558. doi: 10.1038/s41598-024-56276-y

21. Qi X, Wang S, Huang Q, Chen X, Qiu L, Ouyang K, et al. The association between non-high-density lipoprotein cholesterol to high-density lipoprotein cholesterol ratio (NHHR) and risk of depression among US adults: a cross-sectional NHANES study. *J Affect Disord*. (2024) 344:451–7. doi: 10.1016/j.jad.2023.10.064

22. Dimai HP. Use of dual-energy x-ray absorptiometry (DXA) for diagnosis and fracture risk assessment; WHO-criteria, T- and Z-score, and reference databases. *Bone*. (2017) 104:39–43. doi: 10.1016/j.bone.2016.12.016

23. Liu Y, Le S, Liu Y, Jiang H, Ruan B, Huang Y, et al. The effect of calcium supplementation in people under 35 years old: a systematic review and meta-analysis of randomized controlled trials. *eLife*. (2022) 11:e79002. doi: 10.7554/eLife.79002

24. Kushner RF, Ryan DH. Assessment and lifestyle management of patients with obesity: clinical recommendations from systematic reviews. *JAMA*. (2014) 312 (9):943–52. doi: 10.1001/jama.2014.10432

25. Sharma AM, Kushner RF. A proposed clinical staging system for obesity. *Int J Obes (Lond)*. (2009) 33(3):289–95. doi: 10.1038/ijo.2009.2

26. Whelton PK, Carey RM, Aronow WS, Casey DE Jr, Collins KJ, Dennison Himmelfarb C, et al. 2017 ACC/AHA/AAPA/ABC/ACPM/AGS/APhA/ASH/ASPC/NMA/PCNA guideline for the prevention, detection, evaluation, and management of high blood pressure in adults: executive summary: a report of the American College of Cardiology/American Heart Association Task Force on Clinical Practice Guidelines. *Hypertension*. (2018) 71(6):1269–324. doi: 10.1161/HYP.0000000000000066

27. American Diabetes Association Professional Practice Committee. 2. Diagnosis and classification of diabetes: standards of care in diabetes-2024. *Diabetes Care*. (2024) 47(Suppl 1):S20–s42. doi: 10.2337/dc24-S002

28. Johnson CL, Paulose-Ram R, Ogden CL, Carroll MD, Kruszon-Moran D, Dohrmann SM, et al. National health and nutrition examination survey: analytic guidelines, 1999–2010. *Vital Health Stat 2*. (2013) (161):1–24. PMID: 25090154.

29. von Elm E, Altman DG, Egger M, Pocock SJ, Gøtzsche PC, Vandenbroucke JP. The strengthening the reporting of observational studies in epidemiology (STROBE) statement: guidelines for reporting observational studies. *Lancet*. (2007) 370 (9596):1453–7. doi: 10.1016/S0140-6736(07)61602-X

30. Anagnostis P, Stevenson JC, Crook D, Johnston DG, Godsland IF. Effects of menopause, gender and age on lipids and high-density lipoprotein cholesterol subfractions. *Maturitas*. (2015) 81(1):62–8. doi: 10.1016/j.maturitas.2015.02.262

31. Jiang J, Qiu P, Wang Y, Zhao C, Fan S, Lin X. Association between serum high-density lipoprotein cholesterol and bone health in the general population: a large and multicenter study. *Arch Osteoporos*. (2019) 14(1):36. doi: 10.1007/s11657-019-0579-0

32. Li S, Guo H, Liu Y, Wu F, Zhang H, Zhang Z, et al. Relationships of serum lipid profiles and bone mineral density in postmenopausal Chinese women. *Clin Endocrinol*. (2015) 82(1):53–8. doi: 10.1111/cen.12616

33. Chen Y, Wang W, Yang L, Chen W, Zhang H. Association between lipid profiles and osteoporosis in postmenopausal women: a meta-analysis. *Eur Rev Med Pharmacol Sci*. (2018) 22(1):1–9. doi: 10.26355/eurrev_201801_14093

34. Rinonapoli G, Pace V, Ruggiero C, Ceccarini P, Bisaccia M, Meccariello L, et al. Obesity and bone: a Complex relationship. *Int J Mol Sci*. (2021) 22(24):13662. doi: 10.3390/ijms222413662

35. Asomaning K, Bertone-Johnson ER, Nasca PC, Hooven F, Pekow PS. The association between body mass index and osteoporosis in patients referred for a bone mineral density examination. *J Womens Health (Larchmt)*. (2006) 15 (9):1028–34. doi: 10.1089/jwh.2006.15.1028

36. Palermo A, Tuccinardi D, Defeudis G, Watanabe M, D'Onofrio L, Lauria Pantano A, et al. BMI And BMD: the potential interplay between obesity and bone fragility. *Int J Environ Res Public Health*. (2016) 13(6):544. doi: 10.3390/ijerph13060544

37. Ye Z, Lu H, Liu P. Association between essential hypertension and bone mineral density: a systematic review and meta-analysis. *Oncotarget*. (2017) 8(40):68916–27. doi: 10.18632/oncotarget.20325

38. Zhang R, Yin H, Yang M, Lei X, Zhen D, Zhang Z. Advanced progress of the relationship between antihypertensive drugs and bone metabolism. *Hypertension*. (2023) 80(11):2255–64. doi: 10.1161/HYPERTENSIONAHA.123.21648

39. Chuang CH, Yang SF, Liao PL, Huang JY, Chan MY, Yeh CB. Association of thiazide use in patients with hypertension with overall fracture risk: a population-based cohort study. *J Clin Med*. (2022) 11(12):3304. doi: 10.3390/jcm11123304

40. Compston J. Type 2 diabetes mellitus and bone. *J Intern Med*. (2018) 283 (2):140–53. doi: 10.1111/joim.12725

41. Ruan F, Zheng Q, Wang J. Mechanisms of bone anabolism regulated by statins. *Biosci Rep*. (2012) 32(6):511–9. doi: 10.1042/BSR20110118

42. Chamani S, Liberale L, Mobasheri L, Montecucco F, Al-Rasadi K, Jamialahmadi T, et al. The role of statins in the differentiation and function of bone cells. *Eur J Clin Invest*. (2021) 51(7):e13534. doi: 10.1111/eci.13534

43. Wendlová J. Differences in distribution of T-scores and Z-scores among bone densitometry tests in postmenopausal women (a comparative study). *Wien Med Wochenschr*. (2002) 152(23-24):591–5. doi: 10.1046/j.1563-258X.2002.01067.x

44. Afarideh M, Sartori-Valinotti JC, Tollefson MM. Association of sun-protective behaviors with bone mineral density and osteoporotic bone fractures in US adults. *JAMA Dermatol*. (2021) 157(12):1437–46. doi: 10.1001/jamadermatol.2021.4143

frontiers | Frontiers in Neurology

TYPE Systematic Review
PUBLISHED 05 August 2024
DOI 10.3389/fneur.2024.1442145

OPEN ACCESS

EDITED BY
Qingchun Mu,
Second Affiliated Hospital of Soochow University, China

REVIEWED BY
Longfei Shu,
Wuxi Clinical College of Anhui Medical University, China
Feng Gao,
Capital Medical University, China
Sanjeev Nirala,
Tribhuvan University Teaching Hospital, Nepal

*CORRESPONDENCE
Bei Ma
✉ mabei08@163.com
Liming Cheng
✉ limingcheng@tongji.edu.cn

†These authors have contributed equally to this work and share first authorship

RECEIVED 01 June 2024
ACCEPTED 23 July 2024
PUBLISHED 05 August 2024

CITATION
Wang S, Xu W, Wang J, Hu X, Wu Z, Li C, Xiao Z, Ma B and Cheng L (2024) Tracing the evolving dynamics and research hotspots of spinal cord injury and surgical decompression from 1975 to 2024: a bibliometric analysis. *Front. Neurol.* 15:1442145. doi: 10.3389/fneur.2024.1442145

Tracing the evolving dynamics and research hotspots of spinal cord injury and surgical decompression from 1975 to 2024: a bibliometric analysis

Siqiao Wang[1,2†], Wei Xu[1,2,3,4†], Jianjie Wang[1,2,3,4†], Xiao Hu[1,2,3,4], Zhourui Wu[1,2,3,4], Chen Li[1,2,3,4], Zhihui Xiao[1,2], Bei Ma[1,2,3,4*] and Liming Cheng[1,2,3,4*]

[1]Division of Spine, Department of Orthopedics, Tongji Hospital Affiliated to Tongji University School of Medicine, Shanghai, China, [2]Key Laboratory of Spine and Spinal Cord Injury Repair and Regeneration (Tongji University), Ministry of Education, Shanghai, China, [3]Institute of Spinal and Spinal Cord Injury, Tongji University School of Medicine, Shanghai, China, [4]Stem Cell Translational Research Center, Tongji Hospital, Tongji University School of Medicine, Shanghai, China

Background: Exploration of the benefits and timing of surgical decompression in spinal cord injury (SCI) has been a research hotspot. However, despite the higher volume and increasing emphasis on quality there remains no bibliometric view on SCI and surgical decompression. In this study, we aimed to perform bibliometric analysis to reveal the core countries, affiliations, journals, authors, and developmental trends in SCI and surgical decompression across the past 50years.

Methods: Articles and reviews were retrieved from web of science core collection between 1975 and 2024. The bibliometrix package in R was used for data analysis and visualizing.

Results: A total of 8,688 documents were investigated, indicating an ascending trend in annual publications. The USA and China played as the leaders in scientific productivity. The University of Toronto led in institutional productions. Core authors, such as Michael G. Fehlings, showed high productivity, and occasional authors showed widespread interests. Core journals like *Spine* and *Spinal Cord* served as beacons in this field. The interaction of core authors and international collaboration accentuated the cross-disciplinary feature of the field. Prominent documents emphasized the clinical significance of early decompression in 24h post SCI.

Conclusion: Based on comprehensive bibliometric analysis and literature review, we identified the hotspots and future directions of this field: (1) further investigation into the molecular and cellular mechanisms to provide pre-clinical evidence for biological effects of early surgical decompression in SCI animal models; (2) further evaluation and validation of the optimal time window of surgical decompression based on large cohort, considering the inherent heterogeneity of subpopulations in complicated immune responses post SCI; (3) further exploration on the benefits of early decompression on the neurological, functional, and clinical outcomes in acute SCI; (4) evaluation of the optimal surgical methods and related outcomes; (5) applications of artificial intelligence-based technologies in spinal surgical decompression.

KEYWORDS

spinal cord injury, surgical decompression, functional recovery, bibliometric analysis, bibliometrix

1 Introduction

Spinal cord injury (SCI) is devastating, which significantly compromises the life quality of affected patients. Approximately 500,000 new SCI cases per year were reported worldwide with young population accounting for the majority of these cases (1). Patients' symptoms and paralysis resulted from SCI are known as one of the conditions that leads to serious mental and physical impairment. From financial and social points of view, the long-term hospitalization and high cost for therapy imposes a huge burden on patients with SCI and their care givers, which causes great burdens on healthcare systems (2). Hence, it is of necessity to investigate effective treatment strategies for preventing secondary damages and improving functional recovery in SCI patients. SCI treatments have made significant progress in the past years based on the exploration of molecular mechanisms, pathophysiology, neural regeneration, and the improvement of surgery (3, 4). After early operative decompression was proposed in brain injuries (5), early surgical decompression has been widely explored in SCI. Nevertheless, appropriate methods and time window of decompression for SCI remain controversial.

The field of SCI and surgical decompression has produced a variety of significant researches in past decades. These researches were spread over many journals, making it difficult to determine the most impactive sources in the field of SCI and surgical decompression. To date, no research has conducted bibliometric analysis to realize knowledge mining and comprehensively explore the field of SCI and surgical decompression. Hence, we performed a bibliometric analysis to further explore the associated researches, which can reveal significant insights in this dynamic field over the past decades.

Web of Science (WOS) is a commonly used database for technical and scientific literature (6), which help scholars to comprehensively evaluate citation frequency and establish reference co-citation networks for specific research fields. Bibliometrics is a powerful tool for investigating scientific output, developmental trends, and impacts, through evaluating publication characteristics, the geographical distribution feature of research endeavors, critical sources, collaboration networks, and development trends (7). Recently, bibliometric analyses have been performed in multiple clinical fields, including rheumatism, endocrinology, and trauma (7–9). However, the bibliometric views on the research field of SCI and surgical decompression remained a black box. Here, through performing a comprehensive bibliometric analysis, we investigated the research articles and reviews regarding SCI and surgical decompression to determine the knowledge structure, hotspots, and developmental trends in this field.

2 Methods

2.1 Data source

The Web of Science™ (Clarivate™, Philadelphia, PA, United States) was utilized to perform publication retrieval on 14th July 2024. The data sources and inclusion and exclusion criteria were outlined in Figure 1. We utilized Preferred Reporting Items for Systematic Reviews and Meta-Analyses (PRISMA) to document the search processes and results (10).

2.2 Screening strategies

The retrieval strategy was designed as follows: (TS = "spinal cord injury" OR TS = "spinal injuries" OR TS = "spinal cord injuries" OR TS = "spinal injury" OR TS = "spinal cord trauma" OR TS = "spinal cord traumas" OR TS = "spinal cord laceration" OR TS = "spinal cord lacerations" OR TS = "post-traumatic myelopathy" OR TS = "traumatic myelopathies" OR TS = "spinal cord contusion" OR TS = "spinal cord contusions" OR TS = "spinal cord transection" OR TS = "central cord injury") AND (TS = "decompression" OR TS = "surgical" OR TS = "surgery" OR TS = "anterior cervical discectomy and fusion" OR TS = "interbody fusion" OR TS = "arthrodesis" OR TS = "ACDF" OR TS = "endoscopic decompression" OR TS = "discectomy" OR TS = "laminectomy"). Documents published from 1st January 1975 to 14th July 2024 were collected from the WOS Core Collection (WOSCC). Reviews and articles in English were obtained from various publication types.

After excluding documents based on the inclusion criteria of publication types and language, 8,704 documents were extracted. Then, we exported all resulting citations and manually removed duplicates using a bibliographical database manager (EndNote X9). Following duplicate removal, each author reviewed the remaining articles and reviews based on the inclusion criteria independently. Articles and reviews meeting the exclusion criteria were then removed. If any decisions diverged, the research group discussed the results until a consensus was reached.

2.3 Content analysis and the base of extraction

We conducted a content analysis according to the title and abstract, which allowed us to categorize and extract the articles and reviews that were in accordance with the research topics, where more than one theme per article could be extracted for further analysis. The above retrieval strategy was used as a guiding framework for our scoping review. Each article was reviewed by at least two authors on separate occasions to increase replicability of our results. The raw data could be seen in Supplementary materials 1, 2. To prevent bias caused by update of WOSCC, data retrieval and collection were performed on 14th July 2024, which were subjected to bibliometric tools for quality evaluation and subsequent analysis.

2.4 Data analysis

All retrieved documents were exported in a TXT file format, which were processed using "Bibliometrix" package (version 3.2.1) in R (version 4.3.2, Institute for Statistics and Mathematics, Vienna, Austria; www.r-project.org) to perform comprehensive visualization and knowledge mapping (11). Biblioshiny, a web application for bibliometrix, was used to analyze and visualize the raw data. Annual scientific production was investigated to show the general trend within the field of SCI and surgical decompression. The most influential countries, affiliations, authors, and journals were determined by the scientific productions as well as local/global citations. Further, algorithms including Lotka's law (12), Bradford's law (13), and measurement like h-index (14) were utilized to

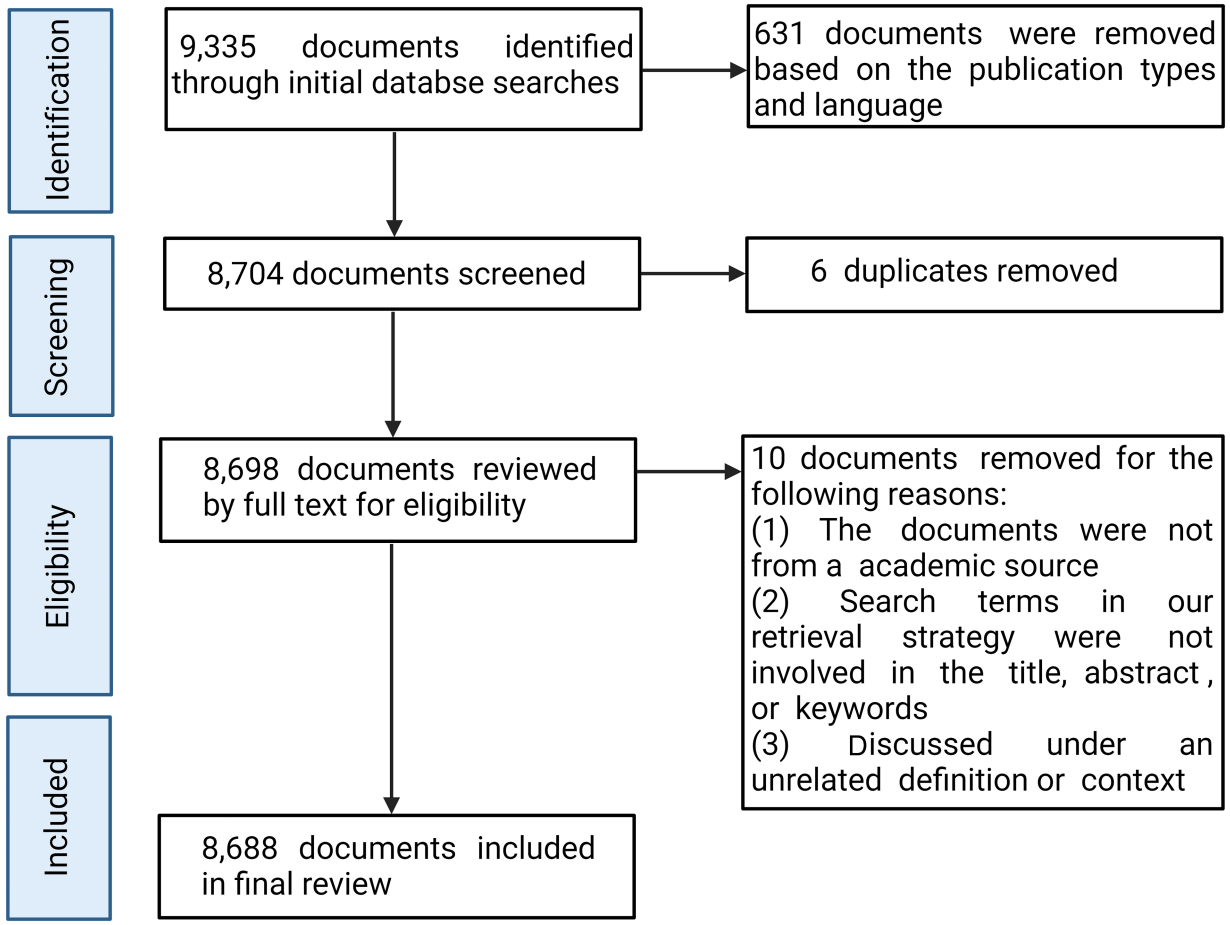

FIGURE 1
Preferred Reporting Items for Systematic Reviews and Meta-Analyses (PRISMA) flow chart detailing the review process and selection of final sample of publications.

determine the core journals and authors. Lotka's law defines that the number of authors who make n contributions is approximately $1/n^a$ of those with one contribution, where a is usually almost two which indicates that the number of authors contributing a particular number of papers is inversely proportional to the number of contributed papers (15). The Lotka's law explains the scientific productivity and the relationship between the authors and their papers through predicting the contribution of an author for a publication. Bradford's law describes the scatter of citations in a given research field, which can be utilized to determine the most highly cited journals or the core journals in a specific research field (16). The h-index, defined as an author's h papers with at least h citations, is utilized as a measure of academic influence in bibliometrics (17). Countries' collaboration of was analyzed to determine the global correlations among different countries. To identify the hot topics, after capturing keywords with high occurrence frequency and the most cited articles, a keyword co-occurrence network was established to show the concrete content of the hotspots. A tree map was constructed to show the most frequent keywords. A thematic map was established to show the different themes through performing a clustering algorithm. The x-axis indicated the centrality (the significance of themes) and the y-axis indicated the density (theme's development degree). Each bubble referred to a theme cluster and the bubble size indicated their occurrences. Thematic evolutions were investigated by dividing the time span into four different slots (1975–2009, 2010–2014, 2015–2019, and 2020–2024).

3 Results

3.1 Literature search results

The initial literature search yielded a total of 9,335 documents published between 1st January 1975 and 14th July 2024 from the WOSCC. A total of 8,704 articles and reviews written in English were extracted. After removing 6 duplicates and 10 documents failing to meet the inclusion and exclusion criteria, we obtained 8,688 articles and reviews in the final list of publications used for bibliometric analysis.

3.2 Analysis of annual publications

Data retrieval strategies and analysis processes were illustrated in Figure 1. From 1st January 1975 to 14th July 2024, 8,688 documents were retrieved from WOSCC. A total of 8,688 documents that met the

inclusion criteria including 7,171 (82.5%) research articles and 1,517 (17.5%) reviews were obtained for the subsequent analysis. The data retrieval date (14th July 2024) accounted for the steep decline in 2024 (Figure 2A). Before 1991, only a limited number of researches were published. Then, from 1991 to 2005, an intermittent and slow increase in annual publications were identified. The most significant increases happened in 2010s, with over 200 papers published per year in this field. Generally, the annual growth rate of publication number was approximately 11.2%, and the average age of documents was about 10.8 years. The growing trend indicated that the field of SCI and surgical decompression was becoming more and more attractive. The trend of annual citations per year in the field of SCI and surgical decompression was shown in Figure 2B. The high peak of the years distribution of citation appeared in the period between 2004 and 2019, implicating that significant research outcomes were gained in this field. The average citations per document was approximately 22.8. However, the overall citation frequency has rapidly declined in the past 5 years.

3.3 Analysis of countries, affiliations, and authors

A total of 88 countries contributed to the field of SCI and surgical decompression. Ranked by accumulated publication number, the top 3 most prolific countries were the USA ($n = 2{,}651$ 30.5%), China

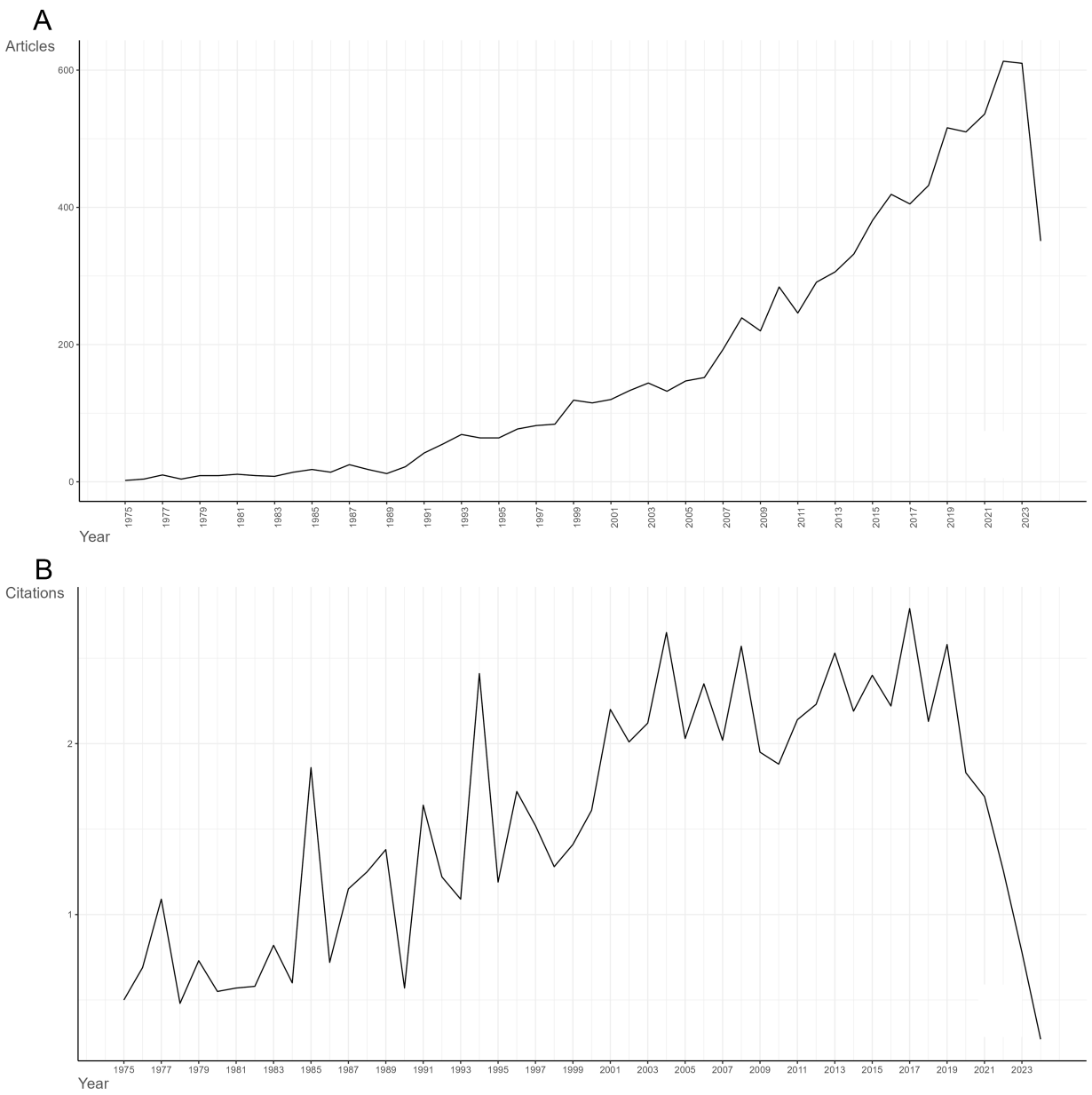

FIGURE 2
Analysis of annual scientific production and annual citation of documents on spinal cord injury (SCI) and surgical decompression. **(A)** The manifestly explosive growth of annual production started from 1991, and the high peak indicated scientific breakthroughs. **(B)** The trend of annual citations per year in the field of SCI and surgical decompression. The high peak implicated that significant research outcomes were gained in this field.

($n = 1,336$, 15.4%), and Japan ($n = 498$, 5.7%). Collaboration strength among different countries can be revealed by the single-country publication (SCP) and multiple-country publication (MCP) rates. Countries showing the highest MCP ratio included the USA, China, Canada, the United Kingdom (UK), and Germany; other countries, such as Japan and Turkey, mainly provided the domestically published articles. Nevertheless, with high number of productions, the overall citation number of articles from China ($n = 16,257$) was considerably less than the USA ($n = 81,340$), which ranked the third among the contributing countries (Figure 3B), indicating the huge influence of the USA within the research field. Besides, Canada ranked the second with 26,492 citations. Country collaboration analysis showed that, China and the USA had the most interactions with others (Figure 3C). There were 819 collaborations across the contributing countries, 74 of which were from the USA to others. In the collaboration map, the connection between China and the USA was the most extensive, highlighting the interactions between these two countries for SCI and surgical decompression-related researches. Generally, the lines between countries were scattered and sparse, indicating the multiple country publications were less than the single country publications.

Currently, a total of 4,527 institutions have participated in the field of SCI and surgical decompression, and the top 10 most prolific institutions were identified (Figure 4). It indicated that University of Toronto ranked the first, with 682 publications, followed by University of California System ($n = 402$), University Health Network Toronto ($n = 307$), Veterans Health Administration ($n = 258$), and University System of Ohio ($n = 249$). These findings were consistent with the results discussed above, which showed the USA and Canada were the pioneers in the field of SCI and surgical decompression.

3.4 Analysis of journals

Publications and citations were utilized for evaluating the overall influence of 1,545 journals in the field of SCI and surgical decompression. The top 10 most productive journals published a total of 2,012 documents from 1975 to 2024, accounting for about 23.2% of all the documents in this field (Supplementary Figure S2A). According to the Bradford's law, the top 23 most prolific journals were defined as the core sources in the research field (Supplementary Figure S2B). Specifically, *Spine* ($n = 365$) was the most productive journal, followed by *Spinal Cord* ($n = 364$), *Journal of Neurotrauma* ($n = 225$), *World Neurosurgery* ($n = 224$), and *Journal of Neurosurgery-Spine* ($n = 194$). Among the journals, *Spine* was the earliest one (year 1984, $n = 5$) to publish articles in the field of SCI and surgical decompression, which continued to rise and remained at the top. However, *World Neurosurgery* was the latest one, with quick growth in publication number (Figure 5A).

The number of local citations was evaluated based on the reference list to evaluate the local impact of journals, whereas global citations covered a broad scope of research fields. In terms of local citations, *Spine* ranked the top of the list with 15,539 citations, followed by *Journal of Neurosurgery* ($n = 7,953$) and *Spinal Cord* ($n = 7,937$), indicating these journals provided a variety of superior quality research (Figure 5B). When h-index was calculated to evaluate the local impact of journals, we identified that *Spine* (h-index = 65), *Journal of Neurotrauma* (h-index = 46), and *Spinal Cord* (h-index = 44) were the top three most impactive sources (Figure 5C).

3.5 Analysis of authors

A total of 32,260 authors have published relevant articles on SCI and surgical decompression since 1975, making efforts to facilitate the development of the field. Lotka's law showed correlations between authors and related publications. In general, it showed the phenomenon that a small proportion of authors provided most of the related articles. Herein, the Lotka's law was used to evaluate the publications in the field of SCI and surgical decompression, as the majority of the relevant documents in this field were published by a rather small population of authors, and about 80% of authors published only one article related to this research field (Supplementary Figure S3A). The top 10 most productive authors were illustrated in Figure 6, among whom Fehlings MG topped the rankings with a total publication number of 202, who has retained an active role until today. Although starting late, Kwon BK, Harrop JS, and Wilson JR continued to be active till now. Additionally, Fehlings MG was the most local cited authors ($n = 2,590$), followed by Aarabi B ($n = 989$; Supplementary Figure S3B). According to the h-index, the top 10 most impactive authors were illustrated in Supplementary Figure S3C. Further, Fehlings MG and Vaccaro AR were the two most impactive authors in this field with the highest h-index.

3.6 Analysis of documents and references

Most cited documents and references served as the future directions for investigating SCI and surgical decompression. Globally cited documents were the articles that were cited in all research fields, whereas locally cited documents were only cited in the field of SCI and surgical decompression. Hence, high number of globally cited documents may represent the overall impact, whereas high number of locally cited documents indicated their influence in the field of SCI and surgical decompression. Figures 7A,B summarized the top 10 most globally cited documents as well as the top 10 most locally cited documents in the field of SCI and surgical decompression, respectively. Specifically, the highest globally cited document, "Prevention of venous thromboembolism," by Geerts WH in 2008 (3,187 global citations) (18), discussed the prevention of venous thromboembolism (VTE). They recommended all major trauma and all SCI patients receive thromboprophylaxis (Grade 1A). In patients admitted to hospital with acute SCI, they recommended thromboprophylaxis with a low-molecular-weight heparin (LMWH), low-dose unfractionated heparin (LDUH), or fondaparinux (each Grade 1A). Furthermore, they recommended that, on admission to the intensive care unit (ICU), all SCI patients be assessed for their VTE risk, and that most of them receive thromboprophylaxis (Grade 1A).

The highest locally cited document, "Early versus Delayed Decompression for Traumatic Cervical Spinal Cord Injury: Results of the Surgical Timing in Acute Spinal Cord Injury Study (STASCIS)" (19), by Fehlings MG, published in 2012 (317 local citations), evaluated the relative effectiveness of early (<24 h after injury) vs. late (≥24 h after injury) surgical decompression post traumatic cervical spinal cord injury (CSCI). They identified that, the odds of at least a 2 grade AIS improvement were 2.8 times higher than those who underwent early surgical decompression as compared with those who underwent late decompressive surgery (OR = 2.83, 95% CI: 1.10,7.28)

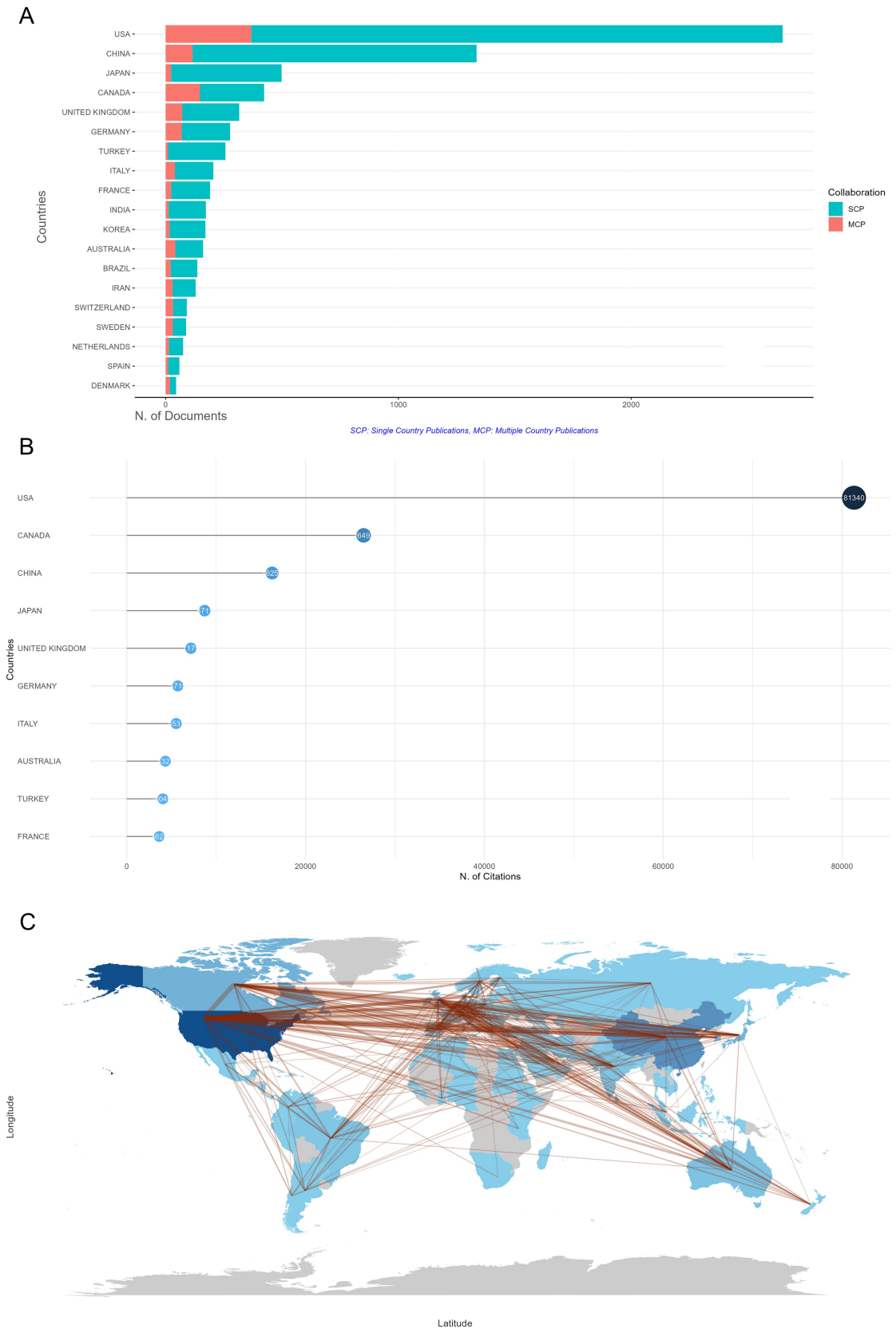

FIGURE 3
Analysis of countries in the field of spinal cord injury (SCI) and surgical decompression. **(A)** Countries' scientific production and collaboration histogram based on the nationality statistics of the corresponding authors in SCI and surgical decompression studies. SCP, single country publications. MCP, multiple country publications. **(B)** Top 10 most cited countries in SCI and surgical decompression researches. **(C)** Country collaboration map in SCI and surgical decompression researches.

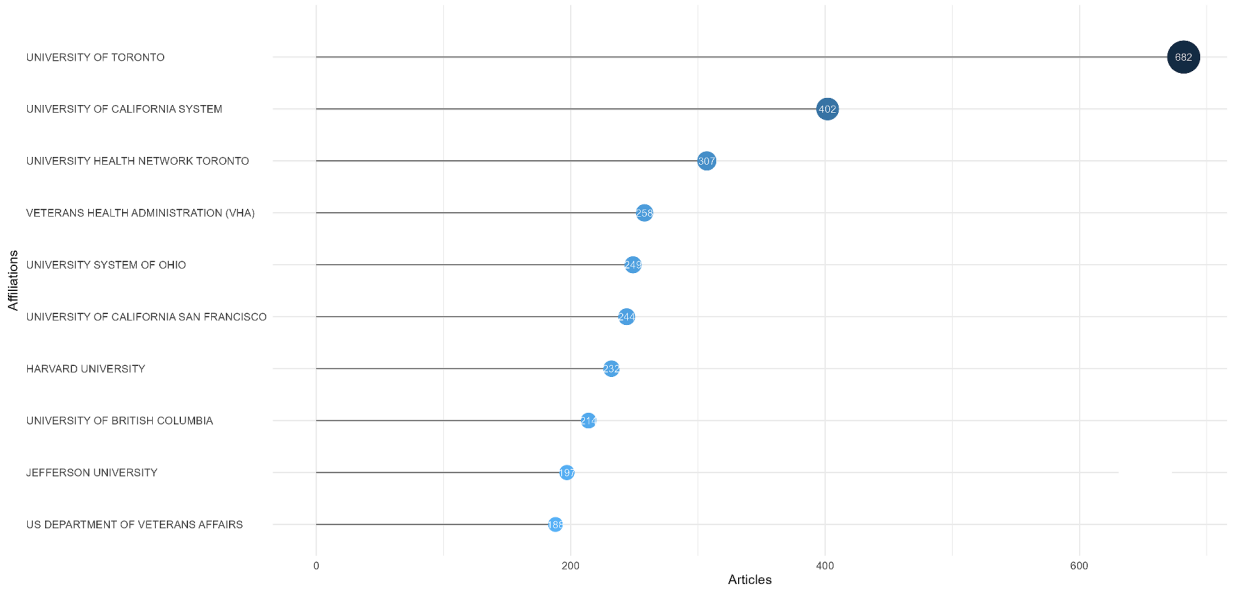

FIGURE 4
Top 10 most productive institutions in spinal cord injury (SCI) and surgical decompression researches.

based on the multivariate analysis. They concluded that, surgical decompression prior to 24 h post SCI could be safely performed, which was related to improved neurologic outcomes.

The top 10 most locally cited references were shown in Figure 7C, "A sensitive and reliable locomotor rating-scale for open-field testing in rats" (20), by Basso DM, published in 1995 (407 local citations), developed an expanded and unambiguous locomotor rating scale for standardizing locomotor outcome measures among laboratories, which can clearly distinguish behavioral outcomes after different injuries and predict anatomical alterations in the injured sites.

3.7 Analysis of keywords

Key words constantly appeared in internalized documents represented the hotspots in a specific research field. As a useful algorithm that is unique to Clarivate databases, KeyWords plus enhances the power of reference searching By searching across disciplines for all the documents that had cited references in common. Based on KeyWords plus analysis (Figure 8A), we identified the top 10 most frequent keywords, including "spinal-cord-injury" (1,203 occurrences), "management" (970 occurrences), "surgery" (844 occurrences), "recovery" (542 occurrences), "injury" (404 occurrences), "outcomes" (395 occurrences), "complications" (378 occurrences), "functional recovery" (309 occurrences), "trauma" (308 occurrences), and "decompression" (294 occurrences), far exceeding other keywords, indicating that this research field concentrated on developing clinically efficient management strategies and surgical methods to improve neurological outcomes, promote functional recovery, and reduce short-term and long-term complications after SCI. The high frequency of appearance of these keywords was further demonstrated and visualized by a keyword tree and word cloud, respectively (Supplementary Figures S4A,B).

A keyword co-occurrence network was constructed to show the internal and external link between the most relevant keywords which occurred more than 10 times in this field (Figure 8A). Link lines indicated the two keywords appeared in one or more articles at the same time. These keywords were grouped into two distinct sub-clusters representing two major themes. Cluster 1 (red) where "spinal-cord-injury," "recovery," "injury," "functional recovery," "expression," "methylprednisolone," "repair," "model," "regeneration," and "rat" were the largest nodes. It chiefly explained the critical role of methylprednisolone in SCI therapy which provided novel therapeutic efficacy and availability in SCI patients and SCI animal models. Cluster 2 (blue) was represented by "management," "surgery," "outcomes," "complications," "trauma," "decompression," "fusion," "risk," "risk-factors," "surgical-treatment," and "classification," which concentrated on the risk factors or risk classification models of different clinical outcomes and complications of SCI patients after surgery.

3.8 Analysis of emerging trends

Based on the historical direct citation network, connections across most of the highly cited documents were unveiled (Figure 9A). The link lines between documents indicated that the earlier research was cited by the latter one, where "Early versus Delayed Decompression for Traumatic Cervical Spinal Cord Injury: Results of the Surgical Timing in Acute Spinal Cord Injury Study (STASCIS)" (19) was the past and had a pivotal role in the citation network.

To identify the future trend topics in the field of SCI and decompression, several popular keywords in the past three decades were obtained for further analysis. To construct the trend topics map, the minimum keyword frequency was set to 10 and the number of keywords per year was set to three. Finally, 90 trend topics were

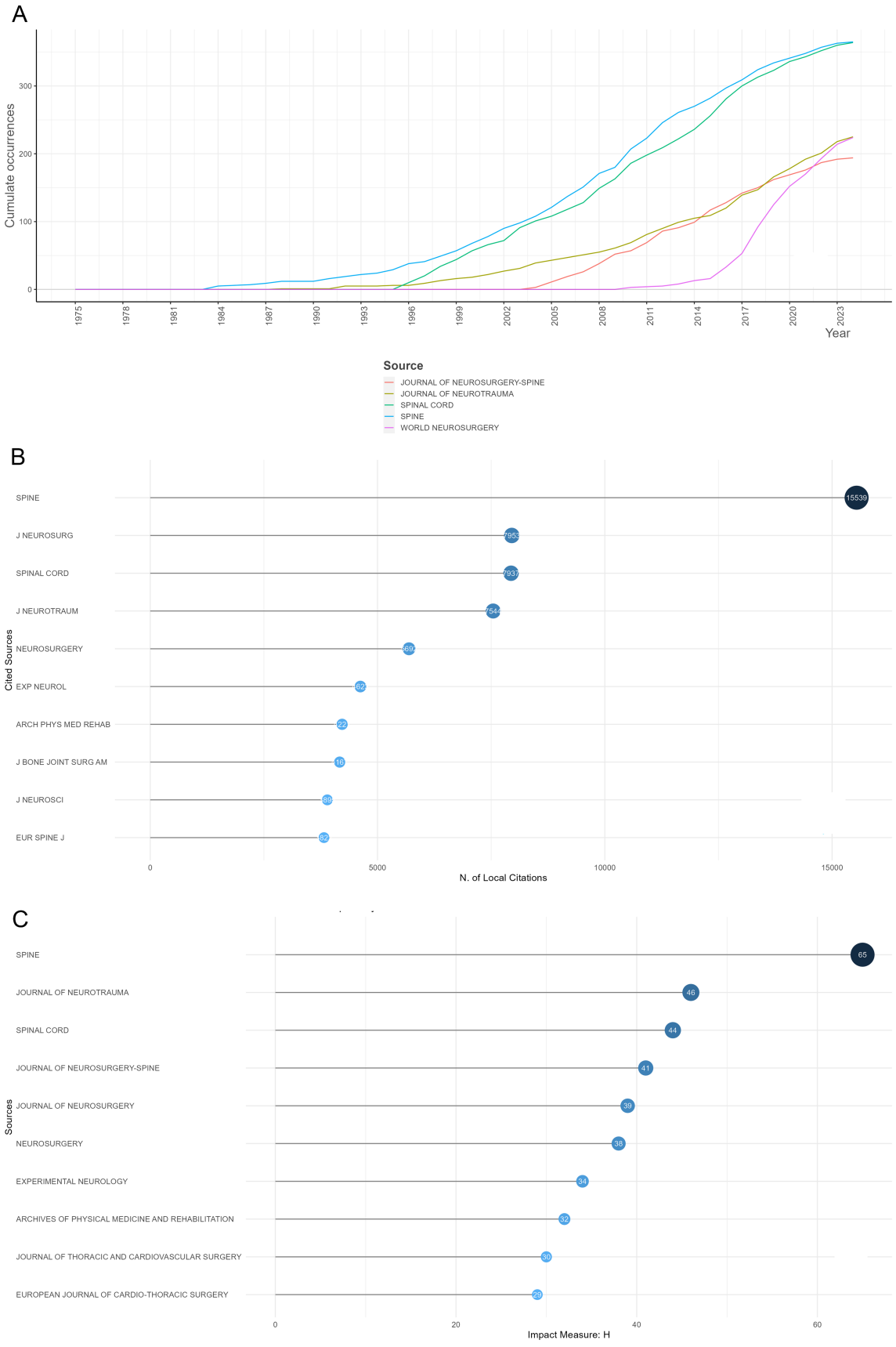

FIGURE 5
Analysis of journals in the field of spinal cord injury (SCI) and surgical decompression. **(A)** The publications' growth of top five productive journals in the field of SCI and surgical decompression. **(B)** Top 10 most local cited journals in the field of SCI and surgical decompression. **(C)** Most local impactive journals measured by h-index in the field of SCI and surgical decompression.

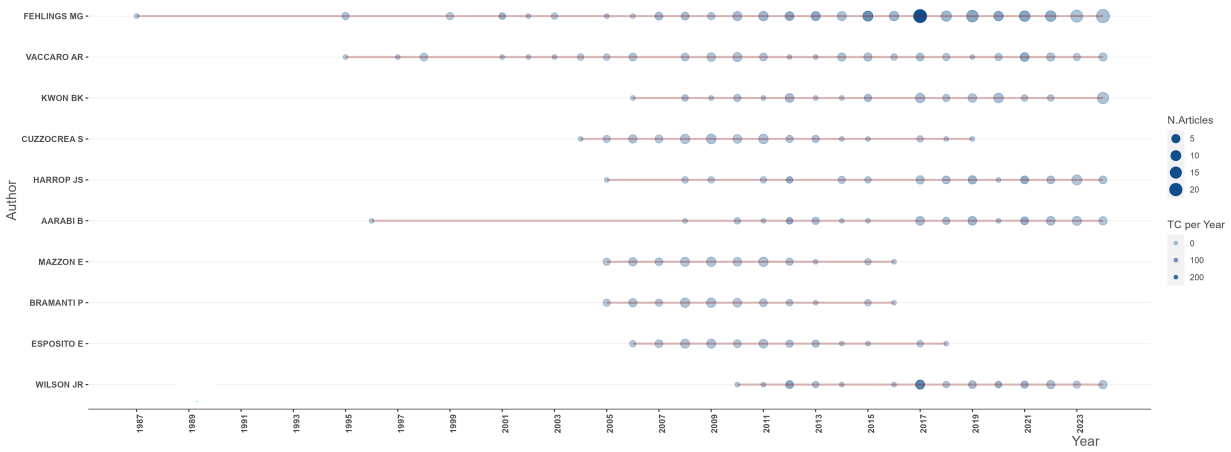

FIGURE 6
Production of the top 10 productive authors over time in the field of spinal cord injury (SCI) and surgical decompression.

identified, and the frequency and popular periods of these research topics were visualized (Figure 9B). Specifically, several trend topics, such as "exosomes," "guideline," "nerve transfers," "hydrogel," "recommendations," "case series," "surgical outcomes," "perfusion-pressure," "intraspinal pressure," "health," and "spondylotic myelopathy" have gained considerable traction over the past 5 years. Dynamic changes within the thematic fields across years (time-period 1975–2009, 2010–2014, 2015–2019, and 2020–2024) were displayed in Figure 9C. Functional recovery is an eternal theme in the field of SCI and surgical decompression. Over time, increasing interests have been attracted by more clinically efficient management strategies of SCI patients who underwent surgical decompression.

3.9 Conceptual analysis

In addition to the dynamics of keywords, the possible relationships across themes with high frequencies also had great significance to better understand the hot topics covered by the research field of SCI and surgical decompression and evolution trends over time. A two-dimensional matrix was constructed to visualize the status of the three major themes in the field of SCI and surgical decompression (Figure 9D). The X axis was labeled with "centrality," representing the relevance degree of the research themes; the Y axis was labeled with "density," indicating the development degree of the research themes. Further, the bubbles were labeled with the most important keywords with the highest occurrences. Generally, four major research themes were distributed in the four quadrants. The green cluster with high development degree and low centrality was described as niche themes, representing that unique gene expression and neural regeneration to promote the functional recovery of SCI patients were highly developed but less associated with the field. The red cluster with high development degree and high centrality was defined as the motor themes the thematic map. Moreover, the blue cluster was located in the quadrant 4, which represented the basic themes. Additionally, deep-vein thrombosis served as the emerging or declining themes, exhibiting a decreasing trend in this research field.

4 Discussion

4.1 General information

Herein, we explored the development trends and hotspots over the past 5 decades and investigated the research frontiers within the field of SCI and surgical decompression in recent years. This bibliometric analysis provided a comprehensive outlook on the associated scientific publications, which shed light on the current research status and identified possible avenues for further investigation. Our results aligned with existing publications, showing an increasing scientific output, multinational collaborations, and emerging thematic alterations within this field (3, 21). Over time, the increased number of publications on SCI and surgical decompression indicated the growing recognition of the critical role that early surgical decompression plays in SCI treatments (22). Surgical decompression for acute SCI aims to reduce secondary ischemia and hypoxia through relieving mechanical pressure. A meta-analysis based on 21 pre-clinical researches showed spinal cord decompression improved the neurological outcomes by 35%, and compressive pressure and duration were critical factors affecting the clinical outcomes (23). Further, previous experimental evidence supported that persistent compression may be a reversible form of secondary injuries (24). Despite its widespread use in acute SCI in North America, the role of surgical decompression in improving neurologic function remained unclear due to the absence of well-designed randomized controlled trials (RCTs). Moreover, the optimal therapeutic window, during which operative decompression could mitigate the secondary SCI, also remained controversial. The logistical and practical challenges associated with early surgical decompression of acute SCI remained important problems.

The wide range of journals publishing on this field, with *Spine*, *Spinal Cord*, and *Journal of Neurosurgery* emerging as the top sources. It indicated that experts from multiple disciplines were actively engaged in this field (25, 26). Such collaboration promoted the depth and breadth of researches on the topic. The analysis of authors revealed the contributions of core authors and occasional authors to the publications related to SCI and surgical

FIGURE 7
Analysis of documents and references in articles regarding spinal cord injury (SCI) and surgical decompression. **(A)** The top 10 most globally cited documents concerning SCI and surgical decompression. The size and darkness of the nodes are in proportion to the number of global citations of each document. **(B)** The top 10 most locally cited documents concerning SCI and surgical decompression. The size and darkness of the nodes are in proportion to the number of local citations of each document. **(C)** The top 10 most locally cited references concerning SCI and surgical decompression. The size and darkness of the nodes are in proportion to the number of local citations of each document.

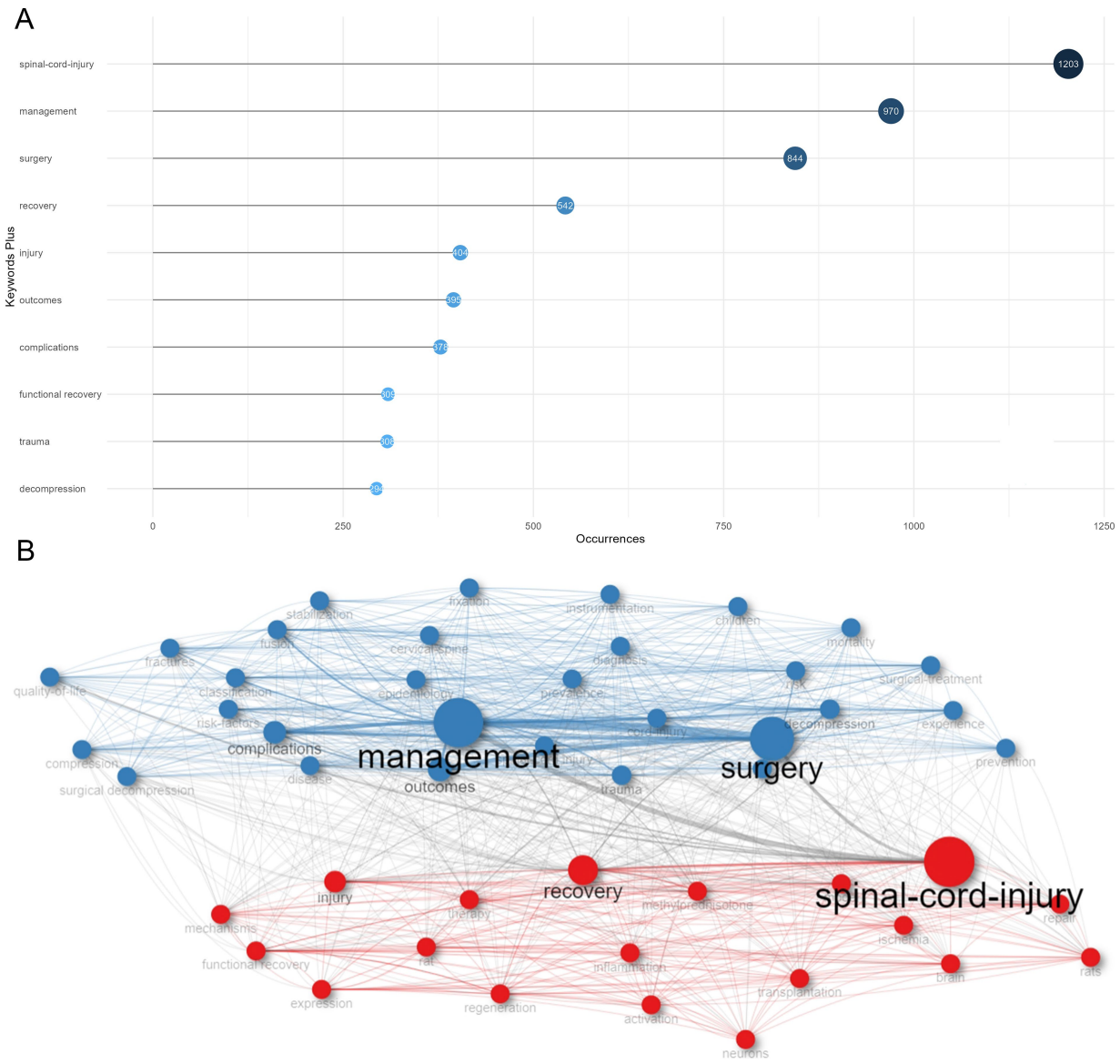

FIGURE 8
Analysis of keywords in the field of spinal cord injury (SCI) and surgical decompression. **(A)** The top 10 most frequent key words selected from KeyWords Plus. The size and darkness of the nodes are in proportion to the number of occurrences of each keyword. **(B)** Co-occurrence analysis of key words. Keywords were divided into two clusters labeled with different colors (blue, red).

decompression. The presence of core authors, such as Michael G. Fehlings and Alexander R Vaccaro, signified their expertise and high productivity within the field. Moreover, the large number of occasional authors suggested a wide engagement of scholars, which emphasized the growing interests in investigating the role of surgical decompression in SCI. Evaluating affiliations provided important insights in the institutional landscape of SCI and surgical decompression research. The prominence of the University of Toronto as the leading affiliation in aspects of publication number indicated a concentrated effort in the field of SCI and surgical decompression. Further, the involvement of institutions from Canada and the USA across the most productive contributors underscored the global collaboration of research on SCI and surgical decompression. The multinational collaboration fostered the exchange of knowledge and promoted the pooling of resources.

The analysis of country scientific output highlighted the USA, China, and Japan as the leading countries in this field. Besides, other countries have also played an important part in the scientific collaboration network, indicating a global effort to overcome the challenges from surgical decompression in SCI. Several experts proposed that, though the recommendations for early surgical decompression in specific patients with acute SCI are well recognized, there is uncertainty about the timing of spinal cord decompression in SCI managements (21). The most locally cited documents provided critical insights in researches that have shaped the research field of SCI and surgical decompression (2, 19, 21, 27–29). The prominent literature entitled "Early versus

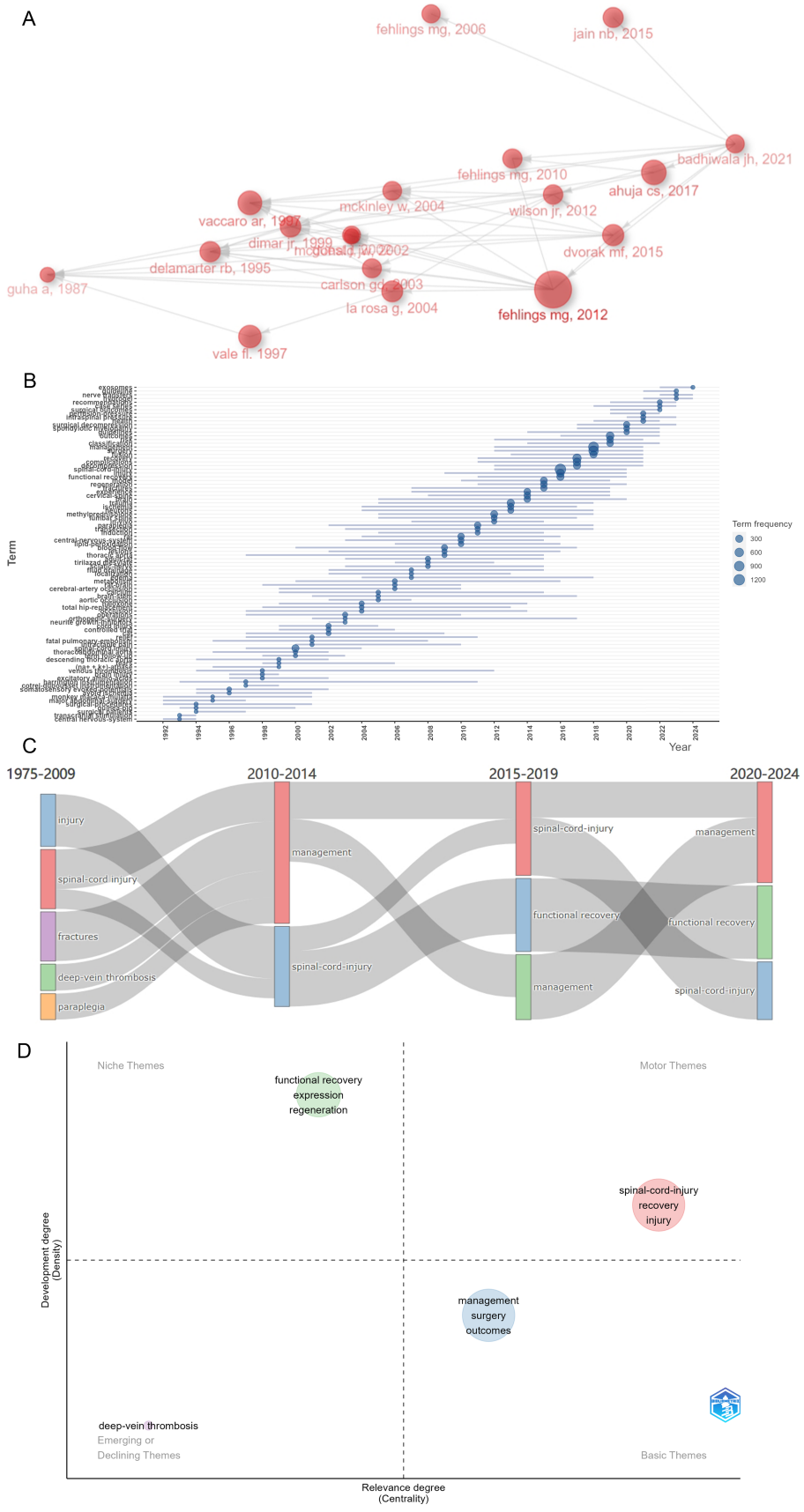

FIGURE 9
Investigating research status of various hot topics on spinal cord injury (SCI) and surgical decompression researches, sketching historical trajectories and revealing research frontiers. **(A)** Historical direct citation network of key documents in SCI and surgical decompression researches. **(B)** Trend Topics

(Continued)

FIGURE 9 (Continued)
Analysis with the 3 keywords per year which occurred at least 10 times in the past decades. **(C)** Sankey plot of the most frequent key words in different time period (1975–2009, 2010–2014, 2015–2019, and 2020–2024). **(D)** Thematic map for SCI and surgical decompression researches. The horizontal coordinate referred to the relevance degree (centrality), and the vertical coordinate represented the development degree (density). Motor themes in the first quadrant represented core themes with high centrality and maturity, niche themes in the second quadrant represented isolated themes with increased maturity, the third quadrant represented emerging or declining themes with low centrality and high maturity, and basic themes in the fourth quadrant indicated popular themes with low maturity.

Delayed Decompression for Traumatic Cervical Spinal Cord Injury: Results of the Surgical Timing in Acute Spinal Cord Injury Study (STASCIS)" represented the most cited and impactive research (19). Fehlings et al. (19) conducted an international, multicenter, prospective cohort study in adults with CSCI aged between 16 and 80. Their results indicated that surgical decompression within 24 h post SCI could be safely conducted and is related to better clinical outcomes (19). Vaccaro et al. (28) performed a prospective analysis to evaluate neurologic outcomes after early vs. late decompressive surgery for CSCI. It revealed no significant neurologic benefits when surgical decompression after CSCI is performed less than 72 h post injury as compared with waiting longer than 5 days. Vale et al. (29) used combined medical and surgical treatments after acute SCI, which demonstrated that early and aggressive medical managements (blood pressure augmentation and volume resuscitation) of patients with SCI can effectively promote the neurological recovery. Fehlings et al. (30) reported that the role of early surgical decompression in SCI patients was only supported by Class III and limited Class II evidence, which can be considered as a practice option only. More prospective and controlled trials are required to investigate the timing and role of early surgical decompression in patients with acute SCI. Furlan et al. (21) reviewed the pre-clinical and clinical evidence regarding the possible influence of timing of decompressive surgery on clinical outcomes post traumatic SCI. There is evidence to demonstrate that early surgical decompression is feasible and safe and that it can optimize neurological outcomes and decrease health care costs (21). Early surgical decompression should be considered in all SCI patients from 8 to 24 h after acute SCI. Ahuja CS et al. also concluded that early surgical decompression requires to be quickly performed after acute SCI (2).

Keyword analysis and thematic clustering provided intriguing insights in the current state of thematic field. The clusters related to spinal cord injury, management, surgery, complications, recovery reflected the multifaceted characteristics of surgical decompression and its influence on SCI functional recovery (3, 31, 32). These clusters highlighted the requirement to investigate the fundamentals, clinical efficiency, post-operative complications of spinal cord decompression. While this study provided critical insights, some research gaps and future directions emerged from this bibliometric analysis. First, there is an urgent need for further exploration on the molecular and cellular mechanisms to provide pre-clinical evidence for biological benefits of early surgical decompression in SCI animal models. It necessitated performing well-designed mechanistic researches, investigating the interplays between surgical decompression and neurological outcomes, and revealing the underlying signaling pathways. Second, there is still much to be explored in terms of the optimal time window for decompression on basis of the current clinical evidence, considering the inherent heterogeneity in complicated inflammatory responses post SCI. Third, further research is warranted to explore the benefits of early surgical decompression on the neurological, functional, and clinical outcomes in SCI.

4.2 The role and timing of early surgical decompression in SCI

Unfortunately, there is no high evidence level analysis investigating the safety and efficacy of early surgical decompression in subpopulations with distinct clinical features (33). Nevertheless, in several analyses, the usefulness of early decompression was supported at the suggestion level (34, 35). In subpopulations according to age, no research compared the efficacy and safety of early surgical decompression and late surgical decompression between younger and elder individuals. Recently, there is an analysis evaluating the clinical outcomes of early decompression between younger and elder patients with acute SCI. Lau et al. (36) reported that, the mortality rate and complication rate of elder patients with acute SCI (≥70 years) were 11 times and 2 times higher than younger patients (<70 years). Nevertheless, there was no statistical difference in discharge American Spinal Injury Association impairment scale (AIS) grade and AIS grade alteration between these two patient groups. In subpopulations according to injury degree, SCI patients with AIS grade B, C, and D at C2-L2 level prior to surgical decompression showed a better motor functional recovery with early decompression (≤24 h) than those with late surgical decompression (>24 h). In SCI patients with AIS grade A, there was no significant benefit of early surgical decompression on motor functional recovery. In SCI patients with AIS grade A or B, early surgical decompression contributed to shorter hospital stay (37). Moreover, as AIS grade altered from A to D at admission, when surgical decompression was conducted in 12 h, the conversion rate from AIS grade at admission to better discharge AIS grade was significantly higher (38). Further, ultra-early surgical decompression (≤12 h) exhibited better improvement in the AIS grade than surgical decompression post 12 h. Particularly, in SCI patients with AIS grade A, if ultra-early surgical decompression was conducted, the AIS grade may improve to stage 1 or 2 post operation (38). Though only for CSCI, other researches showed different time windows of surgical decompression (ultra-early, ≤12 h; early, 12–24 h; and late, >24 h) did not influence conversion of AIS grade (38). Further, in subpopulations according to the preoperative use of steroid pulse, early surgical decompression (≤24 h) in SCI patients with preoperative steroid pulse exhibited better improvement in light touch score, pin prick score, and motor functional recovery than late surgical decompression (>24 h). However, there was no notable difference in the improvement of total motor score between early and late surgical decompression in SCI patients who did not use steroid pulse prior to operation (38).

The optimal time window of surgical decompression post SCI still remained controversial (39). It was challenging to standardize the time window because of inherent heterogeneity in the exact definition of "early decompression" for previous studies, and there were limited studies at high level of recommendation. Importantly, most studies set the time window of definition of "early" as 24 h, which was considered to be the most appropriate method to define "early" (38). Moreover, in 2012, the Surgical Timing in Acute Spinal Cord Injury Study (STASCIS) defined "early" as the first 24 h post SCI, and showed surgical decompression in 24 h post injury was related to better neurologic outcomes, exhibiting more than grade 2 AIS improvement in 6 months follow up (19, 38). Subsequently, various researches showed the beneficial effects of early surgical decompression (<24 h) in SCI patients (21, 38). Nevertheless, despite compelling evidence, timing of decompression for patients with acute SCI was still uncertain. Particularly, in those with central cord syndrome without instability, since spontaneous improvement might happen, surgical decompression of the injured spinal cord might cause worsening neurologic function. Arbeitsgemeinschaft für Osteosynthesefragen spine (AOSpine) evaluated the safety and efficacy of early decompression (≤24 h) and late decompression (>24 h) in SCI patients (35). They reported early surgical decompression should be considered as an important therapeutic strategy in adult SCI patients with traumatic central cord syndrome, and early surgical decompression should be performed in adult patients with acute SCI at any level.

Grossman et al. (40) showed if patients visited the emergency center immediately post SCI, most arrived in 4 h, and that 8 h to spinal cord decompression was critical for achieving better clinical outcomes. In this context, an 8-h time threshold was further proposed. Recent RCTs showed that (41), surgical decompression in 8 h in patients with SCI exhibited more neurological improvement than more than 8 h. Additionally, a previous analysis compared the surgical decompression in 8 h vs. 8 to 24 h, which indicated that neurobehavior outcomes were better in surgical decompression in 8 h than 8 to 24 h post SCI (42). Recently, various researches supported the favorable effect of surgical decompression in 8 h post SCI (43–45). Nevertheless, in several researches, "in 8 h post SCI" was defined as the time taken post arriving in the emergency center. Hence, it was hard to compare the conclusions draw from the previous studies directly. Furthermore, within the narrow time window of 8 h post injury, loss of just 1 h is of vital importance. In clinical practice, decompression in 8 h post SCI was quite difficult because of transport time to the emergency center and lack of available operation rooms. However, a previous study showed negative views on early surgical decompression. Tanaka et al. (46) divided patients in an early decompression group (≤24 h) and a late compression group (>24 h to 1 week). The intensive care unit (ICU) stay, survival rate, and mortality rate of patients showed no significant difference between these two groups (46).

In summary, "time is spine," and the timing of surgical decompression is one of the most significant factors in the treatment of acute SCI. CSCI showed significant improvement with early surgical decompression both in the upper extremities and lower extremities. Early surgical decompression also contributes to better motor outcomes in thoracic SCI as compared with late decompression. Numerous multicenter studies demonstrated that, early surgical decompression significantly promotes long-term neurological improvements (37). Patients with acute SCI should receive decompressive surgery in a center from qualified spinal surgeons as early as possible, but at least in 24 h. Recently, the superiority of the neurological outcomes with decompressive surgery in 8 h has been demonstrated.

4.3 The impact of different surgical methods on different injury segments concerning clinical outcomes

Traumatic SCI is usually unstable, so surgical stabilization is particularly important (32). The aims of surgical therapies post SCI include the stabilization and reduction of the secondary SCI while achieving the anatomical alignment of spine, in which surgical decompression plays a critical role. The surgical procedure promotes early mobilization and rehabilitation. Based on the lesions of the fracture, surgical decompression could be performed posteriorly, anteriorly, or in combination procedures (47).

4.3.1 Optimal surgical methods for CSCI

Early surgical reduction and decompression is critical for CSCI. It is always recommended to restore stability or fusion of the injured segments (48). Atlas fractures happen less frequently in combination with SCI because of the larger diameter of the spinal canal. Atlas arch fractures with a dislocation of at least 7 mm usually indicate the instability of the spinal injury. It is recommended to perform instrumentation of ventral, direct dorsal fusion or dorsal osteosynthesis from C1 to C3. Further, axis fractures are rarely accompanied by SCI. In unstable axis fractures, dorsal stabilization is indicated. Besides, ventral screw osteosynthesis is an alternative, whereas it may play a subordinate role in SCI. Traumatic spondylolisthesis of the C2 and C3 vertebral bodies, also called "hangman's fracture," with an inclination of vertebral bodies of more than 11° or a dislocation of more than 3.5 mm are recommended for surgical stabilization. Anterior discectomy and fusion (ACDF) and posterior fusion using transpedicular dorsal instrumentation has demonstrated satisfactory fusion outcomes (49).

CSCI with disc protrusion requires an anterior approach with early surgical decompression and one-stage fusion utilizing vertebral body replacement or a cage and concomitant ventral plate osteosynthesis (47). A previous study of sub-axial CSCI treated with posterior and anterior stabilization and fusion showed no difference in position, fusion rates, neurological outcomes, or post-operation complications. The approach route with which the respective surgeon is familiar is recommended (50).

The gentle access route from ventral has proven effective in CSCI. Even severe dislocation is often easy to reposition, decompress and stabilize from the anterior. However, if this does not succeed, a dorsal procedure may be necessary (49). There is no difference in fusion rates, postoperative alignment, neurological outcome or long-term complications between the different approaches. Combined anteroposterior stabilizations prove to be advantageous in biomechanical studies and allow early mobilization of patients (48). This should initially be taken into account in the case of longer-distance restorations. Stabilization and fusion of anterior or posterior is unavoidable in the treatment of spinal cord injuries in the cervical spine. To maintain the functionality of the cervical spine, short-range fusions and instrumentation should always be performed.

4.3.2 Optimal surgical methods for thoracic and lumbar SCI

The initial surgical therapy of thoracolumbar spinal cord injuries includes surgical reduction with stabilization (51). Even without a laminectomy, complete decompression of the spinal canal can often be achieved. Dorsal decompression in the sense of a laminectomy can also be performed in the case of injuries to the dura, to relieve an epidural hematoma, to further relieve and/or to retrieve/reduce individual bone fragments.

The choice for spinal cord injuries caused by flexion and distraction injury as well as extension and distraction injuries in the thoracolumbar region is reduction with long-distance dorsal stabilization or fusion (49).

An initial ventral procedure for spinal cord injuries of the thoracic spine is not recommended. Biomechanical studies confirmed a significantly more effective immobilization of the fracture in long-range dorsal instrumentation over at least 2 segments cranial and 2 segments caudal of the fracture compared to short-range instrumentation. In the case of a decision for short-range dorsal instrumentation, the use of index screws in the fractured vertebral body increases stability, but overall, the short-range dorsal instrumentation is inferior to the long-range instrumentation. The use of cross connectors also improves rotational stability (52). In addition to the less effective immobilization of the fractures, short-term stabilization leads to an increased occurrence of subsequent degeneration in the sense of junctural kyphosis compared to long-distance stabilization (53). There is no functional disadvantage for the patients due to the long-distance dorsal instrumentation (54, 55). Patients with a spinal cord injury have unstable fractures, so posterior stabilization and instrumentation alone are not always sufficient. Concomitant decompression in the sense of laminectomy should be performed dorsally in order to perform reduction without iatrogenic worsening of neurological symptoms, and to follow up with posterior fusion using long-distance dorsal spondylodesis at the same time (56). In the case of spinal cord injuries, an exclusively anterior approach can be made caudally from the level of BWK 5. In addition to the protection of the autochthonous back muscles with direct anterior compression, anterior decompression proved to be advantages. In addition, biomechanical studies have shown effective stabilization. Overall, isolated anterior restoration in the thoracolumbar area has practically not been able to establish itself, as the possibilities of reduction are significantly limited compared to posterior restoration and a large number of equipment is required, which makes care in emergency situations more difficult (56). The incidence of postthoracotomy syndrome in these cases is up to 31% (57). In summary, the initial ventral procedure is clearly not recommended for spinal cord injuries of the thoracic spine.

If SCI occurs at the thoracolumbar junction without persistent compression of the spinal cord, stabilization with reduction and fusion without accompanying decompression is primarily recommended (49). If there are concomitant disc injuries or even a rupture/split fracture with a high tendency to pseudarthrosis formation, additive anterior treatment is indicated (58). A corporectomy or partial corporectomy with vertebral body replacement and accompanying cancellous saplasty or expandable cages are often the therapy of choice. Surgical decompression of the myelon by reduction in the context of primary surgical care plays an important role in high thoracic spine, while spinal canal narrowing of up to 50% is not relevant in the area of the thoracolumbar junction. In the area of the lower lumbar spine (lumbar spine), traumatic spinal stenosis can remain without neurological consequences up to 80% of cases. However, fractures of the caudal lumbar spine do not lead to a spinal cord injury (59). Injuries of the thoracolumbar junction with intervertebral disc involvement or bursting fractures often require concomitant anterior care. Long-distance instrumentation in the spinal column achieves a high stability of the spinal cord injuries; there is no difference in functionality in the clinical outcomes of SCI patients compared to short-range care.

In summary, CSCI with disc protrusions requires an anterior approach with decompression and single-stage fusion using a cage. Coarse dislocations can often also be adequately positioned and stabilized by ventrally. In order to maintain functionality, short-distance fusions of the cervical spine should be taken into consideration. Early laminectomy, surgical reduction, and long-term stabilization should be performed for thoracic spinal cord injuries to avoid follow-up degeneration.

4.4 The impact of surgery-related factors on the post-operation complications of SCI

As for surgery-associated factors, a previous study indicated multi-level operation, increased number of surgical segments, prolonged operational duration, excessive intraoperative blood loss, and increased postoperative drainage time were independent predictors for postoperative wound infection (60). Multi-level operation for patients with CSCI may increase the operational duration, and prolonged operation can increase the risk of operational field pollution, and extend operation duration of the CSCI patients' bed rest (61). Furthermore, a previous also showed number of surgical segments and operational duration were independent predictors of postoperative pulmonary infection, which was consistent with our results (62). Multi-segmental cervical spinal operations may prolong the operational duration, and an extended operation duration may increase intraoperative blood loss, eventually increasing the risk of postoperative pulmonary complications.

For the treatment of CSCI, steroid pulse has been recommended for facilitating the neurological function recovery, suppressing inflammatory responses, and improving the clinical outcomes for CSCI patients. Nevertheless, it remained to be clarified whether this therapeutic option can achieve the ideal effects. Clinicians have identified that the occurrence of some perioperative complications, including electrolyte disturbances, gastrointestinal bleeding, hyperglycemia, hypertension, and pulmonary infection, significantly increases with the preoperative use of high-dose hormonal treatment. Preoperative use of steroid pulse might facilitate the motor functional recovery in CSCI patients, whereas no significant difference was identified in long-term clinical outcomes (63). Further, other studies showed steroid pulse not only failed to facilitate neurological functional recovery for CSCI patients, but was more likely to result in pulmonary infection (64, 65).

The preoperative laboratory examination (blood routine test, renal function, liver function, serum electrolytes, D-dimer, and fibrinogen), a fundamental and widely used examination, has been recommended as a critical adjunct for evaluation of CSCI patients.

The combination of laboratory examination parameters and clinical features can make the risk prediction model of SCI patients more reliable and accurate (66, 67). Integrating peripheral blood cells and inflammatory biomarkers may better reflect the complexity of an infection than one single factor, which can contribute to a more reliable prediction of a beginning but not yet clinically apparent pulmonary or wound infection (68). Key molecules and cells can help to identify post-operation complications before clinical or paraclinical signs prompt further diagnostic work-up leading to the diagnosis of the complications after surgical decompression.

4.5 Surgical decompression in animal models

Animal models have contributed to a better understanding of the pathophysiology in SCI and have been widely used in the preclinical testing of new therapeutic strategies. Previous study based on animal experiments showed spinal cord ischemia resulted from hemorrhage and swelling may reach peaks at 8 h post SCI (69). The ideal animal models should anatomically and physiologically resemble SCI in human, require minimal training, be inexpensive and can provide consistent results. Rat models are the most frequently utilized for the research of SCI and are well established and inexpensive, and the injury responses are similar to that identified in human SCI, such as the generation of cystic cavities, formation of glial scar and alterations in the extracellular matrix (ECM) (2). Nevertheless, differences exist in anatomy, size, signaling pathways, and the recovery ability after SCI, which have made the direct translation extremely challenging (70). Unfortunately, various treatments in SCI have been unsatisfactory when translated to homo sapiens from small animal models, because of the inherent biological differences. However, larger animal models, like non-human primates, may overcome these barriers partially, whereas substantial differences in costs and strict housing requirements have made their use less frequent (71). Nevertheless, large animal models may establish critical intermediary models to validate results from rodents through producing data of high safety, biodistribution, and feasibility (72). Evaluating novel surgical strategies in various species is a significant way to bolster pre-clinical evidence before performing clinical trials.

Various pre-clinical studies utilizing different SCI animal models showed the benefits of early spinal cord decompression. A previous study showed that monkeys with 1-min spinal cord compression exhibited better electrophysiological recovery and decreased adverse effects on spinal cord blood flow, compared to animals that underwent spinal cord compression for more than 3 min (73). Further, Rabinowitz et al. (74) performed a prospective and randomized study in dogs comparing early surgical decompression (6 h) with or without methylprednisolone as compared with methylprednisolone alone. It showed that surgical decompression with or without methylprednisolone administration offered better neurological improvement than the use of methylprednisolone alone.

4.6 Molecular and cellular mechanisms of surgical decompression in SCI

The molecular and cellular mechanisms of neural regeneration after surgical decompression in SCI remain fragmentary. Dhillon et al. (75) showed that axonal plasticity was identified during the recovery process of injured spinal cord after decompressive surgery in a rat model of cervical spondylotic myelopathy (CSM). Further, decompressive surgery can attenuate expression of amyloid precursor protein (APP) and increase expression of growth associated protein 43 (GAP43) (75). The accumulation of APP in nerves indicates that there is a certain degree of cytoskeletal breakdown in injured spinal cord (75). GAP43 plays an important role in the axonal regeneration and budding, which is a known biomarker of axonal regeneration in neuronal cells (76). A previous study reported that surgical decompression may decrease the expression of Cacna2d2 (α2δ2) in the injured spinal cord of CSM rat models, and α2δ2 may modulate the expression of GAP43 in the axonal repair of injured spinal cord after surgical decompression (77).

A recent study assessed 5-hydroxytryptamine (5HT) immunohistochemistry after surgical decompression of SCI, which showed a significant increase of serotonergic fibers, below, above, and within the lesion of injured spinal cord (75). This increase might be regulated by localized sprouting responses of serotonergic fibers. The increase of serotonergic fibers is caused by regeneration of axon, which can be reflected by the concomitant presence of GAP43 detected below, above, and within the lesion of previous compression (78, 79). Additionally, after surgical decompression, re-expression of synaptophysin was identified. Expression of synaptophysin may represent the functional synapses (80, 81). These findings demonstrated that surgical decompression may trigger regenerative responses in axons that can help to establish new functional connections after SCI, which required further investigation.

A recent study identified marked microglial responses to surgical compression in SCI rat models which extended to the adjacent tissues below and above the lesion site (75). After surgical decompression, activation of microglia was significantly reduced, which can reduce the inflammatory responses in SCI. Microglia are the resident immune cells and core sensors of danger signals in the spinal cord. After stimulation, resident M2 type (anti-inflammatory) microglia may polarize to the M1 type (pro-inflammatory) (82), which can secrete pro-inflammatory factors (83). Inflammasomes activation in microglia may induce metabolic shift from oxidative phosphorylation to glycolysis, which can contribute to the polarization of microglia to M1 type, eventually leading to neuroinflammation and neurodegeneration (84). Further, a previous study showed that astrocytes were unable to recover after surgical decompression (75). It is suggested that the decreased activity of astrocytes might have attenuated demyelination and promoted axonal sprouting, as identified after experimental regulation of astrocytes in experimental SCI models (85). Unfortunately, there are very few studies evaluating the alterations of microglia and astrocytes in human SCI and SCI animal models (86).

4.7 Applications of artificial intelligence-based technologies combined with surgical decompression in SCI

Recently, various breakthroughs have been made for the applications of artificial intelligence (AI) in SCI and rehabilitation,

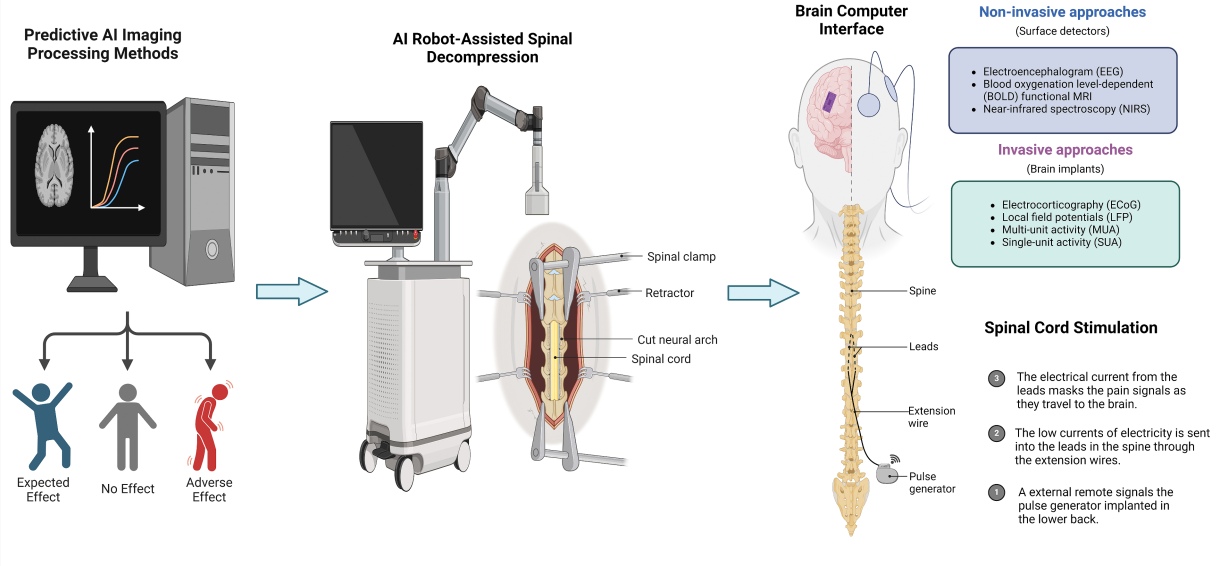

FIGURE 10
Diagram of hotspots of artificial intelligence (AI) research in spinal cord injury and surgical decompression. AI technology has made breakthroughs in spinal cord neural injury and restoration in recent years. We pinpointed several research hotspots for AI research in spinal cord neural injury and surgical decompression: (1) predictive AI imaging processing methods; (2) AI robot-assisted spinal decompression; (3) AI-based brain computer interface; (4) and AI-assisted spinal cord stimulation, positively promoting functional recovery.

such as predictive AI imaging processing methods, AI robot-assisted spinal decompression, AI-based brain computer interface, and AI-assisted spinal cord stimulation, positively promoting functional recovery (Figure 10). AI has been widely applied in neural imaging for patients with SCI. Convolutional neural network (CNN)-based image segmentation models could make tremendous contributions to imaging parameters, accurate diagnosis, and risk stratification of SCI patients (87). AI can be used to track and investigate all neural components of injured spinal cord in real-time, such as neural structure and neuroplasticity (88). Intelligent robots and limb exoskeletons for assisted surgery and rehabilitation emerged as an important research hotspot in the field of SCI and surgical decompression (89). Fang et al. emphasized that robot-assisted gait training (RAGT) can improve the spasticity syndromes and walking capability in patients with SCI, which can normalize muscle tone and improve lower extremity function in patients with SCI without resulting in extra pain (90). AI-based rehabilitation robots are interactive motorized devices which can realize precise measurements and fine limb movements (91). In the future, more efforts can be devoted to developing novel AI models, including supervised learning and feed-forward topological neural networks (92, 93), to enhance the tolerance, safety, and walking functional efficacy of robotic exoskeletons to promote the functional recovery of SCI patients. Furthermore, applications of AI have also been used to repair SCI based on nano-biomaterial technology (94). Sten cell transplantation in the lesions of SCI is a promising therapeutic strategy. However, it remained challenges due to the inflammatory microenvironment within the lesions (95). Using AI for fabricating polymeric nanomaterials could provide the microenvironment needed for the repair and regrowth of neural stem cells (NSCs) to promote remodeling and repair of neural cells (96). Specifically, Li et al. (94) synthesized a 3D-bioactive scaffold and showed that neural networks derived from NSCs modified by pro-myosin receptor kinase C exhibited excellent viability in the scaffold. Moreover, Yuan et al. (97) synthesized DNA hydrogel with high permeability properties using AI to repair a 2-mm spinal cord gap in SCI rat models and implanted the proliferation and differentiation of endogenous stem cells for establishing a nascent neural network. They showed that neural network organization established through transplantation in 3D-bioactive scaffolds was a candidate therapeutic strategy for SCI. Nevertheless, this AI-based nanotechnology has not yet been investigated on a broader scale, and researchers can focus on this research topic in the near future.

Brain-computer interfaces with deep learning algorithms are also one of the latest hotspots in this research field. Brain-computer interface devices are be used to restore lost function and construct electronic "neural bypasses" for circumventing damaged pathways in the injured spinal cord (98, 99). AI techniques applied to brain-computer interfaces can enable disabled patients to control machines as well as other devices. Using implanted intracortical brain-computer interfaces, the patient's cortical signals could be utilized to direct limb movements (100). For instance, Collinger et al. (101) implanted two 96-channel intracortical microelectrodes in a patient's motor cortex and assessed that quadriplegic patients could use the brain-computer interface to realize neural control of high-performance prostheses quickly. Additionally, Ajiboye et al. (101) restored limb movement of paralyzed patients via implanting intracortical brain-computer interfaces and functional electrical stimulation components. They suggested that neuro-electrical stimulation and intracortical brain-computer interface techniques can be integrated to improve the

motor and neurophysiologic status of patients with SCI more effectively. In the future, machine learning algorithms can be used to regulate the activation of nerves and muscles in patients with SCI based on high-resolution and customized electrical stimulation devices. Future neuro-electrical stimulation research could combine AI and deep learning methods like CNNs, and utilize multiple strategies to modulate the neurological and physiological status and promote motor functional recovery in patients with SCI after surgery. Importantly, developing more targeted neuro-electrical and spinal cord stimulation techniques through a wide range of spatially selective stimulation strategies may be critical future research directions.

It is important to emphasize that the data retrieval process in our work may result in sampling bias to some extent. Firstly, the exclusive reliance on literature in English may cause neglect of valuable perspectives from non-English documents. Secondly, the informative feature of bibliometric analysis may potentially overlook unique and niche aspects of the research field. Therefore, when extrapolating our findings to the wider population, caution should be exercised.

5 Conclusion

This study provided a comprehensive outlook of the research on SCI and surgical decompression spanning the last 5 decades. The publication number has significantly increased since 2005, and there is a potential of further growth in scientific output in the near future. Increasing multidisciplinary collaborations and thematic evolutions were identified in this field, revealing the significant role of surgical decompression in SCI therapeutic outcomes. The USA, China, and Japan were the most productive countries in this field, while collaboration among countries in this field should be further promoted. *Spine*, *Spinal Cord*, and *Journal of Neurosurgery* were the most impactive journals. Michael G. Fehlings and Alexander R Vaccaro were the most productive authors. The University of Toronto was the leading affiliation with the highest publication number. While the recommendations for early surgical decompression in specific cases of acute SCI are well recognized, there is considerable uncertainty regarding the role of and the timing of surgical decompression of the spinal cord in the management of SCI patients. Most of the studies defined early surgical decompression as decompression in 24 h post SCI, which was related to better functional recovery in patients with acute SCI. Early surgical decompression exhibited better neurological outcomes in subpopulations according to the injury degree and whether or not preoperative steroid pulse were utilized. Beneficial effects on surgical decompression in 8 h post SCI has been discussed recently, whereas further studies are still urgently needed. Surgical decompression can inhibit microglia activation and trigger regenerative responses in axons that can help to establish new functional connections after SCI, while the underlying molecular and cellular mechanisms, as well as potential signaling pathways required further investigation. AI systems and research on spinal surgical decompression and rehabilitation can mutually reinforce each other and drive medical innovation in the near future.

Data availability statement

The original contributions presented in the study are included in the article/Supplementary material, further inquiries can be directed to the corresponding authors.

Author contributions

SW: Conceptualization, Data curation, Formal analysis, Funding acquisition, Investigation, Methodology, Project administration, Resources, Software, Supervision, Validation, Visualization, Writing – original draft, Writing – review & editing. WX: Conceptualization, Data curation, Investigation, Methodology, Software, Supervision, Writing – original draft. JW: Conceptualization, Data curation, Formal analysis, Investigation, Resources, Supervision, Writing – original draft. XH: Writing – review & editing, Conceptualization, Data curation, Formal analysis, Investigation, Methodology, Software, Supervision. ZW: Writing – review & editing, Conceptualization, Data curation, Formal analysis, Investigation, Methodology, Resources, Software, Supervision, Validation, Visualization. CL: Data curation, Investigation, Methodology, Resources, Software, Supervision, Validation, Writing – review & editing. ZX: Conceptualization, Data curation, Formal analysis, Investigation, Methodology, Software, Supervision, Validation, Writing – review & editing. BM: Data curation, Formal analysis, Investigation, Methodology, Software, Supervision, Writing – review & editing, Conceptualization. LC: Conceptualization, Data curation, Formal analysis, Funding acquisition, Investigation, Methodology, Project administration, Resources, Software, Supervision, Validation, Visualization, Writing – original draft, Writing – review & editing.

Funding

The author(s) declare financial support was received for the research, authorship, and/or publication of this article. This work was funded by National Key Research and Development Program of China (2016YFA0100800), International (Regional) Cooperation and Communication Program of the National Natural Science Foundation of China (81820108013), National Natural Science Foundation of China (NSFC) (81330030), and the Scientific research project of Shanghai Municipal Health Committee (202040075). The funders had no role in study design, data collection and analysis, decision to publish, or preparation of the manuscript.

Acknowledgments

The authors thank the Web of Science™ (WOS) team for using their data.

Conflict of interest

The authors declare that the research was conducted in the absence of any commercial or financial relationships that could be construed as a potential conflict of interest.

Publisher's note

Supplementary material

The Supplementary material for this article can be found online at: https://www.frontiersin.org/articles/10.3389/fneur.2024.1442145/full#supplementary-material

SUPPLEMENTARY FIGURE S1
The Data retrieval strategies and collection process of this study.

SUPPLEMENTARY FIGURE S2
Analysis of core sources in the field of spinal cord injury (SCI) and surgical decompression. **(A)** The top 10 most productive journal in SCI and surgical decompression researches. **(B)** Core journals of SCI and surgical decompression researches based on Bradford's Law.

SUPPLEMENTARY FIGURE S3
Supplementary materials for author analysis in the field of spinal cord injury (SCI) and surgical decompression. **(A)** The frequency distribution of scientific productivity in SCI and surgical decompression researches by Lotka's law. **(B)** Top 10 most local cited authors in SCI and surgical decompression researches. **(C)** Top 10 local impactive authors measured by H-index in SCI and surgical decompression researches.

SUPPLEMENTARY FIGURE S4
Supplementary materials for keyword analysis in the field of spinal cord injury (SCI) and surgical decompression. **(A)** Word Cloud of the top 50 frequent keywords in SCI and surgical decompression researches. **(B)** Tree Map of the top 50 frequent keywords in SCI and surgical decompression researches.

References

1. Quadri SA, Farooqui M, Ikram A, Zafar A, Khan MA, Suriya SS, et al. Recent update on basic mechanisms of spinal cord injury. *Neurosurg Rev*. (2020) 43:425–41. doi: 10.1007/s10143-018-1008-3

2. Ahuja CS, Wilson JR, Nori S, Kotter MRN, Druschel C, Curt A, et al. Traumatic spinal cord injury. *Nat Rev Dis Prim*. (2017b) 3:18. doi: 10.1038/nrdp.2017.18

3. Ahuja CS, Nori S, Tetreault L, Wilson J, Kwon B, Harrop J, et al. Traumatic spinal cord injury-repair and regeneration. *Neurosurgery*. (2017a) 80:S9–S22. doi: 10.1093/neuros/nyw080

4. Qiu YY, Chen YP, Xie Y, Xie HZ, Dong JG. Comparative analysis of the efficacy of early and late surgical intervention for acute spinal cord injury: a systematic review and meta-analysis based on 16 studies. *Int J Surg*. (2021) 94:106098. doi: 10.1016/j.ijsu.2021.106098

5. Rauen K, Reichelt L, Probst P, Schäpers B, Müller F, Jahn K, et al. Decompressive Craniectomy is associated with good quality of life up to 10 years after rehabilitation from traumatic brain injury. *Crit Care Med*. (2020) 48:1157–64. doi: 10.1097/ccm.0000000000004387

6. Li K, Rollins J, Yan E. Web of science use in published research and review papers 1997-2017: a selective, dynamic, cross-domain, content-based analysis. *Scientometrics*. (2018) 115:1–20. doi: 10.1007/s11192-017-2622-5

7. Huang R, Tang J, Wang S, Liu Y, Zhang M, Jin M, et al. Sequencing technology as a major impetus in the advancement of studies into rheumatism: a bibliometric study. *Front Immunol*. (2023b) 14:1067830. doi: 10.3389/fimmu.2023.1067830

8. Huang R, Jin M, Liu Y, Lu Y, Zhang M, Yan P, et al. Global trends in research of fibroblasts associated with rheumatoid diseases in the 21st century: a bibliometric analysis. *Front Immunol*. (2023a) 14:1098977. doi: 10.3389/fimmu.2023.1098977

9. Zhu Y, Lu J, Wang S, Xu D, Wu M, Xian S, et al. Mapping intellectual structure and research hotspots in the field of fibroblast-associated DFUs: a bibliometric analysis. *Front Endocrinol*. (2023) 14:1109456. doi: 10.3389/fendo.2023.1109456

10. Liberati A, Altman DG, Tetzlaff J, Mulrow C, Gotzsche PC, Ioannidis JPA, et al. The PRISMA statement for reporting systematic reviews and Meta-analyses of studies that evaluate health care interventions: explanation and elaboration. *PLoS Med*. (2009) 6:e1000100. doi: 10.1371/journal.pmed.1000100

11. Aria M, Cuccurullo C. Bibliometrix: An R-tool for comprehensive science mapping analysis. *J Informet*. (2017) 11:959–75. doi: 10.1016/j.joi.2017.08.007

12. Pao ML. Lotka Law—a Testing Procedure. *Inf Process Manag*. (1985) 21:305–20. doi: 10.1016/0306-4573(85)90055-x

13. Brookes BC. Bradford's law and the bibliography of science. *Nature*. (1969) 224:953–6. doi: 10.1038/224953a0

14. Hirsch JE. An index to quantify an individual's scientific research output. *Proc Natl Acad Sci USA*. (2005) 102:16569–72. doi: 10.1073/pnas.0507655102

15. Barik N, Jena P. Author productivity pattern and applicability of Lotka's inverse square law: a bibliometric appraisal of selected LIS open access journals. *Digit Libr Perspect*. (2021) 37:223–41. doi: 10.1108/dlp-10-2020-0103

16. Venable GT, Shepherd BA, Roberts ML, Taylor DR, Khan NR, Klimo P. An application of Bradford's law: identification of the core journals of pediatric neurosurgery and a regional comparison of citation density. *Childs Nerv Syst*. (2014) 30:1717–27. doi: 10.1007/s00381-014-2481-9

17. Alonso S, Cabrerizo FJ, Herrera-Viedma E, Herrera F. H-index: a review focused in its variants, computation and standardization for different scientific fields. *J Informet*. (2009) 3:273–89. doi: 10.1016/j.joi.2009.04.001

18. Geerts WH, Bergqvist D, Pineo GF, Heit JA, Samama CM, Lassen MR, et al. Prevention of venous thromboembolism. *Chest*. (2008) 133:381S–453S. doi: 10.1378/chest.08-0656

19. Fehlings MG, Vaccaro A, Wilson JR, Singh A, Cadotte DW, Harrop JS, et al. Early versus delayed decompression for traumatic cervical spinal cord injury: results of the surgical timing in acute spinal cord injury study (STASCIS). *PLoS One*. (2012) 7:e32037. doi: 10.1371/journal.pone.0032037

20. Basso DM, Beattie MS, Bresnahan JC. A sensitive and reliable locomotor rating-scale for open-field testing in rats. *J Neurotrauma*. (1995) 12:1–21. doi: 10.1089/neu.1995.12.1

21. Furlan JC, Noonan V, Cadotte DW, Fehlings MG. Timing of Decompressive surgery of spinal cord after traumatic spinal cord injury: An evidence-based examination of pre-clinical and clinical studies. *J Neurotrauma*. (2011) 28:1371–99. doi: 10.1089/neu.2009.1147

22. Badhiwala JH, Ahuja CS, Fehlings MG. Time is spine: a review of translational advances in spinal cord injury. *J Neurosurg Spine*. (2019) 30:1–18. doi: 10.3171/2018.9.Spine18682

23. Batchelor PE, Wills TE, Skeers P, Battistuzzo CR, Macleod MR, Howells DW, et al. Meta-analysis of pre-clinical studies of early decompression in acute spinal cord injury: a Battle of time and pressure. *PLoS One*. (2013) 8:e72659. doi: 10.1371/journal.pone.0072659

24. Fehlings MG, Perrin RG. The role and timing of early decompression for cervical spinal cord injury: update with a review of recent clinical evidence. *Injury Int J Care Injured*. (2005) 36:S13–26. doi: 10.1016/j.injury.2005.06.011

25. Fehlings MG, Tetreault LA, Wilson JR, Kwon BK, Burns AS, Martin AR, et al. A clinical practice guideline for the Management of Acute Spinal Cord Injury: introduction, rationale, and scope. *Global Spine J*. (2017) 7:84S–94S. doi: 10.1177/2192568217703387

26. Sakaura H, Hosono N, Mukai Y, Ishii T, Yoshikawa H. C5 palsy after decompression surgery for cervical myelopathy—review of the literature. *Spine*. (2003) 28:2447–51. doi: 10.1097/01.Brs.0000090833.96168.3f

27. Sekhon LHS, Fehlings MG. Epidemiology, demographics, and pathophysiology of acute spinal cord injury. *Spine*. (2001) 26:S2–S12. doi: 10.1097/00007632-200112151-00002

28. Vaccaro AR, Daugherty RJ, Sheehan TP, Dante SJ, Cotler JM, Balderstrom RA, et al. Neurologic outcome of early versus late surgery for cervical spinal cord injury. *Spine*. (1997) 22:2609–13. doi: 10.1097/00007632-199711150-00006

29. Vale FL, Burns J, Jackson AB, Hadley MN. Combined medical and surgical treatment after acute spinal cord injury: results of a prospective pilot study to assess the merits of aggressive medical resuscitation and blood pressure management. *J Neurosurg*. (1997) 87:239–46. doi: 10.3171/jns.1997.87.2.0239

30. Fehlings MG, Sekhon LHS, Tator C. The role and timing of decompression in acute spinal cord injury—what do we know? What should we do? *Spine*. (2001) 26:S101–10. doi: 10.1097/00007632-200112151-00017

31. Baroudi M, Rezk A, Daher M, Balmaceno-Criss M, Gregoryczyk JG, Sharma Y, et al. Management of traumatic spinal cord injury: a current concepts review of contemporary and future treatment. *Injury Int J Care Injured*. (2024) 55:111472. doi: 10.1016/j.injury.2024.111472

32. McKinley W, Meade MA, Kirshblum S, Barnard B. Outcomes of early surgical management versus late or no surgical intervention after acute spinal cord injury. *Arch Phys Med Rehabil*. (2004) 85:1818–25. doi: 10.1016/j.apmr.2004.04.032

33. Fehlings MG, Hachem LD, Tetreault LA, Skelly AC, Dettori JR, Brodt ED, et al. Timing of Decompressive surgery in patients with acute spinal cord injury: systematic review update. *Global. Spine J.* (2024) 14:38S–57S. doi: 10.1177/21925682231197404

34. Shi TB, Yu ZX, Chen Z, Wu DW, Wang ZY, Liu WE. The impact of time from injury to surgery on the risk of neuropathic pain after traumatic spinal cord injury. *J Orthop Surg Res.* (2023) 18:857. doi: 10.1186/s13018-023-04355-7

35. Wilson JR, Tetreault LA, Kwon BK, Arnold PM, Mroz TE, Shaffrey C, et al. Timing of decompression in patients with acute spinal cord injury: a systematic review. *Global Spine J.* (2017) 7:95S–115S. doi: 10.1177/2192568217701716

36. Lau D, Ore CLD, Tarapore PE, Huang M, Manley G, Singh V, et al. Value of aggressive surgical and intensive care unit in elderly patients with traumatic spinal cord injury. *Neurosurg Focus.* (2019) 46:E3. doi: 10.3171/2018.12.Focus18555

37. Dvorak MF, Noonan VK, Fallah N, Fisher CG, Finkelstein J, Kwon BK, et al. The influence of time from injury to surgery on motor recovery and length of hospital stay in acute traumatic spinal cord injury: An observational Canadian cohort study. *J Neurotrauma.* (2015) 32:645–54. doi: 10.1089/neu.2014.3632

38. Sterner RC, Brooks NP. Early decompression and short transport time after traumatic spinal cord injury are associated with higher American spinal injury association impairment scale conversion. *Spine.* (2022) 47:59–66. doi: 10.1097/brs.0000000000004121

39. Asif H, Tsan SEH, Zoumprouli A, Papadopoulos MC, Saadoun S. Evolving trends in the surgical, anaesthetic, and intensive care management of acute spinal cord injuries in the UK. *Eur Spine J.* (2024) 33:1213–22. doi: 10.1007/s00586-023-08085-6

40. Grossman RG, Frankowski RF, Burau KD, Toups EG, Crommett JW, Johnson MM, et al. Incidence and severity of acute complications after spinal cord injury. *J Neurosurg Spine.* (2012) 17:119–28. doi: 10.3171/2012.5.Aospine12127

41. Cengiz SL, Kalkan E, Bayir A, Ilik K, Basefer A. Timing of thoracolomber spine stabilization in trauma patients; impact on neurological outcome and clinical course. A real prospective (rct) randomized controlled study. *Arch Orthop Trauma Surg.* (2008) 128:959–66. doi: 10.1007/s00402-007-0518-1

42. Jug M, Kejzar N, Vesel M, Al Mawed S, Dobravec M, Herman S, et al. Neurological recovery after traumatic cervical spinal cord injury is superior if surgical decompression and instrumented fusion are performed within 8 hours versus 8 to 24 hours after injury: a single center experience. *J Neurotrauma.* (2015) 32:1385–92. doi: 10.1089/neu.2014.3767

43. Lee D-Y, Park Y-J, Song S-Y, Hwang S-C, Kim K-T, Kim D-H. The importance of early surgical decompression for acute traumatic spinal cord injury. *Clin Orthop Surg.* (2018) 10:448–54. doi: 10.4055/cios.2018.10.4.448

44. Wutte C, Becker J, Klein B, Mach O, Panzer S, Stuby FM, et al. Early decompression (<8 hours) improves functional bladder outcome and mobility after traumatic thoracic spinal cord injury. *World Neurosurg.* (2020) 134:E847–54. doi: 10.1016/j.wneu.2019.11.015

45. Wutte C, Klein B, Becker J, Mach O, Panzer S, Strowitzki M, et al. Earlier decompression (< 8 hours) results in better neurological and functional outcome after traumatic thoracolumbar spinal cord injury. *J Neurotrauma.* (2019) 36:2020–7. doi: 10.1089/neu.2018.6146

46. Tanaka C, Tagami T, Kaneko J, Fukuda R, Nakayama F, Sato S, et al. Early versus late surgery after cervical spinal cord injury: a Japanese nationwide trauma database study. *J Orthop Surg Res.* (2019) 14:302. doi: 10.1186/s13018-019-1341-4

47. Wilson JR, Fehlings MG. Emerging approaches to the surgical Management of Acute Traumatic Spinal Cord Injury. *Neurotherapeutics.* (2011) 8:187–94. doi: 10.1007/s13311-011-0027-3

48. Dhillon CS, Jakkan MS, Dwivedi R, Medagam NR, Jindal P, Ega S. Outcomes of unstable subaxial cervical spine fractures managed by Posteroanterior stabilization and fusion. *Asian Spine J.* (2018) 12:416–22. doi: 10.4184/asj.2018.12.3.416

49. Dalbayrak S, Yaman O, Yilmaz T. Current and future surgery strategies for spinal cord injuries. *World J Orthop.* (2015) 6:34–41. doi: 10.5312/wjo.v6.i1.34

50. Brodke DS, Anderson PA, Newell DW, Grady MS, Chapman JR. Comparison of anterior and posterior approaches in cervical spinal cord injuries. *J Spinal Disord Tech.* (2003) 16:229–35. doi: 10.1097/00024720-200306000-00001

51. Bohlman HH, Eismont FJ. Surgical techniques of anterior decompression and fusion for spinal-cord injuries. *Clin Orthop Relat Res.* (1981) 154:57–67. doi: 10.1097/00003086-198101000-00011

52. Lazaro BCR, Deniz FE, Brasiliense LBC, Reyes PM, Sawa AGU, Theodore N, et al. Biomechanics of thoracic short versus long fixation after 3-column injury laboratory investigation. *J Neurosurg Spine.* (2011) 14:226–34. doi: 10.3171/2010.10.Spine09785

53. Waqar M, Van-Popta D, Barone DG, Bhojak M, Pillay R, Sarsam Z. Short versus long-segment posterior fixation in the treatment of thoracolumbar junction fractures: a comparison of outcomes. *Br J Neurosurg.* (2017) 31:54–7. doi: 10.1080/02688697.2016.1206185

54. Altay M, Ozkurt B, Aktekin CN, Ozturk AM, Dogan Ö, Tabak AY. Treatment of unstable thoracolumbar junction burst fractures with short- or long-segment posterior fixation in magerl type a fractures. *Eur Spine J.* (2007) 16:1145–55. doi: 10.1007/s00586-007-0310-5

55. Guven O, Kocaoglu B, Bezer M, Aydin N, Nalbantoglu U. The use of screw at the fracture level in the treatment of thoracolumbar burst fractures. *J Spinal Disord Tech.* (2009) 22:417–21. doi: 10.1097/BSD.0b013e3181870385

56. Spiegl UJA, Schnake KJ, Hartmann F, Katscher S, Riehle M, Scheyerer MJ, et al. Traumatic fractures of the thoracic spine: narrative literature review. *Zeitschrift Fur Orthopadie Und Unfallchirurgie.* (2021) 159:373–82. doi: 10.1055/a-1144-3846

57. Zhang SH, Thakur JD, Khan IS, Menger R, Kukreja S, Ahmed O, et al. Anterior stabilization for unstable traumatic thoracolumbar spine burst fractures. *Clin Neurol Neurosurg.* (2015) 130:86–90. doi: 10.1016/j.clineuro.2014.10.020

58. Spiegl UJ, Josten C, Devitt BM, Heyde CE. Incomplete burst fractures of the thoracolumbar spine: a review of literature. *Eur Spine J.* (2017) 26:3187–98. doi: 10.1007/s00586-017-5126-3

59. Blanco JF, De Pedro JA, Hernández PJ, Paniagua DC, Framiñán A. Conservative management of burst fractures of the fifth lumbar vertebra. *J Spinal Disord Tech.* (2005) 18:229–31.

60. Famous KR, Delucchi K, Ware LB, Kangelaris KN, Liu KD, Thompson BT, et al. Acute respiratory distress syndrome subphenotypes respond differently to randomized fluid management strategy. *Am J Respir Crit Care Med.* (2017) 195:331–8. doi: 10.1164/rccm.201603-0645OC

61. Balachandran VP, Gonen M, Smith JJ, DeMatteo RP. Nomograms in oncology: more than meets the eye. *Lancet Oncol.* (2015) 16:E173–80. doi: 10.1016/s1470-2045(14)71116-7

62. Luo K, Huang YQ, Zhu LB, Gan XR, Zhang Y, Xiao SN, et al. Risk factors and nomogram for postoperative pulmonary infection in patients with cervical spinal cord injury. *World Neurosurg.* (2023) 177:E317–24. doi: 10.1016/j.wneu.2023.06.040

63. Evaniew N, Belley-Côté E, Fallah N, Noonan VK, Rivers CS, Dvorak MF. Methylprednisolone for the treatment of patients with acute spinal cord injuries: a systematic review and Meta-analysis. *J Neurotrauma.* (2016) 33:468–81. doi: 10.1089/neu.2015.4192

64. Liu ZY, Yang Y, He L, Pang M, Luo CX, Liu B, et al. High-dose methylprednisolone for acute traumatic spinal cord injury a meta-analysis. *Neurology.* (2019) 93:E841–50. doi: 10.1212/wnl.0000000000007998

65. Sultan I, Lamba N, Liew A, Doung P, Tewarie I, Amamoo JJ, et al. The safety and efficacy of steroid treatment for acute spinal cord injury: a systematic review and meta-analysis. *Heliyon.* (2020) 6:e03414. doi: 10.1016/j.heliyon.2020.e03414

66. Li BC, Su R, Yan HH, Liu JJ, Gao C, Li XF, et al. Immunological risk factors for nonalcoholic fatty liver disease in patients with psoriatic arthritis: new predictive nomograms and natural killer cells. *Front Immunol.* (2022) 13:7729. doi: 10.3389/fimmu.2022.907729

67. Tang NA, Chen H, Chen RD, Tang W, Zhang HJ. Combination of serological biomarkers and clinical features to predict mucosal healing in Crohn's disease: a multicenter cohort study. *BMC Gastroenterol.* (2022) 22:229. doi: 10.1186/s12876-022-02304-y

68. Fluri F, Morgenthaler NG, Mueller B, Christ-Crain M, Katan M. Copeptin, Procalcitonin and routine inflammatory markers-predictors of infection after stroke. *PLoS One.* (2012) 7:e48309. doi: 10.1371/journal.pone.0048309

69. Donnelly DJ, Popovich PG. Inflammation and its role in neuroprotection, axonal regeneration and functional recovery after spinal cord injury. *Exp Neurol.* (2008) 209:378–88. doi: 10.1016/j.expneurol.2007.06.009

70. Tator CH. Review of treatment trials in human spinal cord injury: issues, difficulties, and recommendations. *Neurosurgery.* (2006) 59:957–87. doi: 10.1227/01.Neu.0000245591.16087.89

71. Zhang N, Fang MR, Chen HH, Gou FM, Ding MX. Evaluation of spinal cord injury animal models. *Neural Regen Res.* (2014) 9:2008–12. doi: 10.4103/1673-5374.143436

72. Nout YS, Rosenzweig ES, Brock JH, Strand SC, Moseanko R, Hawbecker S, et al. Animal models of neurologic disorders: a nonhuman primate model of spinal cord injury. *Neurotherapeutics.* (2012) 9:380–92. doi: 10.1007/s13311-012-0114-0

73. Kobrine AI, Evans DE, Rizzoli HV. Experimental acute balloon compression of the spinal-cord—factors affecting disappearance and return of the spinal evoked-response. *J Neurosurg.* (1979) 51:841–5. doi: 10.3171/jns.1979.51.6.0841

74. Rabinowitz RS, Eck JC, Harper CM, Larson DR, Jimenez MA, Parisi JE, et al. Urgent surgical decompression compared to methylprednisolone for the treatment of acute spinal cord injury. *Spine.* (2008) 33:2260–8. doi: 10.1097/BRS.0b013e31818786db

75. Dhillon RS, Parker J, Syed YA, Edgley S, Young A, Fawcett JW, et al. Axonal plasticity underpins the functional recovery following surgical decompression in a rat model of cervical spondylotic myelopathy. *Acta Neuropathol Commun.* (2016) 4:89. doi: 10.1186/s40478-016-0359-7

76. Liu H, Xiong DQ, Pang RZ, Deng Q, Sun NY, Zheng JQ, et al. Effects of repetitive magnetic stimulation on motor function and GAP43 and 5-HT expression in rats with spinal cord injury. *J Int Med Res.* (2020) 48:030006052097076. doi: 10.1177/0300060520970765

77. Liu PS, Li XF, Liu J, Zhang HJ, You ZT, Zhang JF. Cacna2d2 inhibits axonal regeneration following surgical decompression in a rat model of cervical spondylotic myelopathy. *BMC Neurosci.* (2022) 23:42. doi: 10.1186/s12868-022-00727-7

78. Benowitz LI, Routtenberg A. GAP-43: An intrinsic determinant of neuronal development and plasticity. *Trends Neurosci*. (1997) 20:84–91. doi: 10.1016/s0166-2236(96)10072-2

79. Bradbury EJ, Moon LDF, Popat RJ, King VR, Bennett GS, Patel PN, et al. Chondroitinase ABC promotes functional recovery after spinal cord injury. *Nature*. (2002) 416:636–40. doi: 10.1038/416636a

80. Calhoun ME, Jucker M, Martin LJ, Thinakaran G, Price DL, Mouton PR. Comparative evaluation of synaptophysin-based methods for quantification of synapses. *J Neurocytol*. (1996) 25:821–8. doi: 10.1007/bf02284844

81. Gordon SL, Leube RE, Cousin MA. Synaptophysin is required for Synaptobrevin retrieval during synaptic vesicle endocytosis. *J Neurosci*. (2011) 31:14032–6. doi: 10.1523/jneurosci.3162-11.2011

82. Davalos D, Grutzendler J, Yang G, Kim JV, Zuo Y, Jung S, et al. ATP mediates rapid microglial response to local brain injury in vivo. *Nat Neurosci*. (2005) 8:752–8. doi: 10.1038/nn1472

83. Yang S, Magnutzki A, Alami NO, Lattke M, Hein TM, Scheller JS, et al. IKK2/NF-κB activation in astrocytes reduces amyloid β deposition: a process associated with specific microglia polarization. *Cells*. (2021) 10:2669. doi: 10.3390/cells10102669

84. Yu HY, Chang Q, Sun T, He X, An J, Wen LL, et al. Metabolic reprogramming and polarization of microglia in Parkinson's disease: role of inflammasome and iron. *Ageing Res Rev*. (2023) 90:102032. doi: 10.1016/j.arr.2023.102032

85. Li ZW, Li JJ, Wang L, Zhang JP, Wu JJ, Mao XQ, et al. Epidermal growth factor receptor inhibitor ameliorates excessive astrogliosis and improves the regeneration microenvironment and functional recovery in adult rats following spinal cord injury. *J Neuroinflammation*. (2014) 11:71. doi: 10.1186/1742-2094-11-71

86. Shimizu H, Kakita A, Takahashi H. Spinal cord tau pathology in cervical spondylotic myelopathy. *Acta Neuropathol*. (2008) 115:185–92. doi: 10.1007/s00401-007-0321-7

87. Nozawa K, Maki S, Furuya T, Okimatsu S, Inoue T, Yunde A, et al. Magnetic resonance image segmentation of the compressed spinal cord in patients with degenerative cervical myelopathy using convolutional neural networks. *Int J Comput Assist Radiol Surg*. (2023) 18:45–54. doi: 10.1007/s11548-022-02783-0

88. Srisuchinnawong A, Homchanthanakul J, Manoonpong P. NeuroVis: real-time neural information measurement and visualization of embodied neural systems. *Front Neural Circuits*. (2021) 15:101. doi: 10.3389/fncir.2021.743101

89. Tao GY, Yang S, Xu JJ, Wang LZ, Yang B. Global research trends and hotspots of artificial intelligence research in spinal cord neural injury and restoration-a bibliometrics and visualization analysis. *Front Neurol*. (2024) 15:1235. doi: 10.3389/fneur.2024.1361235

90. Fang CY, Tsai JL, Li GS, Lien ASY, Chang YJ. Effects of robot-assisted gait training in individuals with spinal cord injury: a Meta-analysis. *Biomed Res Int*. (2020) 2020:1–13. doi: 10.1155/2020/2102785

91. Wu JY, Liu YB, Zhao J, Zang XZ, Guan YZ. Research on theory and a performance analysis of an innovative rehabilitation robot. *Sensors*. (2022) 22:929. doi: 10.3390/s22103929

92. Gorre N, Carranza E, Fuhrman J, Li H, Madduri RK, Giger M, et al. MIDRC CRP10 AI interface-an integrated tool for exploring, testing and visualization of AI models. *Phys Med Biol*. (2023) 68:074002. doi: 10.1088/1361-6560/acb754

93. Jiang YM, Wang YN, Miao ZQ, Na J, Zhao ZJ, Yang CG. Composite-learning-based adaptive neural control for dual-arm robots with relative motion. *IEEE Trans Neural Netw Learn Syst*. (2022) 33:1010–21. doi: 10.1109/tnnls.2020.3037795

94. Li G, Zhang B, Sun JH, Shi LY, Huang MY, Huang LJ, et al. An NT-3-releasing bioscaffold supports the formation of TrkC−modified neural stem cell-derived neural network tissue with efficacy in repairing spinal cord injury. *Bioact Mater*. (2021) 6:3766–81. doi: 10.1016/j.bioactmat.2021.03.036

95. Liu DD, He JQ, Sinha R, Eastman AE, Toland AM, Morri M, et al. Purification and characterization of human neural stem and progenitor cells. *Cell*. (2023) 186:1179. doi: 10.1016/j.cell.2023.02.017

96. Shende P, Devlekar NP. A review on the role of artificial intelligence in stem cell therapy: An initiative for modern medicines. *Curr Pharm Biotechnol*. (2021) 22:1156–63. doi: 10.2174/1389201021666201007122524

97. Yuan TY, Shao Y, Zhou X, Liu Q, Zhu ZC, Zhou BN, et al. Highly permeable DNA supramolecular hydrogel promotes neurogenesis and functional recovery after completely transected spinal cord injury. *Adv Mater*. (2021) 33:e2102428. doi: 10.1002/adma.202102428

98. Cajigas I, Vedantam A. Brain-computer Interface, Neuromodulation, and Neurorehabilitation strategies for spinal cord injury. *Neurosurg Clin N Am*. (2021) 32:407–17. doi: 10.1016/j.nec.2021.03.012

99. Luo SY, Rabbani Q, Crone NE. Brain-computer Interface: applications to speech decoding and synthesis to augment communication. *Neurotherapeutics*. (2022) 19:263–73. doi: 10.1007/s13311-022-01190-2

100. Colucci A, Vermehren M, Cavallo A, Angerhoefer C, Peekhaus N, Zollo L, et al. Brain-computer Interface-controlled exoskeletons in clinical Neurorehabilitation: ready or not? *Neurorehabil Neural Repair*. (2022) 36:747–56. doi: 10.1177/15459683221138751

101. Wilson ML, Fleming KA, Kuti MA, Looi LM, Lago N, Ru K. Pathology and laboratory medicine in low-income and middle-income countries 1: access to pathology and laboratory medicine services: a crucial gap. *Lancet*. (2018) 391:1927–38. doi: 10.1016/s0140-6736(18)30458-6

frontiers | Frontiers in Neurology

TYPE Original Research
PUBLISHED 02 September 2024
DOI 10.3389/fneur.2024.1445479

OPEN ACCESS

EDITED BY
Jiaao Gu,
First Affiliated Hospital of Harbin Medical University, China

REVIEWED BY
Chao Han,
University of Science and Technology of China, China
Zhongwu Sun,
First Affiliated Hospital of Anhui Medical University, China
Haiming Luo,
Huazhong University of Science and Technology, China

*CORRESPONDENCE
Wanli Dong
✉ wanli_dong@126.com

†These authors have contributed equally to this work

RECEIVED 07 June 2024
ACCEPTED 21 August 2024
PUBLISHED 02 September 2024

CITATION
Yang W, Guan F, Yang L, Shou G, Zhu F, Xu Y, Meng Y, Li M and Dong W (2024) Highly sensitive blood-based biomarkers detection of beta-amyloid and phosphorylated-tau181 for Alzheimer's disease.
Front. Neurol. 15:1445479.
doi: 10.3389/fneur.2024.1445479

Highly sensitive blood-based biomarkers detection of beta-amyloid and phosphorylated-tau181 for Alzheimer's disease

Wei Yang[1,2†], Fulin Guan[3†], Lihui Yang[3], Guangli Shou[2], Fangfang Zhu[2], Yuanyuan Xu[2], Ying Meng[2], Min Li[2] and Wanli Dong[1*]

[1]Department of Neurology, First Affiliated Hospital of Soochow University, Suzhou, China,
[2]Department of Neurology, Second Affiliated Hospital of Bengbu Medical College, Bengbu, China,
[3]Department of Neurology, Suzhou Dushu Lake Hospital, Suzhou, China

Background: Plasma biomarker has the potential to be the reliable and propagable approach in the early stage diagnosis of Alzheimer's disease (AD). However, conventional methods appear powerless in the detection of these biomarkers at low concentrations in plasma. Here, we determined plasma biomarker concentrations of patients across the AD spectrum by an improved digital enzyme-linked immunosorbent assay (ELISA) technique. Confirms the predictive and diagnostic value of this method for AD patients and study the relationships between these biomarkers and cognitive status.

Methods: Plasma concentrations of amyloid-beta 40 (Aβ40), amyloid-beta 42 (Aβ42) and plasma phosphorylated tau at threonine 181 (p-tau181) were determined in 43 AD patients, 33 mild cognitive impairment (MCI) patients and 40 normal cognition (NC) subjects as healthy controls using the improved digital ELISA technique. In addition, all subjects were required to receive neuropsychological assessments.

Results: Plasma p-tau181 level showed certain discrepancies between NC and MCI ($p< 0.05$), AD ($p< 0.01$) groups. The level of plasma Aβ42 ($p< 0.05$) and Aβ40 ($p< 0.01$) was significantly different between AD and NC group. The p-tau181 level was able to distinguish AD (AUC=0.8768) and MCI (AUC=0.7932) from NC with higher accuracy than Aβ42/Aβ40 ratio (AUC=0.8343, AUC=0.6569). Both p-tau181 (CDR: r=0.388 p<0.001; MMSE: r=−0.394 p<0.001) and Aβ42/Aβ40 ratio (CDR: r=−0.413 p<0.001; MMSE: r=0.358 p<0.001) showed stronger positive correlation with clinical dementia rating (CDR) and mini mental state examination (MMSE) scores than Aβ42 (CDR: r=−0.280 p=0.003; MMSE: r=0.266 p=0.005) or Aβ40 (CDR: r=0.373 p<0.001; MMSE: r=−0.288 p=0.002) alone.

Conclusion: Plasma p-tau181 level and Aβ42/Aβ40 ratio showed promising values in diagnosis of AD and MCI. Our results indicate that this improved digital ELISA diagnosis approach can facilitate early recognition and management of AD and pre-AD patients.

KEYWORDS

blood biomarker, Alzheimer's disease, mild cognitive impairment, plasma p-tau181, Aβ40, Aβ42

Introduction

Alzheimer's disease (AD) is the most prevalent cause of dementia among the elderly. The 2021 World Alzheimer Report indicates that over 55 million individuals worldwide are currently suffering from dementia. However, it is estimated that 75% of these cases remain undiagnosed, with this figure potentially rising to 90% in developing countries (1). Recent estimates indicate that the number of individuals aged 60 years or older with AD dementia in China is over 9.83 million (2). The symptoms of AD become progressively worse over time, with brain damage occurring 20 years or more before clinical symptoms appear (3–10). Individuals with MCI do not yet meet the criteria for dementia, but have a greater possibility of developing into this condition (11, 12). MCI is thought to be closely related to the risk of incident dementia, whether due to AD or even earlier, such as subjective cognitive decline (SCD) (13, 14). Therefore, early diagnosis allows for early intervention and treatment trials.

Previous diagnoses of AD mainly rely on cognitive performance, neuropsychological assessment and biomarkers detected in the cerebrospinal fluid (CSF) or through amyloid positron emission tomography (PET) (15). However, the diagnostic latency, invasiveness, expense and dependence on associated infrastructure of those approaches limit their promotion in clinical practice. In contrast, blood biomarkers have a promising value in clinical practice due to their cost-effectiveness, non-invasiveness, and easy accessibility (16). The assessment of blood biomarkers facilitates the early identification of individuals at risk of developing AD, thus representing a pivotal step toward effectively tackling this urgent public health concern (17). In recent years, some ultra-sensitive measurement of low-abundance biomarkers have been gradually applied to the study of AD protein markers, with sensitivity improving by up to 1,000-fold over conventional ELISA (18–20), leading to the availability of detecting AD-relevant biomarkers in blood samples (21). Researchers have examined the core AD biomarkers based on the "A/T/N" framework in a Han Chinese cohort (22). Despite advancements in quantifying plasma biomarkers like amyloid beta (Aβ1-42 and Aβ1-40) and phosphorylated tau (pTau), technical challenges persist due to the varying costs and usage complexities of detection methods, which necessitate further refinement for extensive clinical adoption (23). Standardization is another critical issue; the absence of uniform procedures in blood sample management, from collection to analysis and reporting, could compromise the reliability of biomarker measurements and impede their application in clinical and research realms (24). The quest for accuracy and robustness in diagnosing Alzheimer's disease (AD) using blood biomarkers is fraught with challenges, particularly when dealing with diverse community populations. The interference of confounding factors, both systemic and biological, further complicates the accurate detection of these biomarkers, highlighting the need for more sophisticated analytical techniques to isolate their effects. Early diagnosis of AD is also a significant hurdle, as the subtle pathological changes in the initial stages of the disease are tough to discern without highly sensitive detection methods. Capturing the minute variations in blood biomarkers is equally challenging and demands technology that is not only sensitive but also precise (25). Moreover, the journey from research to clinical practice involves a meticulous implementation roadmap that encompasses various stages, including study design, sample handling, biomarker assessment, and reporting of findings. This transition is a gradual process that is still in progress. Lastly, while blood biomarkers offer the benefits of being less invasive and more cost-effective, it is imperative to weigh these advantages against the overall impact on patients and the healthcare system in practical scenarios (23). In summary, the detection of blood biomarkers still faces multiple challenges in achieving clinical application, and further research and technological development are needed to overcome these issues.

The immunoassay used here is an improved digital ELISA. The achievement of signal amplification through dividing of samples into hundreds of micro-reactors and further sealing the reactor which allow the subsequent enzyme-catalyzed reactions happens in the sealed environment, which enables the detection of low abundance protein in blood. It is characterized by accuracy, efficiency, cost-effectiveness, and ease of operation and holds promise in tackling the current challenges associated with biomarkers. Digital ELISA technology is widely used in clinical simultaneous detection of multiple cytokines (26). For instance, the concentrations of interleukin-4 (IL-4) and IL-6 in the peripheral blood of children with asthma were found to be significantly elevated in comparison to healthy controls, whereas the concentrations of interferon-γ (IFN-γ) were significantly decreased (27). The serum levels of IL-6, IL-8, IL-17 and other cytokines are altered in patients with breast cancer (28, 29). Patients with arthritis have abnormal serum cytokine concentrations, such as tumor necrosis factor-α (TNF-α), IL-1, and IL-17, compared with healthy individuals (30, 31).

Here, we applied the improved digital ELISA technique to detect the levels of Aβ40, Aβ42, p-tau181 at low concentrations in individuals with or without cognitive impairment, in according with the first aim of this study, which was to verify the feasibility of the improved digital ELISA technique for the detection of peripheral biomarkers in pre-AD and AD patients. Subsequently, the associations between peripheral biomarkers and different stages of cognitive function were analyzed, as well as the potential utility of plasma biomarkers to diagnose AD.

Methods

Study participants and neuropsychological tests

All participants underwent a comprehensive cognitive status and neuropsychological assessment, including the Mini Mental State Examination (MMSE), Clinical Dementia Rating (CDR), the Activity of Daily Living Scale (ADL), and the Hachinski Ischemic Scale. All patients were required to have an insider to provide an evaluation of their functional abilities. The CDR score of normal subjects was 0, while those diagnosed with MCI exhibited a CDR of 0.5 and an MMSE score ranging from 20 to 24 (32). AD patients have a CDR value of 1+. The clinical diagnosis of probable MCI or AD was based on the National Institute on Aging–Alzheimer's Association (NIA-AA) guidelines (2018, 33).

It is essential to obtain comprehensive information regarding the participants' demographics, medical history and family history. Meanwhile all MCI and AD patients underwent a battery of tests, including a complete blood count, blood glucose, blood electrolytes, blood urea nitrogen, serology for syphilis, thyroid function, and CT or MRI scans to exclude other potential causes of their dementia.

Informed consent was provided from all volunteers or their legal guardians. The medical ethics committee of Bengbu Medical College approved protocols for this study [2023 (276)].

Inclusion and exclusion criteria

43 AD and 33 MCI patients were recruited over the period from July 2022 to October 2023 from the Department of Neurology in the Second Affiliated Hospital of Bengbu Medical College and the Fourth Affiliated Hospital of Soochow University.

The inclusion criteria were that all the participants must be over 40 years of age, diagnosis of MCI or AD. All the participants were required to have a reliable insider who could assist in the completion of the clinical visits as needed. A total of 40 normal cognition (NC) over 40 years old from the hospital physical examination center, were recruited as control participants, absence of neuropsychiatric disease, stroke, dementia, and underlying diseases.

The exclusion criteria were subjects with any concomitant neurological, psychiatric or significant medical illness known to affect cognitive function including Parkinson's disease, Huntington disease, seizure disorder, multiple sclerosis, cerebrovascular disease and brain tumor, or history of major depression, anxiety, or other mental diseases, which makes patient unable to accomplish the assessment of cognitive impairment.

Sample preparation

Peripheral venous blood samples were collected into EDTA tubes via standard procedures. The collected blood sample was centrifuged for 10 min at 3000 rpm. Subsequently, plasma supernatant was aliquoted into polypropylene tubes and stored at −80°C until further use.

Materials and operational procedure

Materials, including capture beads, streptavidin-β-galactosidase (SβG), detection antibodies, sample diluent, buffer-1/2, microfluidic chip, fluorogenic substrate and sealing oil were purchased from ColorTech (Suzhou) Biotechnology company (Suzhou, China).

Plasma samples were removed from refrigerator and placed at room temperature for 30 min. Samples were then diluted 4x using sample diluent.

The 10 μL of capture beads suspensions, 15 μL of the detection antibody solution and 150 μL sample (or calibrator) were mixed and incubated at room temperature for 30 min (60 min for p-tau181). The beads were separated and washed three times with 200 μL of buffer-1. After washing, 70.0 μL SβG solution was added and incubated for 5 min (10 min for p-tau181). A sandwich structure was formed by magnetic beads, capture antibody, antigen, detection antibody and labeled enzyme (Figure 1A). The beads were separated and washed seven times with 200 μL of buffer-1, and once with 200 μL of buffer-2. Then the beads were resuspended in 20 μL of buffer-2 for further detection.

The beads dispersion was mixed with the fluorogenic substrate and then loaded into the microfluidic chip that has an array of microreactors. The magnet helps the magnetic microbeads enter the holes and increases the filling rate (Figure 1B-I). The size of each microreactor is designed to ensure only one bead can enter. Then the sealing oil was used to seal the microreactors and remove the beads that did not fall into microreactors (Figure 1B-II).

Enzymes on the beads surface will hydrolyze the fluorogenic substrate in the microreactor and the fluorescent products will accumulate with time (Figure 1B-III). The signal will be read and analyzed (Figure 1C). The concentration of the target sample can be obtained by comparing the signal for unknown samples to the calibration curve.

Statistical analysis

The extreme values of each plasma biomarker, defined as those at least three times the standard deviation (SD) of the mean, were excluded. Normally distributed continuous variables were expressed as mean ± SD, while the skewed distributed continuous variables were described by the median and quartile 1 (Q1) to quartile 3 (Q3). Number (*n*) and percentages (%) were employed for categorical variables. Categorical variables were tested using Pearson chi-square tests. One-way analyses of variance (ANOVA) with the Kruskal-Wallis test was employed for the comparison of continuous variables with unequal variance. *Post hoc* pairwise comparisons was used to evaluate differences among multi-groups and adjusted significance by Bonferroni. Categorical variables were compared using the Pearson's chi-squared test.

Scatter plots were used to illustrate the distributions of original plasma biomarkers' levels of the different groups. The associations between CDR, MMSE scores and plasma biomarkers were assessed using partial correlation analyses with the adjustment for age, sex, and education year as covariates. Education was categorized according to its completion within a six-year timeframe.

p-values <0.05 was considered statistically significant. All statistical analyses were analyzed using IBM SPSS Statistics for Windows, version 27.0. The scatter plots and receiver-operating characteristic (ROC) curves were visualized by GraphPad Prism version10.1.2 for Windows with control of age, sex, and education year.

Results

Characteristics of participants

A total of 116 participants were recruited, including 40 individuals with normal cognition (NC), 33 with a clinically diagnosis of MCI, and 43 patients with AD patients, as characterized by the CDR score. The demographic data of the study participants were presented in Table 1. We did not find a apparent discrepancy in sex among the three groups. The AD group exhibited a significant difference in age, education years compared to the MCI group. The NC group did not differ significantly in age from the MCI group, nor in education from the AD group. As expected, the AD group exhibited the lowest level of education. Following Bonferroni correction, MMSE and CDR scores were found to be significantly different among the three groups.

AD biomarkers in plasma across groups

Table 2 and Figure 2 illustrate the levels of plasma biomarkers detected in the different cognitive performance groups. Aβ40 demonstrated significant differences only between participants with NC and AD (Table 2; Figure 2A). No significant discrepancy of Aβ40 was observed between participants with MCI and other groups. Aβ42 and Aβ42/Aβ40 ratio exhibited a descending trend, with the lowest

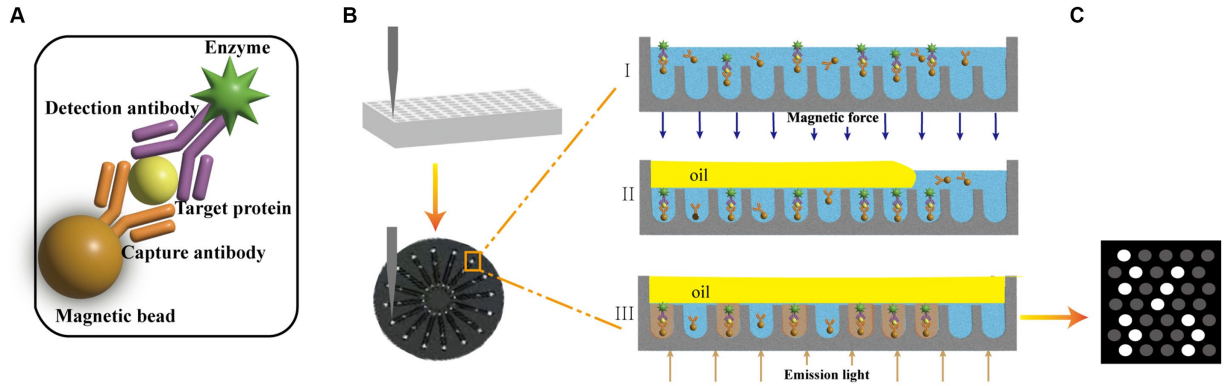

FIGURE 1
(A) Encoded magnetic beads are combined with antigens and enzyme labels to form a sandwich structure complex. **(B)** The plasma mixed with magnetic beads was injected into the flow channel of the disc with 16 integrated microchannels. The coded microbeads automatically enter the chip with the liquid to be analyzed. The magnet helps the magnetic microbeads enter the holes and increases the filling rate (I). The microbeads enter the holes and the enzymes on the beads surface hydrolyze the fluorogenic substrate. A fluorocarbon oil is applied to seal the beads inside different microwells. The beads that are not inside chambers are washed out (II); Light is applied to excite the coding microspheres and liquids in the microwells (III). **(C)** Images of fluorescent molecules are captured dynamically.

TABLE 1 Demographic characteristics of subjects.

	Total (n = 116)	NC (n = 40)	MCI (n = 33)	AD (n = 43)
Gender, M/F	39/77 (50.6%)	18/22 (81.2%)	12/21 (57.1%)	9/34 (26.5%)
Age, years, Mean (SD)	63.8 (12.7)	59.4 (11.7)[c]	58.2 (12.8)[c]	72.3 (8.6)[a, b]
Education, years, ≤6/>6	73/43 (169.7%)	27/13 (207.7%)[b]	14/19 (73.7%)[a, c]	32/11 (290.9%)[b]
MMSE, Median [Q1, Q3]	23.0 [16.0, 28.0]	29.0 [27.0, 30.0][b, c]	23.0 [20.0, 25.0][a, c]	13.0 [9.0,17.0][a, b]
CDR, Median [Q1, Q3]	0.5 [0, 1.0]	0 ± 0[b, c]	0.5 [0.5, 0.5][a, c]	1.0 [1.0, 2.0][a, b]

NC, normal cognition; MCI, mild cognitive impairment; AD, Alzheimer's disease; CDR, Clinical Dementia Rating Scale. SD, standard deviation; MMSE, mini-mental state examination; Q1, quartile 1; Q3, quartile 3; [a]Significant values versus NC (normal cognition). [b]Significant values versus MCI (mild cognitive impairment). [c]Significant values versus AD (Alzheimer's disease).

TABLE 2 Plasma biomarker concentrations and ratios of subjects.

	Total (n = 116)	NC (n = 40)	MCI (n = 33)	AD (n = 43)
Aβ40 (pg/ml), Median [Q1, Q3]	609.98 [493.42, 726.15]	496.19 [430.92, 626.11][c]	620.42 [533.79, 709.83]	680.35 [589.08, 817.20][a]
Aβ42 (pg/ml), Median [Q1, Q3]	4.27 [3.44, 5.48]	4.62 [3.47, 5.82][c]	4.69 [3.60, 5.88][c]	3.95 [2.61, 5.14][a, b]
Aβ42/Aβ40, Median [Q1, Q3]	0.0074 [0.0056, 0.0093]	0.0091 [0.0068, 0.0106][c]	0.0074 [0.0059, 0.0093][c]	0.0058 [0.0035, 0.0080][a, b]
p-tau181 (pg/ml), Median [Q1, Q3]	2.27 [1.49, 4.17]	1.41 [0.46, 2.30][b, c]	2.16 [1.81, 3.26][a, c]	4.76 [2.49, 8.78][a, b]

NC, normal cognition; MCI, mild cognitive impairment; AD, Alzheimer's disease; CDR, Clinical Dementia Rating Scale; SD, standard deviation; MMSE, mini-mental state examination; Q1, quartile 1; Q3, quartile 3; Aβ, amyloid-beta protein; t-tau, total tau; NfL, neurofilament proteinlight chain; p-tau181, tau phosphorylated at threonine 181. [a]Significant values versus NC (normal cognition). [b]Significant values versus MCI (mild cognitive impairment). [c]Significant values versus AD (Alzheimer's disease).

values observed in the AD groups compared to the NC and MCI groups (Table 2; Figures 2B,C). With regard to Aβ42 and Aβ42/Aβ40 ratio, no significant difference was found between participants with NC and MCI. Conversely, plasma p-tau181 exhibited an upward trend across groups, with significant differences observed among the three participant groups (Table 2; Figure 2D).

Associations between plasma biomarkers and cognition

Figures 3, 4 showed the partial correlation matrix between three plasma biomarkers and CDR and MMSE scores after adjusting age, sex and education years.

In Figure 3, Aβ40 showed a positive correlation with CDR (r = 0.352, df = 108, p < 0.001). Aβ42 (r = −0.275, df = 2, p = 0.004) and Aβ42/Aβ40 ratio (r = −0.394, df = 107, p < 0.001) had an inverse correlation with CDR. P-tau181 demonstrated a positive correlation with CDR (r = 0.365, df = 105, p < 0.001). As shown in Figures 3C,D, the cut-off values of Aβ42/Aβ40 ratio and p-tau181 were able to discriminate individuals with cognitive impairment from normal controls. The performance improves with increasing CDR. As demonstrated in Figure 4, Aβ42/Aβ40 ratio (r = 0.358, df = 107, p < 0.001) and p-tau181 (r = −0.394 df = 105, p < 0.001) also showed a stronger correlation with MMSE than Aβ42 (r = 0.266, df = 108, p = 0.005) or Aβ40 (r = −0.288, df = 108, p = 0.002). Higher Aβ40 and p-tau181 were correlated with worse cognitive scores, which correspond to lower Aβ42.

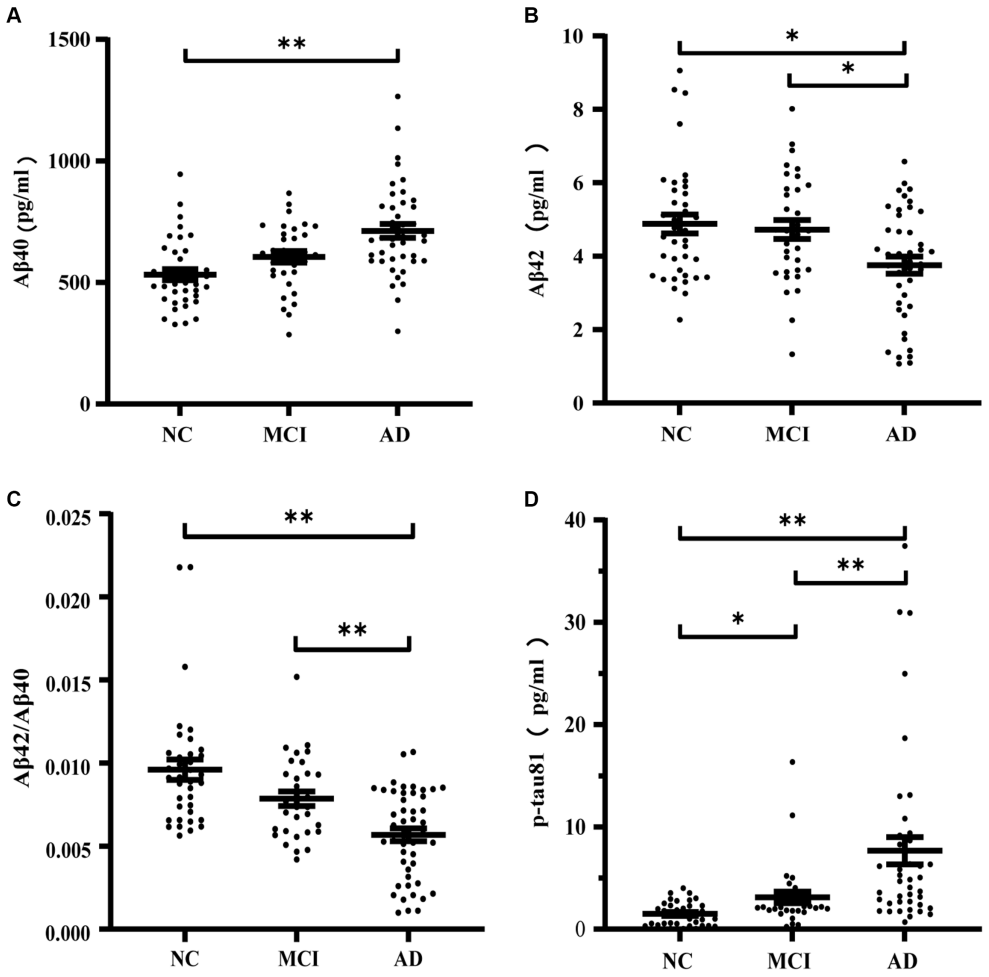

FIGURE 2
Concentrations of Aβ40 **(A)**, Aβ42 **(B)**, Aβ42/Aβ40 **(C)**, p-tau181 **(D)** in normal cognition subjects, MCI and AD patients. *$p \leq 0.05$ and **$p \leq 0.01$.

Figure 5 shows the correlation between plasma biomarkers in each pairwise analysis, respectively. Participants were distributed to four quadrants according to the respective cutoff value for plasma biomarkers of AD. From the distribution in Figure 5A, it can be seen that Aβ42 performed well in distinguishing controls, but not AD subjects. As illustrated in Figures 5B,C, individuals with AD were predominantly located in the double-positive quadrant. P-tau 181 and Aβ42/Aβ40 ratio exhibited the highest concordance (30.8%) in differentiating positive individuals from negative individuals, with 63.4% of AD patients being distinguished.

The value of plasma biomarkers in predicting cognitive status

To figure out if plasma biomarkers are sufficient to identify MCI and AD from non-AD, we performed receiver operator characteristic (ROC) analysis on the diagnostic accuracy of p-tau 181 and the Aβ42/Aβ40 ratio. This analysis demonstrated a higher correlation with cognitive scores. The results demonstrated that p-tau 181 (AUC = 0.8768) and Aβ42/Aβ40 ratio (AUC = 0.8343) were able to classify the AD groups with higher accuracy than MCI (AUC = 0.7932 and 0.6569, respectively) (Figure 6). The performance of p-tau 181 was marginally superior to that of the Aβ42/Aβ40 ratio.

Discussion

The principal findings of the present study were as follows: (1) Plasma Aβ42, and the Aβ42/Aβ40 ratio exhibited a declining trend, whereas plasma Aβ40 and p-tau181 demonstrated an upward trajectory in conjunction with the aggravation of cognitive impairment. (2) Both plasma p-tau181 and the Aβ42/Aβ40 ratio were valuable markers for the diagnosis of AD. P-tau181 was found to be a more effective indicator of clinical cognitive performance. (3) The digital ELISA was identified as a promising and reliable approach for clinical screening of patients with MCI or AD. It has the characteristics of high efficiency and low cost, which would enable early diagnosis and treatment at earlier phases of research, potentially accelerating the discovery of new biomarkers for complex diseases, such as neurological disorders.

Aβ accumulation and hyperphosphorylated tau protein have been considered as potential triggers and/or drivers in the development of AD (33). Plasma concentrations of Aβ42 and the Aβ42/Aβ40 ratio are

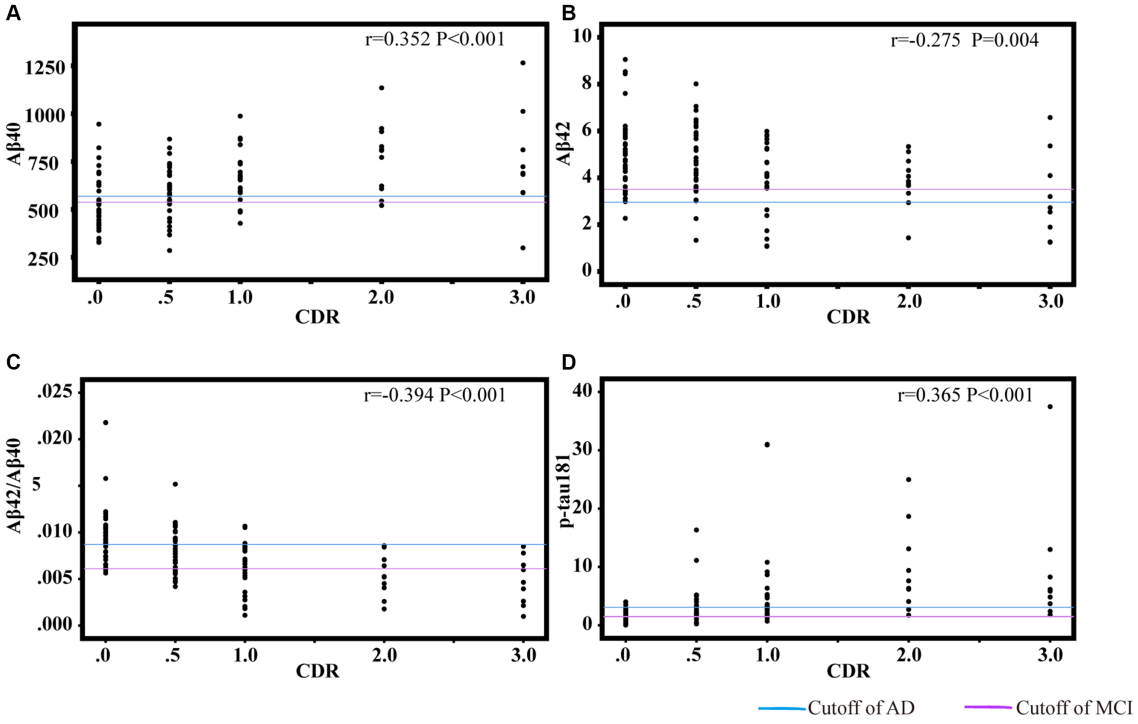

FIGURE 3
Scatter plots of CDR and plasma biomarkers of Aβ40 **(A)**, Aβ42 **(B)**, Aβ42/Aβ40 **(C)**, p-tau181 **(D)**. The partial correlation coefficients (*r*) were adjusted for age, gender, and education year. $p < 0.05$ was considered statistically significant after using multiple comparisons by Bonferroni correction. CDR, clinical dementia rating; Aβ, amyloid-beta protein; p-tau181, tau phosphorylated at threonine 181.

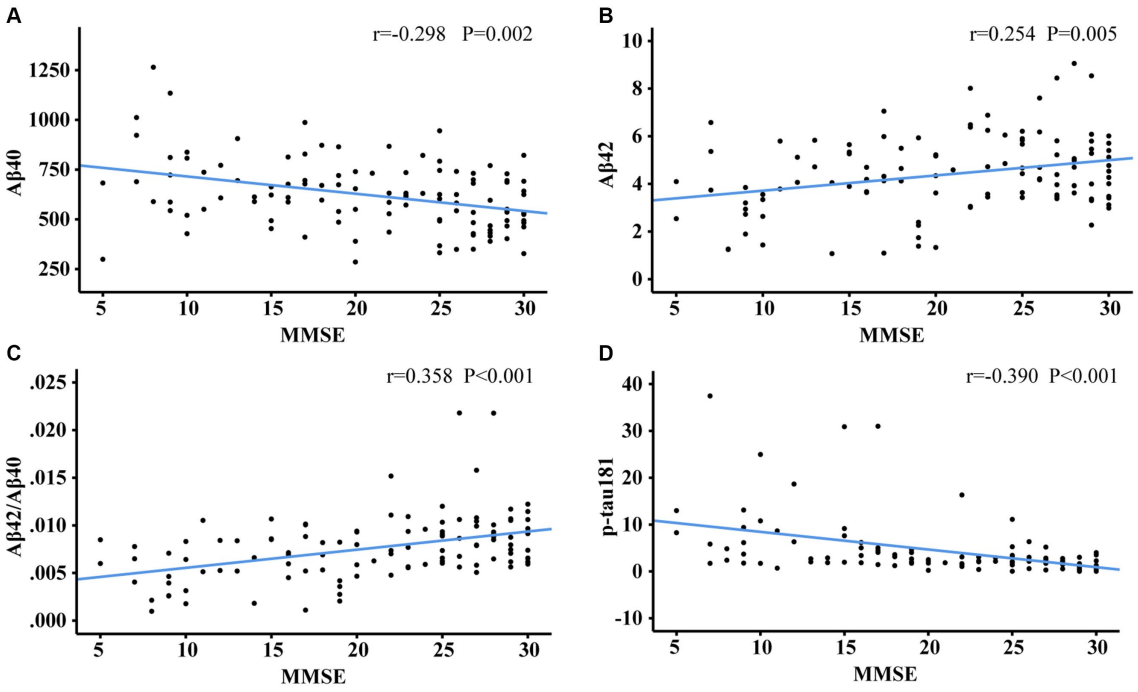

FIGURE 4
Scatter plots of MMSE and plasma biomarkers of Aβ40 **(A)**, Aβ42 **(B)**, Aβ42/Aβ40 **(C)**, p-tau181 **(D)**. The partial correlation coefficients (*r*) were adjusted for age, gender, and education year. $p < 0.05$ was considered statistically significant after using multiple comparisons by Bonferroni correction. MMSE, mini-mental state examination; Aβ, amyloid-beta protein; p-tau181, tau phosphorylated at threonine 181.

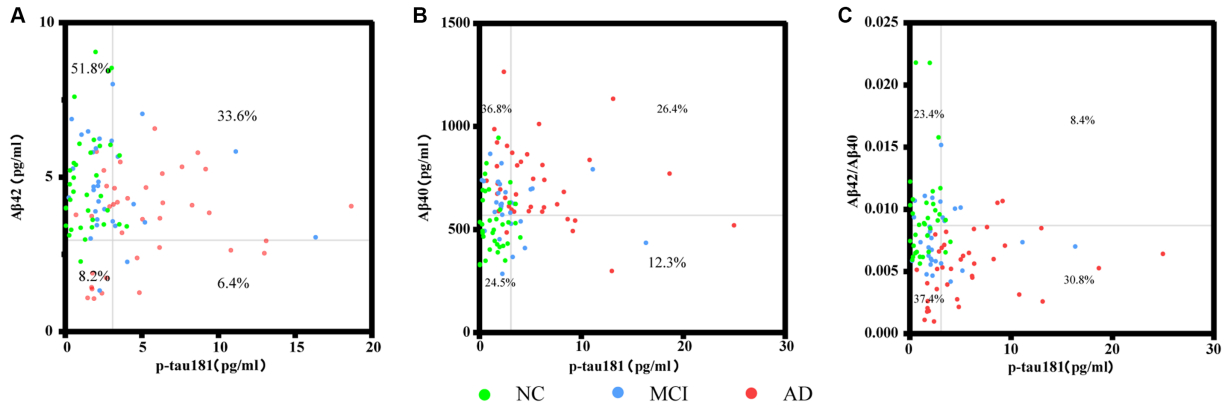

FIGURE 5
Scatter plots represent the correlation between plasma biomarkers in each pairwise analysis among the different groups. Each point refers to the value of indicated measures of a single participant, and the grey lines indicate the cutoff for each biomarker. Percentages indicate the proportions in each quadrant. Four extreme values were not shown in panel **(A)**, and three points in panels **(B,C)** separately, but they were included in the statistical analyses.

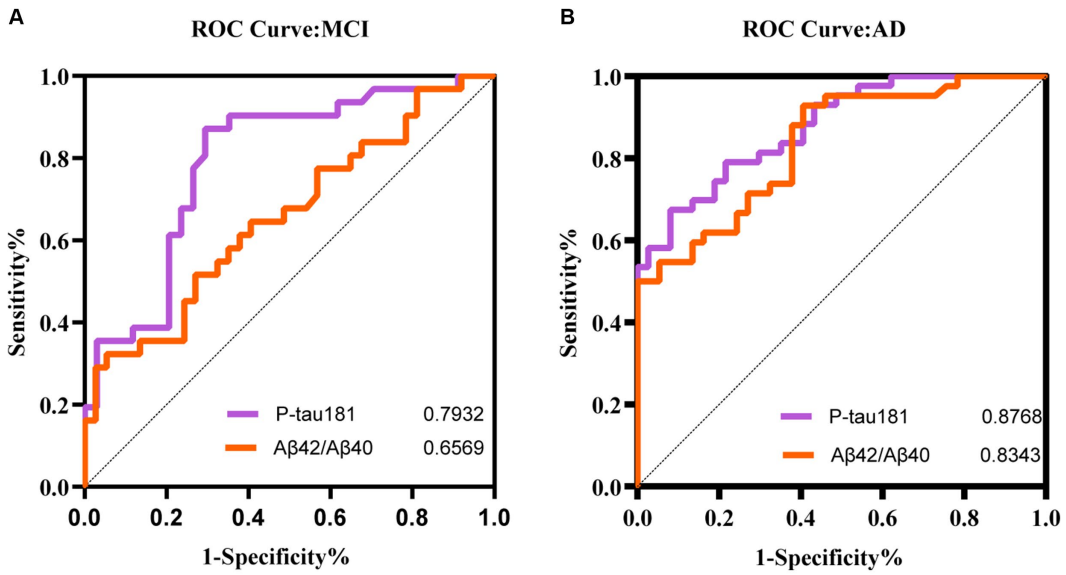

FIGURE 6
ROC curve analyses of different models for MCI **(A)** and AD **(B)** patients.

significantly reduced in AD, indicating the presence of Aβ deposition in the brain. Some have proposed that the Aβ42/Aβ40 ratio offers superior predictive accuracy in determining Aβ status compared to Aβ42 alone (34, 35). Plasma p-tau 181 was inversely changed in AD, which is likely indicative of the presence of neurofibrillary tangles within the brain (36). This study also demonstrated that p-tau 181 and the Aβ42/Aβ40 ratio were tightly correlated with the CDR and MMSE scores, in agreement with previous studies (37, 38). Generally, the p-tau181 biomarker demonstrated the highest sensitivity and specificity in discriminating between control subjects and patients diagnosed with Alzheimer's disease (AD). These results are highly consistent with prior studies. The biomarkers Aβ42, Aβ40, total tau (t-tau) and p-tau181 showed good diagnostic performance (39–41). Furthermore, some studies have confirmed the high predictive value of plasma p-tau in diagnosing AD (16, 37, 42). Nevertheless, the correlations we observed between CDR, MMSE and plasma Aβ42 were weaker even compared with Aβ40 and showed low accuracy for diagnosis of AD. The suboptimal predictive accuracy of plasma Aβ42 may be attributed to the limited sensitivity of this improved digital ELISA technique in quantifying the overall levels of plasma Aβ. Further strengthening improvement of the reagent and procedure is necessary to enhance their effectiveness.

Traditional ELISA is known for its ease of use, cost efficiency, and versatility but is limited by longer processing times, particularly with multiple washing steps, and lower sensitivity. It can also be prone to interferences that may result in false positives or negatives (43). Single Molecule Arrays (SiMoA) offer high sensitivity by detecting individual proteins but require specific complex equipment and techniques (44). The

paper-based lateral flow immunoassay (dLFI) provides a rapid, visual, and practical point-of-care method for detecting AD biomarkers within 30 min, similar to ELISA results, but without the need for specialized equipment. However, it may not match the sensitivity and specificity of laboratory-level ELISA and might not detect all relevant AD biomarkers (45). The immunomagnetic exosomal polymerase chain reaction (iMEP) is a highly sensitive technique for the rapid detection of amyloid-beta and phosphorylated tau proteins in blood exosomes, essential for AD diagnosis. It allows for precise detection and simultaneous analysis of multiple biomarkers but may be limited by its technical complexity and the need for potentially costly specialized equipment and reagents (46). The colorimetric and surface-enhanced Raman scattering (SERS) dual-mode magnetic immunosensor combines colorimetric and SERS techniques for high-sensitivity detection of AD biomarkers, with rapid and intuitive visual color change results. It is particularly adept at identifying low concentrations of p-tau396, 404, aiding in early diagnosis. However, it requires specific SERS equipment, expertise, and may be costly (47, 48). Lastly, the densely aligned carbon nanotube sensor array is a highly sensitive and accurate platform for detecting AD biomarkers at femtomolar concentrations with multiplex detection capabilities. Despite these strengths, its cost and the need for specialized equipment and expertise may limit broader accessibility (49). This was the first study to use the improved digital ELISA to detect of blood biomarkers for AD, which achieves signal amplification by quantifying of single molecules. Digital ELISA represents the latest breakthrough in protein detection, specifically targeting proteins present at minimal concentrations (50–52). Such a platform is urgently needed to unlock the potential biomarker, which is rapidly trending toward low abundance biomarkers associated with disease states.

In our study, we used an external magnetic field to enhance the loading efficiency of the magnetic beads. The low cost of our novel system greatly increases its potential for commercialization. The primary approach to improve the digital ELISA involves evaluating the variation in fluorescence intensity of the liquid in the microwell, which can be used to determine the concentration of the target protein. The traditional digital technique restricts the magnetic bead signal to binary values of 0 or 1, whereas our methodology encompasses a wider range of nuances. Access to its unique ability to quantify single molecules facilitates a more comprehensive understanding of the biological aspects associated with disease progression or the impact of treatments during initial stages of investigation, potentially accelerating the identification of novel biomarkers for complex conditions such as neurodegenerative diseases, facilitating the identification and diagnosis of neurological conditions. The implementation of this proactive strategy will empower individuals at risk to proactively engage in preventive measures, effectively delaying the development of, disease. This progress signifies a notable step toward prompt early intervention and improved clinical management, ultimately delivering tangible benefits to both researchers and patients.

There were several limitations to our study. First and foremost, the sample size was small. This small sample size was partly due to the Corona Virus Disease 2019 (COVID-19) epidemic, but mainly because the rigorous exclusion criteria for participants. The reliability of cytokines is a important issue that can be greatly influenced by confounding variables such as concurrent medical conditions and the use of other medications. In the case of COVID-19 infection, infected blood samples were being available. The stringent selection procedure enabled us to achieve a high level of reliability in our analyses. Secondly, it was not possible to determine whether plasma biomarkers (Aβ40, Aβ42, and P-tau181) correlated with corresponding CSF biomarkers of AD, as CSF collection was rarely accepted by both patients and controls. Further research with larger sample sizes is necessary to validate our findings. Thirdly, the individuals involved in our research were sourced from two different backgrounds, which inevitably led to some inequality. Age, gender and year of education were adjusted for in the statistical models. Fourthly, learning effects (53, 54) and intrusion errors are inevitable in tests evaluating comparable cognitive domains, which may result in potential fluctuations in assessing the cognitive performance of the study subjects. Fifthly, the diagnosis of AD was primarily based on clinical standards rather than pathological evidence from CSF or amyloid/tau PET scans. The lack of a gold standard has impeded us from classifying the 'ATN' framework (55). Finally, the pre-sample processing of the improved digital ELISA used in this work is artificially based. There is an urgent need to make this improved digital ELISA technique fully automate in order to minimize the operational errors. We are also developing the technology's multiplex detection capabilities to enable the simultaneous detection of multiple AD core biomarkers.

Conclusion

In conclusion, we detected Aβ42, Aβ40 and p-tau181 levels in the plasma of AD, MCI and control groups with a high degree of accuracy using this improved digital ELISA technique. Therefore, this technique has the potential to expedite the identification of individuals at risk of dementia, thus contributing to the advancement of AD early screening and clinical drug development for Alzheimer's disease. Of note, multi-centre, longitudinal and more holistic studies are necessary to verify this methodology and to further substantiate the correlation between plasma biomarkers and cognitive manifestations.

Data availability statement

The raw data supporting the conclusions of this article will be made available by the authors, without undue reservation.

Ethics statement

The studies involving humans were approved by Bengbu Medical College Ethics Committee. The studies were conducted in accordance with the local legislation and institutional requirements. The participants provided their written informed consent to participate in this study.

Author contributions

WY: Writing – original draft, Writing – review & editing. FG: Investigation, Methodology, Writing – review & editing. LY: Data curation, Writing – review & editing. GS: Data curation, Writing – review & editing. FZ: Data curation, Writing – review & editing. YX: Data curation, Writing – review & editing. YM: Data curation, Writing – review & editing. ML: Data curation, Writing – review & editing. WD: Conceptualization, Methodology, Project administration, Resources, Supervision, Writing – review & editing.

Funding

The author(s) declare that financial support was received for the research, authorship, and/or publication of this article. This work was supported by the Foundation of Anhui Provincial Department of Education, Anhui Province, China (Grant No. 2022AH051490).

Acknowledgments

We would like to thank ColorTech (Suzhou) Biotechnology Company for its contribution in the manufacturing of the system and partial technical guidance in plasma detection.

Conflict of interest

The authors declare that the research was conducted in the absence of any commercial or financial relationships that could be construed as a potential conflict of interest.

Publisher's note

All claims expressed in this article are solely those of the authors and do not necessarily represent those of their affiliated organizations, or those of the publisher, the editors and the reviewers. Any product that may be evaluated in this article, or claim that may be made by its manufacturer, is not guaranteed or endorsed by the publisher.

References

1. Gauthier SWC, Servaes S, Morais JA, Rosa-Neto P. World Alzheimer report 2022 life after diagnosis: Navigating treatment, care and support. London: Alzheimer's Disease International (2022).

2. Jia L, Du Y, Chu L, Zhang Z, Li F, Lyu D, et al. Prevalence, risk factors, and management of dementia and mild cognitive impairment in adults aged 60 years or older in China: a cross-sectional study. *Lancet Public Health*. (2020) 5:e661–71. doi: 10.1016/S2468-2667(20)30185-7

3. Quiroz YT, Zetterberg H, Reiman EM, Chen Y, Su Y, Fox-Fuller JT, et al. Plasma neurofilament light chain in the presenilin 1 E280A autosomal dominant Alzheimer's disease kindred: a cross-sectional and longitudinal cohort study. *Lancet Neurol*. (2020) 19:513–21. doi: 10.1016/S1474-4422(20)30137-X

4. Barthelemy NR, Li Y, Joseph-Mathurin N, Gordon BA, Hassenstab J, Benzinger TLS, et al. A soluble phosphorylated tau signature links tau, amyloid and the evolution of stages of dominantly inherited Alzheimer's disease. *Nat Med*. (2020) 26:398–407. doi: 10.1038/s41591-020-0781-z

5. Villemagne VL, Burnham S, Bourgeat P, Brown B, Ellis KA, Salvado O, et al. Amyloid beta deposition, neurodegeneration, and cognitive decline in sporadic Alzheimer's disease: a prospective cohort study. *Lancet Neurol*. (2013) 12:357–67. doi: 10.1016/S1474-4422(13)70044-9

6. Reiman EM, Quiroz YT, Fleisher AS, Chen K, Velez-Pardo C, Jimenez-Del-Rio M, et al. Brain imaging and fluid biomarker analysis in young adults at genetic risk for autosomal dominant Alzheimer's disease in the presenilin 1 E280A kindred: a case-control study. *Lancet Neurol*. (2012) 11:1048–56. doi: 10.1016/S1474-4422(12)70228-4

7. Jack CR Jr, Lowe VJ, Weigand SD, Wiste HJ, Senjem ML, Knopman DS, et al. Serial PIB and MRI in normal, mild cognitive impairment and Alzheimer's disease: implications for sequence of pathological events in Alzheimer's disease. *Brain*. (2009) 132:1355–65. doi: 10.1093/brain/awp062

8. Bateman RJ, Xiong C, Benzinger TL, Fagan AM, Goate A, Fox NC, et al. Clinical and biomarker changes in dominantly inherited Alzheimer's disease. *N Engl J Med*. (2012) 367:795–804. doi: 10.1056/NEJMoa1202753

9. Gordon BA, Blazey TM, Su Y, Hari-Raj A, Dincer A, Flores S, et al. Spatial patterns of neuroimaging biomarker change in individuals from families with autosomal dominant Alzheimer's disease: a longitudinal study. *Lancet Neurol*. (2018) 17:241–50. doi: 10.1016/S1474-4422(18)30028-0

10. Braak H, Thal DR, Ghebremedhin E, Del Tredici K. Stages of the pathologic process in Alzheimer disease: age categories from 1 to 100 years. *J Neuropathol Exp Neurol*. (2011) 70:960–9. doi: 10.1097/NEN.0b013e318232a379

11. Etgen T, Sander D, Bickel H, Forstl H. Mild cognitive impairment and dementia: the importance of modifiable risk factors. *Dtsch Arztebl Int*. (2011) 108:743–50. doi: 10.3238/arztebl.2011.0743

12. Petersen RCJAN. Mild cognitive impairment: clinical characterization and outcome. *Arch Neurol*. (1999) 56:303. doi: 10.1001/archneur.56.3.303

13. Molinuevo JL, Rabin LA, Amariglio R, Buckley R, Dubois B, Ellis KA, et al. Implementation of subjective cognitive decline criteria in research studies. *Alzheimers Dement*. (2017) 13:296–311. doi: 10.1016/j.jalz.2016.09.012

14. Jessen F, Amariglio RE, Buckley RF, van der Flier WM, Han Y, Molinuevo JL, et al. The characterisation of subjective cognitive decline. *Lancet Neurol*. (2020) 19:271–8. doi: 10.1016/S1474-4422(19)30368-0

15. Scheltens P, Blennow K, Breteler MM, de Strooper B, Frisoni GB, Salloway S, et al. Alzheimer's disease. *Lancet*. (2016) 388:505–17. doi: 10.1016/S0140-6736(15)01124-1

16. Janelidze S, Mattsson N, Palmqvist S, Smith R, Beach TG, Serrano GE, et al. Plasma P-tau 181 in Alzheimer's disease: relationship to other biomarkers, differential diagnosis, neuropathology and longitudinal progression to Alzheimer's dementia. *Nat Med*. (2020) 26:379–86. doi: 10.1038/s41591-020-0755-1

17. O'Bryant SE, Mielke MM, Rissman RA, Lista S, Vanderstichele H, Zetterberg H, et al. Blood-based biomarkers in Alzheimer disease: current state of the science and a novel collaborative paradigm for advancing from discovery to clinic. *Alzheimers Dement*. (2017) 13:45–58. doi: 10.1016/j.jalz.2016.09.014

18. Cohen L, Walt DR. Highly sensitive and multiplexed protein measurements. *Chem Rev*. (2019) 119:293–321. doi: 10.1021/acs.chemrev.8b00257

19. Ren AH, Diamandis EP, Kulasingam V. Uncovering the depths of the human proteome: antibody-based Technologies for Ultrasensitive Multiplexed Protein Detection and Quantification. *Mol Cell Proteomics*. (2021) 20:100155. doi: 10.1016/j.mcpro.2021.100155

20. Duffy DC. Digital detection of proteins. *Lab Chip*. (2023) 23:818–47. doi: 10.1039/D2LC00783E

21. Blennow K, Zetterberg H. Biomarkers for Alzheimer's disease: current status and prospects for the future. *J Intern Med*. (2018) 284:643–63. doi: 10.1111/joim.12816

22. Gao F, Lv XY, Dai LB, Wang Q, Wang P, Cheng ZZ, et al. A combination model of AD biomarkers revealed by machine learning precisely predicts Alzheimer's dementia: China aging and neurodegenerative initiative (CANDI) study. *Alzheimers Dement*. (2023) 19:749–60. doi: 10.1002/alz.12700

23. Teunissen CE, Verberk IMW, Thijssen EH, Vermunt L, Hansson O, Zetterberg H, et al. Blood-based biomarkers for Alzheimer's disease: towards clinical implementation. *Lancet Neurol*. (2022) 21:66–77. doi: 10.1016/S1474-4422(21)00361-6

24. Zeng X, Chen Y, Sehrawat A, Lee J, Lafferty TK, Kofler J, et al. Alzheimer blood biomarkers: practical guidelines for study design, sample collection, processing, biobanking, measurement and result reporting. *Mol Neurodegener*. (2024) 19:40. doi: 10.1186/s13024-024-00711-1

25. Wang J, Chen M, Masters CL, Wang YJ. Translating blood biomarkers into clinical practice for Alzheimer's disease: challenges and perspectives. *Alzheimers Dement*. (2023) 19:4226–36. doi: 10.1002/alz.13116

26. Tighe P, Negm O, Todd I, Fairclough L. Utility, reliability and reproducibility of immunoassay multiplex kits. *Methods*. (2013) 61:23–9. doi: 10.1016/j.ymeth.2013.01.003

27. Yang SM, Bi Q, Zhang WJ, Cui X, Zhou Y, Yuan C, et al. Highly accurate multiprotein detection on a digital ELISA platform. *Lab Chip*. (2022) 22:3015–24. doi: 10.1039/D2LC00388K

28. Hartman ZC, Poage GM, den Hollander P, Tsimelzon A, Hill J, Panupinthu N, et al. Growth of triple-negative breast Cancer cells relies upon coordinate autocrine expression of the Proinflammatory cytokines IL-6 and IL-8. *Cancer Res*. (2013) 73:3470–80. doi: 10.1158/0008-5472.CAN-12-4524-T

29. Coffelt SB, Kersten K, Doornebal CW, Weiden J, Vrijland K, Hau C-S, et al. IL-17-producing γδ T cells and neutrophils conspire to promote breast cancer metastasis. *Nature*. (2015) 522:345–8. doi: 10.1038/nature14282

30. Robert M, Miossec P. Interleukin-17 and lupus: enough to be a target? For which patients? *Lupus*. (2019) 29:6–14. doi: 10.1177/0961203319891243

31. Mateen S, Zafar A, Moin S, Khan AQ, Zubair S. Understanding the role of cytokines in the pathogenesis of rheumatoid arthritis. *Clin Chim Acta*. (2016) 455:161–71. doi: 10.1016/j.cca.2016.02.010

32. Petersen RC, Doody R, Kurz A, Mohs RC, Morris JC, Rabins PV, et al. Current concepts in mild cognitive impairment. *Arch Neurol*. (2001) 58:1985–92. doi: 10.1001/archneur.58.12.1985

33. Hansson O. Biomarkers for neurodegenerative diseases. *Nat Med*. (2021) 27:954–63. doi: 10.1038/s41591-021-01382-x

34. Hansson O, Lehmann S, Otto M, Zetterberg H, Lewczuk P. Advantages and disadvantages of the use of the CSF amyloid beta (Abeta) 42/40 ratio in the diagnosis of Alzheimer's Disease. *Alzheimers Res Ther*. (2019) 11:34. doi: 10.1186/s13195-019-0485-0

35. Lewczuk P, Matzen A, Blennow K, Parnetti L, Molinuevo JL, Eusebi P, et al. Cerebrospinal fluid Abeta 42/40 corresponds better than Abeta 42 to amyloid PET in Alzheimer's Disease. *J Alzheimers Dis*. (2017) 55:813–22. doi: 10.3233/JAD-160722

36. Ossenkoppele R, Reimand J, Smith R, Leuzy A, Strandberg O, Palmqvist S, et al. Tau PET correlates with different Alzheimer's disease-related features compared to CSF and plasma p-tau biomarkers. *EMBO Mol Med*. (2021) 13:e14398. doi: 10.15252/emmm.202114398

37. Karikari TK, Pascoal TA, Ashton NJ, Janelidze S, Benedet AL, Rodriguez JL, et al. Blood phosphorylated tau 181 as a biomarker for Alzheimer's disease: a diagnostic performance and prediction modelling study using data from four prospective cohorts. *Lancet Neurol*. (2020) 19:422–33. doi: 10.1016/S1474-4422(20)30071-5

38. Xiao Z, Wu X, Wu W, Yi J, Liang X, Ding S, et al. Plasma biomarker profiles and the correlation with cognitive function across the clinical spectrum of Alzheimer's disease. *Alzheimers Res Ther*. (2021) 13:123. doi: 10.1186/s13195-021-00864-x

39. Lantero Rodriguez J, Karikari TK, Suarez-Calvet M, Troakes C, King A, Emersic A, et al. Plasma p-tau 181 accurately predicts Alzheimer's disease pathology at least 8 years prior to post-mortem and improves the clinical characterisation of cognitive decline. *Acta Neuropathol*. (2020) 140:267–78. doi: 10.1007/s00401-020-02195-x

40. Cullen NC, Leuzy A, Palmqvist S, Janelidze S, Stomrud E, Pesini P, et al. Individualized prognosis of cognitive decline and dementia in mild cognitive impairment based on plasma biomarker combinations. *Nat Aging*. (2021) 1:114–23. doi: 10.1038/s43587-020-00003-5

41. Park JC, Han SH, Yi D, Byun MS, Lee JH, Jang S, et al. Plasma tau/amyloid-beta1-42 ratio predicts brain tau deposition and neurodegeneration in Alzheimer's disease. *Brain*. (2019) 142:e19. doi: 10.1093/brain/awz033

42. Palmqvist S, Tideman P, Cullen N, Zetterberg H, Blennow K, et al. Prediction of future Alzheimer's disease dementia using plasma phospho-tau combined with other accessible measures. *Nat Med*. (2021) 27:1034–42. doi: 10.1038/s41591-021-01348-z

43. Zhang L, Yang C, Li Y, Niu S, Liang X, Zhang Z, et al. Dynamic changes in the levels of amyloid-beta(42) species in the brain and periphery of APP/PS1 mice and their significance for Alzheimer's Disease. *Front Mol Neurosci*. (2021) 14:723317. doi: 10.3389/fnmol.2021.723317

44. Rissin DM, Kan CW, Campbell TG, Howes SC, Fournier DR, Song L, et al. Single-molecule enzyme-linked immunosorbent assay detects serum proteins at subfemtomolar concentrations. *Nat Biotechnol*. (2010) 28:595–9. doi: 10.1038/nbt.1641

45. Zhang L, Du X, Su Y, Niu S, Li Y, Liang X, et al. Quantitative assessment of AD markers using naked eyes: point-of-care testing with paper-based lateral flow immunoassay. *J Nanobiotechnol*. (2021) 19:366. doi: 10.1186/s12951-021-01111-z

46. Hu S, Zhang L, Su Y, Liang X, Yang J, Luo Q, et al. Sensitive detection of multiple blood biomarkers via immunomagnetic exosomal PCR for the diagnosis of Alzheimer's disease. Science. *Advances*. (2024) 10:3088. doi: 10.1126/sciadv.abm3088

47. Zhang L, Cao K, Su Y, Hu S, Liang X, Luo Q, et al. Colorimetric and surface-enhanced Raman scattering dual-mode magnetic immunosensor for ultrasensitive detection of blood phosphorylated tau in Alzheimer's disease. *Biosens Bioelectron*. (2023) 222:114935. doi: 10.1016/j.bios.2022.114935

48. Zhang L, Su Y, Liang X, Cao K, Luo Q, Luo H. Ultrasensitive and point-of-care detection of plasma phosphorylated tau in Alzheimer's disease using colorimetric and surface-enhanced Raman scattering dual-readout lateral flow assay. *Nano Res*. (2023) 16:7459–69. doi: 10.1007/s12274-022-5354-4

49. Kim K, Kim MJ, Kim DW, Kim SY, Park S, Park CB. Clinically accurate diagnosis of Alzheimer's disease via multiplexed sensing of core biomarkers in human plasma. *Nat Commun*. (2020) 11:119. doi: 10.1038/s41467-019-13901-z

50. Hasegawa T, Shibayama S, Osumi Y, Sentsui H, Kato M. Quantitative performance of digital ELISA for the highly sensitive quantification of viral proteins and influenza virus. *Anal Bioanal Chem*. (2023) 415:1897–904. doi: 10.1007/s00216-023-04600-2

51. Wang ZY, Wei P. Shifting the paradigm in RNA virus detection: integrating nucleic acid testing and immunoassays through single-molecule digital ELISA. *Front Immunol*. (2024) 14:7. doi: 10.3389/fimmu.2023.1331981

52. Dong RK, Yi N, Jiang DC. Advances in single molecule arrays (SIMOA) for ultra-sensitive detection of biomolecules. *Talanta*. (2024) 270:125529. doi: 10.1016/j.talanta.2023.125529

53. Weuve J, Proust-Lima C, Power MC, Gross AL, Hofer SM, Thiebaut R, et al. Guidelines for reporting methodological challenges and evaluating potential bias in dementia research. *Alzheimers Dement*. (2015) 11:1098–109. doi: 10.1016/j.jalz.2015.06.1885

54. Scharfen J, Jansen K, Holling H. Retest effects in working memory capacity tests: a meta-analysis. *Psychon Bull Rev*. (2018) 25:2175–99. doi: 10.3758/s13423-018-1461-6

55. Jack CR Jr, Bennett DA, Blennow K, Carrillo MC, Dunn B, Haeberlein SB, et al. NIA-AA research framework: toward a biological definition of Alzheimer's disease. *Alzheimers Dement*. (2018) 14:535–62. doi: 10.1016/j.jalz.2018.02.018

frontiers | Frontiers in Neurology

TYPE Original Research
PUBLISHED 13 September 2024
DOI 10.3389/fneur.2024.1454061

OPEN ACCESS

EDITED BY
Qingchun Mu,
Second Affiliated Hospital of Soochow University, China

REVIEWED BY
Madiha Zahra Syeda,
Zhejiang University, China
Jiangwei Ding,
First Affiliated Hospital of Zhengzhou University, China
Hua Shen,
University of Southern California, United States

*CORRESPONDENCE
Shenyu Li
✉ swlishenyu@163.com
Famu Lin
✉ sdlinfamu@126.com

†These authors have contributed equally to this work and share first authorship

RECEIVED 24 June 2024
ACCEPTED 26 July 2024
PUBLISHED 13 September 2024

CITATION
Fu T, Mao C, Chen Z, Huang Y, Li H, Wang C, Liu J, Li S and Lin F (2024) Disease characteristics and clinical specific survival prediction of spinal ependymoma: a genetic and population-based study.
Front. Neurol. 15:1454061.
doi: 10.3389/fneur.2024.1454061

Disease characteristics and clinical specific survival prediction of spinal ependymoma: a genetic and population-based study

Tengyue Fu[1,2†], Chuxiao Mao[1†], Zhuming Chen[1†], Yuxiang Huang[1], Houlin Li[1], Chunhua Wang[3], Jie Liu[4], Shenyu Li[4]* and Famu Lin[5]*

[1]Guangdong-Hong Kong-Macau Institute of CNS Regeneration (GHMICR), Jinan University, Guangzhou, China, [2]The Department of Neurosurgery, The First Affiliated Hospital of Jinan University, Guangzhou, China, [3]College of Life Science and Technology, Mudanjiang Normal University, Mudanjiang, China, [4]The Department of Neurosurgery, The Second Affiliated Hospital of Guilin Medical University, Guilin, China, [5]The Department of Neurosurgery, Shunde Hospital of Southern Medical University, Foshan, China

Background: Spinal Ependymoma (SP-EP) is the most commonly occurring tumor affecting the spinal cord. Prompt diagnosis and treatment can significantly enhance prognostic outcomes for patients. In this study, we conducted a comprehensive analysis of RNA sequencing data, along with associated clinical information, from patients diagnosed with SP-EP. The aim was to identify key genes that are characteristic of the disease and develop a survival-related nomogram.

Methods: We first accessed the Gene Expression Integrated Database (GEO) to acquire the microarray dataset pertaining to SP-EP. This dataset was then processed to identify differentially expressed genes (DEGs) between SP-EP samples and normal controls. Furthermore, machine learning techniques and the CIBERSORT algorithm were employed to extract immune characteristic genes specific to SP-EP patients, thereby enhancing the characterization of target genes. Next, we retrieved comprehensive information on patients diagnosed with SP-EP between 2000 and 2020 from the Surveillance, Epidemiology, and End Results Database (SEER). Using this data, we screened for predictive factors that have a significant impact on patient outcomes. A nomogram was constructed to visualize the predicted overall survival (OS) rates of these patients at 3, 5, and 8 years post-diagnosis. Finally, to assess the reliability and clinical utility of our predictive model, we evaluated it using various metrics including the consistency index (C-index), time-dependent receiver operating characteristic (ROC) curves, area under the curve (AUC), calibration curves, and decision curve analysis (DCA).

Results: A total of 5,151 DEGs were identified between the SP-EP sample and the normal sample. Analysis of Gene Ontology (GO) and Kyoto Encyclopedia of Genes and Genomes (KEGG) pathways revealed that these DEGs were primarily involved in cellular processes, including cell cycle regulation and cell sensitivity mechanisms. Furthermore, immune infiltration analysis was utilized to identify the core gene *CELF4*. Regarding the survival rates of patients with SP-EP, the 3-year, 5-year, and 8-year survival rates were 72.5, 57.0, and 40.8%, respectively. Diagnostic age ($p < 0.001$), gender ($p < 0.001$), and surgical approach ($p < 0.005$) were identified as independent prognostic factors for OS. Additionally, a nomogram model was constructed based on these prognostic

factors, demonstrating good consistency between predicted and actual results in the study's validation process. Notably, the study also demonstrated that more extensive surgical resection could extend patients' OS.

Conclusion: Through bioinformatics analysis of microarray datasets, we identified *CELF4* as a central gene associated with immune infiltration among DEGs. Previous studies have demonstrated that *CELF4* may play a pivotal role in the pathogenesis of SP-EP. Furthermore, this study developed and validated a prognostic prediction model in the form of a nomogram utilizing the SEER database, enabling clinicians to accurately assess treatment risks and benefits, thereby enhancing personalized therapeutic strategies and prognosis predictions.

KEYWORDS

spinal ependymoma, *CELF4*, SEER, nomogram, prognosis

1 Introduction

SP-EP is a rare primary tumor of the central nervous system, typically arising from ependymoma cells in the spinal cord's central canal. Its incidence peaks in adults aged 40–45 years (1, 2). Based on the WHO grading system, SP-EP is categorized into grades I-III, reflecting differences in cell heterogeneity and proliferative activity. Notably, the 2022 WHO diagnostic criteria for ependymoma saw mucinous papillary ependymoma elevated to grade II, with the anaplastic subtype no longer classified. Instead, specific subtypes are described histopathologically (3, 4). Clinical manifestations of SP-EP vary depending on tumor location, size, and growth rate, causing significant physical and mental distress to patients (5, 6). Surgical resection remains the primary treatment aiming for maximum safety. Guidelines recommend adjuvant radiotherapy (RT) for grade II primary SP-EP and all grade III cases post-surgery. However, the use of radiotherapy is controversial, and optimal dosing and prognostic benefits remain undetermined (7, 8). Systemic chemotherapy's role in treating SP-EP is limited, with minimal lasting efficacy. Its impact on progression-free survival is also restricted. Therefore, chemotherapy is typically reserved as an adjuvant for recurrent cases where resection or radiotherapy is not feasible (9, 10).

Bioinformatics analysis, a powerful tool, uncovers potential molecular markers of disease by comparing gene expression patterns between patients and healthy controls (11). Nowadays, in-depth transcriptome bioinformatics analysis offers a fresh perspective in searching for diagnostic markers, prognostic indicators, and therapeutic targets. Nomogram, as a tool for comprehensive analysis and visual representation of prognostic risk factors, enable more accurate risk quantification. Notably, nomogram have been extensively utilized in prognostic assessments of intracranial mass lesions, including meningiomas, gliomas, and central lymphoma (12–14). However, due to limited data availability, there is currently no clinical prediction model tailored for SP-EP in practical application. Therefore, developing a novel model for this patient group is imperative. The GEO database[1] serves as a widely accessed gene sequencing resource, enabling us to retrieve SP-EP-specific genetic information. Furthermore, the SEER database[2] represents a reliable and extensive online platform for collecting cancer statistics in the US population.

2 Materials and methods

2.1 Data collection and analysis

In this study, RNA sequencing data from 14 SP-EP patients were retrieved from two chips in the GEO database: GSE66354 and GSE50161. To eliminate potential batch effects, the Combat method was applied to preprocess all RNA seq data. Subsequently, the annotation library "hgu133plus2.db" was utilized to map probe sets to their respective gene symbol identifiers. Probe sets annotated to the same gene symbol identifier were then aggregated using their average values (15). For the GSE54934 dataset, the "limma" package in R software was employed to identify DEGs between tumor samples and normal samples (16). DEGs were selected using a cutoff criterion of $|\log2FC| > 1$ and an adjusted p-value (P adj) < 0.05 (15, 17). This approach allowed us to filter out significant DEGs for further analysis.

2.2 Functional enrichment analysis

To identify DEGs between two subgroups and understand their functional clustering, the "clusterProfiler" package in R software is utilized. This package performs statistical analysis and visualization of gene set functional clustering, providing insights into the biological roles of the identified DEGs (18). Furthermore, KEGG pathway enrichment analysis is conducted using the "clusterProfiler" package to investigate the main metabolic and signaling pathways associated with the DEGs (19). This analysis helps to identify the key biological processes and interactions underlying the observed gene expression differences. Gene Ontology (GO) is a comprehensive ontology in bioinformatics, encompassing three core domains: biological processes (BP), cellular components (CC), and molecular functions

1 https://www.ncbi.nlm.nih.gov/geo/

2 https://seer.cancer.gov/

(MF) (20). Through KEGG pathway annotation and analysis of DEGs, the primary metabolic and signaling pathways associated with these genes can be identified (21). A significance threshold of $p < 0.05$ is adopted for enrichment analysis.

2.3 Utilizing machine learning techniques to identify disease-specific characteristic genes

To search for disease characteristic genes among differentially expressed genes, we initially employed the LASSO regression method. This approach utilized the "glmnet" package in R software to filter the expression levels of differentially expressed genes. Cross-validation was then conducted to identify the gene with the minimum error as the disease characteristic gene. Furthermore, we also screened disease characteristic genes using the SVM-RFE method. This involved filtering differential gene expression through the "e1071," "kernlab," and "caret" packages in R software. Similarly, cross-validation was employed to determine the gene with the lowest error as the disease characteristic gene. Finally, we intersected the disease characteristic genes identified by both methods and generated a VENN diagram to select the final set of disease characteristic genes.

2.4 Immune infiltration analysis of chips: a methodological perspective

Utilizing R software (version 4.3.1), along with the CIBERSORT algorithm, we conducted an analysis of the previously obtained and corrected gene expression matrix from the joint chip. This analysis aimed to identify genes with a significance level of $p < 0.05$ and to assess the proportion of 22 distinct species present in each sample. Furthermore, the CIBERSORT algorithm was employed to quantify the proportion of infiltrating immune cells. Additionally, the "limma" package within R software was leveraged to compare the ratios between high-risk and low-risk groups.

2.5 Research design and data collection

The SEER research data is accessible for public utilization by registered users, and the committee has exempted the necessity for informed consent, thereby eliminating the requirement for patient consent (license number: 13950, November 2021). Leveraging the SEER database, which was released in April 2024, we identified 1,696 patients diagnosed with SP-EP. The data retrieval process was facilitated by the SEER*Stat software, specifically version 8.4.3. To pinpoint patients with SP-EP, we utilized the primary tumor site code (C72.0), as stipulated in the third edition of the International Classification of Diseases for Oncology. Additionally, the histological code (ICD-O-3:9391/3) specific to ependymoma was employed for further classification. During our selection process, we excluded patients with the following characteristics: (1) unknown race and marital status, (2) unspecified tumor size (codes: 000/990/991/994/995/999), and (4) undetermined radiation therapy status. Consequently, as illustrated in Figure 1, 826 cases were ultimately included in our subsequent research and were randomly allocated to the training and validation sets in a 7:3 ratio.

2.6 Variable selection and research design

Clinical information is derived from the SEER database, encompassing various patient characteristics such as age at diagnosis, gender (male or female), racial categories (white, black, or other), marital status (married, unmarried, or unknown), tumor dimensions, tumor count (single or multiple), surgical intervention details, radiation therapy status (received or not received), and chemotherapy administration (administered or not administered). The X-tile program is utilized to categorize patients based on age into two groups: those aged ≤64 years and those >64 years. Tumor size is categorized using the median value as the cutoff. Surgical resection extents are classified into three categories: non-surgical resection, biopsy/STR, and total resection. The primary endpoint for measurement is OS. The conclusion of the follow-up period is set as December 31, 2020.

2.7 Construction and validation of nomograms

Using the cph() function in the RMS package of R language software, we constructed a predictive model that relies on independent prognostic factors to forecast the 1-year, 2-year, and 3-year OS rates among patients with SP-EP. Subsequently, we employed the plot() functions to generate corresponding survival prediction nomograms and visualize the prediction model. To identify independent prognostic variables, univariate and multivariate Cox regression analysis was conducted on the training dataset. The significant variables derived from this analysis were then utilized to develop nomograms for predicting the OS of SP-EP. To assess the performance of the nomograms, we utilized various evaluation methods. Specifically, the calibration curve was used to demonstrate the accuracy of nomogram predictions. Additionally, the time-dependent ROC curve and AUC were calculated to evaluate the nomograms' ability to discriminate between different patient groups over time. Finally, to confirm the robustness of our findings, the nomograms were tested on the validation dataset and reanalyzed accordingly.

2.8 Clinical correlation

Perform DCA to evaluate the clinical utility of nomograms for practical clinical applications. The optimal critical value for each patient's risk score is determined using the ROC curve. After calculating the risk score, patients in the training and validation cohorts are classified into high-risk and low-risk groups. To evaluate survival differences, we employed K-M survival curves to analyze OS differences between these groups. Additionally, we examined the influence of various surgical conditions on survival times between high-risk and low-risk patients.

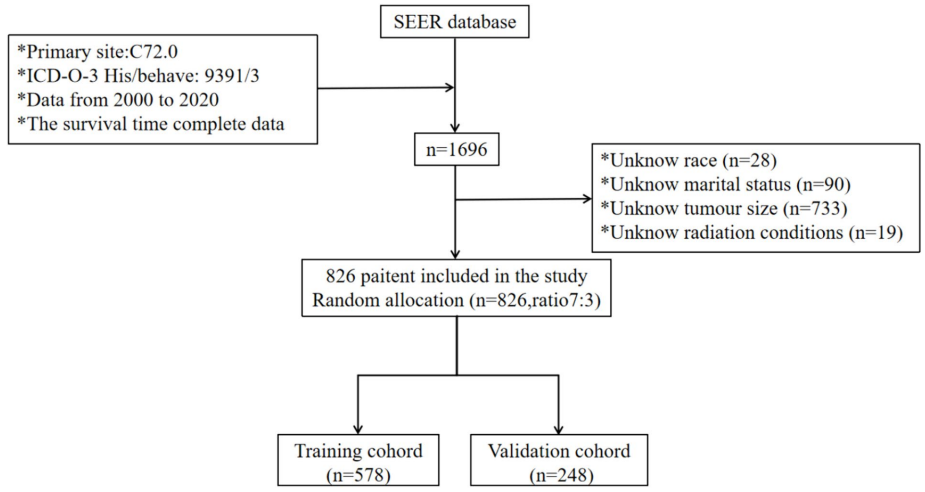

FIGURE 1
Participant inclusion and exclusion flowchart. SEER, Surveillance, Epidemiology, and End Result Program; ICD-0-3, International Classification of Disease for Oncology, Third Edition.

2.9 Statistical analysis

We apply χ^2. We verify the clinical variables between the training set and validation set and conduct univariate and multivariate Cox proportional hazards regression analysis to identify independent predictors of survival specifically within the training set. The consistency index (C-index) serves as a metric to assess the authenticity and reliability of the model represented by the nomogram. A calibration chart is constructed to assess the agreement between predicted and observed values. DCA is used to analyze the effectiveness of commonly used nomograms and prognostic indicators in clinical practice. Kaplan Meier method and logarithmic rank test are utilized for survival analysis. All statistical analyses were conducted using R software (version 4.3.1). The R packages used in this study include "rms," "survival," "surveyor," and "ggDCA." All statistical significance in this study was determined using a $p < 0.05$.

3 Results

3.1 RNA-seq gene differential analysis

To delve into the pathogenic core genes of SP-EP, we first retrieved mRNA expression profiles of SP-EP and normal tissues from GEO (GSE50161 and GSE66354). Subsequently, we filtered and identified DEGs for comparison with normal tissues. Our analysis revealed a total of 5,151 DEGs, of which 2,679 genes were upregulated (log2 FC > 1) and 2,472 genes were downregulated (log2 FC < −1). This finding is illustrated in Figure 2.

3.2 Functional enrichment analysis

To delve deeper into the functions of the 5,151 DEGs in SP-EP, statistical analysis and visualization of their functional clustering were conducted using the "clusterprofile" package in R software. Table 1 presents the top 5 GO items of DEGs, sorted by *p*-values. From the BP analysis, it emerged that these DEGs primarily participate in processes such as chromosome segregation, nuclear chromosome segregation, sister chromatid segregation, mitotic sister chromatid segregation, and mitotic nuclear division. In the CC analysis, they were significantly associated with spindle, mitotic spindle, chromosome centromeric region, chromosomal region, and condensed chromosome. Furthermore, the MF analysis revealed that the DEGs are primarily involved in microtubule binding, tubulin binding, microtubule motor activity, cytoskeletal motor activity, and CXCR chemokine receptor binding. To gain additional insights into the crucial pathways of these DEGs, we conducted a KEGG pathway analysis. The results, depicted in Figure 3 and Table 2, revealed that the top 10 enriched KEGG pathways, ranked by *p*-values, primarily encompassed Cell cycle, Cellular senescence, Oocyte meiosis, Motor proteins, IL-17 signaling pathway, Viral protein interaction with cytokine and cytokine receptor, Progesterone-mediated oocyte maturation, p53 signaling pathway, and Human T-cell leukemia virus 1 infection.

3.3 Machine learning method for obtaining disease characteristic genes

We applied LASSO regression to filter differential gene expression using the R software "glmnet" package. Seven genes with the lowest error values were selected as disease characteristic genes, and relevant visualization graphs were drawn (Figures 4A,B). The vertical axis represents the error size, the horizontal axis represents the number of genes, and gene errors were ranked from high too low to obtain *UNC13C*, *CNTNAP4*, *SYN1*, *CELF4*, *CYP4X1*, *SEC14L5*, and *CLEC2L*. Furthermore, we utilized the SVM-RFE method to screen disease characteristic genes, employing the R software packages "e1071," "kernlab," and "caret" to filter differential gene expression. We employed cross-validation to identify the disease characteristic genes with minimal error and conducted visual analysis (Figure 4C). The vertical axis represents the error size, and the horizontal axis

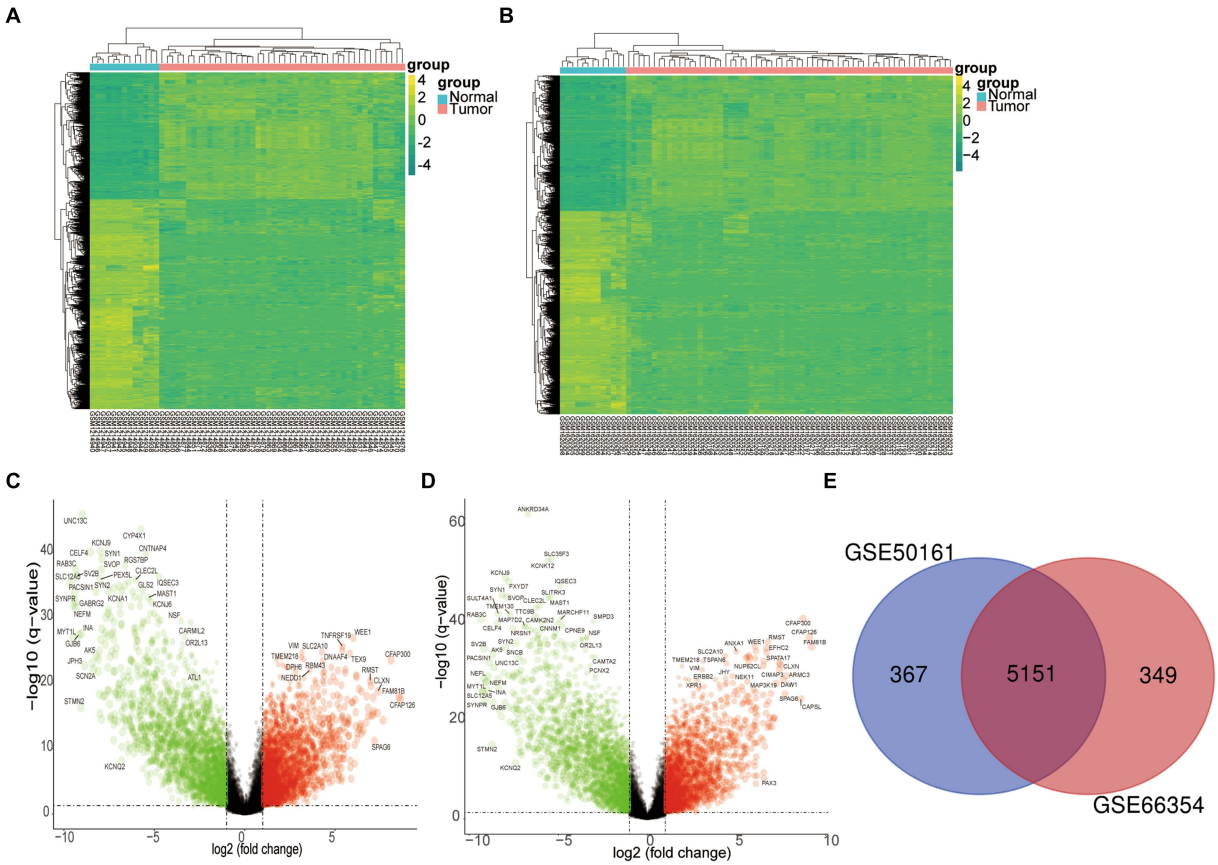

FIGURE 2
Differentially expressed genes. **(A)** The heatmap of DEGs in GSE50161 was generated using R software, with expression profiles above the mean depicted in yellow and those below in green. **(B)** Similarly, a heatmap for DEGs in GSE66354 was created through R software. **(C)** A volcano plot was constructed to visualize the differentially expressed genes in GSE50161, log FC: log2 fold change. **(D)** A volcano plot was also generated for the differentially expressed genes in GSE66354. **(E)** A Venn diagram illustrates the intersection of DEGs between GSE50161 and GSE66354 databases.

TABLE 1 GO enrichment analysis of DEGs in SP-EP.

Category	Term	Count	Gene ratio	*p*-value
BP	Chromosome segregation	34	34/99	2.43E-31
BP	Nuclear chromosome segregation	30	30/99	6.47E-30
BP	Sister chromatid segregation	27	27/99	1.56E-29
BP	Mitotic sister chromatid segregation	25	25/99	9.75E-29
BP	Mitotic nuclear division	28	28/99	1.23E-28
CC	Spindle	24	24/100	1.07E-18
CC	Mitotic spindle	18	18/100	1.68E-18
CC	Chromosome, centromeric region	20	20/100	1.85E-18
CC	Chromosomal region	23	23/100	2.91E-18
CC	Condensed chromosome	20	20/100	9.95E-18
MF	Microtubule binding	14	14/97	1.56E-10
MF	Tubulin binding	14	14/97	1.09E-08
MF	Microtubule motor activity	7	7/97	6.54E-08
MF	Cytoskeletal motor activity	7	7/97	2.03E-06
MF	CXCR chemokine receptor binding	4	4/97	2.06E-06

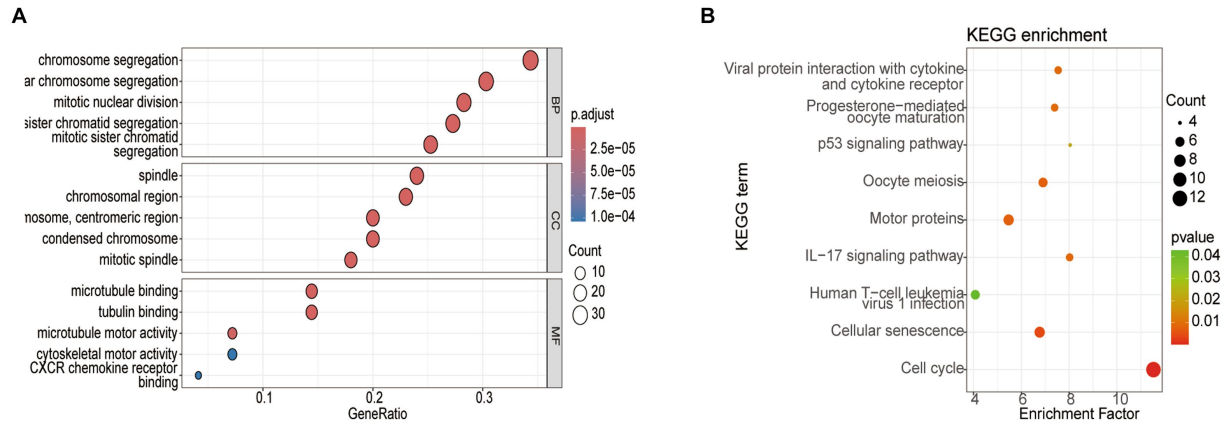

FIGURE 3
Analysis of the top 5 enriched GO and top 10 KEGG pathways in DEGs. **(A)** GO enrichment analysis. **(B)** KEGG enrichment pathway analysis. Node size represents the proportion of genes; The node color represents the *p*-value.

TABLE 2 KEGG enrichment analysis of DEGs in SP-EP.

Category	Term	Count	Gene ratio	*p*-value
hsa04110	Cell cycle	12	12/58	3.21E-10
hsa04218	Cellular senescence	7	7/58	7.04E-05
hsa04114	Oocyte meiosis	6	6/58	0.000215
hsa04814	Motor proteins	7	7/58	0.000265
hsa04657	IL-17 signaling pathway	5	5/58	0.000377
hsa04061	Viral protein interaction with cytokine and cytokine receptor	5	5/58	0.000501
hsa04914	Progesterone-mediated oocyte maturation	5	5/58	0.000549
hsa04115	p53 signaling pathway	4	4/58	0.001491
hsa05166	Human T-cell leukemia virus 1 infection	6	6/58	0.003364

represents the number of genes. Thirty-one genes with minimal error expressions were identified. The intersection of the disease characteristic genes obtained from both methods was taken, and a Venn diagram was drawn (Figure 4D) to obtain *SYN1*, *CELF4*, and *CYP4X1*.

3.4 Immune infiltration analysis

Based on 22 immune-related gene sets, we conducted immune infiltration analysis, which revealed the subtypes of immune cells, their corresponding abundances, and variations in the proportions of various immune cells across tumor samples. As depicted in Figures 5A,B, the proportions of Macrophages M2, CD4+ memory resting T cells, Eosinophils, Monocytes, and Neutrophils were comparatively high in SP-EP tumor tissue, whereas the proportions of other immune cell types were relatively low. To further investigate the association between three key genes and immune cell infiltration, patients were stratified into high-and low-risk groups. The results are presented in Figures 5C–E. Notably, a significant difference was observed in the proportions of follicular helper T cells and Monocytes between the two groups in the context of *CELF4* ($p < 0.05$). However, no significant differences were detected for *SYN1* and *CYP4X1* ($p > 0.05$).

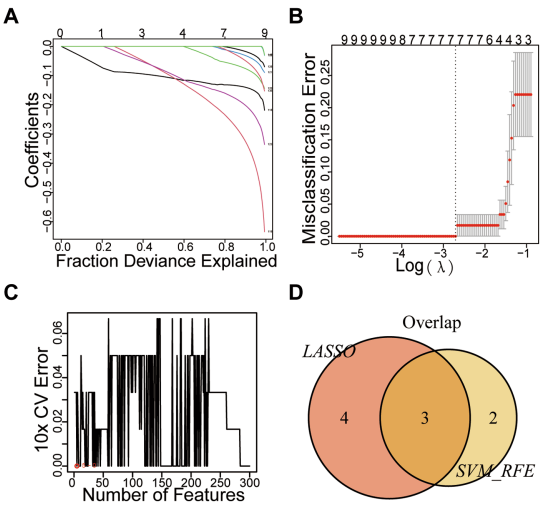

FIGURE 4
Mechanical Learning Method for Identifying Disease-Specific Genes. **(A)** LASSO Coefficient Curve Depicting Prognostic DEGs. **(B)** Cross-Validation for Selecting Optimal Regularization Parameters (λ). **(C)** SVM-RFE Diagram. **(D)** VENN Diagram.

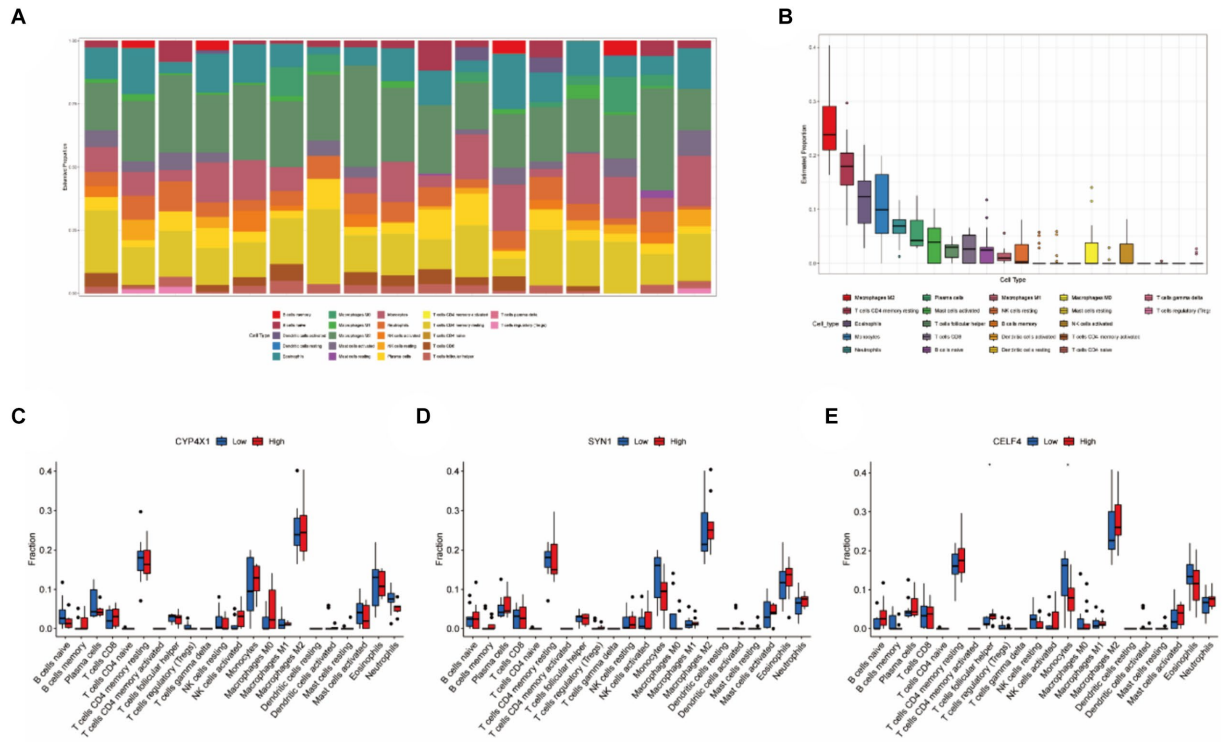

FIGURE 5
Immune infiltration analysis based on 22 immune related gene sets. **(A)** Representing 22 subtypes of immune cells, each bar chart abundance represents the proportion of immune cells in each sample, and different colors represent each subtype. **(B)** Differences in the proportion of 22 subtypes of immune cells. **(C–E)** Comparative analysis of the proportion of immune infiltrating cells between the high-risk and low-risk groups of *CELF4*, *SYN1*, and *CYP4X1* (*$p < 0.05$).

3.5 Clinical characteristics of patients

Our study encompassed 826 patients diagnosed with SP-EP in the SEER database spanning the years 2000–2020. Of these patients, the training set comprised 578 individuals (70%) and the validation set consisted of 248 individuals (30%). In terms of age distribution, the majority of patients (87.3%) fell within the young age bracket of ≤64 years, with 12.7% belonging to the elderly group (>64 years). Regarding gender, 47.2% were male and 52.8% were female. Notably, young women under 64 years of age constituted the primary affected group, accounting for 45.9 and 46.5% in the training and validation sets, respectively. In terms of tumor characteristics, male patients exhibited an average tumor size of 34.6 mm, whereas female patients had an average tumor size of 27.9 mm. When it came to treatment options, surgical intervention was the most preferred method, with 78.3% of patients opting for it. Radiotherapy followed as the second most common choice, accounting for 16.3% of patients. Chemical drug treatment, however, was chosen by only a minuscule proportion of 0.4%, and none of these patients underwent either surgery or radiation therapy. It is important to mention that sequential variables related to surgery, radiotherapy, and chemotherapy are not recorded in the SEER database. Similarly, detailed information about the drugs used in chemotherapy is also unavailable. For a comprehensive overview of the clinical data, please refer to Table 3.

3.6 Variable selection

In this study, the optimal cutoff value for continuous variables was determined using X-Tile software (version 3.6.1). The patient's age was categorized into two groups: ≤64 years old and >64 years old, as depicted in Figure 6. To assess the interaction among various covariates, relevant factors with $p < 0.05$ in both univariate and multivariate Cox proportional risk models were combined to identify independent prognostic factors. The findings revealed that age ($p < 0.001$), gender ($p < 0.001$), and surgical method ($p < 0.005$) served as independent predictors of prognosis, as summarized in Table 4. Notably, younger age, female gender, and complete surgical resection were factors that significantly contributed to improved overall survival (OS) in patients with SP-EP.

3.7 Nomogram validation

Based on Cox univariate/multivariate regression analysis, we constructed prognostic models for 3-year, 5-year, and 8-year overall survival (OS) in SP-EP patients. The results, visualized in Figure 7 as nomogram, reveal that age is the most significant prognostic factor, followed by surgical methods and gender differences. Each factor level is assigned a grade score, enabling visual calculation through the nomogram. Summing the scores across all factors provides the corresponding OS value. In both the

10.3389/fneur.2024.1454061

TABLE 3 Patient characteristics and socio-demographic.

Characteristics	Training cohort (n = 578), n (%)	Validation cohort (n = 248), n (%)	p-value
Age (n%)			
≤64 years	501 (86.7%)	220 (88.7%)	721 (87.3%)
>64 years	77 (13.3%)	28 (11.3%)	105 (12.7%)
Sex (n%)			
Male	272 (47.1%)	118 (47.6%)	390 (47.2%)
Female	306 (52.9%)	130 (52.4%)	436 (52.8%)
Race (n%)			
White	488 (84.4%)	219 (88.3%)	707 (85.6%)
Black	52 (9.0%)	11 (4.4%)	63 (7.6%)
Other	38 (6.6%)	18 (7.3%)	56 (6.8%)
Marital status (n%)			
Single	151 (26.1%)	62 (25.0%)	213 (25.8%)
Married	343 (59.3%)	158 (63.7%)	501 (60.7%)
Others	84 (14.5%)	28 (11.3%)	112 (13.6%)
Size (n%)			
<30 mm	353 (61.1%)	160 (64.5%)	513 (62.1%)
≥30 mm	225 (38.9%)	88 (35.5%)	313 (37.9%)
Number (n%)			
Single	494 (85.5%)	217 (87.5%)	711 (86.1%)
Multiple	84 (14.5%)	31 (12.5%)	115 (13.9%)
Surgery (n%)			
GTR	163 (28.2%)	86 (34.7%)	249 (30.1%)
Biopsy/STR	288 (49.8%)	110 (44.4%)	398 (48.2%)
NO surgery	127 (22.0%)	52 (21.0%)	179 (21.7%)
Radiation (n%)			
Yes	99 (17.1%)	36 (14.5%)	135 (16.3%)
No	479 (82.9%)	212 (85.5%)	691 (83.7%)
Chemotherapy (n%)			
Yes	2 (0.3%)	1 (0.4%)	3 (0.4%)
No	576 (99.7%)	247 (99.6%)	823 (99.6%)

GTR, total resection; RT, radiotherapy; STR, subtotal resection.

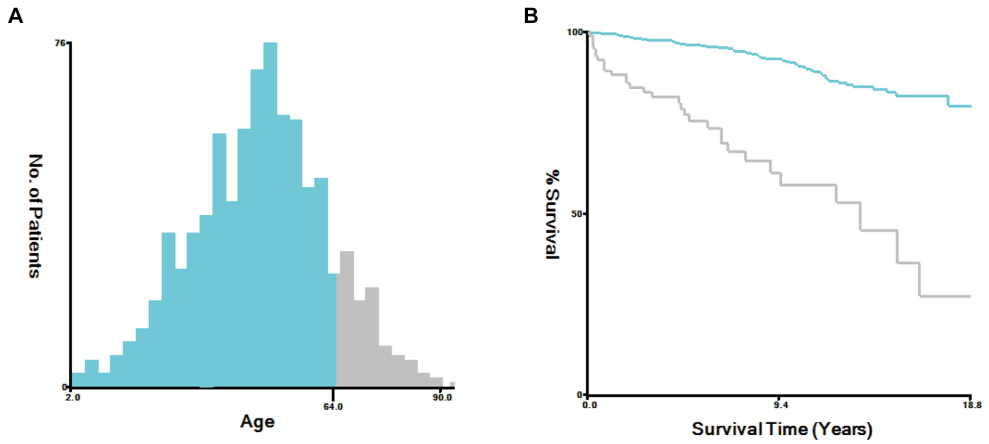

FIGURE 6
Sing X-Tile software to determine the optimal cutoff values for age. **(A)** Age-Survival Histogram. **(B)** Age-Survival Kaplan Meier diagram.

TABLE 4 Univariate and multivariate analyses of characteristics for predicting overall survival (OS) in patients with SP-EP.

Variables	Univariate			Multivariate		
	HR	95%CI	*p*-value	HR	95%CI	*p*-value
Age (years)						
≤64	Ref.			Ref.		
>64	6.1	3.9–9.5	$p < 0.001$*	5.2633	2.6847–8.6682	$p < 0.001$*
Sex						
Male	Ref.			Ref.		
Female	0.58	0.38–0.89	$p < 0.001$*	0.6418	0.3697–1.0803	$p < 0.001$*
Race						
White	Ref.			Ref.		
Black	−0.04	0.52–2.5	$p = 0.95$	1.6197	0.6102–4.2958	$p = 0.333$
Others	−0.04	0.39–2.4		1.6474	0.4935–5.4941	$p = 0.417$
Marital status						
Single	Ref.			Ref.		
Married	0.44	0.51–1.4	$p = 0.089$	0.4858	0.3800–1.4747	$p = 0.552$
Divorced/separated/widowed	0.44	0.83–2.9		1.0883	0.4880–2.4275	$p = 0.803$
Size (mm)						
≤30	Ref.			Ref.		
>30	1.23	0.64–1.5	$p = 0.94$	1.2460	0.7203–2.1572	$p = 0.431$
Tumor number						
Single	Ref.			Ref.		
Multiple	3.7	2.4–5.7	$p = 0.013$*	3.3463	1.8936–5.9127	$p = 0.093$
Surgery						
GTR	Ref.			Ref.		
Biopsy/STR	0.84	0.82–2.5		1.3168	0.6426–2.6946	$p = 0.452$
NO surgery	0.84	1.4–3.9	$p = 0.0046$*	9.1490	1.3045–4.7786	$p < 0.005$*
Radiation						
Yes	Ref.			Ref.		
No	0.73	0.44–1.2	$p = 0.22$	7.6595	0.4126–1.422	$p = 0.398$
Chemotherapy						
Yes	Ref.			Ref.		
No	0.2	0.028–1.5	$p = 0.11$	1.3764	0.0000-Inf	$p = 0.996$

GTR, total resection; RT, radiotherapy; STR: subtotal resection. *$p < 0.05$; HR, hazard ratio; CI, confidence interval.

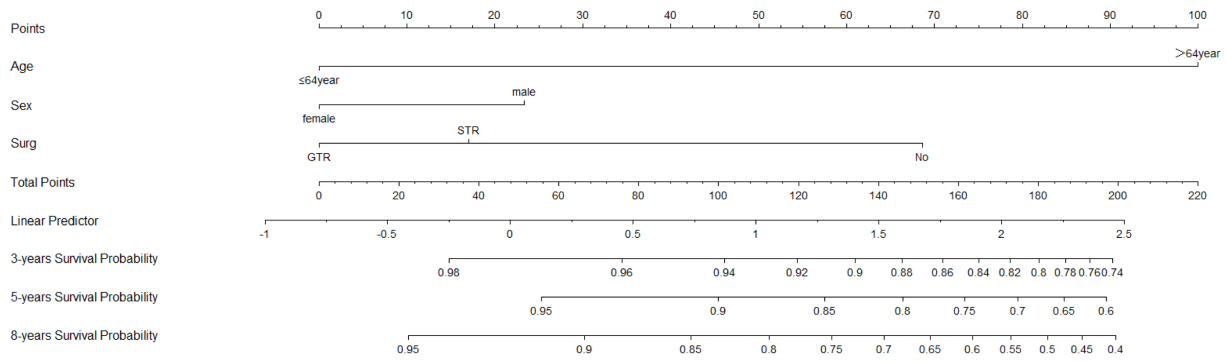

FIGURE 7
The nomograms to predict OS at 3-, 5-, and 8-year with SP-EP. SEER, Surveillance, Epidemiology, and End Result Program; OS, overall survival.

training and validation sets, the C-index of the OS prediction model is 0.741 and 0.747, respectively (Table 5). Additionally, the AUC values for 3, 5, and 8 years indicate good discriminability of the prediction model (Figure 8). To assess the calibration level of the OS prediction models, we employed calibration curve graphs. Both the modeling and validation groups demonstrate a high overlap between the calibration curve and the standard line (Figure 9), indicating a strong correlation between the predicted and observed survival rates. Furthermore, we evaluated the clinical applicability of the prediction model using DCA (Figure 10). The results demonstrate a wide threshold probability range and a high net benefit for predicting 3-year, 5-year, and 8-year survival rates in SP-EP patients.

TABLE 5 C-index for training and validation sets in OS nomograms.

	Training set		Validation set	
	C-index	95%CI	C-index	95%CI
OS	0.741		0.747	

C-index, concordance index; OS, overall survival; CI, confidence interval.

4 Discussion

In this study, we retrieved spinal meningioma data from the GEO database and conducted a comprehensive analysis of the genetic profiles of affected patients. Differential gene analysis revealed a significant enrichment of genes primarily associated with chromosome segregation, nuclear chromosome segregation, and sister chromatid segregation. These genes are intricately involved in cellular processes such as cell cycle regulation, cellular sensitivity mechanisms, meiotic events in oocytes, motor protein functions, and the IL-17 signaling pathway—all of which are closely linked to immunological functions. Subsequently, we identified three core genes: *CELF4*, *SYN1*, and *CYP4X1*. Notably, *CYP4X1* appears to play a pivotal role in the pathogenesis and immune infiltration associated with SP-EP.

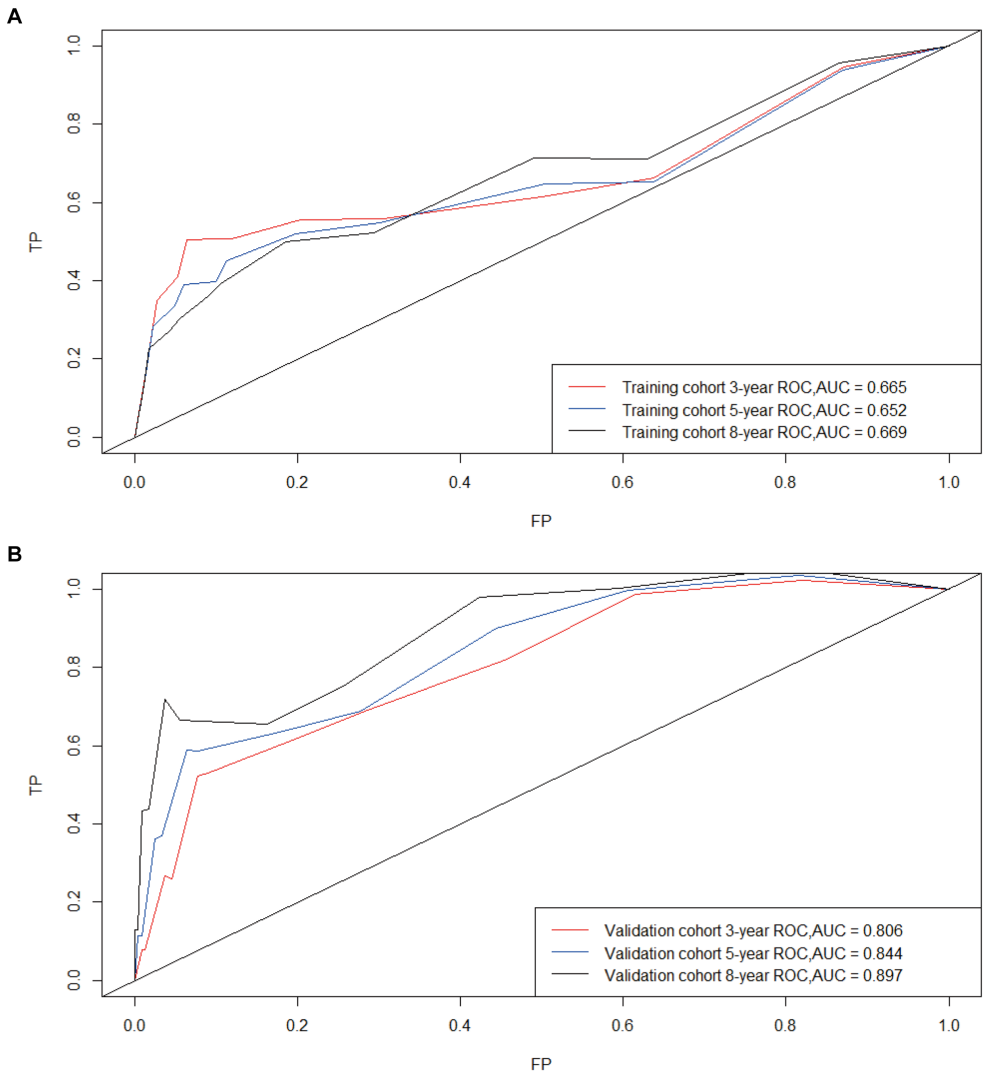

FIGURE 8
Time-dependent curves (ROC) of the nomogram for 3-, 5-, and 8-year predictions; AUC for predicting OS in the training cohort **(A)** and validation cohort **(B)**.

CELF4 (CUGBP Elav Like Family Member 4), an RNA-binding protein, plays diverse roles in cellular processes such as RNA splicing and mRNA stability. Its expression has been shown to influence the immune response within the tumor microenvironment. Specifically, studies suggest that *CELF4* might suppress the anti-tumor immune response by regulating immune checkpoint molecules (22, 23). Additionally, *CELF4* expression has been associated with poor prognosis in colorectal cancer, indicating its significance in the pathogenesis of this malignancy (24). Immune tumor infiltration is crucial in cancer development, metastasis, and immune escape, affecting patient prognosis (25–27).

CELF4 is widely expressed, with high levels observed in the central nervous system (28). SP-EP, a rare tumor originating from ependymal cells, remains understudied regarding the role of *CELF4*. However, insights can be drawn from studies on *CELF4*'s function in other CNS tumors, such as glioblastoma, which suggest its involvement in tumor progression and aggressiveness (29–31). The exact mechanism underlying *CELF4*'s influence on tumor immune infiltration in SP-EP remains elusive. Based on findings in other cancers, it is hypothesized that *CELF4* may regulate the expression of genes involved in antigen presentation, cytokine signaling, and immune cell recruitment within the tumor microenvironment (22, 32). Future research is warranted to delve deeper into the specific role of *CELF4* in SP-EP and its intricate interplay with the tumor immune response. Studies exploring *CELF4* expression levels in patients with SP-EP and their correlation with immune cell infiltration would be highly valuable. Additionally, functional studies aimed at elucidating the precise mechanisms by which *CELF4* regulates immune infiltration in this specific cancer type are urgently needed.

In addition, we conducted an extensive retrospective study focusing on the clinical data of SP-EP patients, thereby presenting the most recent evidence for their epidemiological analysis. Utilizing the SEER database, we developed clinical prognostic models that encompassed 3-year, 5-year, and 8-year survival probabilities by extracting potential prognostic factors specific to patients with

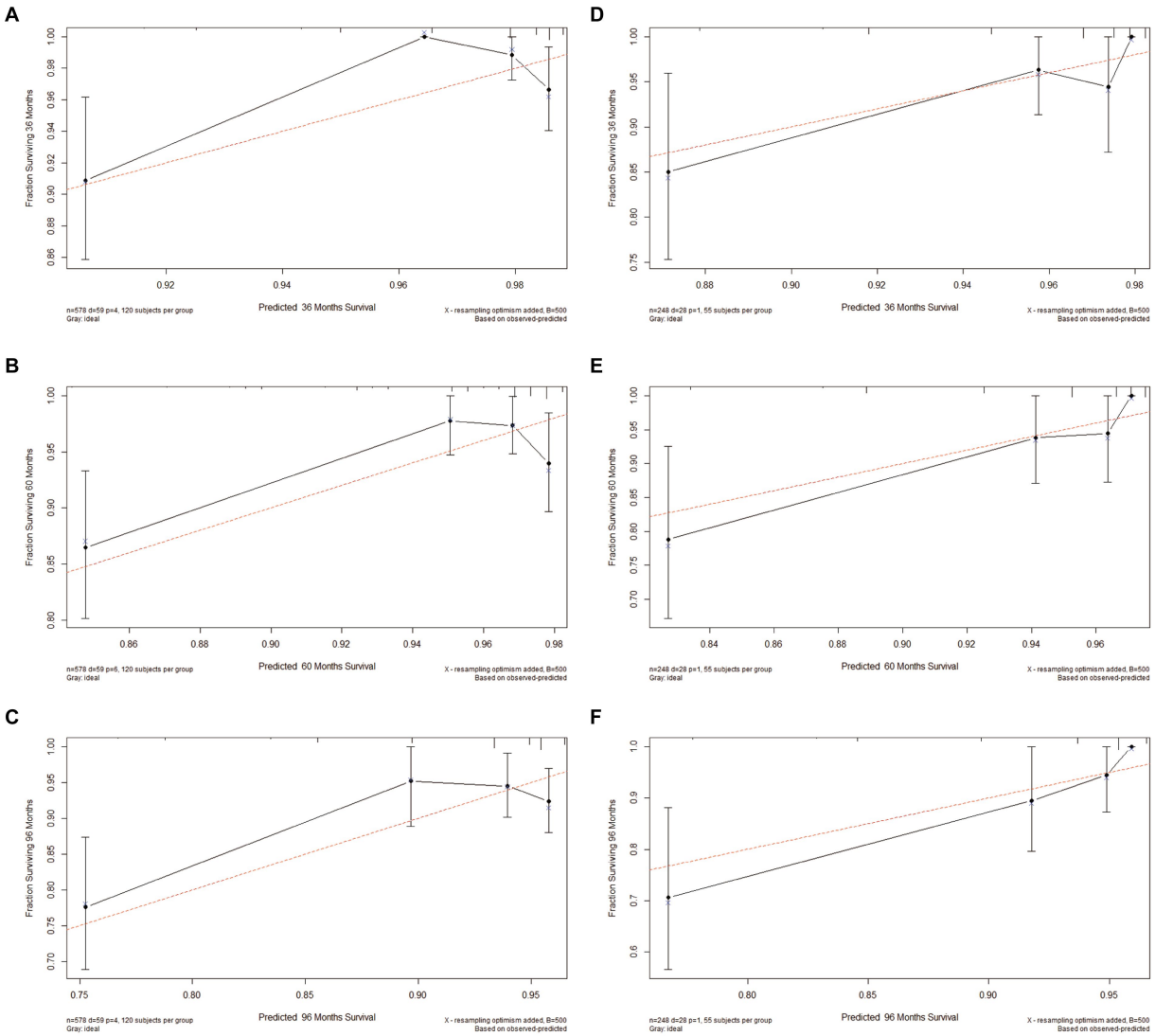

FIGURE 9
Calibration plots of 3-, 5-, and 8-year OS for patients with intramedullary SP-EP. **(A–C)** Calibration plots of 3-, 5-, and 8-year OS in the training cohort. **(D–F)** Calibration plots of 3-, 5-, and 8-year OS in the validation cohort.

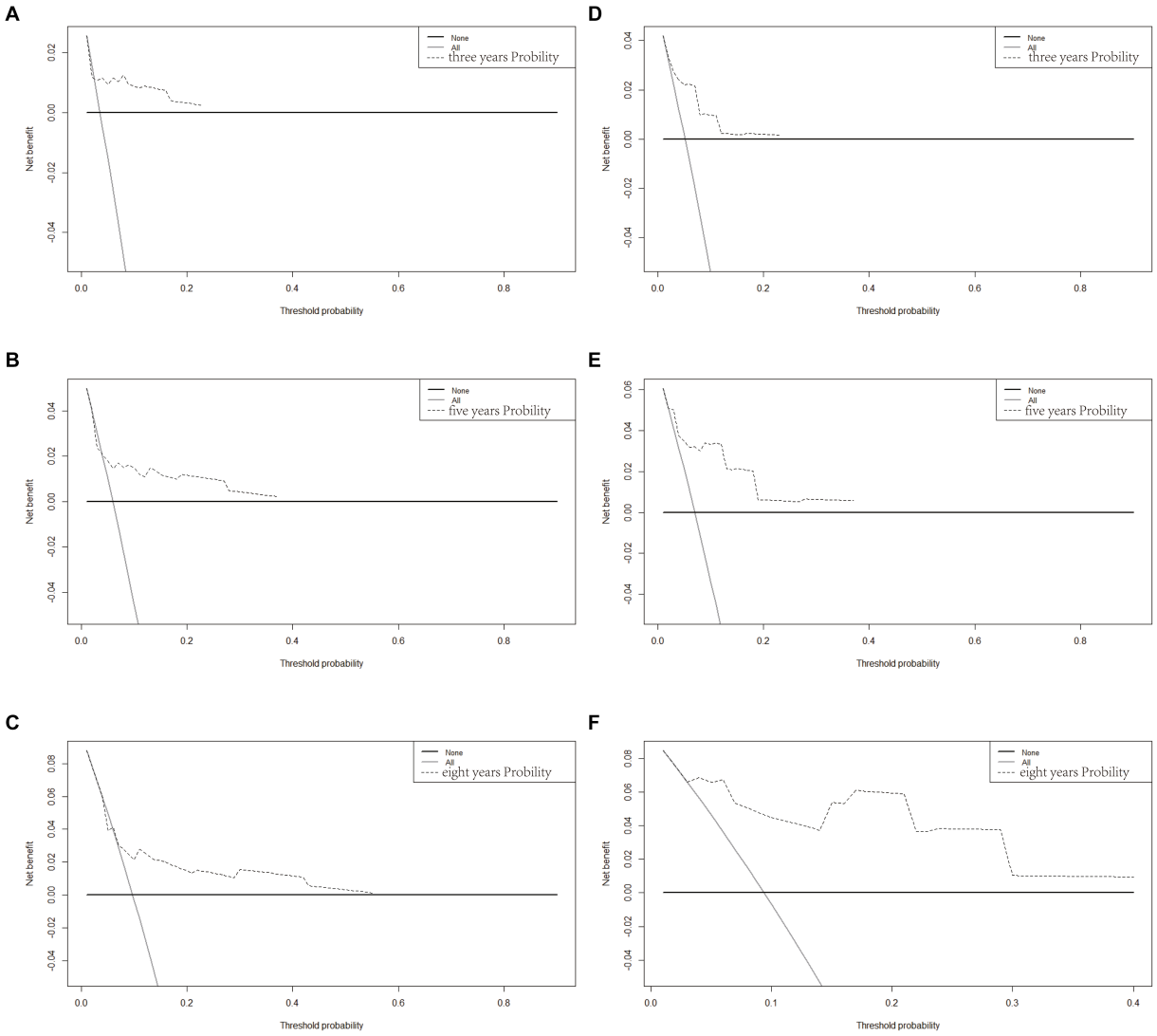

FIGURE 10
Decision curve analysis of the OS-associated nomograms. DCA curves of 3-, 5-, and 8-year OS in the training cohort **(A–C)** and validation cohort **(D–F)**.

SP-EP. Our findings indicate that age, gender, and surgical approach are potentially significant predictors of survival outcomes for SP-EP patients.

Consistent with previous findings by Boström et al. (33), age serves as a crucial factor influencing the prognosis of SP-EP patients. In cases where other tumor characteristics remain constant, the overall survival rate (OS) among older patients is significantly lower compared to younger patients, displaying a statistically significant difference (34). Through a combination of univariate/multivariate Cox regression analysis and the clinical prediction nomogram established, it becomes evident that an increase in age is inversely associated with patients' overall survival time. This could be attributed to the higher incidence of postoperative long-term sequelae in older patients, including secondary hydrocephalus, neurological dysfunction, and nutritional and metabolic disorders (35, 36). Additionally, this trend may also be linked to age-related declines in immune function and gene repair capacity (9). Male gender emerges as a significant prognostic indicator for poorer outcomes in ependymoma, particularly among young boys under 15 years of age (37–40). According to population-based cancer registry data analyzed by Soon et al. (41), there is a notable trend indicating an improved survival rate among female patients. Notably, the median OS for female patients diagnosed with malignant ependymoma is significantly longer than that of males (262 months versus 196 months). However, the precise reasons underlying the overall longer survival time observed in female patients remain elusive.

Surgical resection has traditionally been regarded as the primary treatment approach for SP-EP. Our research aligns with this consensus, revealing that patients undergoing ependymoma surgery fare better, with the extent of resection serving as a significant prognostic factor (42, 43). Notably, across various studies, patients who undergo gross total resection (GTR) surgery exhibit superior outcomes compared to those undergoing subtotal resection (STR) surgery (37, 44). Our findings echo these previous observations, emphasizing the need to prioritize maximal tumor tissue removal

while safeguarding neurological function to mitigate recurrence risks. Advancements in microsurgical techniques and endoscopic surgery have significantly enhanced the prognostic outlook for patients with SP-EP.

The utilization of postoperative radiotherapy (RT) in the management of ependymoma is gradually escalating (45). Nevertheless, our investigation reveals that adjuvant radiotherapy did not markedly enhance the overall survival (OS) of patients regardless of whether they underwent complete or incomplete resection surgery. Furthermore, certain studies concur that radiotherapy confers no notable advantage in terms of OS for ependymoma patients. In contrast to our findings, prior studies have advocated for high-dose adjuvant radiotherapy in patients undergoing subtotal resection (STR) (45, 46). However, it is noteworthy that our research may be constrained by the limitations inherent in the SEER database, which precludes us from obtaining detailed information regarding tumor radiation dose and radiation field.

Over the past decade, tumor prediction models have increasingly been adopted, with nomogram emerging as one of the preferred methods. In our study, we also employed nomogram to predict patient outcomes. Compared to older prediction models, nomogram exhibit greater accuracy and effectiveness in forecasting patient outcomes, thanks to their balanced consideration of various factors (47). Furthermore, our analysis revealed that nomogram can precisely predict patient survival rates. Leveraging this approach, we developed a risk classification system that stratifies patients into high, medium, and low-risk OS categories. This system serves as a valuable tool for guiding patient risk adaptation counseling and clinical treatment decisions. However, it's worth noting that our study has several limitations. Firstly, being a retrospective cohort study, it is inevitably prone to potential selection bias, which typically renders such studies less robust than large randomized controlled trials. Secondly, our validation process was limited to internal data, and we eagerly anticipate external validation using other datasets in the future. Additionally, the SEER database lacks detailed information on chemotherapy usage, radiation methods, and specific radiation levels, thus hindering our ability to correlate delayed treatment effects with precise radiation doses/volumes or specific chemotherapy administrations.

In conclusion, we have successfully developed and internally validated a nomogram-based OS prediction model for patients with SP-EP. Despite its limitations, the model demonstrates acceptable accuracy and clinical applicability, offering medical professionals a practical tool for intuitive and personalized risk analysis in clinical practice.

Data availability statement

Publicly available datasets were analyzed in this study. This data can be found at: SEER (https://seer.cancer.gov/) and GEO database (https://www.ncbi.nlm.nih.gov/geo/) with accession numbers: GSE66354 and GSE50161.

Ethics statement

Ethical approval was not required for the study involving humans in accordance with the local legislation and institutional requirements. Written informed consent to participate in this study was not required from the participants or the participants' legal guardians/next of kin in accordance with the national legislation and the institutional requirements.

Author contributions

TF: Data curation, Formal analysis, Funding acquisition, Investigation, Methodology, Project administration, Supervision, Validation, Visualization, Writing – original draft. CM: Conceptualization, Data curation, Formal analysis, Investigation, Methodology, Project administration, Supervision, Validation, Visualization, Writing – original draft, Resources. ZC: Conceptualization, Data curation, Investigation, Methodology, Project administration, Resources, Supervision, Validation, Visualization, Writing – original draft. YH: Conceptualization, Methodology, Project administration, Validation, Visualization, Writing – original draft. HL: Investigation, Methodology, Project administration, Validation, Visualization, Writing – original draft, Conceptualization, Data curation, Formal analysis, Resources, Software. CW: Funding acquisition, Investigation, Project administration, Conceptualization, Data curation, Formal analysis, Methodology, Writing – review & editing. JL: Conceptualization, Data curation, Formal analysis, Funding acquisition, Investigation, Methodology, Project administration, Resources, Supervision, Validation, Visualization, Writing – review & editing, Software. SL: Conceptualization, Data curation, Investigation, Project administration, Resources, Software, Validation, Visualization, Writing – review & editing. FL: Conceptualization, Data curation, Funding acquisition, Investigation, Project administration, Resources, Visualization, Writing – review & editing, Formal analysis, Methodology, Supervision, Validation.

Funding

The author(s) declare financial support was received for the research, authorship, and/or publication of this article. This work was supported in part by the Heilongjiang Natural Science Foundation Project (Grant No LH2021C096).

Conflict of interest

The authors declare that the research was conducted in the absence of any commercial or financial relationships that could be construed as a potential conflict of interest.

Publisher's note

References

1. Sun XY, Kong C, Lu SB, Sun SY, Guo MC, Ding JZ. Survival outcomes and prognostic factors of patients with intramedullary grade II ependymomas after surgical treatments. *J Clin Neurosci*. (2018) 57:136–42. doi: 10.1016/j.jocn.2018.08.001

2. Villanueva-Castro E, Meraz-Soto JM, Hernández-Dehesa IA, Tena-Suck ML, Hernández-Reséndiz R, Mateo-Nouel EJ, et al. Spinal ependymomas: an updated WHO classification and a narrative review. *Cureus*. (2023) 15:e49086. doi: 10.7759/cureus.49086

3. Candanedo-Gonzalez F, Ortiz-Arce CS, Rosales-Perez S, Remirez-Castellanos AL, Cordova-Uscanga C, Gamboa-Dominguez A. Immunohistochemical features of giant cell ependymoma of the filum terminale with unusual clinical and radiological presentation. *Diagn Pathol*. (2017) 12:7. doi: 10.1186/s13000-016-0595-y

4. Rudà R, Bruno F, Pellerino A, Soffietti R. Ependymoma: evaluation and management updates. *Curr Oncol Rep*. (2022) 24:985–93. doi: 10.1007/s11912-022-01260-w

5. Cachia D, Johnson DR, Kaufmann TJ, Lowe S, Andersen S, Olar A, et al. Case-based review: ependymomas in adults. *Neurooncol Pract*. (2018) 5:142–53. doi: 10.1093/nop/npy026

6. Farooqi S, Tebha SS, Qamar MA, Singh S, Alfawares Y, Ramanathan V, et al. Clinical characteristics, management, and outcomes of intramedullary spinal cord ependymomas in adults: a systematic review. *World Neurosurg*. (2023) 173:237–250.e8. doi: 10.1016/j.wneu.2023.02.098

7. Chamberlain MC, Tredway TL. Adult primary intradural spinal cord tumors: a review. *Curr Neurol Neurosci Rep*. (2011) 11:320–8. doi: 10.1007/s11910-011-0190-2

8. Nabors LB, Portnow J, Ahluwalia M, Baehring J, Brem H, Brem S, et al. Central nervous system cancers, version 3.2020, NCCN clinical practice guidelines in oncology. *J Natl Compr Cancer Netw*. (2020) 18:1537–70. doi: 10.6004/jnccn.2020.0052

9. Cerretti G, Pessina F, Franceschi E, Barresi V, Salvalaggio A, Padovan M, et al. Spinal ependymoma in adults: from molecular advances to new treatment perspectives. *Front Oncol*. (2023) 13:1301179. doi: 10.3389/fonc.2023.1301179

10. Zhang D, Liu H, Zhang M, Cao J. Adult supratentorial extraventricular anaplastic ependymoma with cerebrospinal fluid dissemination metastases: a case report. *Front Neurol*. (2024) 15:1351674. doi: 10.3389/fneur.2024.1351674

11. Wang Q, Chen J, Wang A, Sun L, Qian L, Zhou X, et al. Differentially expressed circRNAs in melanocytes and melanoma cells and their effect on cell proliferation and invasion. *Oncol Rep*. (2018) 39:1813–24. doi: 10.3892/or.2018.6263

12. Feng S, Li J, Fan F, Wang Z, Zhang Q, Zhang H, et al. Prognostic factors and treatment strategies for elderly patients with malignant meningioma: a SEER population-based study. *Front Oncol*. (2022) 12:913254. doi: 10.3389/fonc.2022.913254

13. Li X, Shao Y, Wang Z, Zhu J. Risk prediction and treatment assessment in glioma patients using SEER database: a prospective observational study. *BMJ Open*. (2023) 13:e079341. doi: 10.1136/bmjopen-2023-079341

14. Tang D, Chen Y, Shi Y, Tao H, Tao S, Zhang Q, et al. Epidemiologic characteristics, prognostic factors, and treatment outcomes in primary central nervous system lymphoma: a SEER-based study. *Front Oncol*. (2022) 12:817043. doi: 10.3389/fonc.2022.817043

15. Zeng Y, Li N, Zheng Z, Chen R, Peng M, Liu W, et al. Screening of hub genes associated with pulmonary arterial hypertension by integrated bioinformatic analysis. *Biomed Res Int*. (2021) 2021:6626094–16. doi: 10.1155/2021/6626094

16. Abernathy DG, Kim WK, McCoy MJ, Lake AM, Ouwenga R, Lee SW, et al. MicroRNAs induce a permissive chromatin environment that enables neuronal subtype-specific reprogramming of adult human fibroblasts. *Cell Stem Cell*. (2017) 21:332–348.e9. doi: 10.1016/j.stem.2017.08.002

17. Liu J, Wan Y, Li S, Qiu H, Jiang Y, Ma X, et al. Identification of aberrantly methylated differentially expressed genes and associated pathways in endometrial cancer using integrated bioinformatic analysis. *Cancer Med*. (2020) 9:3522–36. doi: 10.1002/cam4.2956

18. Yu G, Wang LG, Han Y, He QY. clusterProfiler: an R package for comparing biological themes among gene clusters. *OMICS*. (2012) 16:284–7. doi: 10.1089/omi.2011.0118

19. Liu J, Feng M, Li S, Nie S, Wang H, Wu S, et al. Identification of molecular markers associated with the progression and prognosis of endometrial cancer: a bioinformatic study. *Cancer Cell Int*. (2020) 20:59. doi: 10.1186/s12935-020-1140-3

20. Harris MA, Clark J, Ireland A, Lomax J, Ashburner M, Foulger R, et al. The gene ontology (GO) database and informatics resource. *Nucleic Acids Res*. (2004) 32:258D–2261D. doi: 10.1093/nar/gkh036

21. Kanehisa M, Goto S. KEGG: Kyoto encyclopedia of genes and genomes. *Nucleic Acids Res*. (2000) 28:27–30. doi: 10.1093/nar/28.1.27

22. Ladd AN. CUG-BP, Elav-like family (CELF)-mediated alternative splicing regulation in the brain during health and disease. *Mol Cell Neurosci*. (2013) 56:456–64. doi: 10.1016/j.mcn.2012.12.003

23. Mu Q, Lv Y, Luo C, Liu X, Huang C, Xiu Y, et al. Research progress on the functions and mechanism of circRNA in cisplatin resistance in tumors. *Front Pharmacol*. (2021) 12:709324. doi: 10.3389/fphar.2021.709324

24. Fan X, Liu L, Shi Y, Guo F, Wang H, Zhao X, et al. Integrated analysis of RNA-binding proteins in human colorectal cancer. *World J Surg Oncol*. (2020) 18:222. doi: 10.1186/s12957-020-01995-5

25. Li HX, Wang SQ, Lian ZX, Deng SL, Yu K. Relationship between tumor infiltrating immune cells and tumor metastasis and its prognostic value in cancer. *Cells*. (2022) 12:64. doi: 10.3390/cells12010064

26. Allam M, Hu T, Lee J, Aldrich J, Badve SS, Gökmen-Polar Y, et al. Spatially variant immune infiltration scoring in human cancer tissues. *NPJ Precis Oncol*. (2022) 6:60. doi: 10.1038/s41698-022-00305-4

27. Mu Q, Yao K, Syeda MZ, Wan J, Cheng Q, You Z, et al. Neutrophil targeting platform reduces neutrophil extracellular traps for improved traumatic brain injury and stroke theranostics. *Adv Sci*. (2024) 11:e2308719. doi: 10.1002/advs.202308719

28. GTEx Consortium. The genotype-tissue expression (GTEx) project. *Nat Genet*. (2013) 45:580–5. doi: 10.1038/ng.2653

29. Siddaway R, Milos S, Vadivel AKA, Dobson THW, Swaminathan J, Ryall S, et al. Splicing is an alternate oncogenic pathway activation mechanism in glioma. *Nat Commun*. (2022) 13:588. doi: 10.1038/s41467-022-28253-4

30. Alors-Pérez E, Pedraza-Arevalo S, Blázquez-Encinas R, García-Vioque V, Agraz-Doblas A, Yubero-Serrano EM, et al. Altered CELF4 splicing factor enhances pancreatic neuroendocrine tumors aggressiveness influencing mTOR and everolimus response. *Mol Therapy Nucleic Acids*. (2024) 35:102090. doi: 10.1016/j.omtn.2023.102090

31. Syeda MZ, Hong T, Huang C, Huang W, Mu Q. B cell memory: from generation to reactivation: a multipronged defense wall against pathogens. *Cell Death Discov*. (2024) 10:117. doi: 10.1038/s41420-024-01889-5

32. Nasiri-Aghdam M, Garcia-Garduño TC, Jave-Suárez LF. CELF family proteins in Cancer: highlights on the RNA-binding protein/noncoding RNA regulatory axis. *Int J Mol Sci*. (2021) 22:11056. doi: 10.3390/ijms222011056

33. Boström A, von Lehe M, Hartmann W, Pietsch T, Feuss M, Boström JP, et al. Surgery for spinal cord ependymomas: outcome and prognostic factors. *Neurosurgery*. (2011) 68:302–8; discussion 9. doi: 10.1227/NEU.0b013e3182004c1e

34. Wang C, Yuan X, Zuo J. Individualized prediction of overall survival for primary intramedullary spinal cord grade II/III ependymoma. *World Neurosurg*. (2020) 143:e149–56. doi: 10.1016/j.wneu.2020.07.049

35. Mohammed W, Farrell M, Bolger C. Spinal cord ependymoma—surgical management and outcome. *J Neurosci Rural Pract*. (2019) 10:316–20. doi: 10.4103/jnrp.jnrp_267_18

36. Deng X, Zhang X, Yang L, Lu X, Fang J, Yu L, et al. Personalizing age-specific survival prediction and risk stratification in intracranial grade II/III ependymoma. *Cancer Med*. (2020) 9:615–25. doi: 10.1002/cam4.2753

37. Rodríguez D, Cheung MC, Housri N, Quinones-Hinojosa A, Camphausen K, Koniaris LG. Outcomes of malignant CNS ependymomas: an examination of 2408 cases through the surveillance, epidemiology, and end results (SEER) database (1973-2005). *J Surg Res*. (2009) 156:340–51. doi: 10.1016/j.jss.2009.04.024

38. Jia Z, Yan Y, Wang J, Yang H, Zhan H, Chen Q, et al. Development and validation of prognostic nomogram in ependymoma: a retrospective analysis of the SEER database. *Cancer Med*. (2021) 10:6140–8. doi: 10.1002/cam4.4151

39. Elsamadicy AA, Koo AB, David WB, Lee V, Zogg CK, Kundishora AJ, et al. Comparison of epidemiology, treatments, and outcomes in pediatric versus adult ependymoma. *Neurooncol Adv*. (2020) 2:vdaa019. doi: 10.1093/noajnl/vdaa019

40. Wang Y, Mu Q, Sheng M, Chen Y, Jian F, Li R. A nomogram for predicting overall survival of patients with primary spinal cord glioblastoma. *Neurospine*. (2024) 21:676–89. doi: 10.14245/ns.2448082.041

41. Soon WC, Goacher E, Solanki S, Hayes J, Kapetanstrataki M, Picton S, et al. The role of sex genotype in paediatric CNS tumour incidence and survival. *Childs Nerv Syst*. (2021) 37:2177–86. doi: 10.1007/s00381-021-05165-0

42. Leblond P, Massimino M, English M, Ritzmann TA, Gandola L, Calaminus G, et al. Toward improved diagnosis accuracy and treatment of children, adolescents, and young adults with ependymoma: the international SIOP ependymoma II protocol. *Front Neurol*. (2022) 13:887544. doi: 10.3389/fneur.2022.887544

43. Samuel N, Tetreault L, Santaguida C, Nater A, Moayeri N, Massicotte EM, et al. Clinical and pathological outcomes after resection of intramedullary spinal cord tumors: a single-institution case series. *Neurosurg Focus*. (2016) 41:E8. doi: 10.3171/2016.5.Focus16147

44. Korshunov A, Golanov A, Sycheva R, Timirgaz V. The histologic grade is a main prognostic factor for patients with intracranial ependymomas treated in the microneurosurgical era: an analysis of 258 patients. *Cancer*. (2004) 100:1230–7. doi: 10.1002/cncr.20075

45. Tensaouti F, Ducassou A, Chaltiel L, Sevely A, Bolle S, Padovani L, et al. Imaging biomarkers of outcome after radiotherapy for pediatric ependymoma. *Radiother Oncol*. (2018) 127:103–7. doi: 10.1016/j.radonc.2018.02.008

46. Macdonald SM, Sethi R, Lavally B, Yeap BY, Marcus KJ, Caruso P, et al. Proton radiotherapy for pediatric central nervous system ependymoma: clinical outcomes for 70 patients. *Neuro Oncol*. (2013) 15:1552–9. doi: 10.1093/neuonc/not121

47. Iasonos A, Schrag D, Raj GV, Panageas KS. How to build and interpret a nomogram for cancer prognosis. *J Clin Oncol*. (2008) 26:1364–70. doi: 10.1200/jco.2007.12.9791

frontiers | Frontiers in Oncology

TYPE Case Report
PUBLISHED 19 September 2024
DOI 10.3389/fonc.2024.1402550

OPEN ACCESS

EDITED BY
Ning Li,
Southeast University, China

REVIEWED BY
Xiang Fang,
Sichuan University, China
Xiangyi Meng,
First Affiliated Hospital of Harbin Medical University, China
Sanjeev Nirala,
Tribhuvan University Teaching Hospital, Nepal

*CORRESPONDENCE
Xiuchun Yu
13969132190@163.com

†These authors share first authorship

RECEIVED 17 March 2024
ACCEPTED 29 August 2024
PUBLISHED 19 September 2024

CITATION
Miao Z, Han Z, Zheng K, Xu M, Yu X, Han C and Yu X (2024) Denosumab combined with microwave ablation excisional scraping for giant cell tumor of the thoracic spine: a case report and literature review.
Front. Oncol. 14:1402550.
doi: 10.3389/fonc.2024.1402550

Denosumab combined with microwave ablation excisional scraping for giant cell tumor of the thoracic spine: a case report and literature review

Zukang Miao[1†], Zhiwei Han[2†], Kai Zheng[1], Ming Xu[1], Xue Yu[3], Changsheng Han[1] and Xiuchun Yu[1*]

[1]Department of Orthopaedic Surgery, The 960th Hospital of the People's Liberation Army Joint Logistics Support Force, Jinan, Shandong, China, [2]Department of Joint Surgery, Central Hospital Affiliated to Shandong First Medical University, Jinan, Shandong, China, [3]School of Anesthesia, Shandong Second Medical University, Weifang, Shandong, China

Denosumab has recently become an important part of the treatment regime for spinal giant cell tumors of the bone (GCTB). Its use has significantly reduced the risk of surgery and postoperative complications in patients with spinal GCTB. However, the use of denosumab has not yet been optimized to reap the maximum benefits. Here, we have reported the case of a patient who was treated with denosumab in combination with excision and scraping for GCTB of the T10 vertebrae, which achieved good tumor control and no recurrence at the 2-year postoperative follow-up. We have also reviewed the case in the light of relevant literature as well as presented our ideas and recommendations for the optimal use of denosumab.

KEYWORDS

denosumab, excisional scraping, giant cell tumor of bone, case report, literature review

1 Introduction

Giant cell tumor of the bone (GCTB) is an aggressive tumor with a very high recurrence rate (1). The most common sites of its occurrence are the long bones of the extremities, with 1–5% involvement of the spine (including the vertebrae, pelvis, and sacrum) (2). For spinal GCTB, surgery is the sure-fire treatment approach and it includes total *en bloc* spondylectomy and intra-lesional curettage. Total *en bloc* spondylectomy (TES) is the treatment of choice for spinal GCTB; however, considering the special anatomy of the spine, its location, and the extent of the tumor, serious complications may occur (3). Relatively, intra-lesional curettage surgery is less traumatic for patients and has fewer postoperative complications, albeit the chance of tumor recurrence is 15–30% (4). Therefore, it is important to achieve complete curettage, reduce the postoperative

recurrence rates, and establish an effective adjuvant treatment for GCTB in difficult-to-treat areas.

Denosumab is a human immunoglobulin (Ig) G2 monoclonal antibody that targets and inhibits RANKL activation. It functions similarly to osteoprotegerin (OPG), which inhibits osteoclast activation and differentiation by competitively binding to RANKL, which, in turn, reduces bone resorption and increases bone mass (5). The Chinese Society of Clinical Oncology (CSCO) guidelines mention the treatment of GCTB (Class 2A evidence). However, there are still some unresolved issues regarding the use of denosumab in clinical practice, including the rapid recurrence after discontinuation of the drug after long-term use and the use of the drug before curettage as it may increase the risk of local recurrence (6). Therefore, it remains elusive as to how denosumab should be used to maximize patient benefit. Here, we have reported the case of a patient who underwent denosumab treatment in combination with excision and scraping for GCTB in T10 vertebrae; the patient showed no tumor recurrence or uncomfortable symptoms at 24-month postoperative follow-up, indicating that the intervention achieved good clinical outcome.

2 Case report

A 45-year-old woman was admitted to our hospital on January 21, 2022, with the complaint of "lower back pain and restricted movement for more than 2 months". Her pre-existing physical fitness revealed no family history of genetic disorders. Specialist examination showed no evident deformity of the spine, limited flexion, extension, and rotation. Significant pressure and percussion pain in the thoracolumbar region were noted, albeit there was no radiating pain. Normal skin sensation of the trunk and lower limbs, normal muscle strength, and tone of both lower limbs were recorded. Physiological reflexes were present, while pathological reflexes were not elicited. Her blood tests showed no significant abnormalities. Imaging, X-ray, and computed tomography (CT) revealed an irregular morphology of the T10 vertebral body with abnormal bone destruction. The magnetic resonance imaging (MRI) displayed flattening of the T10 vertebral body with uneven signal changes and compression of the spinal canal (Figures 1A1–C4). CT-guided aspiration biopsy of the T10 vertebral tumor showed aspiration pathology, indicating GCTB (Figure 1D). The cumulative observations of the abovementioned clinical manifestations and examination outcomes led to the preliminary diagnosis of T10 vertebrae GCTB.

The condition and associated risks were explained in detail to the patient and his family, who then agreed to the treatment plan of using the drugs in combination with surgery. Three separate subcutaneous injections of 120 mg denosumab were administered on days 1, 8, and 15 along with the concomitant oral administration of calcium carbonate D3, 600 mg, qd. After 3 weeks of medication, imaging was reviewed: the T10 vertebral body tumor was observed to be significantly smaller than earlier, partially ossified (Figures 2A1–C4). A microwave inactivation and scraping of the T10 vertebral body tumor via the posterior approach was performed on March 8, 2022, for internal fixation with bone grafting. After routine intraoperative incision and exposure, exposure of the T8-T12 bilateral articular processes and vertebral plates, pedicle screws

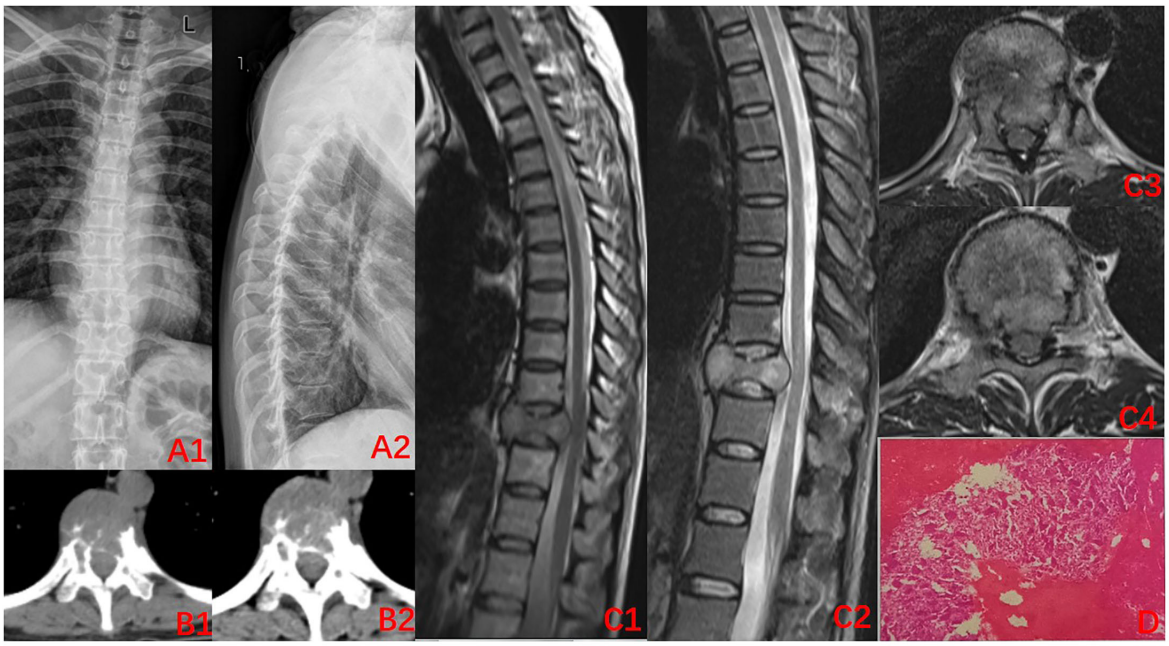

FIGURE 1
Imaging at the time of initial diagnosis (2022–01). **(A1-B2)** X-ray of the thoracic spine. CT: Decreased density of T10 vertebral body, destruction of the vertebral bone, and discontinuity of the bone cortex; **(C1–C4)** MRI of the thoracic spine: centric flattening of the T10 vertebral body, heterogeneous signal changes within the vertebral body, dural compression, and narrowing of the spinal canal; **(D)** Puncture pathology: a large number of osteoclasts can be seen with the invasion of normal bone tissue, indicative of giant cell tumor of the bone.

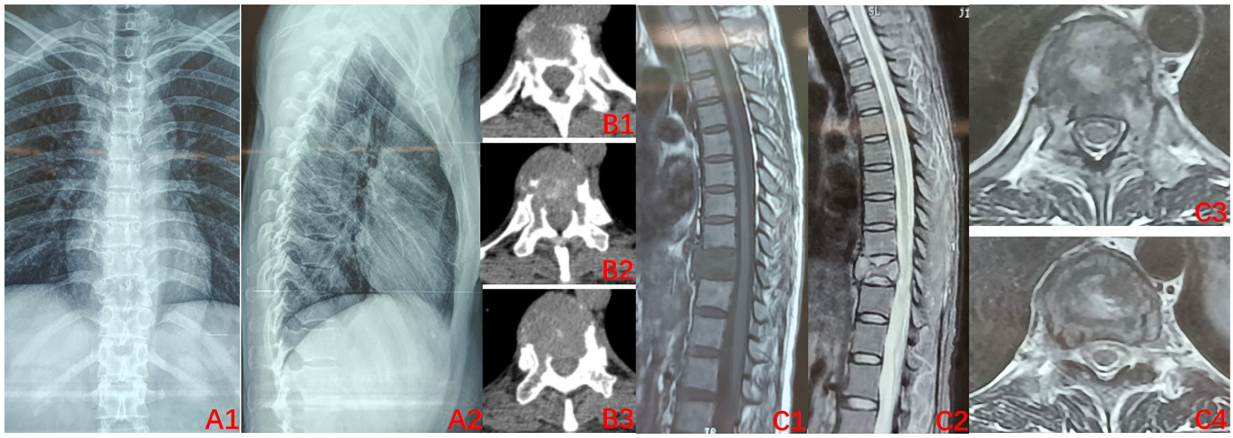

FIGURE 2
Preoperative imaging after 3 doses of denosumab (2022–03). **(A1–B3)** X-ray of the thoracic spine. CT: Bone density of the T10 vertebral body was significantly improved relative to that previously, uneven ossification was observed within the vertebral body, and bone formation was evident at the posterior margin of the vertebral body; **(C1–C4)** MRI of the thoracic spine: vertebral signal inhomogeneity was altered, tumor size is reduced, and intravertebral occupancy was improved.

of an appropriate length were implanted in T8, T9, T11, and T12, and a titanium rod of an appropriate length was placed on one side for temporary fixation, followed by ultrasonic osteotome cutting of the T10 plate, resection of T9 inferior articular process and T10 superior articular process and exposure of the dura mater and nerve roots, and cutting of the T10 nerve root. A microwave needle was then inserted into the T10 vertebral body through one side of the pedicle, with the microwave needle setting power at 60 W; the microwave inactivation of the tumor was conducted thrice unilaterally at multiple points and directions, while ice-water rinsing was performed, and the thermometer needle was continuously measured to maintain a temperature <42°C to protect the spinal cord, while the contralateral side was treated similarly for a total of six times. After microwave inactivation, the vertebral body was cut and scraped from both sides to achieve complete resection, and the lower endplate of T9 and the upper endplate of T11 were processed to expose the normal oozing bone. Then implantation of allograft bone at the anterior margin of the vertebral body a titanium cage filled with allograft bone of the appropriate length was placed. After the examination of the c-arm X-ray machine, the position of the internal fixation is satisfactory, a titanium rod was implanted, the drainage was left in place, and the incision was sutured (Figures 3A1, A2). The postoperative pathology was consistent with GCTB (Figure 3B).

The radiographs were reviewed 1 month after the surgery and displayed a satisfactory position of the internal fixation (Figures 3C1, C2), as such the use of denosumab was resumed. It was planned to be used every 3 months for the first 2 years after the surgery and then every 6 months in the third year. Finally, it was used once every year in the fourth and fifth years of the surgery. A repeat MRI was conducted in March 2024, which revealed no significant abnormalities (Figures 4A1–A4). Currently, at 24 months after the surgery, denosumab has been used a total of 7 times, the patient has not experienced any significant discomfort, and the follow-up is still ongoing.

3 Discussion

GCTB consists mainly of neoplastic stromal cells, multinucleated giant cells, and their monocytic precursors (7). Stromal cells express RANKL, a tumor component of GCTB that stimulates the proliferation of multinucleated giant cells and their monocytic precursor aggregates. Multinucleated giant cells express RANK, which binds to RANKL, disrupting normal bone homeostasis and causing excessive bone resorption (8, 9). Denosumab inhibits osteoclast activation and promotes bone deposition, and its specificity and affinity for RANKL is higher than that of RANK, blocking the RANK/RANKL signaling pathway by binding to RANKL and thus inhibiting the interaction between neoplastic stromal cells and multinucleated giant cells, which is closely associated with tumor recurrence (10).

The valuable role of denosumab in GCTB has gained a consensus, albeit the duration of use for the pharmacological treatment and the timing of its use that can maximize the benefits to the patients remain debatable. The preoperative use of denosumab can make the lesion site more amenable to surgical treatment, especially in patients with larger, destructive, recurrent GCTB (11). Rutkowski et al. (12) reported that the preoperative use of denosumab was effective in reducing the staging of GCTB, with more than one-third (38%) of the patients showing reduced grading of their surgery, which subsequently reduced the need for a more invasive procedure as well as stabilized or improved the neurological status without increasing the risk of neurological deterioration (13). Preoperative adjuvant therapy with denosumab also reduced the blood supply to the tumor tissues and hardened the lesion, thereby facilitating tumor resection (14). In addition, it was effective in improving patients' pain symptoms, overall functioning, tumor size, and histological features, thereby providing a reference for timing and the certainty of surgery (15).

However, in contrast, a study by Guo et al. (16) found that 43% of the patients who used denosumab preoperatively experienced

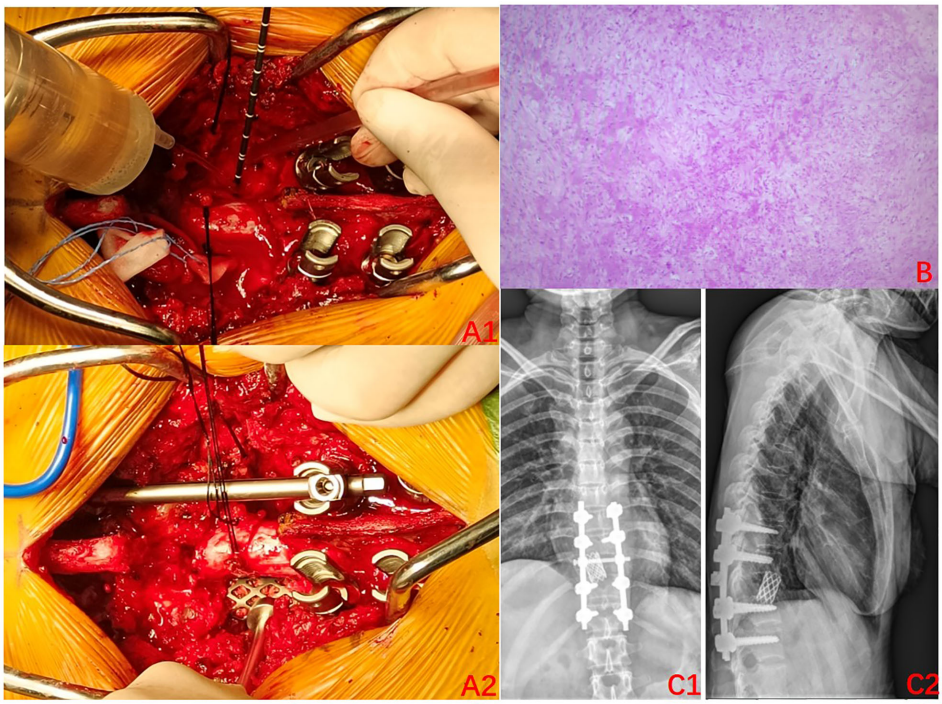

FIGURE 3
Surgery-related imaging. **(A1)** Intraoperative photos (2022–03): Microwave inactivation of vertebral tumors; **(A2)**: Implanted titanium cage;. **(B)** Postoperative pathology: focal new bone formation can be seen, with some areas of degenerative-like necrosis of the bone tissues. **(C1–C2)** Postoperative X-rays (2022–04); A satisfactory position of the internal fixation can be seen.

recurrence, which suggests that the preoperative use of denosumab may increase the risk of local recurrence of GCTB treated with scraping. Moreover, the local recurrence rate after a curettage procedure following the preoperative use of denosumab was significantly higher when compared to that directly after a curettage procedure (17). This difference can be attributed to the fact that although the use of denosumab significantly reduced the tumor size, it increased the risk of recurrence due to the central

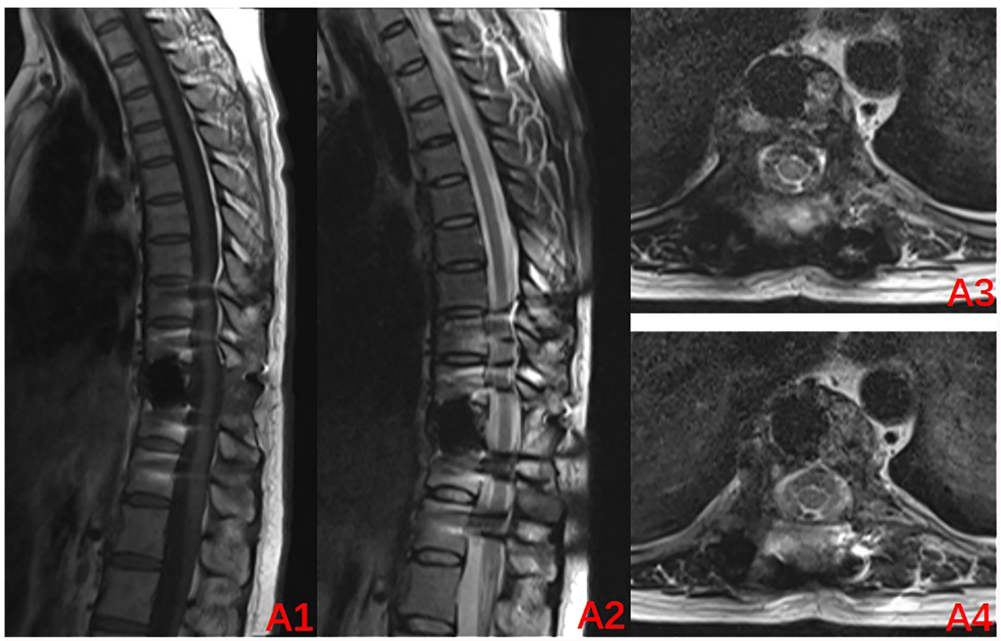

FIGURE 4
Review MRI at 24 months after the surgery (2024–03): **(A1–A4)** Internal fixation artifacts can be seen in the T10 vertebral body, with no abnormal signal in the spinal canal and a normal sagittal diameter.

sclerosis sign and peripheral bone formation. This occurred because of the inadequate scraping of the tumor considering that that the tumor area could not be correctly identified intraoperatively, which ultimately leads to the retention of the tumor tissues (18). GCTB is an aggressive tumor and there is no evidence of blood or lymphatic transmission.

Boriani et al. (19) proposed that denosumab should be used preoperatively for ≥6 months in patients undergoing intra-lesional curettage of the tumor lesion, which can be extended by up to 12 months in patients with an insignificant local response to the tumor. Most authors recommend an estimated duration of 3–6 months, with an initial loading consisting of 120 mg of denosumab administered subcutaneously thrice a week at the start and then continued thereafter at the same rate once a month. The prolonged preoperative use (>9 months) of denosumab has been associated with more surgical complications and a higher risk of vertebral fracture; the prolonged use results in excessive ossification of the original tumor, making it impossible to determine the safe boundaries of tumor resection, which, in turn, increases the risk of local recurrence (20). Currently, short courses of preoperative denosumab have demonstrated effectiveness in reducing surgical grading and in achieving tumor control. Zhang et al. (21) suggested a recurrence rate of 27% in patients undergoing surgery with a short-term (6 doses) denosumab course, stating more potential benefit from shortening the number of preoperative medications when used again. In sacral GCTB, a short course (≤3 doses) of preoperative denosumab treatment not only achieves the local control of the tumor but also improves the likelihood of intraoperative neurological and postoperative functional preservation (22). Relevant imaging evaluations revealed that short-term (≤3 weeks) preoperative neoadjuvant treatment of spinal GCTB with denosumab induces a radiological and histological response that sclerosis the tumor, reduces the soft-tissue component of the tumor, and prevents adhesion to the dura mater, nerve roots, and other important tissue structures, thereby facilitating the achievement of optimal oncological and functional outcomes (23). Ultra-short-term (<3 months) denosumab treatment before the surgery can help achieve the therapeutic effect of a conventional treatment course as well as reduce the risk of local recurrence (14). In a single-center retrospective study by Hindiskere et al. (24), no difference was noted between short (≤3) and long (>3) preoperative courses of denosumab treatment in terms of the MSTS scores, radiological and histological responses, and recurrence-free survival, showing that that drug toxicity response could be achieved at lesser expense (25). Denosumab is also effective in advanced severe GCTB, and a short course of its treatment can make surgery more effective when conducted after a reasonable assessment of the risk of postoperative recurrence (18).

Denosumab inhibits the binding of RANKL to RANK and the maturation and differentiation of osteoclast precursors to osteoblasts. Histological manifestations of GCTB after denosumab treatment include osteoclast disappearance and bone formation (26). However, it does not affect the mesenchymal cells of the tumor, that is, denosumab does not eliminate the tumor cells, but rather only inhibits their activity (27). Mak et al. (28) reported that the RANKL expression was almost eliminated in patients treated with denosumab, but the tumor mesenchymal cells continued to proliferate, which importantly contributed to tumor recurrence. Therefore, preoperative use of denosumab followed by surgical intervention is necessary and the postoperative use of the drug plays an important role in controlling tumor recurrence.

Intra-lesional curettage surgery should be performed, and denosumab should be administered even after surgery and continued for at least 6–12 months after the surgery to reduce tumor recurrence (20). Guo et al. (29) noted that patients undergoing sacral nerve-sparing sacral osteoblastoma curettage with the preservation of the sacral nerves achieved good recurrence-free survival and the continued use of denosumab for 24 months postoperatively was effective in controlling the early recurrence of the tumor. Pharmacological studies have indicated that denosumab has a half-life of approximately 4 weeks and that the inhibitory effect on osteolysis lasts for at least 3 months (30), albeit the optimal dosing schedule for maintenance therapy has not yet been determined. Jianru Xiao et al. (31) suggested that, for patients with spinal GCTB, denosumab should be continued for 2 years postoperatively (120 mg/4 weeks) that the decision to discontinue the drug should be based on the assessment of the risk of recurrence. Denosumab administered at 4-week intervals prevented bone-related events. Extended dosing intervals may reduce toxicity, drug costs, and the number of clinical visits if the efficacy remains unchanged, albeit there is no clear evidence on the efficacy and safety of extended interval use of denosumab (32). Jiang et al. (33) demonstrated that prolonged intervals of denosumab administration provided a similar tumor control and a significantly lower incidence of adverse bone-related events when compared to the standard dose intervals. A very recent study proposed that denosumab, in combination with the targeted drug Sunitinib, can achieve better outcomes (17). Alternatively, with the adjunctive use of radiotherapy, denosumab can be discontinued early for withdrawal, such that good tumor control can be achieved (34), albeit this aspect warrants more in-depth study before any conclusive inference.

Microwave ablation (MWA) induces high-speed vibration of polar molecules in tumor tissues by applying microwave electromagnetic fields, and these molecules collide with friction, which converts kinetic energy into thermal energy, thereby causing irreversible damage or coagulative necrosis of tumor cells (35, 36). Compared to other thermal ablation technologies, MWA can obtain higher heating efficiency, better tissue conductance, and heat conduction (37). Current studies have shown that it has achieved similar efficacy to surgery in solid organ tumors such as early-stage lung cancer and percutaneous puncture for liver cancer (38). As for bone tumors, it can be used as a preoperative adjuvant therapy to effectively reduce intraoperative blood loss and minimize the risk of tumor contamination in the surrounding tissues (39). It effectively manages GCTB with soft tissue extensions, which can be effectively inactivated without damaging the surrounding normal tissues when detected by a pycnometer needle (40). For GCTB occurring in the extremities, using MWA combined with cement-filled internal fixation can maximize the preservation of joint function without violating the articular surface, and the recurrence rate is not significantly different from that of total resection (41). It can

maintain the integrity of the joint and achieve biological repair of the bone defect lesion (42). MWA has been used in the treatment of bone tumors for more than 30 years. It can be used as an independent percutaneous minimally invasive treatment for some benign bone tumors and bone metastases, or as an auxiliary treatment for hemostasis, tumor inactivation, or improving the safety of tumor resection boundary (43).

Our analysis revealed that the prolonged use of denosumab preoperatively, the use of a simple curettage without any adjuvant therapy, the lack of continued use of denosumab, or premature discontinuation of denosumab postoperatively were the main contributors to the high recurrence rate of GCTB. The use of adjuvants has now been shown to significantly reduce the recurrence rate of GCTB. Local adjuvants, including high-speed burring, ethanol, and cryosurgery were used in conjunction with intra-lesional scraping to improve the local control aspect. However, due to the special anatomical location of the spine, the use of these adjuvants can greatly increase the risk of spinal cord and nerve damage (44). However, microwave ablation-assisted lesion scraping, by adjusting the working power and controlling the microwave ablation temperature by real-time intraoperative monitoring, can protect the spinal cord, nerves, and other important tissues, as well as maximize the killing and removal of the tumor cells, which has already demonstrated its absolute advantages in the treatment of extremity GCTB (45), while avoiding the risks of other adjuvant therapies.

In summary, in the present case, denosumab was used thrice preoperatively to reduce the size of the tumor and cause local ossification. Intraoperative tumor scraping when assisted by microwave ablation achieved maximum tumor debulking. Tumor control was achieved with the use of denosumab at progressively longer intervals in the postoperative period to taper off the drug, which significantly reduced the rate of tumor recurrence. Thus, the present review and case experience provide a new perspective on the clinical application of denosumab.

Data availability statement

The original contributions presented in the study are included in the article/Supplementary Material. Further inquiries can be directed to the corresponding author.

Ethics statement

The studies involving humans were approved by The 960th Hospital of the PLA Joint Logistics Support Force. The studies were conducted in accordance with the local legislation and institutional requirements. The participants provided their written informed consent to participate in this study. Written informed consent was obtained from the individual(s) for the publication of any potentially identifiable images or data included in this article.

Author contributions

ZM: Data curation, Formal analysis, Writing – original draft, Writing – review & editing. ZH: Data curation, Investigation, Resources, Writing – original draft, Writing – review & editing. KZ: Data curation, Writing – review & editing. MX: Data curation, Validation, Writing – review & editing. XY: Resources, Validation, Writing – review & editing. CH: Resources, Validation, Writing – review & editing. XCY: Conceptualization, Supervision, Validation, Writing – review & editing.

Funding

The author(s) declare that no financial support was received for the research, authorship, and/or publication of this article.

Conflict of interest

The authors declare that the research was conducted in the absence of any commercial or financial relationships that could be construed as a potential conflict of interest.

Publisher's note

Supplementary material

The Supplementary Material for this article can be found online at: https://www.frontiersin.org/articles/10.3389/fonc.2024.1402550/full#supplementary-material

References

1. Li J, Zhou J, Liu Y, Sun X, Song W. Comprehensive treatment for multicentric giant cell tumors of the pelvis and spine using apatinib: A case report and literature review. *J Cancer Res Ther*. (2020) 16:1020–6. doi: 10.4103/jcrt.JCRT_892_19

2. Sereno M, Franco SR, de la Reina L, Campo-Cañaveral de la Cruz JL, Muñoz de Legaría M, Casado Saénz E. Conversion in a resectable tumor after denosumab neoadjuvant in a large dorsal giant cells tumor: A case report and a literature review. *Curr Oncol*. (2023) 30:9335–45. doi: 10.3390/curroncol30100675

3. Bandiera S, Boriani S, Donthineni R, Amendola L, Cappuccio M, Gasbarrini A. Complications of en bloc resections in the spine. *Orthop Clin North Am*. (2009) 40:125–vii. doi: 10.1016/j.ocl.2008.10.002

4. Rekhi B, Dave V. Giant cell tumor of bone: An update, including spectrum of pathological features, pathogenesis, molecular profile and the differential diagnoses. *Histol Histopathol*. (2023) 38:139–53. doi: 10.14670/HH-18-486

5. Ren B, Ren X, Wang L, Tu C, Zhang W, Liu Z, et al. A bibliometric research based on hotspots and frontier trends of denosumab. *Front Pharmacol*. (2022) 13):929223. doi: 10.3389/fphar.2022.929223

6. Tan X, Zhang Y, Wei D, Yang Y, Xiang F. Denosumab for giant cell tumors of bone from 2010 to 2022: a bibliometric analysis. *Clin Exp Med*. (2023) 23:3053–75. doi: 10.1007/s10238-023-01079-0

7. Thomas DM. RANKL, denosumab, and giant cell tumor of bone. *Curr Opin Oncol*. (2012) 24:397–403. doi: 10.1097/CCO.0b013e328354c129

8. Roessner A, Smolle M, Haybäck J. Riesenzelltumor des Knochens: Morphologie, molekulare Pathogenese und Differenzialdiagnose [Giant cell tumor of bone: Morphology, molecular pathogenesis, and differential diagnosis. *Pathologe*. (2020) 41:134–42. doi: 10.1007/s00292-020-00760-5

9. Wülling M, Delling G, Kaiser E. The origin of the neoplastic stromal cell in giant cell tumor of bone. *Hum Pathol*. (2003) 34:983–93. doi: 10.1053/s0046-8177(03)00413-1

10. Skubitz KM. Giant cell tumor of bone: current treatment options. *Curr Treat Options Oncol*. (2014) 15:507–18. doi: 10.1007/s11864-014-0289-1

11. Puri A, Gulia A, Hegde P, Verma V, Rekhi B. Neoadjuvant denosumab: its role and results in operable cases of giant cell tumour of bone. *Bone Joint J*. (2019) 101-B:170–7. doi: 10.1302/0301-620X.101B2.BJJ-2018-0907.R2

12. Rutkowski P, Ferrari S, Grimer RJ, Stalley PD, Dijkstra SP, Pienkowski A, et al. Surgical downstaging in an open-label phase II trial of denosumab in patients with giant cell tumor of bone. *Ann Surg Oncol*. (2015) 22:2860–8. doi: 10.1245/s10434-015-4634-9

13. Al Farii H, McChesney G, Patel SS, Rhines LD, Lewis VO, Bird JE. The risk of neurological deterioration while using neoadjuvant denosumab on patients with giant cell tumor of the spine presenting with epidural disease: a meta-analysis of the literature. *Spine J*. (2024) 24:1056–64. doi: 10.1016/j.spinee.2024.01.016

14. Xiang F, Liu H, Deng J, Ma W, Chen Y. Progress on denosumab use in giant cell tumor of bone: dose and duration of therapy. *Cancers (Basel)*. (2022) 14:5758. doi: 10.3390/cancers14235758

15. Rath BK, G A, Mohanty P, Tripathy A, Sahoo JP. Repercussions of denosumab in patients with giant cell tumor of bone: an observational study. *Cureus*. (2023) 15: e48702. doi: 10.7759/cureus.48702

16. Zhao Y, Cai Z, Tang X, Du Z, Yang Y, Guo W. Preoperative Denosumab may increase the Risk of Local Recurrence of Giant-cell Tumor of Bone Treated with Curettage: A Systematic Review and Meta-analysis. *J Cancer*. (2021) 12:508–17. doi: 10.7150/jca.50575

17. Imre A, Zoltán S, Miklós S. Current indications for denosumab in benign bone tumours. *EFORT Open Rev*. (2023) 8:895–905. doi: 10.1530/EOR-23-0138

18. van der Heijden L, Lipplaa A, van Langevelde K, Bovée JVMG, van de Sande MAJ, Gelderblom H. Updated concepts in treatment of giant cell tumor of bone. *Curr Opin Oncol*. (2022) 34:371–8. doi: 10.1097/CCO.0000000000000852

19. Boriani S, CecChinato R, Cuzzocrea F, Bandiera S, Gambarotti M, Gasbarrini A. Denosumab in the treatment of giant cell tumor of the spine. Preliminary report, review of the literature and protocol proposal. *Eur Spine J*. (2020) 29:257–71. doi: 10.1007/s00586-019-05997-0

20. Xará-Leite F, Coutinho L, Fleming C, Magalhães M, Oliveira V, Rodrigues-Pinto R, et al. Can Denosumab cure giant cell tumors of the spine? A case report and literature review. *Eur J Orthop Surg Traumatol*. (2020) 30:19–23. doi: 10.1007/s00590-019-02554-9

21. Zhang RZ, Ma TX, Qi DW, Zhao M, Hu T, Zhang GC. Short-term preoperative denosumab with surgery in unresectable or recurrent giant cell tumor of bone. *Orthop Surg*. (2019) 11:1101–8. doi: 10.1111/os.12561

22. Liang H, Liu X, Yang Y, Guo W, Yang R, Tang X, et al. Ultra-short course of neoadjuvant denosumab for nerve-sparing surgery for giant cell tumor of bone in sacrum. *Spine (Phila Pa 1976)*. (2022) 47:691–701. doi: 10.1097/BRS.0000000000004318

23. Tang Q, Lu J, Zhu X, Song G, Wu H, Xu H, et al. The efficacy and safety of short-course neoadjuvant denosumab for en bloc spondylectomy in spinal giant cell tumor of bone: a preliminary report. *Eur Spine J*. (2023) 32:4297–305. doi: 10.1007/s00586-023-07770-w

24. Hindiskere S, Errani C, Doddarangappa S, Ramaswamy V, Rai M, Chinder PS. Is a short-course of preoperative denosumab as effective as prolonged therapy for giant cell tumor of bone? *Clin Orthop Relat Res*. (2020) 478:2522–33. doi: 10.1097/CORR.0000000000001285

25. Thomas D, Henshaw R, Skubitz K, Chawla S, Staddon A, Blay JY, et al. Denosumab in patients with giant-cell tumour of bone: an open-label, phase 2 study. *Lancet Oncol*. (2010) 11:275–80. doi: 10.1016/S1470-2045(10)70010-3

26. Agawa R, Kato I, Kawabata Y, Takeyama M, Fujii S. Histological and immunohistochemical analyses of osteoclast maturation in giant cell tumor of bone. *Pathol Res Pract*. (2024) 254:155128. doi: 10.1016/j.prp.2024.155128

27. Girolami I, Mancini I, Simoni A, Baldi GG, Simi L, Campanacci D, et al. Denosumab treated giant cell tumour of bone: a morphological, immunohistochemical and molecular analysis of a series. *J Clin Pathol*. (2016) 69:240–7. doi: 10.1136/jclinpath-2015-203248

28. Mak IW, Evaniew N, Popovic S, Tozer R, Ghert M. A translational study of the neoplastic cells of giant cell tumor of bone following neoadjuvant denosumab. *J Bone Joint Surg Am*. (2014) 96:e127. doi: 10.2106/JBJS.M.01332

29. Lim CY, Liu X, He F, Liang H, Yang Y, Ji T, et al. Retrospective cohort study of 68 sacral giant cell tumours treated with nerve-sparing surgery and evaluation on therapeutic benefits of denosumab therapy. *Bone Joint J*. (2020) 102-B:177–85. doi: 10.1302/0301-620X.102B2.BJJ-2019-0813.R1

30. Body JJ, Facon T, Coleman RE, Lipton A, Geurs F, Fan M, et al. A study of the biological receptor activator of nuclear factor-kappaB ligand inhibitor, denosumab, in patients with multiple myeloma or bone metastases from breast cancer. *Clin Cancer Res*. (2006) 12:1221–8. doi: 10.1158/1078-0432.CCR-05-1933

31. Leng A, Yang M, Sun H, Dai Z, Zhu Z, Wan W, et al. Surgical strategy for recurrent giant cell tumor in the thoracolumbar spine. *Orthop Surg*. (2024) 16:78–85. doi: 10.1111/os.13911

32. Keisner SV. Prevention of skeletal-related events with extended-interval denosumab: A review of the literature. *Ann Pharmacother*. (2024) 58:174–84. doi: 10.1177/10600280231168456

33. Jiang CY, Zhao L, Schuetze SM, Chugh R. Giant cell tumor of bone: effect of longer dosing intervals of denosumab on tumor control and bone-related complications. *Oncologist*. (2022) 27:595–9. doi: 10.1093/oncolo/oyac066

34. Miao Z, Xu M, Zheng K, Gong H, Yan N, Chen Q, et al. Denosumab combined with precision radiotherapy for recurrent giant cell tumor of the thoracic spine: a case report and literature review. *Front Neurol*. (2024) 14:1308600. doi: 10.3389/fneur.2023.1308600

35. Sidoff L, Dupuy DE. Clinical experiences with microwave thermal ablation of lung Malignancies. *Int J Hyperthermia*. (2017) 33:25–33. doi: 10.1080/02656736.2016.1204630

36. Zhong L, Sun S, Shi J, Cao F, Han X, Bao X, et al. Clinical analysis on 113 patients with lung cancer treated by percutaneous CT-guided microwave ablation. *J Thorac Dis*. (2017) 9:590–7. doi: 10.21037/jtd.2017.03.14

37. Hu X, Hu Q, He Y, Yi X, Wu Z, Hu H, et al. Efficacy and safety of microwave ablation and its synergistic potential in the treatment of early-stage non-small cell lung cancer. *Clin Imaging*. (2024) 107:110070. doi: 10.1016/j.clinimag.2023.110070

38. Fang T, Lv H, Lv G, Li T, Wang C, Han Q, et al. Tumor-derived exosomal miR-1247-3p induces cancer-associated fibroblast activation to foster lung metastasis of liver cancer. *Nat Commun*. (2018) 9:191. doi: 10.1038/s41467-017-02583-0

39. Cornman-Homonoff J, Miller ZA, Smirniotopoulos J, May BJ, Winokur RS, Pua BB, et al. Preoperative percutaneous microwave ablation of long bone metastases using a parallel medullary approach for reduction of operative blood loss. *J Vasc Interv Radiol*. (2017) 28:1069–71. doi: 10.1016/j.jvir.2017.03.004

40. Goldberg SN. Comparison of techniques for image-guided ablation of focal liver tumors. *Radiology*. (2002) 223:304–7. doi: 10.1148/radiol.2232012152

41. Jiao YQ, Yang HL, Xu L, Liu J, Hu YC. Surgical treatment of distal radius giant cell tumors. *Handb Surg Rehabil*. (2021) 40:150–5. doi: 10.1016/j.hansur.2020.12.004

42. Ke J, Cheng S, Yao MY, Chu X, Wang M, Zeng XL, et al. Novel strategy of curettage and adjuvant microwave therapy for the treatment of giant cell tumor of bone in extremities: A preliminary study. *Orthop Surg*. (2021) 13:185–95. doi: 10.1111/os.12865

43. Zheng K, Yu X, Hu Y, Zhang Y, Wang Z, Wu S, et al. Clinical guideline for microwave ablation of bone tumors in extremities. *Orthop Surg*. (2020) 12:1036–44. doi: 10.1111/os.12749

44. Machak GN, Snetkov AI. The impact of curettage technique on local control in giant cell tumour of bone. *Int Orthop*. (2021) 45:779–89. doi: 10.1007/s00264-020-04860-y

45. Zheng K, Yu XC, Xu M, Wang JM. Conservative surgery with microwave ablation for recurrent bone tumor in the extremities: a single-center study. *BMC Cancer*. (2022) 22:1122. doi: 10.1186/s12885-022-10233-y

frontiers | Frontiers in Oncology

TYPE Case Report
PUBLISHED 12 November 2024
DOI 10.3389/fonc.2024.1387005

OPEN ACCESS

EDITED BY
Gerardo Caruso,
University Hospital of Policlinico G. Martino, Italy

REVIEWED BY
Mahmoud Messerer,
Centre Hospitalier Universitaire Vaudois (CHUV), Switzerland
Tuo Shao,
First Affiliated Hospital of Harbin Medical University, China

*CORRESPONDENCE
Qingchun Mu
muq@suda.edu.cn
Rujun Li
newjun_li@163.com

RECEIVED 24 February 2024
ACCEPTED 18 September 2024
PUBLISHED 12 November 2024

CITATION
Wang Y, Zhu Q, Chen A, Dai C, Xu L, Sheng M, Huang Q, Lan Q, Mu Q and Li R (2024) Integrated surgical intervention for intradural extramedullary hemangioblastoma of the cervical spine: a case report and literature review. *Front. Oncol.* 14:1387005. doi: 10.3389/fonc.2024.1387005

Integrated surgical intervention for intradural extramedullary hemangioblastoma of the cervical spine: a case report and literature review

Yao Wang[1], Qing Zhu[1], Ailin Chen[1], Chungang Dai[1], Longjiang Xu[2], Minfeng Sheng[1], Qiang Huang[1], Qing Lan[1], Qingchun Mu[1]* and Rujun Li[1]*

[1]Department of Neurosurgery, Second Affiliated Hospital of Soochow University, Suzhou, Jiangsu, China, [2]Department of Pathology, Second Affiliated Hospital of Soochow University, Suzhou, Jiangsu, China

Introduction: The incidence of hemangioblastoma is low, constituting only 1-5% of all spinal cord tumors. Specifically, intradural extramedullary hemangioblastoma without Von Hippel-Lindau syndrome represents an exceedingly rare condition.

Methods: We report the first documented case of cervical intradural extramedullary hemangioblastoma in China. A 53-year-old male patient presented with a 3-year history of mild right hemiplegia, segmental muscle strength and sensation impairment, and a positive pyramidal tract sign. MRI showed an abnormal oval signal focus in the intradural and extramedullary region at the C6-C7 vertebral level. Before surgery, angiography was performed to identify the supplying arteries and draining veins. Subsequent interventional therapy achieved over 90% occlusion of blood vessels, creating optimal conditions for complete resection of the spinal tumor.

Results: The patient demonstrated satisfactory postoperative recovery with significant restoration of sensory and motor functions. Pathological examination showed a significant upregulation of CD31 in tumor cells and a substantial presence of the neuro-specific marker S100 in the tumor stroma, consistent with the diagnostic criteria for spinal hemangioblastoma.

Conclusion: The rarity of cervical intradural extramedullary hemangioblastoma without Von Hippel-Lindau syndrome was reaffirmed by a comprehensive review of the existing literature. Complete tumor resection remains the optimal approach for managing this uncommon condition, generally resulting in a favorable prognosis. Traditional open fenestration surgery is linked to elevated risks of bleeding and trauma. Meanwhile, endovascular injection of embolic agents may lead to residual lesions and an increased risk of recurrence. Therefore, we recommend a one-time combined treatment conducted in a

hybrid operating room to achieve complete resection and effectively reduce intraoperative bleeding risk. Despite presenting challenges and requiring high proficiency, we still recommend this type of combined surgery as a suitable therapeutic option for such diseases.

KEYWORDS

spinal hemangioblastoma, intradural extramedullary, Von Hippel-Lindau syndrome, rare diseases, integrated surgical intervention, case report

1 Introduction

Hemangioblastomas (HBs) are rare, low-grade benign tumors, representing 1-3% of central nervous system (CNS) tumors (1). Of these, approximately 70-80% are found in the cerebellar hemisphere, 10-15% in the vermis, 10% in the brainstem, and only 3.2% in the spinal cord, where they account for 1–5% of intramedullary spinal tumors in surgical series (1–4). However, the spinal hemangioblastoma is characterized by its slow growth and high vascularity, making up only 2-15% of primary malignant tumors in the spinal cord (5). The intramedullary form accounts for 41 to 84% of spinal HBs, while both intramedullary and extramedullary forms are observed in 11 to 37%, and only 3 to 22% present as purely extramedullary lesions. Despite the known endothelial cell origin of HBs, their incidental extramedullary pathogenesis remains unclear (6). Additionally, HBs are also associated with Von Hippel-Lindau (VHL) syndrome, which is caused by mutations in the VHL gene located on chromosome 3p25-26 (7). At the same time, compared with patients with sporadic HBs (20.5%), patients with intradural extramedullary (IDEM) HBs associated with VHL syndrome (88.2%) were more common (8, 9). Therefore, IDEM spinal HBs without VHL syndrome are extremely rare. In this article, we will introduce the compound treatment plan for such rare diseases launched by our center, and discuss the specific diagnosis and treatment methods combined with the literature.

2 Case presentation

2.1 History

The patient, a 53-year-old man, presented with unexplained neck discomfort that started 3 years ago. He also experienced numbness and weakness in his right limb as well as difficulty walking. Physical examination revealed mild sensory segmental impairment and positive pyramidal signs. The patient had a history of hypertension and suffered from cerebral infarction 3 years ago, for which he had been taking orally administered enteric-coated aspirin tablets for an extended period of time. This patient did not have a family history of spinal HBs. Clinical evaluation for VHL syndrome did not reveal any retinopathy. Imaging studies of the chest, abdomen, head, and pelvis showed no evidence of other lesions. The patient had no relevant medical treatment history.

2.2 Imaging

The MRI imaging of the neck revealed a space-occupying lesion at the C6-C7 level, causing compression on the spinal cord and exhibiting evident enhancement effect (Figures 1A–C). Within and above the lesion, empty vascular shadows were observed in the dorsal spinal cord. A vascular mass was identified between both sides of the vertebral arteries on CTA and CT, possibly receiving blood supply from the superior thyroid artery (Figures 1G, H). The findings on DSA were consistent with those on CTA (Figure 1K), indicating an arteriovenous malformation or spinal hemangioblastoma. The two types of diseases we have inferred are both benign, with a high probability of having a good prognosis.

2.3 Surgical intervention

The primary surgical approach for IDEM typically includes gross total resection (GTR) or subtotal resection (STR), optionally preceded by preoperative endovascular embolization or intraoperative venous drainage division (10–13). For tumors that cannot be fully resected, stereotactic radiotherapy and antiangiogenic therapy are viable alternatives (14–18). Preoperative endovascular embolization is an effective adjunct, reducing surgical bleeding and operative risks in selected cases (10–13). However, clear evidence supporting the benefits of preoperative endovascular embolization for improving tumor removal quality remains lacking (12). Considering the high likelihood of intraoperative bleeding and the necessity of complete tumor resection, we counseled the patient that right radial artery puncture cerebral angiography and embolization would be required prior to resection. This specific surgical procedure can be summarized as follows: “Puncture of the right radial artery for cerebral angiography, embolization of the tumor feeding artery, and resection of the tumor in the spinal canal under neuroelectrophysiological monitoring”. The patient was placed in the supine position after general anesthesia. Under the monitoring of the road map, the X-pedion10 microtubule guide wire shaped into a “J” shape at the tip was used to guide three Marathon microcatheters with straight tips to be placed into the three tumor feeding arteries (Figure 1L). The balloon was filled and a total of 2.5ml of Onyx18 glue was slowly injected. Angiography showed occlusion of more

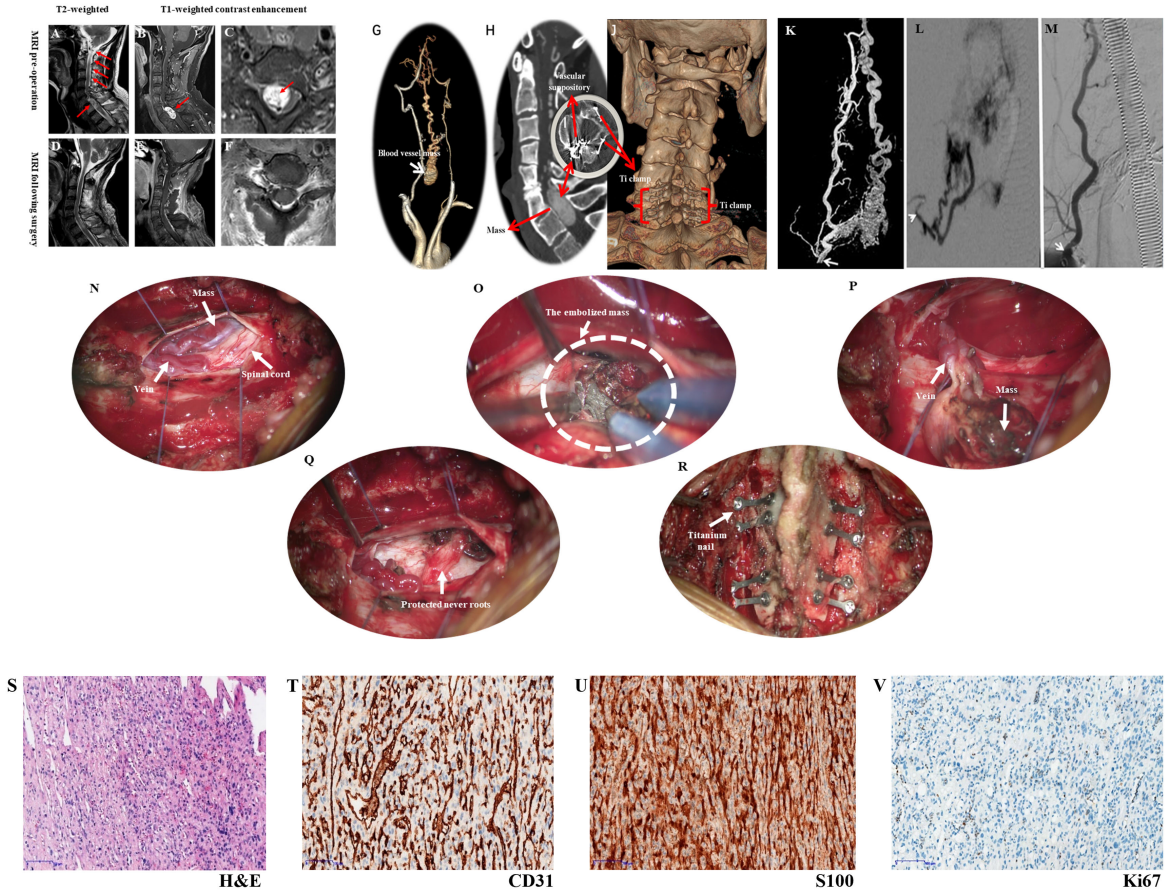

FIGURE 1
Presents the imaging examination, surgical procedure, and pathological findings. Figure 1 **(A)** MRI shows a mass at the C6 and C7 levels, along with a beaded vascular flow shadow on the dorsal side of the spinal cord above it; **(B, C)** MRI reveals oval abnormal signal foci in the spinal canal at the level of C6-7 vertebral bodies, measuring approximately 16mm×11mm×26mm, exhibiting evident enhancement, as well as small patchy vascular flow shadows (red arrows) and changes indicative of spinal cord compression; **(D–F)** Depict images from postoperative period illustrating complete disappearance of the mass when compared to **(A–C)**; **(G)** The CTA reveals a vascular mass located between the bilateral vertebral arteries, potentially supplied by the superior thyroid artery; **(H)** Preoperative CT scan exhibits a rounded mass with lightly increased signal intensity within the spinal canal at C6-7; **(I)** Postoperative CT demonstrates complete disappearance of the mass, revealing residual shadows of the embolic agent; **(J)** Three-dimensional CT reconstruction confirms satisfactory fixation of vertebral plates in laminoplasty using titanium nails. **(K)** Selective angiography involved injecting a contrast agent through the distal end of the 4F VER catheter, entering the opening of the right thyroid neck trunk (white arrow). This depicted contrast agent entry into the tumor via the intervertebral foramen, causing hyperstaining and backflow towards the medulla oblongata; **(L)** The Echelon10 microcatheter was super selected into a branch of the tumor feeding artery from the superior thyroid artery (white arrow), resulting in tumor staining after contrast injection; **(M)** Following Onyx18 injection, angiography of the right thyrocervical trunk displayed well-developed main trunk arteries (white arrow) with nearly complete absence of tumor staining. **(N)** The dissection of the dura allows for the observation of varicose veins, tumors, and compression of the spinal cord; **(O)** After cutting the arachnoid membrane and flowing out the cerebrospinal fluid, the embolized tumor can be seen on the lateral side of the spinal cord; **(P)** The tumor has been dissociated and turned out of the tumor cavity; **(Q)** The nerve root is completely preserved; **(R)**. Reposition and titanium needle fixation of the lamina fix the vertebral plate, and maintain the stability of the spine. Pathological findings (×100 magnification) observed under a light microscope, **(S)** H&E staining revealed numerous fusiform tumor cells with irregular lumens and thin-walled blood vessels; **(T)** CD31 staining showed prominent vascular endothelial cells, with the presence of numerous irregular thin-walled blood vessels and some anastomosed blood vessels; **(U)** S100 expression was strongly positive in tumor cells; **(V)** Ki67 expression indicated a low tumor growth index of approximately 1%.

than 90% of the vessels in the vascular mass (Figure 1M). Then, the whole lamina and spinous process of C6-C7 were removed. The dura mater was cut and suspended, and a well-demarcated vascular mass with a size of 2.5cm×1.5cm×1.5cm filled with embolic agent was located at the right side of the spinal canal at C6 and C7 levels. The mass was located on the right side of the spinal cord, within the arachnoid, and originated from the region of the C6-C7 intervertebral foramen. Along the border of the mass, there was a gradual cessation of blood supply to the C6-C7 intervertebral foramen. The adhesion of the mass to the spinal cord and nerves was separated, and ultimately, the mass was completely removed. There was no evidence of residual tumor and the spinal cord remained intact. Subsequently, the removed C6 and C7 partial laminae combined with spinous process were reduced as a whole and fixed with 8 titanium connecting pieces and 16 titanium nails to consolidate the stability of the spine, and the wound was closed in a standard manner (Figures 1N–R). The intraoperative blood loss was only 300ml and the procedure lasted a total of 8 hours.

2.4 Postoperative course

Pathological examination of the resected tumor tissue was conducted post-surgery. The findings revealed that the tumor consisted of spindle-shaped tumor cells and blood sinuses. CD31 exhibited strong positivity, with immune complexes deposited irregularly on the vascular endothelium of the tumor, forming a grid-like pattern. S100 also demonstrated strong positivity, with immune complexes deposited on nerve bundles within the tumor stroma. These observations collectively supported the diagnosis of hemangioblastoma (Figures 1S–V). The postoperative recovery was satisfactory, as muscle strength returned to normal and sensory disturbances resolved. A follow-up MRI performed 9 days after surgery displayed effusion behind the lamina, edema in interspinous soft tissues, complete disappearance of mass shadow, and absence of residual lesions (Figures 1D–F). Postoperative CT scans show complete mass resolution, with only residual embolic agent shadows remaining (Figure 1I). Three-dimensional CT reconstruction further confirms successful vertebral plate fixation with titanium nails during laminoplasty (Figure 1J). During the postoperative follow-up for 6 months, the patient's limb pain and numbness resolved, and normal gait. The Modified McCormick functional schema score (19) and Sensory pain scale score (19) decreased from 3 points before the operation to 1 point after the operation. The patient consistently adhered to the treatment regimen and did not experience any tolerability issues throughout the course of treatment. No significant complications were encountered. The timelines for crucial stages in patient diagnosis and care were meticulously devised (Figure 2).

3 Results

We conducted a comprehensive literature review on this rare disease, covering the period from 1978 to 2023, and identified 27 cases of primary IDEM spinal HBs (3, 4, 6, 7, 14, 20–38). The criteria for including and excluding these literatures, along with specific patient information, are detailed in Figure 3 and Tables 1, 2. Of these cases, 12 were male (44.4%) and 15 were female (55.6%). The mean age at onset was 54.81 ± 15.33 years old, ranging from 17 to 82 years old. The tumors were most commonly located in the lumbar spine (n=7, 26%), followed by the cervical spine (n=6, 22%), thoracic spine (n=6, 22%), conus (n=3,11%), and cervicomedullary junction (n=2, 7%). What is more, the tumor also can span or accumulate more than one segment (n=3, 11%). The preoperative clinical manifestations of all patients can be summarized as follows: only sensory disorders (n=11, 41%), only motor disorders (n=2, 7%), combined sensory and motor disorders (n=13, 48%), and sensory and motor disorders accompanied by sphincter dysfunction (n=1, 4%) such as constipation.

MRI is a highly accurate imaging modality for diagnosing spinal hemangioblastoma and has been widely utilized in clinical practice (3, 4, 6, 7, 14, 22–38). Therefore, most patients underwent MRI examination (n=25, 93%), while a few of patients (n=2, 7%) did not undergo such examination. Similarly, only a few of patients underwent CTA or CT, most of patients (n=23, 85%) did not undergo CTA examination. Although spinal angiography was beneficial for differential diagnosis, it was not conducted in over half of the patients (n=9, 33%). Additionally, only 3 patients (including this case) received interventional embolization to occlude the feeding artery.

In the majority of cases, GTR was performed with clear tumor boundaries (n=23, 85%). Only 2 patients underwent marginal resection due to spinal cord adhesion and severe nerve root involvement, while another 2 patients underwent STR. The majority of patients had a favorable postoperative prognosis with recovery of neurological function and resolution of pain or sensory disturbances (n=23, 85%). Transient urinary retention and intestinal retention were observed in only 2 patients after surgery but subsequently improved. Post-surgery, only 1 patient encountered acute cerebellar hemorrhage, while another exhibited progressive sensory and motor function decline, ultimately resulting in death.

Postoperative pathology confirmed 24 cases, 3 cases of IDEM hemangioblastoma that did not yield a clear pathological diagnosis. Only 1 patient's diagnosis was made through autopsy examination.

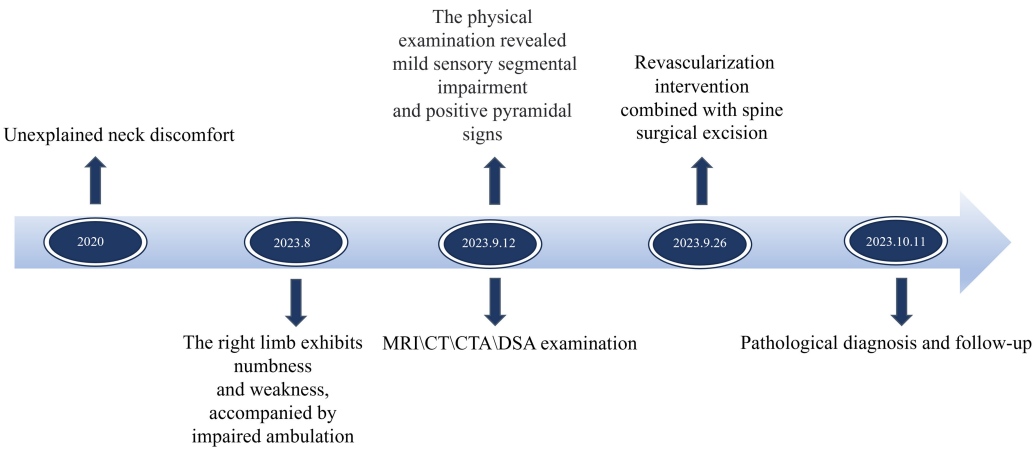

FIGURE 2
Presents a timeline of key points in the patient's diagnosis and treatment.

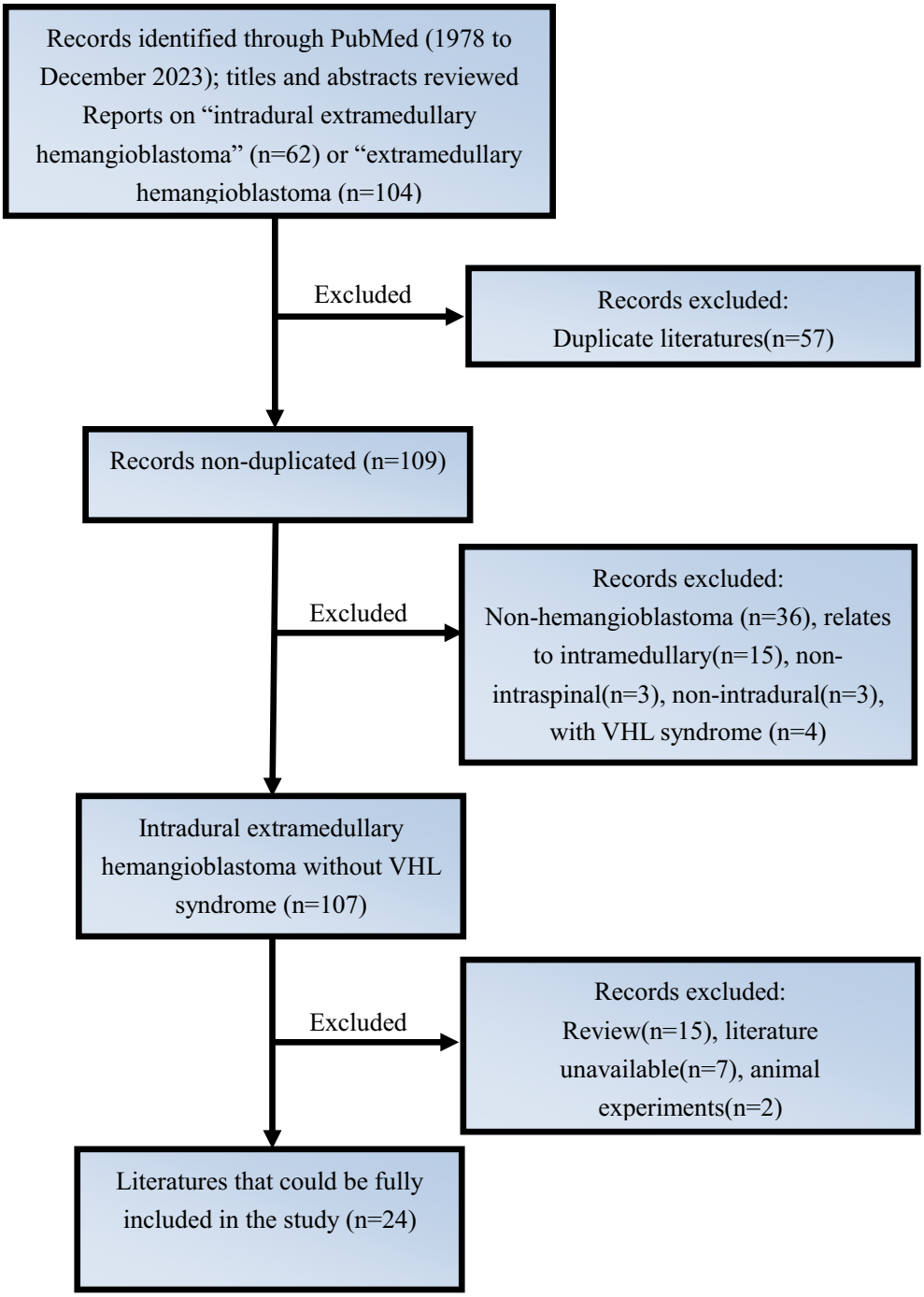

FIGURE 3
The final flowchart for literature enrollment.

4 Discussion

Although the clinical symptoms of spinal hemangioblastoma may overlap with those of various spinal degenerative diseases, and the MRI imaging features may resemble a range of tumors and vascular malformations (such as arteriovenous malformations and dural arteriovenous fistulas), MRI examination remains the preferred diagnostic modality for spinal hemangioblastoma (4, 35). The key to MRI diagnosis of hemangioblastoma lies in the identification of abnormally dilated blood vessels located beyond the peritumoral region (24). Due to the location and size of spinal HBs, there may be various imaging manifestations. For instance, smaller lesions typically exhibit solid and homogeneous characteristics with prominent enhancement on T1-weighted images (T1WI), often accompanied by edema and cavity formation on T2-weighted images (T2WI). Conversely, larger lesions demonstrate heterogeneous enhancement on both T1WI and T2WI (6, 13, 26, 39).

TABLE 1 Intradural Extramedullary Hemangioblastomas (1976-2023).

N	Author, Year	Age (Years)/ Sex	Location	MRI	CTA	AG	PL	ET	Preoperative Symptoms	EOR	Postoperative Outcome
1	Wisoff et al.,1978 (20)	59/M	Conus	No	No	No	Yes	No	Sensory and motor	GTR	Improved
2	Kitanaka et al.,1993 (21)	59/F	T6	No	CT	No	Yes	No	Sensory and motor	GTR	Improved
3	Minami,1998 (22)	48/M	Cervico medullary junction	Yes	No	Yes	Yes	No	Sensory only	GTR	Improved
4	Brisman,2000 (23)	57/F	Conus	Yes	No	Yes	Yes	No	Sensory and motor	GTR	Improved
5	Toyoda et al.,2004 (24)	46/M	C5-C7	Yes	No	No	Yes	No	Sensory only	GTR	Improved
6	Kashiwazaki et al.,2007 (25)	31/M	T4-T6	Yes	No	No	Yes	No	Motor only	GTR	Improved
7	Na et al., 2007 (26)	53/F	C3-C4	Yes	No	No	NS	No	Sensory and motor	GTR	Improved
8		66/M	C7-T1	Yes	No	No	NS	No	Sensory and motor	GTR	Improved
9		35/F	Cervico medullary junction	Yes	No	No	NS	No	Sensory and motor	GTR	Improved
10	Ramachandran et al.,2008 (27)	75/F	C4-C6	Yes	No	No	Autopsy	No	Sensory and motor	GTR	Continued to worsen; death
11	Taniguchi et al.,2009 (29)	65/F	T4-T5	Yes	No	No	Yes	No	Sensory and motor	Marginal resection	Improved
12	Barbosa-Silva et al.,2009 (28)	66/F	T10-T11	Yes	No	No	Yes	No	Sensory and motor	GTR	Improved
13	Chauvet et al.,2014 (30)	51/F	T2、L3、L4	Yes	No	Yes	Yes	No	Sensory only	GTR	Cerebellar hemorrhage associated with acute hydrocephalus; improved
14	Law et al.,2014 (31)	59/M	L4	Yes	CT	Yes	Yes	Yes	Sensory and motor	STR	Improved
15	Blaty et al.,2017 (14)	82/M	L4	Yes	No	No	Yes	No	Sensory only	STR	Improved; temporary urinary and bowel retention
16	Martins et al., 2019 (32)	28/F	L2	Yes	No	No	Yes	No	Sensory only	GTR	Improved
17	Li et al.,2021 (33)	72/M	C5	Yes	Yes	Yes	Yes	No	Sensory only	GTR	Improved
18	Kawanishi et al.,2021 (3)	58/F	T2-T3	Yes	No	No	Yes	No	Sensory and motor	GTR	Improved
19	Sereke et al.,2021 (34)	17/F	T10-T12	Yes	No	No	Yes	No	Sensory, motor and sphincter	GTR	Improved
20	Thippeswamy et al.,2021 (6)	52/F	L1-3	Yes	No	No	Yes	No	Motor only	GTR	Improved

(Continued)

10.3389/fonc.2024.1387005

TABLE 1 Continued

N	Author, Year	Age (Years)/ Sex	Location	MRI	CTA	AG	PL	ET	Preoperative Symptoms	EOR	Postoperative Outcome
21	Um et al.,2021 (35)	70/F	L2-3	Yes	No	Yes	Yes	Yes	Sensory only	GTR	Improved
22	Shields et al.,2021 (4)	65/M	T12-L1	Yes	CT	No	Yes	No	Sensory only	GTR	Improved
23	Fanous et al.,2022 (37)	62/M	C4-C5	Yes	No	No	Yes	No	Sensory only	GTR	Improved
24	Kehayov et al., 2022 (7)	40/M	Conus	Yes	No	No	Yes	No	Sensory only	GTR	Improved
25	D' Oria S et al.,2022 (36)	49/F	L1/2	Yes	No	Yes	Yes	No	Sensory and motor	GTR	Improved; temporary urinary and bowel retention
26	Fujii et al.,2022 (38)	66/F	L3	Yes	No	Yes	Yes	No	Sensory only	Marginal resection	Improved
27	Present case	53/M	C6-C7	Yes	Yes	Yes	Yes	Yes	Sensory and motor	GTR	Improved

MRI, magnetic resonance imaging; CTA, CT angiography; AG, angiography; PL, pathology; ET, embolization therapy; EOR, extent of resection; M, male; F, female; NS, not specific; GTR, gross total resection; STR, subtotal resection.

Additionally, the pathological diagnosis remains indispensable. Although the histogenesis mechanism of HBs remains elusive, several studies have indicated that HBs demonstrate positive staining for inhibin-α, CD56, and S100, while showing negative staining for CD34 and CD31 (40, 41). Meanwhile, Vimentin, a protein found in intermediate filaments, is expressed within endothelial cells. Ki67, an antigen associated with cellular proliferation, serves as an accurate indicator of tumor cell proliferative activity and is commonly employed for definitive diagnosis (29).

Relevant literature has also indicated that selective spinal angiography demonstrates a sensitivity of up to 90% in the diagnosis of hemangioblastoma (8), which aids in distinguishing it from other tumors and vascular malformations, such as arteriovenous malformations, dural arteriovenous fistulas, and cavernous malformations (10, 42). The utilization of spinal angiography additionally offers comprehensive information regarding the feeding arteries of the lesion, particularly focusing on the anterior spinal arteries, as well as venous drainage. Consequently, this further enhances preoperative preparation (10, 43, 44). In addition, some investigators argue that preoperative embolization can effectively mitigate the risk of intraoperative bleeding (4, 10, 42), while others contend that preoperative embolization does not offer a definitive therapeutic benefit but may potentially incite bleeding or result in medullary infarction during the embolization procedure (45–47). Therefore, it is imperative for personnel performing spinal angiography to possess a high level of technical proficiency and extensive experience.

Due to the rapid deterioration of symptoms in patients with spinal HBs, microsurgical intervention is often necessary. Currently, microsurgery can be classified into GTR and STR based on the extent of resection. Wang et al. (13) suggest that for sporadic or isolated spinal cord HBs, GTR can effectively cure the disease, alleviate clinical symptoms, and have a low recurrence rate. Meanwhile, Imagama S et al. (11) proposed that STR may not effectively address the cavity and edema surrounding hemangioblastoma, potentially exacerbating the patient's symptoms. The majority of cases advocate a posterior approach for achieving complete tumor resection due to the sufficient space provided by posterior laminectomy, facilitating tumor exposure (48, 49). It is worth noting that despite the limited availability of conclusive evidence, certain scholars contend that stereotactic radiotherapy and antiangiogenic therapy may serve as viable treatment modalities for spinal hemangioblastoma in cases where complete resection is not feasible (14–18). Additionally, it is widely acknowledged among investigators that the prognosis for patients with VHL syndrome is often suboptimal, characterized by a recurrence rate as high as 33.3%. In contrast, sporadic HBs exhibit a lower recurrence rate ranging from 6.25% to 20% (2, 4, 13, 38). Consequently, GTR remains the current preferred treatment for spinal HBs whenever feasible.

The IDEM hemangioblastoma is a rare condition that lacks specific clinical features, but its prominent imaging feature is the vascular flow void effect shown by MRI (39, 50–52). However, it should be noted that arteriovenous malformations and other hypervascular tumors can also exhibit this vascular flow void effect. Therefore, despite completing comprehensive CTA and MRI examinations prior to surgery in our

TABLE 2 Summary of patient demographics and case characteristics of patient with intradural extramedullary hemangioblastomas.

	Total patients (n=27)	Male (n=12,44.4%)	Female (n=15,55.6%)
Mean age (range, years)	54.81 ± 15.33	56.73 ± 14.86	53.00 ± 16.54
Location			
Cervical	6 (22%)	4 (33%)	2 (13%)
Cervicomedullary junction	2 (7%)	1 (8%)	1 (7%)
Thoracic	6 (22%)	1 (8%)	5 (33%)
Lumbar	7 (26%)	2 (17%)	5 (33%)
Conus	3 (11%)	2 (17%)	1 (7%)
Multiple segment	3 (11%)	2 (17%)	1 (7%)
MRI			
Yes	25 (93%)	11 (92%)	14 (93%)
No	2 (7%)	1 (8%)	1 (7%)
CTA			
Yes	2 (7%)	2 (17%)	0 (0%)
No	23 (85%)	8 (67%)	15 (100%)
CT	2 (7%)	2 (27%)	0 (0%)
AG			
Yes	9 (33%)	4 (33%)	5 (33%)
No	18 (67%)	8 (67%)	10 (67%)
PL			
Autopsy	1 (4%)	0 (0%)	1 (7%)
Yes	23 (85%)	11 (92%)	12 (80%)
NS	3 (11%)	1 (8%)	2 (13%)
ET			
Yes	3 (11%)	2 (17%)	1 (7%)
No	24 (89%)	10 (83%)	13 (93%)
EOR			
GTR	23 (85%)	10 (83%)	13 (87%)
STR	2 (7%)	2 (17%)	0 (0%)
Marginal resection	2 (7%)	0 (0%0	2 (13%)
Preoperative Symptoms			
Sensory only	11 (41%)	7 (58%)	4 (27%)
Motor only	2 (7%)	1 (8%)	1 (7%)
Sensory and motor	13 (48%)	4 (33%)	9 (60%)
Sensory, motor and sphincter	1 (4%)	0 (0%)	1 (7%)
Postoperative Outcome			
Improved	23 (85%)	11 (92%)	12 (80%)
Improved; temporary urinary and bowel retention	2 (7%)	1 (8%)	1 (7%)
Cerebellar hemorrhage associated with acute hydrocephalus; improved	1 (4%)	0 (0%)	1 (7%)
Continued to worsen; death	1 (4%)	0 (0%)	1 (7%)

MRI, magnetic resonance imaging; CTA, CT angiography; AG, angiography; PL, pathology; ET, embolization therapy; EOR, extent of resection; GTR, gross total resection; STR, subtotal resection.

center, it is crucial to differentiate between these two distinct vascular variants - arteriovenous malformation or hemangioblastoma. Furthermore, while DSA currently serves as the most accurate cerebral angiography method with high resolution capabilities, its contribution to the diagnosis of hemangioblastoma still requires evaluation. We firmly believe that pathology remains the gold standard for diagnosing solid tumors due to its ability to assess cellular and molecular landscapes as well as identify benign and malignant tumors.

Up to the present time, the International Society for the Study of Vascular Anomalies (ISSVA) has established a widely acknowledged classification system for vascular anomalies. In recent years, with the flourishing development of genetic testing and imaging technology, there has been a significant enhancement in diagnosing such diseases. Genetic testing has become increasingly comprehensive, aiding in identifying specific genetic mutations and informing treatment decisions. However, when it comes to hemangioblastoma, there still exists an unbridged gap in effective targeted molecule therapy. Furthermore, advanced imaging techniques like MRI and CT have greatly improved our diagnostic capabilities by enabling visualization and detection of vascular abnormalities, thereby creating conditions for achieving more precise diagnoses. Nevertheless, despite advancements in genetic testing and imaging techniques, diagnosis remains challenging due to the rarity of these disorders and their wide range of underlying symptoms. This necessitates a combination of medical resource allocation within the responsible department to minimize risks associated with curative interventions.

After conducting extensive literature analysis, we have observed that a majority of investigators generally advocate for the complete resection of tumors as it effectively reduces tumor recurrence rates. Despite the remarkable outcomes achieved through the application of keyhole minimally invasive techniques in intraspinal space-occupying lesions (53), this particular patient presented with IDEM

hemangioblastoma characterized by an abundance of blood vessels and involvement of high segments. Therefore, to ensure surgical safety, a surgical approach involving laminectomy and spinous process resection was chosen subsequent to interventional embolization. Additionally, to ensure spinal stability, we have incorporated the use of commonly employed titanium nails for lamina fixation during vertebroplasty (Figure 1R). It is worth mentioning that preoperative imaging examination revealed a significant abundance of tumor vessels within the tumor itself. Consequently, in a hybrid operating room setting, we performed endovascular intervention and successfully occluded over 90% of these tumor vessels using Onyx18, resulting in substantial reduction in intraoperative bleeding.

5 Conclusion

Our case illustrates that a combined approach involving endovascular embolization and laminectomy for cervical intramedullary dural HBs, unrelated to VHL syndrome, can effectively minimize intraoperative blood loss, improve surgical field visibility, and enable precise micromanipulation, ensuring complete tumor resection. This comprehensive treatment strategy significantly reduces intraoperative risks and achieves superior therapeutic outcomes. In conclusion, we recommend giving full consideration to preoperative embolization in cases where such procedures are sufficiently qualified. Last but not the least, we advocate for further research to investigate the efficacy of comprehensive treatment strategies for these benign yet high-risk hypervascular tumors.

Data availability statement

The datasets presented in this article are not readily available because of ethical and privacy restrictions. Requests to access the datasets should be directed to the corresponding authors.

Ethics statement

The studies involving humans were approved by The Second Affiliated Hospital of Soochow University. The studies were conducted in accordance with the local legislation and institutional requirements. Written informed consent for participation was not required from the participants or the participants' legal guardians/next of kin in accordance with the national legislation and institutional requirements. Written informed consent was obtained from the individual(s) for the publication of any potentially identifiable images or data included in this article.

Author contributions

YW: Conceptualization, Formal analysis, Resources, Writing – original draft, Writing – review & editing. QZ: Writing – review & editing, Data curation, Methodology, Supervision, Validation. AC: Methodology, Supervision, Validation, Writing – review & editing. CD: Data curation, Supervision, Writing – review & editing. LX: Data curation, Methodology, Writing – review & editing. MS: Methodology, Resources, Writing – review & editing. QH: Conceptualization, Data curation, Formal analysis, Funding acquisition, Investigation, Methodology, Project administration, Resources, Software, Supervision, Validation, Visualization, Writing – original draft, Writing – review & editing. QL: Data curation, Methodology, Supervision, Validation, Writing – review & editing. RL: Conceptualization, Investigation, Methodology, Supervision, Validation, Writing – original draft, Writing – review & editing. QM: Investigation, Validation, Writing – review & editing.

Funding

The author(s) declare financial support was received for the research, authorship, and/or publication of this article. 2024 Jiangsu Graduate Practice Innovation Plan (SJCX24_1818). Postgraduate Research & Practice Innovation Program of Jiangsu Province (SJCX24_1818) Jiangsu Provincial Medical Key Discipline (Laboratory) (JSDW202225) Subject construction lifting project (XKTJ-XK202402).

Acknowledgments

The authors sincerely acknowledge the patients and their families for granting their informed consent to participate in this study, and express deep gratitude for their invaluable support.

Conflict of interest

The authors declare that the research was conducted in the absence of any commercial or financial relationships that could be construed as a potential conflict of interest.

Publisher's note

References

1. Messerer M, Cossu G, Pralong E, Daniel RT. Intramedullary hemangioblastoma: microsurgical resection technique. *Neurochirurgie*. (2017) 63:376–80. doi: 10.1016/j.neuchi.2015.11.002

2. Tucer B, Ekici MA, Kazanci B, Guclu B. Hemangioblastoma of the filum terminale associated with von hippel-lindau disease: a case report. *Turk Neurosurg*. (2013) 23:672–75. doi: 10.5137/1019-5149.JTN.6172-12.1

3. Kawanishi M, Tanaka H, Itoh Y, Yokoyama K, Yamada M, Sugie A, et al. Intradural extramedullary hemangioblastoma of the thoracic cord: a case report. *Surg Neurol Int*. (2021) 12:126. doi: 10.25259/SNI_795_2020

4. Shields L, Harpring JE, Highfield HA, Zhang YP, Shields CB. Intradural, extramedullary hemangioblastoma at the level of the conus medullaris: illustrative case. *J Neurosurg Case Lessons*. (2021) 1:CASE2145. doi: 10.3171/CASE2145

5. Colamaria A, Fochi NP, Laguado Y, Blagia M, Leone A, Carbone F. Cervical intra and extramedullary hemangioblastoma with associated syringomyelia: a case report and review of the literature. *Surg Neurol Int*. (2022) 13:448. doi: 10.25259/SNI_814_2022

6. Thippeswamy PB, Soundararajan D, Kanna RM, Kuna VS, Rajasekaran S. Sporadic intradural extramedullary hemangioblastoma of cauda equina with large peritumoral cyst-a rare presentation. *Indian J Radiol Imaging*. (2021) 31:1057–61. doi: 10.1055/s-0041-1741047

7. Kehayov I, Angelova P, Batakliev I, Belovezhdov V, Kitov B. Monoradiculopathy caused by sporadic hemangioblastoma of the conus medullaris: case report and literature review. *Cureus*. (2022) 14:e24099. doi: 10.7759/cureus.24099

8. Couch V, Lindor NM, Karnes PS, Michels VV. Von hippel-lindau disease. *Mayo Clin Proc*. (2000) 75:265–72. doi: 10.4065/75.3.265

9. Yousef A, Rutkowski MJ, Yalcin CE, Eren OC, Caliskan I, Tihan T. Sporadic and von-hippel lindau disease-associated spinal hemangioblastomas: institutional experience on their similarities and differences. *J Neurooncol*. (2019) 143:547–52. doi: 10.1007/s11060-019-03189-w

10. Biondi A, Ricciardi GK, Faillot T, Capelle L, Van Effenterre R, Chiras J. Hemangioblastomas of the lower spinal region: report of four cases with preoperative embolization and review of the literature. *Ajnr Am J Neuroradiol*. (2005) 26:936–45.

11. Imagama S, Ito Z, Wakao N, Sakai Y, Kato F, Yukawa Y, et al. Differentiation of localization of spinal hemangioblastomas based on imaging and pathological findings. *Eur Spine J*. (2011) 20:1377–84. doi: 10.1007/s00586-011-1814-6

12. Saliou G, Giammattei L, Ozanne A, Messerer M. Role of preoperative embolization of intramedullary hemangioblastoma. *Neurochirurgie*. (2017) 63:372–75. doi: 10.1016/j.neuchi.2016.01.004

13. Wang H, Zhang L, Wang H, Nan Y, Ma Q. Spinal hemangioblastoma: surgical procedures, outcomes and review of the literature. *Acta Neurol Belg*. (2021) 121:973–81. doi: 10.1007/s13760-020-01420-4

14. Blaty D, Malos M, Palmrose T, McGirr S. Sporadic intradural extramedullary hemangioblastoma of the cauda equina: case report and literature review. *World Neurosurg*. (2018) 109:436–41. doi: 10.1016/j.wneu.2017.10.104

15. Moss JM, Choi CY, Adler JJ, Soltys SG, Gibbs IC, Chang SD. Stereotactic radiosurgical treatment of cranial and spinal hemangioblastomas. *Neurosurgery*. (2009) 65:79–85. doi: 10.1227/01.NEU.0000348015.51685.D2

16. Pan J, Jabarkheel R, Huang Y, Ho A, Chang SD. Stereotactic radiosurgery for central nervous system hemangioblastoma: systematic review and meta-analysis. *J Neurooncol*. (2018) 137:11–22. doi: 10.1007/s11060-017-2697-0

17. Schuch G, de Wit M, Holtje J, Laack E, Schilling G, Hossfeld DK, et al. Case 2. Hemangioblastomas: diagnosis of von hippel-lindau disease and antiangiogenic treatment with su5416. *J Clin Oncol*. (2005) 23:3624–26. doi: 10.1200/JCO.2005.01.184

18. Takeuchi S, Tanaka R, Fujii Y, Abe H, Ito Y. Surgical treatment of hemangioblastomas with presurgical endovascular embolization. *Neurol Med Chir (Tokyo)*. (2001) 41:246–51,251-52. doi: 10.2176/nmc.41.246

19. Naito K, Yamagata T, Ohata K, Takami T. Safety and efficacy of syringoperitoneal shunting with a programmable shunt valve for syringomyelia associated with extensive spinal adhesive arachnoiditis: technical note. *World Neurosurg*. (2019) 132:14–20. doi: 10.1016/j.wneu.2019.08.103

20. Wisoff HS, Suzuki Y, Llena JF, Fine DI. Extramedullary hemangioblastoma of the spinal cord. Case report. *J Neurosurg*. (1978) 48:461–64. doi: 10.3171/jns.1978.48.3.0461

21. Kitanaka C, Kuwahara M, Teraoka A. Intradural, purely extramedullary hemangioblastoma of the spinal cord–case report. *Neurol Med Chir (Tokyo)*. (1993) 33:377–80. doi: 10.2176/nmc.33.377

22. Minami M, Hanakita J, Suwa H, Suzui H, Fujita K, Nakamura T. Cervical hemangioblastoma with a past history of subarachnoid hemorrhage. *Surg Neurol*. (1998) 49:278–81. doi: 10.1016/s0090-3019(97)00196-1

23. Brisman JL, Borges LF, Ogilvy CS. Extramedullary hemangioblastoma of the conus medullaris. *Acta Neurochir (Wien)*. (2000) 142:1059–62. doi: 10.1007/s007010070063

24. Toyoda H, Seki M, Nakamura H, Inoue Y, Yamano Y, Takaoka K. Intradural extramedullary hemangioblastoma differentiated by mr images in the cervical spine: a case report and review of the literature. *J Spinal Disord Tech*. (2004) 17:343–47. doi: 10.1097/01.bsd.0000083630.91606.af

25. Kashiwazaki D, Hida K, Yano S, Seki T, Iwasaki Y. Subpial hemangiopericytoma with marked extramedullary growth: case report. *Neurosurgery*. (2007) 61:E1336–37. doi: 10.1227/01.neu.0000306116.93291.94

26. Na JH, Kim HS, Eoh W, Kim JH, Kim JS, Kim ES. Spinal cord hemangioblastoma: diagnosis and clinical outcome after surgical treatment. *J Korean Neurosurg Soc*. (2007) 42:436–40. doi: 10.3340/jkns.2007.42.6.436

27. Ramachandran R, Lee HS, Matthews B, Shatzel A, Tihan T. Intradural extramedullary leptomeningeal hemangioblastomatosis and paraneoplastic limbic encephalitis diagnosed at autopsy: an unlikely pair. *Arch Pathol Lab Med*. (2008) 132:104–08. doi: 10.5858/2008-132-104-IELHAP

28. Barbosa-Silva E, Carvalho GT, Frota MO, Sousa AA, Souza CB. Intradural extramedullary hemangioblastoma. *Arq Neuropsiquiatr*. (2009) 67:530–33. doi: 10.1590/s0004-282x2009000300033

29. Taniguchi S, Ogikubo O, Nakamura T, Yamagishi I, Hayakawa K, Otsuka T, et al. A rare case of extramedullary-intradural hemangioblastoma in the thoracic spine. *Spine (Phila Pa 1976)*. (2009) 34:E969–72. doi: 10.1097/BRS.0b013e3181b8e4f4

30. Chauvet D, Silhouette B, Engrand N, Pradier F, Piotin M, Lot G. Multiple spinal hemangioblastomas complicated with postoperative remote cerebellar hemorrhage: review of the literature of two rare entities. *World Neurosurg*. (2014) 81:841–43. doi: 10.1016/j.wneu.2012.11.054

31. Law EK, Lee RK, Griffith JF, Siu DY, Ng HK. Spinal nerve root haemangioblastoma associated with reactive polycythemia. *Case Rep Radiol*. (2014) 2014:798620. doi: 10.1155/2014/798620

32. Martins HO, Brock RS, Taricco MA, Junior J, de Oliveira MF. Sporadic hemangioblastoma of cauda equina: an atypical case report. *Surg Neurol Int*. (2019) 10:60. doi: 10.25259/SNI-127-2019

33. Li D, Choe S, Borys E, Serrone JC, Germanwala AV. Primary intradural extramedullary sporadic spinal hemangioblastomas: case report and systematic review. *World Neurosurg*. (2021) 152:84–94. doi: 10.1016/j.wneu.2021.05.105

34. Sereke SG, Bongomin F, Owor G. Dumbbell-shaped extramedullary hemangioblastoma of the thoracic spine as a diagnostic dilemma of solitary fibrous tumor. *Int Med Case Rep J*. (2021) 14:77–81. doi: 10.2147/IMCRJ.S294759

35. Um MK, Lee E, Lee JW, Lee KS, Kang Y, Ahn JM, et al. Sporadic intradural extramedullary hemangioblastoma not associated with von hippel-lindau syndrome: a case report and literature review. *Taehan Yongsang Uihakhoe Chi*. (2021) 82:700–07. doi: 10.3348/jksr.2020.0040

36. D' OS, Giraldi D, Flores D, Murrone D, D' AV, Chaurasia B. Sporadic hemangioblastoma of cauda equina: a case report and brief literature review. *J Craniovertebr Junction Spine*. (2022) 13:265–70. doi: 10.4103/jcvjs.jcvjs_87_22

37. Fanous A, Mugge L, Kurzejewski K, Cournoyer A, Ziu M. Intradural extramedullary hemangioblastoma of the cervical spine: case report and literature review. *Cureus*. (2022) 14:e25125. doi: 10.7759/cureus.25125

38. Fujii Y, Nishisho T, Tezuka F, Iwanami A, Yamashita K, Toki S, et al. Hemangioblastoma of the cauda equina: a case report and review of the literature. *J Med Invest*. (2022) 69:312–15. doi: 10.2152/jmi.69.312

39. Baker KB, Moran CJ, Wippold FN, Smirniotopoulos JG, Rodriguez FJ, Meyers SP, et al. Mr imaging of spinal hemangioblastoma. *Ajr Am J Roentgenol*. (2000) 174:377–82. doi: 10.2214/ajr.174.2.1740377

40. Epari S, Bhatkar R, Moyaidi A, Shetty P, Gupta T, Kane S, et al. Histomorphological spectrum and immunohistochemical characterization of hemangioblastomas: an entity of unclear histogenesis. *Indian J Pathol Microbiol*. (2014) 57:542–48. doi: 10.4103/0377-4929.142645

41. Shi H, Li H, Zhen T, Zhang F, Han A. Hemangioblastoma of pelvic cavity: report of a case and review of literature. *Int J Clin Exp Pathol*. (2014) 7:7054–58.

42. Beall DP, Googe DJ, Emery RL, Thompson DB, Campbell SE, Ly JQ, et al. Extramedullary intradural spinal tumors: a pictorial review. *Curr Probl Diagn Radiol*. (2007) 36:185–98. doi: 10.1067/j.cpradiol.2006.12.002

43. Nadkarni TD, Menon RK, Desai KI, Goel A. Hemangioblastoma of the filum terminale. *J Clin Neurosci*. (2006) 13:285–88. doi: 10.1016/j.jocn.2005.02.025

44. Kern M, Naeini R, Lehmann TN, Benndorf G. Imaging of a thoracic spinal nerve haemangioblastoma by three-dimensional digital angiography. *J Clin Neurosci*. (2006) 13:929–32. doi: 10.1016/j.jocn.2005.12.034

45. Ampie L, Choy W, Khanna R, Smith ZA, Dahdaleh NS, Parsa AT, et al. Role of preoperative embolization for intradural spinal hemangioblastomas. *J Clin Neurosci*. (2016) 24:83–7. doi: 10.1016/j.jocn.2015.09.006

46. Chang H, Li J, Wang P, Lu X, Li B. Microsurgical treatment of cervical spinal hemangioblastoma. *Neurochirurgie*. (2020) 66:56–60. doi: 10.1016/j.neuchi.2019.11.005

47. Takai K, Taniguchi M, Takahashi H, Usui M, Saito N. Comparative analysis of spinal hemangioblastomas in sporadic disease and von hippel-lindau syndrome. *Neurol Med Chir (Tokyo)*. (2010) 50:560–67. doi: 10.2176/nmc.50.560

48. Roonprapunt C, Silvera VM, Setton A, Freed D, Epstein FJ, Jallo GI. Surgical management of isolated hemangioblastomas of the spinal cord. *Neurosurgery*. (2001) 49:321–27,327-28. doi: 10.1097/00006123-200108000-00012

49. Yasargil MG, Antic J, Laciga R, de Preux J, Fideler RW, Boone SC. The microsurgical removal of intramedullary spinal hemangioblastomas. Report of twelve cases and a review of the literature. *Surg Neurol*. (1976) 3):141–48.

50. Colombo N, Kucharczyk W, Brant-Zawadzki M, Norman D, Scotti G, Newton TH. Magnetic resonance imaging of spinal cord hemangioblastoma. *Acta Radiol Suppl*. (1986) 369:734–37.

51. Chu BC, Hida K, Furukawa M, Abe S, Miyasaka K. Mr findings in spinal hemangioblastoma: correlation with symptoms and with angiographic and surgical findings. *Ajnr Am J Neuroradiol*. (2001) 22:206–17.

52. Fahrendorf G, Sartor K, Gado MH. Magnetic resonance imaging of spinal cord hemangioblastomas and arteriovenous malformations. *Acta Radiol Suppl*. (1986) 369:730–33.

53. Chen Y, Yu P, Xu H, Li S, Wang Q, Wu C, et al. Efficacy of minimally invasive tubular approaches for management of the lumbar spinal synovial cysts: a meta-analysis. *Eur J Med Res*. (2023) 28:494. doi: 10.1186/s40001-023-01481-0

frontiers | Frontiers in Oncology

TYPE Case Report
PUBLISHED 02 December 2024
DOI 10.3389/fonc.2024.1422958

OPEN ACCESS

EDITED BY
Cheng-Ying Ho,
Johns Hopkins Medicine, United States

REVIEWED BY
Sheng-Che Hung,
University of North Carolina at Chapel Hill, United States
Thomas Zaikos,
University of California, Irvine, United States

*CORRESPONDENCE
Qingchun Mu
muq@suda.edu.cn
Xiaofeng Chen
chenxiaofeng2008@hotmail.com

†These authors have contributed equally to this work

RECEIVED 26 April 2024
ACCEPTED 11 November 2024
PUBLISHED 02 December 2024

CITATION
Guo H, Wang Y, Wang L, Han D, Meng X, Mu Q and Chen X (2024) Intramedullary schwannoma of conus medullaris with syringomyelia: a case report and literature review.
Front. Oncol. 14:1422958.
doi: 10.3389/fonc.2024.1422958

Intramedullary schwannoma of conus medullaris with syringomyelia: a case report and literature review

Hua Guo[1†], Yao Wang[2†], Liankun Wang[3†], Dianhui Han[1], Xiangyi Meng[1], Qingchun Mu[2*] and Xiaofeng Chen[1*]

[1]Department of Neurosurgery, The First Affiliated Hospital of Harbin Medical University, Harbin, Heilongjiang, China, [2]Department of Neurosurgery, The Second Affiliated Hospital of Soochow University, Suzhou, Jiangsu, China, [3]Department of Neurology, Heilongjiang Province Hospital, Harbin, Heilongjiang, China

Intramedullary schwannomas in the conus medullaris are very rare and are usually not associated with syringomyelia. We report a unique case of intramedullary schwannoma in the conus medullaris with long-segment syringomyelia. The patient was a 60-year-old male, initially presenting with left dorsalgia, subsequently developing weakness in the right lower extremity. As the symptoms progressed, the patient exhibited ataxia in gait, accompanied by sphincter insufficiency and voiding dysfunction. Lumbar MRI revealed the presence of two tumors at the L3 and T11-L1 levels, accompanied by syringomyelia extending from T4 to T10. During surgery, it was determined that the tumor located at the T11-L1 vertebral level was intramedullary, whereas the tumor situated at the L3 level exhibited an extramedullary intradural configuration. Pathological examination conclusively identified both the intramedullary and extramedullary tumors as schwannomas. Although intramedullary schwannomas at the conus medullaris are very rare, schwannoma remains a diagnosis that cannot be ignored when facing patients with intramedullary tumors with syringomyelia. Intramedullary schwannoma can have a good neurological prognosis after surgical treatment.

KEYWORDS

intramedullary schwannoma, syringomyelia, conus medullaris, surgical treatment, case report

Introduction

Schwannomas are one of the most common primary spinal tumors. It usually originates from Schwann cells of the peripheral nervous system, and most of them are solitary and accompanied by a capsule. Based on the different positional relationships with the spinal dura mater, spinal schwannomas can be classified into three types: epidural (8-32%),

intradural-extramedullary (1-19%), and intradural(49-83%) (3, 4). The vast majority of schwannomas are located in the intradural space. Intradural schwannomas can be categorized into extramedullary intradural and intramedullary(IM) schwannomas. IM schwannomas are considered rare neoplasms, comprising only 1.1% of spinal schwannomas and 0.3% of all IM tumors (7). The most common site of IM schwannomas is the cervical spine and the level of the conus medullaris are less common, and those with syringomyelia are even rarer (11). We describe the first-ever instance to our knowledge of IM schwannoma of conus medullaris with long segment syringomyelia.

Case report

Anal sphincter weakness, urinary difficulties for two months, right lower limb weakness and walking instability for half a year, and left back pain for a year all are the symptoms which brought the 60-year-old male patient to the hospital. Neurological examination revealed sensory impairment below the inguinal plane, disappearance of abdominal wall reflex and cremasteric reflex. After admission, ultrasound examination showed that the residual urine volume in the bladder after urination was 530 ml. The patient did not have any previous major illness and had only taken oral pain medication in the past, this was his first visit to the hospital. Even with painkillers, his symptoms got worse. None of the patient's family members had a history of schwannoma.

We conducted a comprehensive MRI scan of the patient's entire spine, which included T1-weighted imaging (T1WI), T2-weighted imaging (T2WI), and enhanced scanning following the injection of a contrast agent. The tumors showed mixed signals on MRI plain scan and heterogeneous enhancement on enhanced MRI.MRI examination showed two tumors at L3 level and T11-L1 level respectively, measuring 8 × 8 × 10 mm and 24 × 54 × 20 mm. At the same time, syringomyelia at T4-T10 level appeared above the tumor at T11-L1 level (Figure 1). Based on the patient's clinical manifestations and MRI examination, the preoperative preliminary diagnosis was schwannoma or ependymoma. Other differential diagnoses included glioma, astrocytoma, calcified tuberculoma etc.

Subsequently, both tumors were removed simultaneously. The patient was placed in the prone position and two incisions were made at T12-L1 and L3 spinous processes. The skin and fascia were dissected layer by layer, and the muscles on both sides of the spinous process were separated and pulled. The bilateral laminae of T12, L1 and L3 were opened to expose the tumors, revealing that the tumor at the T11-L1 level was IM, while the tumor at L3 was extramedullary intradural.

Both tumors were completely resected under the microscope, the patient's neurological symptoms improved after the operation. Pathological examination showed that both tumors were schwannomas (Figure 2).

At the time of discharge, the patient's condition was significantly better than that on admission, the weakness of the right lower limb was significantly relieved, and he could basically walk normally. He still had weakness of the anal sphincter and difficulty in bowel and defecation. The lumbar incision healed well. Physical examination showed grade 5 muscle strength in the right lower extremity and Babinski signs were negative. Three months later, the patient's bladder and stool function was significantly improved compared with that before surgery, and he could walk completely independently. MRI reexamination showed that the tumor was completely removed and no recurrence was observed, and syringomyelia significantly shrank (Figure 1). During the one-year post-operative telephone follow-up, the patient is currently able to walk normally, with urinary and bowel functions having largely returned to normal, and the preoperative symptoms have essentially dissipated.The treatment timeline is shown in Figure 3.

Discussion

IM schwannomas are very rare, pathologist James Kernohan first reported IM schwannoma in 1931 (17). The last possible literature review was done in 2021 by V. M. Swiatek et al. that listed 166 IM schwannoma instances that were documented at the time (11). The cervical spine accounted for 63% of recorded cases of IM schwannoma, with the thoracic spine of the spinal cord coming in second at 26% and the lumbar spine at 11% (21). We conducted a systematic review of the literature in PubMed up to January 1, 2023 using the keywords "intramedullary" and "schwannoma" to retrieve all relevant studies and case reports of IM schwannoma. Inclusion criteria were as follows (1): at least one histologically confirmed IM schwannoma was reported (2), the tumor was located at the site of the conus medullaris, and (3) clinical information on the patient was available. We did not include the cases with neurofibromatosis. Only 15 cases—not including this one—of IM schwannoma in the spinal cord's conus have ever been documented in the literature (1, 2, 5, 6, 8–10, 12, 13, 15, 16, 18–20, 22) (Table 1).

By reviewing 16 cases with IM schwannomas in the conus of the spinal cord including our case, the age range was found to be 11–70 years old, with an average age of 40.1 ± 16.2 years. In a 2:1 ratio, men are more affected than women, which is consistent with the previous literature (11). The mean interval between the symptom onset and diagnosis was 16.9 months. This may be because IM schwannoma often grows slowly and infrequently exhibits clinical signs in its early stages. Among the 16 cases, the main symptom of about 57% was low back pain, 43% had movement disorders, 21% had paresthesia, 14% had sphincter dysfunction, and 1 patient had hypolibido or sexual dysfunction. Depending on where the tumor is located, the symptomatology of schwannomas might include neurological impairments as well as signs and symptoms (6). Prior research focusing on the clinical characteristics and surgical outcomes of patients with IM schwannomas has consistently demonstrated that pain or sensory disturbance constitutes the most prevalent initial symptom, followed by motor dysfunction, with sphincter dysfunction ultimately manifesting in the late stages (14).

Since there are no Schwann cells in the central nervous system's white matter, the pathophysiology of IM schwannomas is up for discussion (23). Intramural Schwann cells arising from the embryonal neural tube; Schwann cells transforming from neuroectoderm into pial cells; Schwann cells migrating into the cord in response to cord trauma; Schwann cells proliferating in the spinal

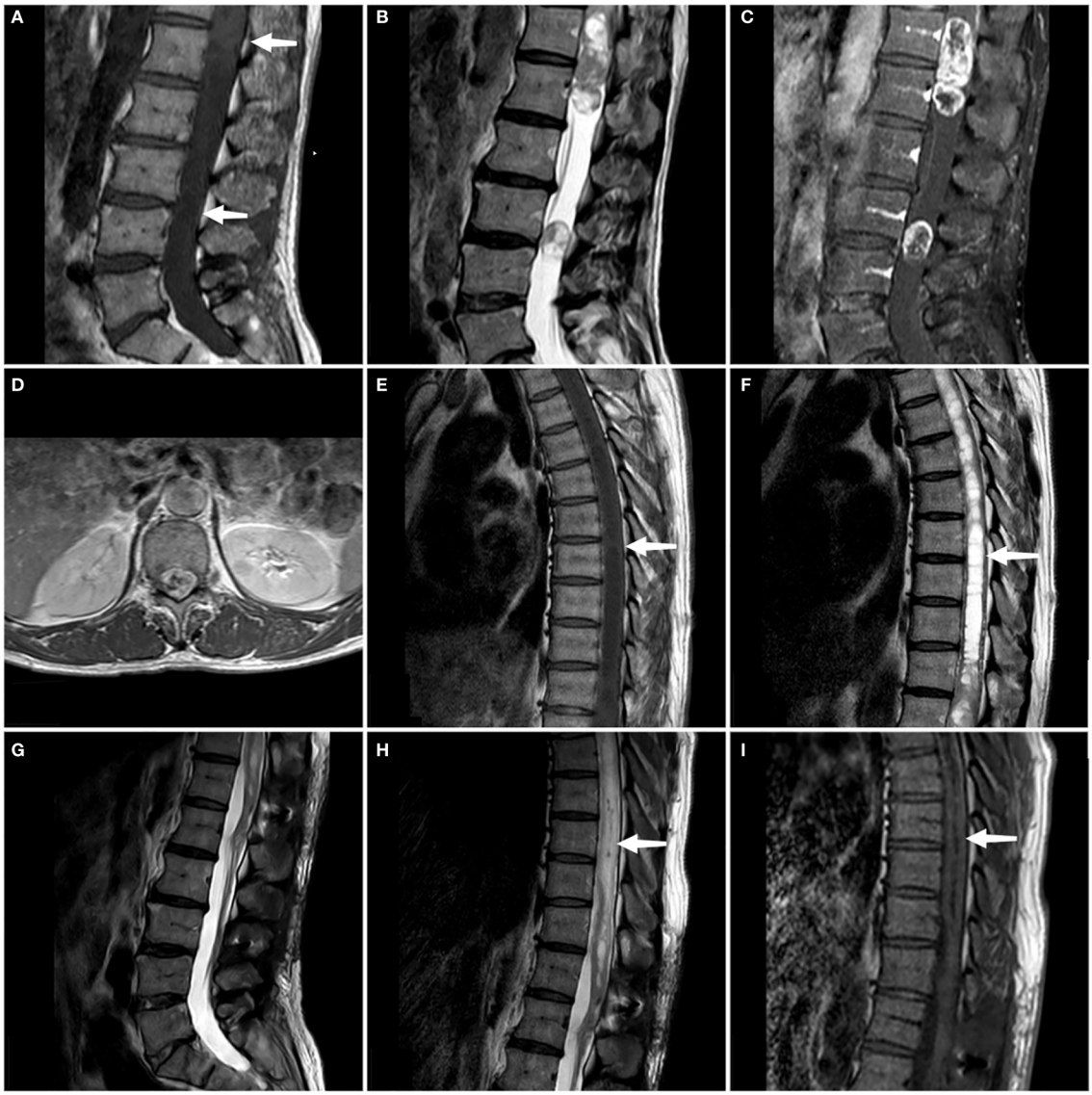

FIGURE 1
On the sagittal T1WI sequence, iso-signal occupying lesions (at the white arrow) are discernible separately within the T11-L1 segment and the L3 segment **(A)**. On the sagittal T2WI sequence, both tumors exhibit mixed signals **(B)**. Enhanced T1WI scans in both sagittal and axial planes reveal significant and heterogeneous enhancement of both lesions **(C, D)**. A persistent intramedullary abnormal signal at T4-T10 was seen above the lesion (at the white arrow), showing hypointense on the T1WI and hyperintense on the T2WI **(E, F)**. Follow-up MRI at 3 months confirmed complete tumor removal with no recurrence **(G)**. Sagittal T1- and T2-weighted thoracic MRI images reveal a marked reduction in syringomyelia compared to preoperative findings (white arrow) **(H, I)**.

artery nerve fibers; Schwann cells extending into cord from the region where spinal nerve roots enter pia mater are some of the theories regarding the origin of IM schwannomas (5, 24, 25). The Neurospinal Society of Japan conducted a nationwide analysis on IM Schwannoma of the spinal cord (26). Two primary categories of tumor location and extension can be distinguished: intramedullary to extramedullary extension and fully intramedullary extension. Each type may have a distinct developing pathway in light of these mechanisms and the location of the tumor. The shape of the tumor may depend on where in the spinal cord the aforementioned mechanisms take place. For instance, it is believed that tumors arising in more central parts of the spinal cord have intramedullary lesions, whereas tumors arising at the surface of the spinal cord have exophytic lesions.

Preoperative diagnosis might be challenging. MRI is the modality of choice for diagnosing IM schwannomas. On T1-weighted images, these IM schwannomas often show low to intermediate signal strength. They may be heterogeneous on T2-weighted imaging, showing collagen deposition, hemorrhage, and focal areas of hyper- and hypo-intensity (18). Strong contrast enhancement is typically seen in schwannomas, most likely as a result of open-gap junctions, which are short, straight, patent, and readily communicate with a sizable extracellular space (9). Of the 15 cases we reviewed, MRI data of 11 patients could be obtained, and the other 4 patients only had the relevant description of myelography. Uniform or nodular strong contrast enhancement was seen in all but one case (no T1 enhanced scan was performed),

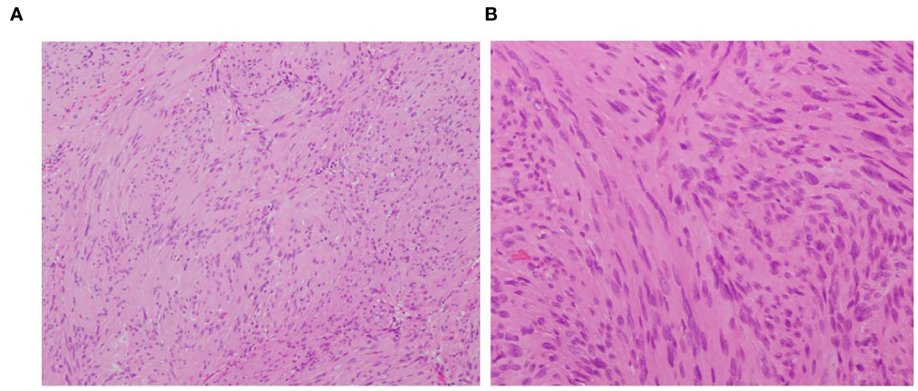

FIGURE 2
(A) observing under a microscope, the tumor shows cellular and hypocellular areas (H&E×200). **(B)** plumped spindle-shaped cells with palisading nuclei can be seen (H&E ×400).

which may be due to the abundant blood supply of the schwannoma. Of them, syringomyelia was present in just 3 cases, whereas 3 cases had uneven enhancement and 7 cases had uniform enhancement. In our case, both lesions showed isointensity on sagittal T1-weighted images, with a long strip of hypointense shadow above the lesion at T11-L1. A heterogeneously low-signal lesion at T11-L1 with a noticeable high signal extending upward is visible on the sagittal T2-weighted MRI, which is consistent with syringomyelia. Both lesions showed significant uneven enhancement and well-delineated masses on coronal enhanced T1-weighted images. Differential diagnosis typically encompasses all IM lesions with contrast enhancement, such as ependymomas, astrocytomas, hemangioblastomas, and metastatic tumors, which generally exhibit unclear tumor boundaries and are associated with spinal cord edema and tumor cysts (27). While a well-defined enhancement pattern can serve as a distinguishing feature between IM schwannomas and other IM tumors, our review identified that 27% (3/11) of the cases did not conform to this pattern, manifesting as heterogeneous or rim enhancement. Peritumoral edema or tumor cysts are also prevalent in IM schwannomas, as observed in our cases. In conclusion, it is challenging to establish a definitive preoperative diagnosis of IM schwannoma solely based on MRI findings.

After analyzing preoperative MRI characteristics of IM schwannomas that had previously been documented in the literature, Ho et al. (7) came to the conclusion that the lack of syringomyelia was a diagnostic MRI sign of IM schwannomas. However, some cases with IM schwannomas also have syringomyelia associated with them. Nine of the twenty instances with IM schwannoma reported by Yang et al. (22) had syringomyelia. The study conducted by V. M. Swiatek et al. (11) reported that 20.9% of the 165 IM schwannomas patients were found to have association with syringomyelia. In our case, the MRI showed very long segment syringomyelia at the level of T4-T10. The review of 16 cases, including the present one, resulted in the exclusion of 2 cases due to missing imaging data and the identification of 4 cases associated with syringomyelia (9, 12, 22). We speculate that a tumor that obstructed the flow of cerebrospinal fluid in the central canal produced the syringomyelia. As a result, our conclusion is that the absence of syringomyelia, although prevalent, lacks specificity. For tumors such as IM ependymoma, astrocytoma, and hemangioblastoma, which require differentiation from IM schwannoma, the presence of

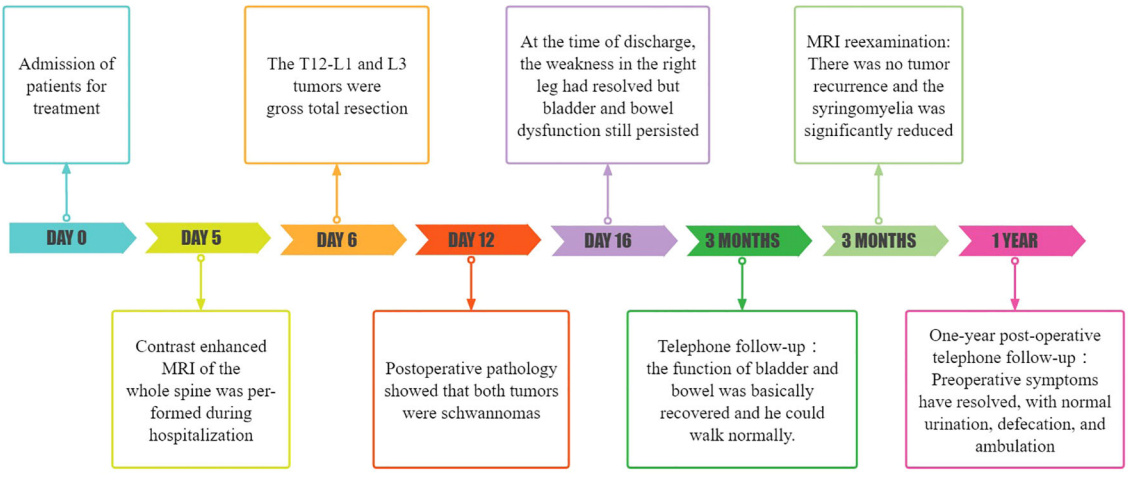

FIGURE 3
Treatment timeline of the patient.

TABLE 1 Summary of conus intramedullary schwannomas (in non-neurofibromatosis patients) reported to date.

Author reference	S. No.	Age (years)	Sex	Date	Tumor level	Symptom; duration	SM	MRI	Clinico-radiological differentials	Treatment	Resection	Follow up details available
Our case	1	60	M	2023	T11-L1	Back pain; 1 year	Yes	Inhomogeneous enhancement	Ependymoma Astrocytoma	T11-L1laminectomy	GTR	3 months, recovering well
Rahul Varshney et al. (2)	2	70	M	2020	T11-L2	Paraparesis, sphincter dysfunction; 2.5 year	No	Inhomogeneous enhancement	Ependymoma Astrocytoma	D12-L1 laminectomy	GTR	3 months, recovering well
Ritika Singh et al. (6)	3	27	F	2018	Conus	Lower backache; 1 year	No	Heterogenous rim enhancement	Ependymoma Astrocytoma	T12-L1 laminectomy	STR	1 year, recovering well
Karatey et al. (9)	4	30	F	2017	T12–L1	Back pain, walking difficulty; 2 months	Yes	Homogeneous enhancement	Astrocytoma	T12 laminectomy	GTR	N/A
Jagannatha et al. (12)	5	11	M	2016	T11–12	Weakness of both legs; 1 year	Yes	Homogeneous enhancement	Ependymoma Astrocytoma Calcified tuberculoma	T10–D12 laminotomy	GTR	6 months, recovering well
Yang et al. (14)	6	35	M	2014	T11–L2	Lower back pain, weakness in the left leg; 2 years	Yes	Inhomogeneous enhancement	Ependymoma	T11–12 laminectomy	GTR	9 months, full recovery
Kumar et al. (16)	7	40	F	2014	Conus	Back pain, walking difficulty; 1.5–2 years	N/A	Homogeneous enhancement	N/A	T10–L1 laminectomy	GTR	1 month, partial recovery
Canbay et al. (18)	8	49	F	2011	Conus	Lower back pain; 2 years	No	Inhomogeneous enhancement	N/A	T12–L1 laminectomy	GTR	N/A
Ohtonari et al. (19)	9	29	M	2009	Conus	Bladder dysfunction, paresthesia; 8 months	No	Homogeneous, well-enhanced,cystic lesion	N/A	T12–L1 laminectomy	STR	Patient being closely monitored for recurrence
M N Saiful Azl et al. (20)	10	54	M	2007	Conus	Low back pain; 2 years	No	Heterogenously enhanced	Ependymoma	laminectomy	GTR	N/A
Kahilogullari et al. (1)	11	338	F	2005	Conus	Waist and legs pain; 7 months	No	Homogeneous, well-enhanced	N/A	T12–L1 laminectomy	STR	Partial recovery postop
O'Brien et al. (5)	12	448	M	2003	T11-L1	Weakness in the legs; 6 months	No	Equal signal on T2	N/A	T11–L1 laminectomy	STR	6 months, no recurrence
Lesoin et al. (8)	13	N/A	M	1983	Conus	Weakness in the legs; 5 years	N/A	N/A	N/A	N/A	GTR	Slight weakness in left leg at 11 months
Schmitt (10)	14	N/A	M	1975	Conus	Paresthesia; 1.5 months	N/A	N/A	N/A	Autopsy finding	N/A	N/A
Guidetti (13)	15	N/A	N/A	11965	Conus	N/A	N/A	N/A	N/A	N/A	GTR	N/A
McCormik (15)	16	N/A	M	1964	L2	1.5 months	N/A	N/A	N/A	Autopsy finding	N/A	N/A

N/A, not applicable.

10.3389/fonc.2024.1422958

syringomyelia also lacks specificity. Notably, ependymoma, due to its location at the center of the spinal cord, is often accompanied by syringomyelia (28). Therefore, we propose that the absence of syringomyelia may have a certain role in the diagnosis of IM schwannoma, albeit lacking specificity. Pathological diagnosis constitutes an indispensable component in confirming the diagnosis of schwannomas. Histopathological examination typically reveals the tumor tissue arranged in alternating hypercellular and hypocellular areas (Antoni A and B), with tumor cells dispersed within a loose, mucinous stroma. These cells display an oval to spindle shape and form palisading patterns (Figure 2). Immunohistochemical staining often demonstrates positive expression for S-100 protein and Leu-7 (4).

As schwannoma is benign, gross total resection (GTR) is the preferred treatment for IM schwannoma. Nonetheless, not every patient may be able to achieve GTR. A well-defined tumor-spinal cord anatomical plane is critical for obtaining GTR; therefore, an ill-defined anatomical plane may mean that the tumor is difficult to achieve GTR even if it is benign. STR may also be necessary to prevent deterioration of neurological function if the lesion is adherent to the neural tissue (21). Furthermore, the residual tumor may be removed with a second surgery (29). After reporting 20 cases with IM schwannomas, 16 of which had GTR and 4 of which had subtotal resection (STR), Yang et al. (22) came to the conclusion that GTR or STR could result in a favorable clinical outcome. By reviewing reported 14 IM schwannoma cases (2 cases were excluded because surgical information was not available), GTR was achieved in 79% (11/14) of patients. In the study conducted by Yang et al. (14), the syrinx shrank in 77.8% (7/9) of patients with IM schwannoma accompanied by syringomyelia who underwent tumor resection only, with no syrinx enlargement observed. In our case, the shrinkage of syringomyelia was also observed during the radiological reassessment conducted three months post-surgery. Therefore, for syringomyelia secondary to IM schwannoma, additional drainage of the syrinx may not be necessary, as the syrinx may collapse following tumor resection (28). Adjuvant treatment modalities, such as radiotherapy and chemotherapy, have failed to exhibit favorable therapeutic outcomes in the context of IM spinal cord schwannomas. Conversely, adjuvant radiotherapy and chemotherapy may be utilized in the management of partially resected or recurrent IM spinal cord tumors, encompassing gliomas and ependymomas.Research is ongoing to develop novel therapeutic strategies for these patients, including targeted drug delivery and nanomedicine technologies (30).

Recurrence of IM schwannoma tumors is rare, even in cases with STR (14). M. Swiatek et al. (11) reported 165 patients with IM schwannomas with a mean follow-up of 34 months, and tumor recurrence was observed in only 4% of cases. Of the 15 cases of conical IM schwannomas we collected, follow-up information was not available in 6 cases. Tumor recurrence was not observed in the remaining 9 cases, even though 4 of them only achieved STR. During the follow-up period with an average duration of 6 months, almost all cases exhibited improved neurological function post-operatively, including 4 patients who underwent STR. In our case, the tumor achieved GTR because both tumors had clear boundaries with the surrounding tissue. Three months following surgery, a follow-up MRI revealed no signs of tumor recurrence and a considerable reduction in the edema surrounding the tumor. In conclusion, our analysis suggests that the prompt surgical management of symptomatic IM schwannomas, irrespective of the surgical approach employed (either GTR or STR), holds the potential to elicit substantial improvements in patient prognosis.

Conclusion

In conclusion, although IM schwannomas in the conus medullaris are rare tumors, they should still be an option when diagnosing intramedullary tumors, especially with syringomyelia. As a benign tumor, intramedullary schwannoma can achieve good neurological outcome after surgical treatment.

Data availability statement

The datasets presented in this article are not readily available because of ethical and privacy restrictions. Requests to access the datasets should be directed to the corresponding authors.

Ethics statement

The studies involving humans were approved by the Ethics Committee of First Affiliated Hospital of Harbin Medical University. The studies were conducted in accordance with the local legislation and institutional requirements. The participants provided their written informed consent to participate in this study. Written informed consent was obtained from the individual(s) for the publication of any potentially identifiable images or data included in this article.

Author contributions

HG: Writing – original draft, Writing – review & editing. YW: Writing – original draft, Writing – review & editing. LW: Writing – original draft, Writing – review & editing. DH: Writing – review & editing. XM: Writing – review & editing. XC: Writing – original draft, Writing – review & editing. QM: Funding acquisition, Writing – review & editing.

Funding

The author(s) declare financial support was received for the research, authorship, and/or publication of this article. The Heilongjiang Welfare Fund Organization of Disabled Persons (HJ2022-1), the Postdoctoral Science Foundation of Heilongjiang Province (LBH-Z19076), and the National Natural Science Foundation of China (82360366) provided funding for this study.

Conflict of interest

The authors declare that the research was conducted in the absence of any commercial or financial relationships that could be construed as a potential conflict of interest.

Publisher's note

References

1. Kahilogullari G, Aydin Z, Ayten M, Attar A, Erdem A. Schwannoma of the conus medullaris. *J Clin Neurosci*. (2005) . 12:80–1. doi: 10.1016/j.jocn.2004.02.016

2. Varshney R, Bharadwaj P, Choudhary A, Paliwal P, Kaushik K. A rare case of intramedullary schwannoma at conus medullaris: A case report with review of literature. *Surg Neurol Int*. (2020) . 11:454. doi: 10.25259/sni_718_2020

3. Conti P, Pansini G, Mouchaty H, Capuano C, Conti R. Spinal neurinomas: retrospective analysis and long-term outcome of 179 consecutively operated cases and review of the literature. *Surg Neurol*. (2004) . 61:34–43. doi: 10.1016/s0090-3019(03)00537-8

4. Seppälä MT, Haltia MJ, Sankila RJ, Jääskeläinen JE, Heiskanen O. Long-term outcome after removal of spinal schwannoma: a clinicopathological study of 187 cases. *J Neurosurg*. (1995) . 83:621–6. doi: 10.3171/jns.1995.83.4.0621

5. O'Brien DF, Farrell M, Fraher JP, Bolger C. Schwann cell invasion of the conus medullaris: case report. *Eur Spine J*. (2003) . 12:328–31. doi: 10.1007/s00586-002-0484-9

6. Singh R, Chaturvedi S, Pant I, Singh G, Kumari R. Intramedullary schwannoma of conus medullaris: rare site for a common tumor with review of literature. *Spinal Cord Ser Cases*. (2018) . 4:99. doi: 10.1038/s41394-018-0134-z

7. Ho T, Tai KS, Fan YW, Leong LL. Intramedullary spinal schwannoma: case report and review of preoperative magnetic resonance imaging features. *Asian J Surg*. (2006) . 29:306–8. doi: 10.1016/s1015-9584(09)60108-1

8. Lesoin F, Delandsheer E, Krivosic I, Clarisse J, Arnott G, Jomin M, et al. Solitary intramedullary schwannomas. *Surg Neurol*. (1983) . 19:51–6. doi: 10.1016/0090-3019(83)90211-2

9. Karatay M, Koktekir E, Erdem Y, Celik H, Sertbas I, Bayar MA. Intramedullary schwannoma of conus medullaris with syringomyelia. *Asian J Surg*. (2017) . 40:240–42. doi: 10.1016/j.asjsur.2014.04.004

10. Schmitt HP. Epi-" and intramedullary neurilemmoma of the spinal cord with denervation atrophy in the related skeletal muscles. *J Neurol*. (1975) . 209:271–8. doi: 10.1007/bf00314366

11. Swiatek VM, Stein KP, Cukaz HB, Rashidi A, Skalej M, Mawrin C, et al. Spinal intramedullary schwannomas-report of a case and extensive review of the literature. *Neurosurg Rev*. (2021) . 44:1833–52. doi: 10.1007/s10143-020-01357-5

12. Jagannatha AT, Joshi KC, Rao S, Srikantha U, Varma RG, Mahadevan A. Paediatric calcified intramedullary schwannoma at conus: A common tumor in a vicarious location. *J Pediatr Neurosci*. (2016) . 11:319–21. doi: 10.4103/1817-1745.199474

13. Guidetti B. Intramedullary tumours of the spinal cord. *Acta Neurochir (Wien)*. (1967) . 17:7–23. doi: 10.1007/bf01670413

14. Yang T, Wu L, Deng X, Yang C, Xu Y. Clinical features and surgical outcomes of intramedullary schwannomas. *Acta Neurochir (Wien)*. (2014) . 156:1789–97. doi: 10.1007/s00701-014-2168-8

15. McCormick WF. Intramedullary spinal cord schwannoma. A unique case. *Arch Pathol*. (1964) . 77:378–82.

16. Kumar R, Mittal RS. Intramedullary schwannoma of conus medullaris: case report and review of the literature. *World Spinal Column J*. (2014), 1–5.

17. Kernohan JW, Woltman HW, Adsion AW. Intramedullary tumors of the spinal cord: a review of fifty-one cases, with an attempt at histologic classification. *Arch Neurol Psychiatry*. (1931) . 25:679–701. doi: 10.1001/aurpsyc.1931.02230040013001

18. Canbay S, Hasturk AE, Markoc F, Caglar S. Schwannoma of the conus medullaris: a rare case. *Chin J Cancer*. (2011) . 30:867–70. doi: 10.5732/cjc.011.10213

19. Ohtonari T, Nishihara N, Ota T, Ota S, Koyama T. Intramedullary schwannoma of the conus medullaris complicated by dense adhesion to neural tissue. *Neurol Med Chir (Tokyo)*. (2009) . 49:536–8. doi: 10.2176/nmc.49.536

20. Saiful Azli MN, Abd Rahman IG, Md Salzihan MS. Ancient schwannoma of the conus medullaris. *Med J Malaysia*. (2007) . 62:256–8.

21. Navarro Fernández JO, Monroy Sosa A, Cacho Díaz B, Arrieta VA, Ortíz Leyva RU, Cano Valdez AM, et al. Cervical intramedullary schwannoma: case report and review of the literature. *Case Rep Neurol*. (2018) . 10:18–24. doi: 10.1159/000467389

22. Yang T, Wu L, Yang C, Deng X, Xu Y. Coexisting intramedullary schwannoma with an ependymal cyst of the conus medullaris: A case report. *Oncol Lett*. (2015) . 9:903–06. doi: 10.3892/ol.2014.2786

23. Kodama Y, Terae S, Hida K, Chu BC, Kaneko K, Miyasaka K. Intramedullary schwannoma of the spinal cord: report of two cases. *Neuroradiology*. (2001) . 43:567–71. doi: 10.1007/s002340100540

24. Wood WG, Rothman LM, Nussbaum BE. Intramedullary neurilemoma of the cervical spinal cord. *Case Rep J Neurosurg*. (1975) . 42:465–8. doi: 10.3171/jns.1975.42.4.0465

25. Nayak R, Chaudhuri A, Chattopadhyay A, Ghosh SN. Thoracic intramedullary schwannoma: A case report and review of literature. *Asian J Neurosurg*. (2015) . 10:126–8. doi: 10.4103/1793-5482.145155

26. Hara T, Mizuno M, Hida K, Sasamori T, Miyoshi Y, Uchikado H, et al. Intramedullary schwannoma of the spinal cord: A nationwide analysis by the neurospinal society of Japan. *Neurospine*. (2023) . 20:747–55. doi: 10.14245/ns.2346376.188

27. Lee SE, Chung CK, Kim HJ. Intramedullary schwannomas: long-term outcomes of ten operated cases. *J Neurooncol*. (2013) . 113:75–81. doi: 10.1007/s11060-013-1091-9

28. Wang K, Zhao J, Zhang Y, Su Y. Pediatric intramedullary schwannoma with syringomyelia: a case report and literature review. *BMC Pediatr*. (2018) . 18:374. doi: 10.1186/s12887-018-1341-2

29. Hida K, Yano S, Iwasaki Y. Staged operation for huge cervical intramedullary schwannoma: report of two cases. *Neurosurgery*. (2008) 62:ONS456–60. doi: 10.1227/01.neu.0000326035.54714.cc

30. Tobin MK, Geraghty JR, Engelhard HH, Linninger AA, Mehta AI. Intramedullary spinal cord tumors: a review of current and future treatment strategies. *Neurosurg Focus*. (2015) . 39:E14. doi: 10.3171/2015.5.Focus15158

Frontiers in Neurology

Explores neurological illness to improve patient care

The third most-cited clinical neurology journal explores the diagnosis, causes, treatment, and public health aspects of neurological illnesses. Its ultimate aim is to inform improvements in patient care.

Discover the latest Research Topics

See more →

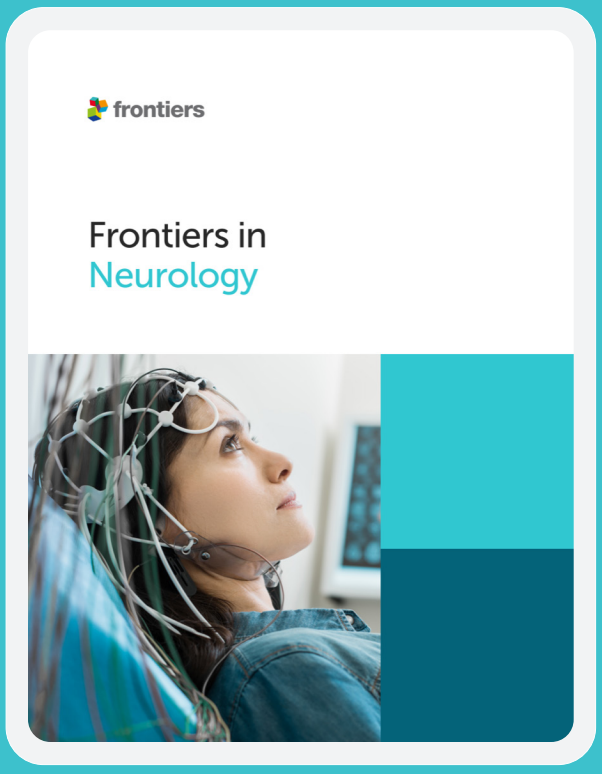

Frontiers

Avenue du Tribunal-Fédéral 34
1005 Lausanne, Switzerland
frontiersin.org

Contact us

+41 (0)21 510 17 00
frontiersin.org/about/contact